



UvA-DARE (Digital Academic Repository)

Microenvironmental regulation of multiple myeloma and malignant lymphoma: the role of HGF, Wnts, heparan sulfate proteoglycans, and N-cadherin

Groen, R.W.J.

Publication date

2010

Document Version

Final published version

[Link to publication](#)

Citation for published version (APA):

Groen, R. W. J. (2010). *Microenvironmental regulation of multiple myeloma and malignant lymphoma: the role of HGF, Wnts, heparan sulfate proteoglycans, and N-cadherin*. [Thesis, fully internal, Universiteit van Amsterdam].

General rights

It is not permitted to download or to forward/distribute the text or part of it without the consent of the author(s) and/or copyright holder(s), other than for strictly personal, individual use, unless the work is under an open content license (like Creative Commons).

Disclaimer/Complaints regulations

If you believe that digital publication of certain material infringes any of your rights or (privacy) interests, please let the Library know, stating your reasons. In case of a legitimate complaint, the Library will make the material inaccessible and/or remove it from the website. Please Ask the Library: <https://uba.uva.nl/en/contact>, or a letter to: Library of the University of Amsterdam, Secretariat, Singel 425, 1012 WP Amsterdam, The Netherlands. You will be contacted as soon as possible.

Microenvironmental regulation of Multiple Myeloma and Malignant Lymphoma



Richard W. J. Groen

Microenvironmental regulation of Multiple Myeloma and Malignant Lymphoma

Richard W. J. Groen



Microenvironmental regulation of Multiple Myeloma and Malignant Lymphoma

The role of HGF, Wnts, heparan sulfate proteoglycans,
and N-cadherin

Cover images: Sarah Newbury, the first documented patient with multiple myeloma. Adapted from Solly with permission. Solly S. Remarks on the pathology of mollities ossium with cases. *Med Chir Trans Lond* 1844; 27:435–461.

This thesis was prepared at the Department of Pathology, Academic Medical Center, University of Amsterdam, the Netherlands.

The research described in this thesis was funded by the Department of Pathology, Academic Medical Center and by the Dutch Cancer Society.

Printing of this thesis was financially supported by Celgene B.V., Biospace Lab, the Dutch Cancer Society, the Department of Pathology, Academic Medical Center, and the University of Amsterdam.



Printing: Ipskamp Drukkers, Enschede, the Netherlands

Lay-out: Wilfried Meun and Wim van Est

Microenvironmental regulation of Multiple Myeloma and Malignant Lymphoma:

The role of HGF, Wnts, heparan sulfate proteoglycans, and N-cadherin

Richard W.J. Groen

ISBN 978-90-9025768-6

Voor mijn moeder

Microenvironmental regulation of Multiple Myeloma and Malignant Lymphoma

The role of HGF, Wnts, heparan sulfate proteoglycans,
and N-cadherin

ACADEMISCH PROEFSCHRIFT

ter verkrijging van de graad van doctor
aan de Universiteit van Amsterdam
op gezag van de Rector Magnificus
prof. dr. D.C. van den Boom
ten overstaan van een door het college voor promoties
ingestelde commissie,
in het openbaar te verdedigen in de Agnietenkapel
op donderdag 18 november 2010, te 14.00 uur

door

Richard Wilhelmus Johannes Groen

geboren te Heemskerk

Promotiecommissie:

Promotor: Prof. dr. S.T. Pals
Co-promotor: Dr. M. Spaargaren

Overige leden: Prof. dr. M.H.J. van Oers
Prof. dr. H. Spits
Prof. dr. R. Versteeg
Prof. dr. H. Lokhorst
Prof. dr. B. Klein
Prof. dr. K. Vanderkerken

Faculteit der Geneeskunde

Table of Contents

Chapter 1	General introduction	9
	Innate and adaptive immunity	
	Lymphocyte development	
	Lymphoid malignancies	
	Multiple myeloma	
	Microenvironmental signals in the pathogenesis of multiple myeloma and malignant lymphoma	
	Mouse models for multiple myeloma	
	Aims and outline of this thesis	
Chapter 2	Functional analysis of HGF/MET signaling and aberrant HGF-activator expression in diffuse large B cell lymphoma	55
Chapter 3	Illegitimate Wnt pathway activation by β -catenin mutation or autocrine stimulation in T cell malignancies	75
Chapter 4	Transcriptional silencing of the Wnt-antagonist Dickkopf-1 by promoter methylation unleashes aberrant Wnt signaling in advanced multiple myeloma	97
Chapter 5	A bioluminescence imaging based in vivo model for preclinical testing of novel cellular immunotherapy strategies to improve Graft versus Myeloma	117
Chapter 6	Targeting EXT1 reveals a crucial role for heparan sulfate in the growth of multiple myeloma	135
Chapter 7	N-cadherin-mediated adhesion of multiple myeloma cells inhibits osteoblast differentiation	149
Chapter 8	General discussion	169
Chapter 9	Summary	185
	Nederlandse samenvatting	191
	Dankwoord	195
	Curriculum Vitae	199
	Publications by the author	201

1

General introduction

1

General introduction

Innate and adaptive immunity

The body is constantly exposed to infectious organisms. Our immune system, comprised of the innate (non-specific) and the adaptive (specific) immune system, enables us to resist these infections.

Innate immunity serves as the first line of defense against pathogens. This system is made up of several distinct components, including physical barriers, *i.e.* the skin and internal epithelial layers, and specialized phagocytic cells such as monocytes, macrophages and granulocytes. The innate immune system responds in a non-specific manner, meaning the response is not antigen (Ag) specific and reacts equally well to a variety of pathogens. Upon detection of infection, the innate system initiates an inflammatory response by recruiting white blood cells, activating the complement cascade, and finally activating the adaptive immune system.

The adaptive immunity, which acts as a second line of defense, is Ag-specific and demonstrates immunological memory, in other words it “remembers” that it has encountered a pathogen and reacts more rapidly to a subsequent exposure with the same pathogen. The activation of this system is initiated when invading bacteria are taken up through phagocytosis by an antigen-presenting cell (APC), such as a dendritic cell or macrophage. These APCs migrate to the draining lymph nodes, where the bacterium is digested and its Ags are processed and presented to the lymphocytes. The lymphocytes, naive B and T cells, all exhibit their own Ag receptor specificity. In response to the right Ag, T cells become activated and start secreting messengers as interleukin-2 (IL-2), which induces the expansion of the T cells. These activated T cells become T-helper cells (Th cells) in the case of CD4⁺ or cytotoxic T cells (CTLs) if they are CD8⁺ T cells. The Th cells will secrete cytokines inducing proliferation and activation of effector cells, like CTLs, natural killer cells and macrophages, which will execute the cellular immune response. At the same time the Th cells are also required for the humoral immune response. For proper activation, B cells not only need high-affinity binding of antigen to the B cell receptor (BCR), but also co-stimulation by the Th cells through CD40-CD40L interaction, initiating a germinal center (GC) reaction. Activated B cells can then either develop directly into antibody-secreting cells, or mature into GC-precursor B cells and move to the primary follicle to engage in a GC reaction ¹. After several rounds of proliferation and diversification of the variable region of the immunoglobulin (Ig) gene, those B cells that express newly generated modified antibodies are selected for improved Ag binding and survive. Finally, these B cells will differentiate into memory cells or antibody-producing plasma cells. These antibodies will circulate and constitute the humoral immune defense. As this process takes 4-5 days, several forms of memory have been established to reduce the response time in a recurrent infection, namely long-lived plasma cells residing in the bone marrow (BM) for many years, and memory B and T cells, which can be reactivated by encountering the same pathogen.

1

Lymphocyte development

All different classes of blood cells originate from the hematopoietic stem cells (HSCs) ², which reside in specialized niches in the BM. Hematopoietic cells can be divided in two major groups: cells originating from the common lymphoid progenitor (CLP) including B, T and natural killer cells, and cells originating from the common myeloid progenitor (CMP) with the neutrophils, megakaryocytes/platelets, monocyte/macrophages, and the erythrocytes or red blood cells. Here we will focus on the development of the lymphoid lineage, in particular the B and T cells, the malignant transformation and the importance of the microenvironment in these processes.

B cell development

In adults, B cell development takes place in the BM, where offspring of CLPs, differentiate into immature B cells (Figure 1). During the first stages of their differentiation, which are Ag-independent, the B cells depend on the pre-BCR for survival ^{3;4}. The BCR is formed by rearrangement of the variable (V), the diversity (D) and joining (J) regions of the Ig heavy chain gene (IgH) locus located on chromosome 14. Signaling via the pre-BCR will induce rearrangements of the V and J segments of the Ig light chains (the κ or λ locus) to produce a mature BCR of the IgM isotype. The immature B cells expressing a mature BCR migrate to secondary lymphoid organs like peripheral lymph nodes, spleen, or mucosal-associated lymphoid tissue (MALT), where they differentiate into naïve, mature B cells. The secondary lymphoid organs are designed to facilitate optimal Ag presentation. Upon challenge with Ag mature B cells can undergo Ag-specific B cell differentiation. In case of Ag recognition by the BCR, they will internalize and process the Ag. The B cells will present Ag-derived peptides on MHC class II molecules to Th cells at the border of the T cell and the B cell area. This interaction will provide the B cells with co-stimulatory signals that are indispensable for further differentiation. Some of the activated B cells will now develop into antibody-producing (Figure 1), while others migrate into the primary follicle, initiating the formation of a GC ^{4;5}. The GC, a specialized microenvironment in the B cell follicle of the secondary lymphoid organs, can be subdivided based on histological grounds into a dark and light zone ³. In the dark zone, the B cells, which have become centroblasts, undergo a rapid clonal expansion and somatic hypermutation (SHM) of their Ig-genes ⁶⁻⁹. During SHM, mutations are introduced in the Ig-genes by an enzyme called activation-induced cytidine deaminase (AID), which deaminates cytidines to uracils resulting in C to T and G to A transitions ¹⁰. The mutated B cells, now centrocytes, migrate into the light zone of the GC (Figure 1). Here the selection starts, based on the affinity of their BCRs for Ag presented by the follicular dendritic cells (FDCs) ^{3;11}. B cells expressing low affinity or auto-reactive mutant BCRs will die by apoptosis, while cells expressing high affinity BCRs will receive survival and proliferation signals from the FDCs and Th cells ^{9;12;13}. The surviving B cells will process the Ag and present Ag-specific peptides to Ag-specific T cells ¹⁴. These cells, which have been activated by dendritic cells, provide stimulatory signals to the B cells (e.g. T cell receptor (TCR)/CD3-MHC class II, CD40-CD40L, CD80/86-CD28, and several cytokines) ¹⁵⁻¹⁸, which result in class switch recombination (CSR) and differentiation into either memory B cells or plasma cells ^{5;19} (Figure 1).

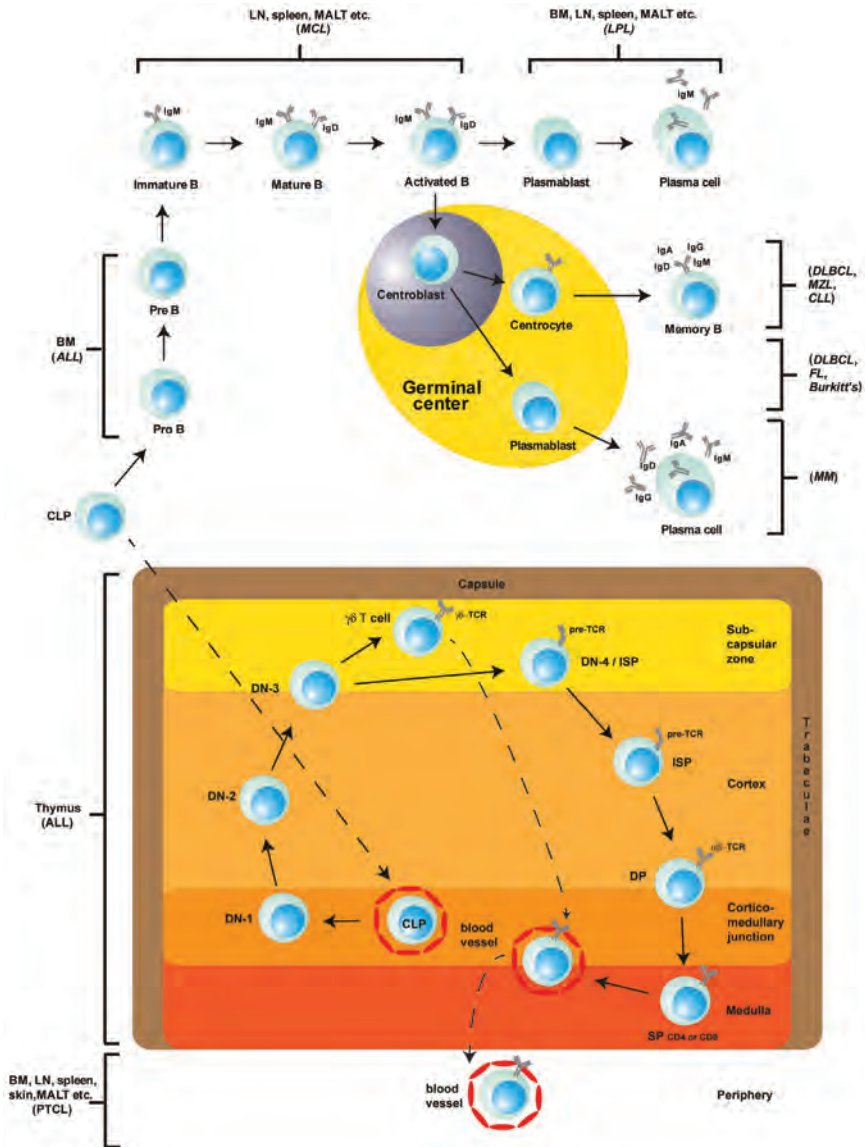


Figure 1. B and T cell development and the corresponding neoplasia.

Schematic representation of B and T cell development and differentiation. The malignant counterparts are indicated in parenthesis. See text for more detail. BM, bone marrow; LN, lymph node; MALT; mucosa associated lymphoid tissue; CLP, common lymphoid precursor; ALL, acute lymphoblastic leukemia; MCL, mantle cell lymphoma; LPL, lymphoplasmacytic lymphoma; DLBCL, diffuse large B cell lymphoma; MZL, marginal zone lymphoma; CLL, chronic lymphatic leukemia/lymphoma; FL, follicular lymphoma; MM, multiple myeloma; DN, double negative; ISP, immature single positive; DP, double positive; SP, single positive; TCR, T cell receptor; PTCL, peripheral T cell lymphoma.

T cell development

Initially, the thymus is seeded with CLPs, which is a chemotactic process controlled by chemokines and adhesion molecules²⁰⁻²³. This starts as early as the eighth week of gestation in humans²⁴. Significant roles have been assigned to two CC-chemokines, *i.e.* CC-chemokine ligand 21 (CCL21) and CCL25, and their corresponding receptors, CCR7 and CCR9 respectively^{25;26}. Mice deficient for CCL21, CCR7, or CCR9 all showed reduced numbers of thymocytes during embryonic development^{27;28}. Next to chemokines, adhesion molecules, like CD44 and P-selectin glycoprotein ligand 1 (PSGL1), have been implicated in thymic settling, since interference with one of these molecules was shown to block the colonization of the thymus^{29;30}. Following entry into the thymus, the progenitors develop into T cells through distinct phenotypic stages, which take place at defined anatomical places within the thymus (Figure 1). These locations, or stromal compartments, contain specialized epithelial cells, providing growth and differentiation signals to the developing T cells^{26;31}. The CLPs enter the thymus at the cortico-medullary junction³², which develop into double negative T cells (DN), in man subsequently CD34⁺CD1a⁻ and CD34⁺CD1a⁺, and finally they lose expression of CD34^{33;34}. During these early DN stages, the T cells migrate to the subcapsular region, where the first T cell rearrangements take place. Rearrangements of the different TCR genes occur in a fixed order, the *TCRD* locus rearranges first, followed by the *TCRG* genes, which if successful could result in a functional $\gamma\delta$ -TCR and the development of a $\gamma\delta$ T cell. Alternatively, a cell may enter the $\alpha\beta$ -lineage by rearranging the β -chain, which locus starts rearranging shortly after *TCRG*. During the ISP stage, the functionality of the TCR β chain is tested by expressing it on the cell surface together with the invariant pre-TCR α chain^{25;26}. The successful expression of the pre-TCR complex on the cell surface, together with the Delta-Notch interaction, triggers the differentiation into DP cells that express $\alpha\beta$ -TCRs. As T cells progress through the immature single positive (ISP; CD4⁺CD3⁺) and double positive (DP; CD4⁺CD8⁺) stages, they travel in opposite direction through the cortex, toward the medulla (Figure 1). Here, close to the cortico-medullary junction these DP cells undergo a series of selection processes (positive and negative selection). Upon TCR recognition of peptide-MHC ligands, DP cells are selected based on the avidity of the interaction^{26;35;36}. While low avidity interactions induce signals for survival and differentiation, high avidity interactions leads to apoptosis (positive selection). T cells that survive positive selection migrate towards the corticomedullary junction, where they are again presented with self-antigen in complex with MHC molecules on APCs. T cells that interact too strongly with the Ag receive an apoptotic signal that leads to cell death (negative selection). Only 3-5% of the developing T cells survive these checkpoints^{37;38}. The selected DP cells are induced to differentiate into single positive cells (SP; CD4⁺CD8⁻ or CD4⁺CD8⁺) and relocate from the cortex to the medulla³⁹ where they undergo further maturation⁴⁰⁻⁴². In addition to the stringent repertoire selection, the T cells need to be in close contact with the thymic epithelial cells. This contact is highly important, since these cells express Notch ligands and also produce essential factors, like IL-7 and Wnts, which promote T cell development and survival^{26;31;43}. Finally the resulting mature, but naive, T cells emigrate from the thymus, a process controlled by G protein-coupled receptors⁴⁴, *e.g.* S1P₁⁴⁵, CCR7⁴⁶ and CXCR4⁴⁷. The role of Wnt signaling in (T-) lymphocyte development and malignant transformation will be discussed in more detail later in this chapter.

Lymphoid malignancies

The first cases of lymphoid malignancy were published by the English physician Thomas Hodgkin in 1832. The disease was subsequently named Hodgkin's disease⁴⁸. The multinucleated cells (Reed-Sternberg cells), characteristic for this disease, were first described by Dorothy Reed and Carl Sternberg around 1900. Since these cells are known to be of lymphoid origin, it was renamed to Hodgkin lymphoma⁴⁹. The WHO classification still makes the distinction between Hodgkin and non-Hodgkin lymphoma (NHL). However, nowadays the NHLs can be divided based on clinical presentation, morphology, immunophenotype, and genetic and molecular features into three groups of neoplasms, *i.e.* B cell, T cell, and NK cell neoplasms, with numerous distinctive subtypes. In the western world, about 20 new cases of lymphoma are diagnosed per 100,000 people per year, which are predominantly of B cell origin⁴⁹⁻⁵¹.

Table 1. WHO 2008 classification of T cell neoplasms^{1,2}.

Precursor T cell neoplasms

Precursor T acute lymphoblastic leukemia/lymphoma (T-LBL/ALL)

Mature T cell neoplasms

Leukemic or disseminated

T cell prolymphocytic leukemia

T cell large granular lymphocytic leukemia

Adult T cell lymphoma/leukemia (HTLV1-positive)

Systemic EBV-positive T cell lymphoproliferative disorders of childhood

Extranodal

Extranodal NK/T cell lymphoma, nasal type^a

Enteropathy-associated T cell lymphoma

Hepatosplenic T cell lymphoma

Extranodal-cutaneous

Mycosis fungoides

Sezary syndrome

Primary cutaneous CD30+ lymphoproliferative disorders

Primary cutaneous anaplastic large cell lymphoma

Lymphomatoid papulosis

Subcutaneous panniculitis-like T cell lymphoma

*Primary cutaneous gamma-delta T cell lymphoma**

*Primary cutaneous aggressive epidermotropic CD8+ cytotoxic T cell lymphoma**

*Primary cutaneous small/medium CD4+ T cell lymphoma**

Nodal

Angioimmunoblastic T cell lymphoma (AITL)

Anaplastic large cell lymphoma (ALCL), ALK-positive

*Anaplastic large cell lymphoma (ALCL), ALK-negative**

Peripheral T cell lymphoma, not otherwise specified (PTCL, NOS)

^a Most cases are derived from NK cells and only a minority from T cells. *These represent provisional entities or provisional subtypes of other neoplasms. Diseases shown in italics are newly included in the 2008 WHO classification.

- de Leval L, Bisig B, Thielen C, Boniver J, Gaulard P. Molecular classification of T-cell lymphomas. *Crit Rev Oncol Hematol*. 2009;72:125-143.
- Jaffe ES. The 2008 WHO classification of lymphomas: implications for clinical practice and translational research. *Hematology Am Soc Hematol Educ Program*. 2009:523-531.

T-lineage malignancies

1

T cell malignancies comprise two major entities: precursor T cell neoplasms, *i.e.* precursor T lymphoblastic lymphoma/acute lymphoblastic leukemia (T-LBL/ALL), derived from the thymocytes, and peripheral T cell lymphomas (PTCL), developing from mature post-thymic T cells^{52;53}. T-LBL/ALL is an aggressive disease that mainly develops in children, especially adolescent males. This disease frequently presents with extensive BM and blood involvement, and to a lesser extent as a mediastinal mass^{49;53}. An abnormal karyotype is detected in approximately 50% of the cases, which comprise translocations, deletions and duplications. Most of the translocations, juxtapose the regulatory region of one of the *TCR* loci and transcription factor genes, such as *TAL1*, *LYL1*, *LCK*, *TAN1*, *TLX1* and *TLX3*^{31;54}. Many of these oncogenic transcription factors are downregulated after the first DN stages of development, indicating this disease is driven by signal transduction pathways that control T cell development in the thymus^{53;54}. Other translocations cause gene fusion, which results in chimeric proteins. A frequent genetic abnormality found in T-LBL/ALL, involving 50% of the cases, are activating mutations in the key regulator of T cell fate, *NOTCH1*⁵⁵. These mutations involve the heterodimerization or the PEST-domain, resulting in ligand-independent signaling and an increased half-life of the intracellular part of the protein, respectively. Both lead to constitutive activation of the Notch1 signaling pathway. In addition, activating mutations in *JAK1*, involved in cytokine signal transduction, occur in approximately 20% of adult T-LBL/ALL⁵⁶. Although T-ALL and T-LBL are generally considered as two manifestations of the same disease, recent gene expression profiling (GEP) studies showed that T-ALL and T-LBL samples segregated into distinct clusters, suggesting underlying difference in their biology^{57;58}. PTCL encompass many entities based on the clinical presentation of the disease (Table 1), however PTCL not otherwise specified (PTCL NOS), angioimmunoblastic T cell lymphoma (AITL), and anaplastic large cell lymphoma (ALCL) are the most prevalent entities in Europe, together accounting for 79% of PTCLs^{53;59}. PTCL NOS consist of a large heterogeneous group of PTCL, which accounts for up to one-third of the PTCL. This group is sometimes referred to as the “waste-basket” since most cases lack specific features that would allow characterization within another entity. The clinical course of this tumor is highly aggressive, with a 5-year survival of 20-30%^{53;59}. Complex cytogenetic aberrations are common, with loss of 5q and 6p seen in 25-30% of cases. Furthermore, recurrent chromosomal gains have been observed in 7q and 8q, which involve *CDK6* and *MYC*. Recently, it has been shown that compared to normal T cells, PTCL NOS appears to be closely related to activated T cells, characterized by deregulation of genes related to proliferation, apoptosis, cell adhesion and matrix remodeling⁶⁰. AITL has distinctive pathological features, a diffuse polymorphous infiltrate, prominent arborizing vessels, proliferation of FDCs, and almost always contain Epstein-Barr virus (EBV)-positive B cells^{52;61}. Genetic abnormalities, like trisomy 3 and 5, and an additional X chromosome are frequently observed. Chromosomal translocations that involve the *TCR* loci appear to be extremely rare⁵³. GEP analysis of AITL cases has revealed that the neoplastic cells were enriched for genes normally expressed by follicular Th cells⁶². A hallmark of the ALCL are the large CD30-positive cells. Chromosomal translocations that involve the anaplastic lymphoma kinase (ALK) gene on chromosome 2p23 are characteristic for the disease, dividing this lymphoma subtype into ALK-positive and ALK-negative ALCLs^{63;64}. Multiple translocation partners have been identified, however the most common translocation is the t(2;5)(p23;q35), resulting in the fusion gene NPM-ALK. All translocations juxtapose the catalytic domain of ALK to a partner protein, resulting in a chimeric protein with constitutive activation of the tyrosine kinase ALK⁵³.

B-lineage malignancies

The vast majority of malignant lymphomas are of B cell origin (Figure 1), which presumably is related to the fact that B cells during development and differentiation undergo a series of DNA-modifying processes, *i.e.* Ig V(D)J recombination, SHM and CSR, that can all cause non-physiological genetic alterations^{1,51;65}. During the Ig V(D)J recombination double-stranded DNA breaks are introduced by the recombination activating genes (RAG1 and RAG2), after which the intervening DNA is excised. Next, the selected Ig gene segments are joined by DNA repair processes (non-homologous end-joining). However, there is now ample evidence that such a process can contribute to chromosomal translocations in lymphoma^{65;66}. This is best exemplified by the canonical translocations found in follicular lymphoma (FL), t(14;18), and the t(11;14) in mantle zone B cell lymphoma, which juxtapose the *BCL2* and *CCND1*, to the IgH enhancer locus, respectively, resulting in the enhanced expression of the anti-apoptotic BCL-2 and the cell cycle progression regulator cyclin-D1^{67;68}. Although the GC reaction is beneficial during the immune response against invading pathogens, the fact that most mature B cell lymphomas are derived from GC or post-GC B cells, reveals the risk of combining DNA-modifications, like SHM and CSR, with high proliferation rates that occur in the GC^{1;65;69}. Since both processes, which essentially depend on the mutator-enzyme AID, are associated with the occurrence of single and double-stranded DNA breaks, it is believed that they predispose to chromosomal translocations⁷⁰. Chromosomal translocations that involve the *IgH* switch region, indicative of invalid CSR, have indeed been identified in FL, diffuse large B cell lymphoma (DLBCL), Burkitt's lymphoma, and multiple myeloma (MM), and include translocation partners as *BCL-6*, *MYC*, *CCND1*, *CCND3*, *FGFR3-MMSET*, and *c-MAF*^{66;71-73}. In addition, AID can introduce mutations in nonimmunoglobulin genes, *e.g.* the oncogenes *BCL6*, *MYC*, *PIM1*, *PAX-5*, *RhoH/TFF*⁷⁴, in GC B cells, which might accumulate because of a deficiency in DNA mismatch repair or clonogenic selection^{65;75}. Today, the WHO classification recognizes around 30 different B-NHL entities (Table 2)^{52;76}, which are classified based on morphology, configuration of the BCR, and expression of membrane proteins and large scale GEP. Most prevalent B cell malignancies include DLBCL, FL, and MM⁵¹.

Diffuse large B cell lymphoma

DLBCL is the most common B-NHL, accounting for more than 30% of newly diagnosed lymphomas in the western world^{65;77;78}. Although DLBCL can occur at any age, including childhood, median presentation is in the seventh decade^{49;78}. DLBCL frequently present as nodal disease, however in up to 40% of patients the site of presentation is extranodal. Commonly affected organs include, gastrointestinal tract, central nervous system, testis, spleen, liver and BM. In addition to *de novo* disease, DLBCL can arise as a progression/transformation of a underlying low-grade lymphoma, *i.e.* chronic lymphocytic leukemia (CLL; Richter's syndrome), FL, or marginal zone lymphoma^{49;77;78}. A broad spectrum of genetic aberrations have been reported in DLBCL, which include translocations, amplifications, deletions and point mutations, involving genes controlling proliferation, apoptosis and differentiation^{77;79}. Common genetic abnormalities involve 3q27, *BCL-6* translocation (30%), the t(14;18) translocation, involving *BCL-2* (20%), and *MYC* rearrangements^{77;78}.

GEP has revealed that DLBCLs are actually a mixture of distinct cancers. With this technique, DLBCL can be divided in three distinct groups, associated with different prognosis^{80;81}. The first group, the germinal center B cell-like subtype (GC-DLBCL), has a GEP signature corresponding with normal GC. These GC-DLBCLs have highly mutated Ig genes and the

Table 2. WHO 2008 classification of B cell neoplasms ¹.**Precursor B cell neoplasms**

Precursor B acute lymphoblastic leukemia/lymphoma (B-LBL/ALL)

Mature B cell neoplasms

Chronic lymphocytic leukemia/small lymphocytic lymphoma

B cell prolymphocytic leukemia

Splenic marginal zone lymphoma

Hairy cell leukemia

*Splenic lymphoma/leukemia, unclassifiable**Splenic diffuse red pulp small B cell lymphoma ***Hairy cell leukemia-variant **

Lymphoplasmacytic lymphoma

Waldenström macroglobulinemia

Heavy chain diseases

Alpha heavy chain disease

Gamma heavy chain disease

Mu heavy chain disease

Plasma cell myeloma

Solitary plasmacytoma of bone

Extrasosseous plasmacytoma

Extranodal marginal zone B cell lymphoma of mucosa-associated lymphoid tissue (MALT lymphoma)

Nodal marginal zone B cell lymphoma (MZL)

Pediatric type nodal MZL

Follicular lymphoma

Pediatric type follicular lymphoma

Primary cutaneous follicle center lymphoma

Mantle cell lymphoma

Diffuse large B cell lymphoma (DLBCL), not otherwise specified

T cell/histiocyte rich large B cell lymphoma

*DLBCL associated with chronic inflammation**Epstein-Barr virus (EBV)+ DLBCL of the elderly*

Lymphomatoid granulomatosis

Primary mediastinal (thymic) large B cell lymphoma

Intravascular large B cell lymphoma

Primary cutaneous DLBCL, leg type

ALK+ large B cell lymphoma

Plasmablastic lymphoma

Primary effusion lymphoma

Large B cell lymphoma arising in HHV8-associated multicentric Castleman disease

Burkitt lymphoma

B cell lymphoma, unclassifiable, with features intermediate between diffuse large B cell lymphoma and Burkitt lymphoma

B cell lymphoma, unclassifiable, with features intermediate between diffuse large B cell lymphoma and classical Hodgkin lymphoma

*These represent provisional entities or provisional subtypes of other neoplasms. Diseases shown in italics are newly included in the 2008 WHO classification

1. Jaffe ES. The 2008 WHO classification of lymphomas: implications for clinical practice and translational research. Hematology.Am.Soc.Hematol.Educ.Program. 2009;523-531.

malignant clone continues to undergo SHM⁸². Genetic lesions that specifically occur in GCB lymphomas are the t(14;18) translocation, *PTEN* deletion, amplification of the microRNA cluster miR17-92, and mutations in *p53*⁶⁵. The second largest group, have the plasma cell profile, including the transcription factor XBP-1, which corresponds to an expression profile similar to activated B cells. These activated B cell-like DLBCLs (ABC-DLBCLs), have heavily mutated IgH genes, but have not undergone CSR and express IgM^{65,83,84}. Genetic aberrations characteristic for ABC-DLBCLs, include amplification of *BCL2* and deletion of the *INK4A-ARF* locus⁶⁵. The ABC-DLBCLs display constitutive activation of the NF- κ B pathway, which has shown to be essential for survival⁸⁵. In addition, by activation of downstream targets, which collectively block apoptosis, constitutive activation of this pathway may contribute to the poor response to chemotherapy^{65,86}. Furthermore, a recent screen revealed that the activation of NF- κ B in ABC-DLBCLs is dependent on three proteins: *CARD11*, *BCL10*, and *MALT1*. In normal B cells this complex is formed after BCR activation, and activates NF- κ B signaling via I κ B kinase and I κ B α ^{65,87}. In ABC-DLBCL, genetic aberrations in *CARD11*⁸⁸ and *CD79A*, or *CD79B* (signaling subunits of the BCR)⁸⁹ have been found to underlie the constitutive activation of NF- κ B. These studies imply that chronic BCR signaling is a critical step in the pathogenesis of ABC-DLBCL⁶⁵. The third subtype of DLBCL lack the expression of genes associated with GCB lymphomas or ABC-DLBCL⁸¹. Importantly, compared to patients with ABC-DLBCL, patients with GC-DLBCL have a more favorable prognosis, with a 3-year progression-free survival of 40% and 74%, respectively⁶⁵. The prognosis of the third is intermediate⁸¹. Although much progress has been made in unraveling the pathogenesis of DLBCL with GEP, the contribution of the microenvironment has remained largely unexplored.

Multiple Myeloma

Multiple myeloma (MM) is the second most common B cell neoplasm characterized by a clonal expansion of malignant plasma cells in the BM. It accounts for 1% of all cancer-related deaths⁹⁰⁻⁹³, with an incidence of 5.6 per 100,000 inhabitants in the Netherlands⁹⁴. Recent studies have shown that all MMs are preceded by a pre-malignant expansion of plasma cells called monoclonal gammopathy of undetermined significance (MGUS)^{95,96}. MGUS has a prevalence of 3% and 5% in persons older than 50 and 70 years respectively⁹⁷, with a risk of progression to MM of 1% per year⁹⁸. So far no discriminative genetic or phenotypic markers that can distinguish MGUS from MM tumor cells have been identified, which makes it impossible to predict if and when an MGUS will progress to MM⁹⁹. Despite intense efforts and an enormous increase in our understanding of the pathogenesis of MM, the median survival after conventional treatments is 3-4 years, whereas high-dose treatment followed by an autologous stem cell transplantation can extend the median survival to 5-7 years¹⁰⁰. The evolution of MM is nowadays viewed as a multistep process in which MGUS progresses through smoldering (asymptomatic) MM, symptomatic (intramedullary) MM, and extramedullary MM/plasma cell leukemia^{91,93,99} (Figure 2). These stages can be distinguished with the use of the International Myeloma Working Group (IMWG) criteria. Based on these criteria, a patient with smoldering MM has serum monoclonal (M)-protein levels of ≥ 30 g/L and/or $\geq 10\%$ plasma cells in the BM in the absence of end-organ damage (CRAB – hypercalcaemia, renal insufficiency, anaemia, or bone lesions), while a patient with symptomatic MM has M-protein in the serum and/or urine, $\geq 10\%$ of BM plasma cells, and end-organ damage that can be attributed to the underlying plasma cell proliferative disorder¹⁰¹.

Although MM is characterized by markedly heterogeneous chromosomal aberrations, it can be subdivided in two cytogenetic groups: A hyperdiploid subgroup (48-75 chromosomes) with infrequent (<10%) IgH-translocations or other structural chromosomal abnormalities, and a non-hyperdiploid subgroup (<48 or >75 chromosomes) with a high prevalence of translocations of the IgH locus^{90,91,93,103} (Figure 2). The hyperdiploid subgroup is defined by the presence of multiple trisomies that happen to be odd numbered, including 3, 5, 7, 9, 11, 15, 19, and 21. The translocations in the non-hyperdiploid subgroup juxtapose potent Ig gene enhancers next to an array of oncogene-harboring partner loci: Translocations involving 11q13 (*CCND1*), 4p16 (*FGFR3* and *MMSET*), 16q23 (*c-MAF*), 6p21 (*CCND3*), and 20q11 (*MAFB*), account for approximately 40% of cases with Ig translocations⁹¹. In addition, loss of chromosome 13 is also considered to be an early event in the pathogenesis of MM, involving approximately half of the MGUS cases, and overlapping with both groups. Although no known transcriptional, cytogenetic, or mutational event can discriminate MGUS from MM, several secondary translocations and gene mutations have been identified and implicated in disease progression, *e.g.* translocations involving *MYC*, activating mutations in *KRAS*, *NRAS*,

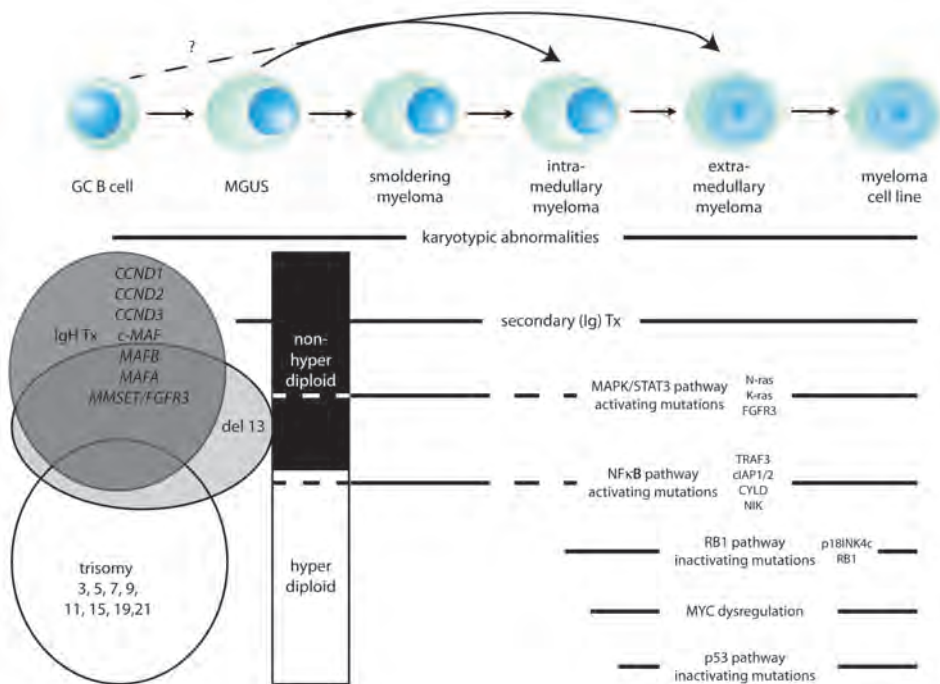


Figure 2. Disease stages and timing of oncogenic events.

Genetic aberrations occurring in multiple myeloma (MM). Many oncogenic events are already present in monoclonal gammopathy of undetermined significance (MGUS). Based on cytogenetics MM can be divided into two groups with minimal overlap: non-hyperdiploid with high prevalence of translocations of the IgH locus, and hyperdiploid with infrequent translocations or other structural chromosomal abnormalities. However, both groups show substantial overlap with the del 13-group. The translocation partner in the IgH translocation (Tx) group are listed according to increasing frequency of coexistence with del 13. Secondary translocations may occur at every stage of disease progression. Although *MYC* can also be deregulated by IgH Tx, this usually occurs as a secondary translocation. At later timepoints, several signaling pathways can be (in)activated by late oncogenic events, driving disease progression. Adapted and modified from Chng *et al.* (2007) Best Pract Res Clin Haematol¹⁰².

and *FGFR3*, inactivating mutations or deletions of *TRAF3*, *CYLD*, *TP53*, *RB1*, and *PTEN*^{91;93;103} (Figure 2). The genetic heterogeneity is further reflected by the results of gene expression profiling studies performed on MM patient samples, which identified at least seven molecular subtypes, including PR (cell cycle progression and proliferation), HY (hyperdiploid), LB (low incidence of bone lesions), MS (*MMSET*-translocation), MF (*MAF*-translocations), CD-1 (*CCND1* or *CCND3*-translocations), and CD-2 (*CCND1* or *CCND3*-translocations, with CD20 expression)^{104;105}. These subgroups allow risk-stratification of newly diagnosed patients, a high-risk being associated with the MS, PR, and MF, corresponding to a 3-year estimate of event-free survival of 39%, 44%, and 50%, respectively¹⁰⁴. Interestingly, genomic profiling also revealed that dysregulation of cyclin D might be a universal event in the pathogenesis of MM. Plasma cells of MM patients exhibit increased and/or dysregulated expression of either *CCND1*, *CCND2*, or *CCND3*⁹⁹. Another pathway constitutively activated in the majority of MM samples is the NF- κ B pathway, which is often associated with genetic or epigenetic alteration of components of the pathway for example *TRAF3*, *CYLD*, *BIRC2/BIRC3*, *CD40*, *NFKB1*, or *NFKB2*^{106;107}. Moreover, this pathway was found to induce *IRF4* expression, a gene found to be essential for MM cell survival¹⁰⁸. In addition to regulation by NF- κ B, *IRF4* is translocated in a few MM patients, but more importantly it has been shown to form a positive feedback loop with *MYC*, a oncogene frequently translocated in MM¹⁰⁷.

Role of the microenvironment in the pathogenesis of multiple myeloma

In 1889, Stephen Paget proposed the “seed and soil” hypothesis, *i.e.* postulated that the initiation of tumor metastasis is being influenced by the cross-interaction between cancer cells (“seed”) and specific organ microenvironments (“soil”)^{109;110}. MM can be viewed as a prototypical disease model of this hypothesis, as reflected by the inability of MM cells to grow outside of the “soil”, the BM, during the initial stages of the disease. This together with the absence of real definitive genetic differences between MGUS and MM, underscores the essential role of the BM microenvironment in development, maintenance, and progression of MM^{91;93;111}. Thus, the behavior of MM cells is not solely determined by their genetic background, but also by the BM microenvironment^{91;110-113}.

During the last decades, it has become apparent that the interaction between MM cells and the local BM microenvironment is bidirectional: MM cells radically perturb the normal BM homeostasis, resulting in anemia and osteolytic lesions. Conversely, the BM microenvironment, either directly via adhesion molecules or indirectly via the production of cytokines, chemokines, and growth factors, induces proliferation and survival of the MM cells^{90;91;110-113}. MM cells can express a wide variety of adhesion molecules on their surface, including integrins, selectins, CD44, MUC-1, and N-CAM. These molecules mediate homing of the MM cells to the BM, and subsequently facilitate binding to extracellular matrix (ECM) proteins and BM stromal cells (BMSCs)^{111;112;114} (Figure 3). Besides direct interactions, the BM provides the MM cells with a wide array of soluble factors, that are mainly secreted by the BMSCs and MM cells themselves. These soluble factors include interleukins (*e.g.* IL-1 β ¹¹⁵, IL-3¹¹⁶, IL-6¹¹⁷, and IL-7¹¹⁸), growth factors (*e.g.* HGF^{119;120}, IGF-1¹²¹, VEGF¹²², Wnts¹²³, and TGF- β ¹²⁴), chemokines (SDF-1 α ¹²⁵, MCP-1¹²⁶, and MIP-1 α ¹²⁷), as well as angiopoietin-1¹²⁸, and matrix metalloproteinases (MMP-2 and MMP-9^{129;130}). These interactions not only localizes the tumor cells in the BM microenvironment but also have important functional consequences (Figure 3), including increased proliferation, survival, and drug-resistance of

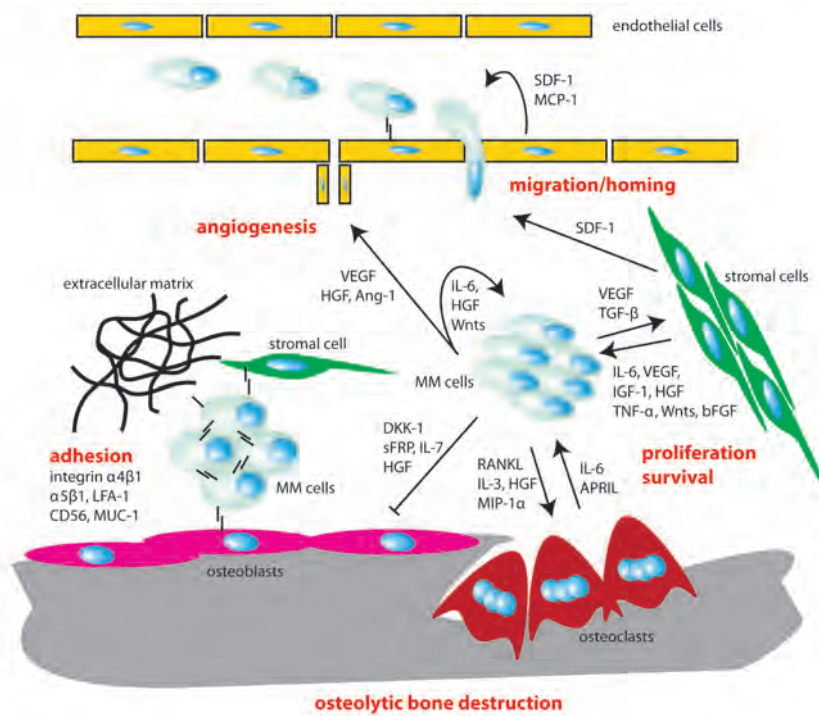


Figure 3. The interaction of multiple myeloma cells with bone marrow microenvironment.

A schematic overview of the interactions in the multiple myeloma (MM) bone marrow (BM) niche. MM cells enter the BM, directed by the chemokines MCP-1 and SDF-1. Within the BM, MM cells interact with the microenvironment either directly via adhesion molecules or indirectly via auto- and paracrine produced proliferation and survival-inducing factors. Besides, MM cells produce factors that induce angiogenesis, while others induce osteolytic bone disease by inhibition of osteoblast differentiation and stimulation of osteoclast activity. Arrows indicate activation and blunted arrows indicate inhibition. For more details see text.

the MM cells, induction of angiogenesis, as well as increased bone resorbing activity^{90;91;110-112}. Osteolytic bone disease is one of the most important clinical sequelae of MM, and presents in up to 90% of the patients¹³¹⁻¹³³. Under physiological conditions structural remodelling of the bone is a continuous process in which osteoclast-mediated resorption of “old” bone tissue is subsequently followed by new bone formation by the osteoblasts^{91;103}. This process is tightly regulated by co-ordinate expression of receptor activator of NF- κ B ligand (RANKL) and osteoprotegerin (OPG). RANKL is produced by osteoblasts and BMSCs and binds to its receptor RANK on osteoclastic cells, activating the development of osteoclasts. OPG functions as a decoy-receptor for RANKL, mainly produced by BMSCs¹⁰³. At an early stage of MM, there is an elevation of both osteoclasts and osteoblast numbers. However, during progression osteoblast activity is suppressed, shifting the balance towards an increase in bone resorption^{132;134}. In addition, osteoclast activity is potentiated by: (1) upregulation of RANKL expression in BMSCs¹³⁵; (2) decreased levels of OPG^{136;137}; (3) upregulation of pro-osteoclastogenic cytokines (e.g. IL-1, IL-3, IL-6, IL-11, HGF, MIP-1 α)^{91;131;132}; (4) increased levels, in a subset of patients, of Dickkopf-1 (DKK1), which inhibits differentiation of osteoblast precursor cells, while enhancing osteoclastogenesis by enhancing RANK/RANKL interactions^{132;138;139}.

Taken together, the findings discussed above show the importance of the microenvironment, providing growth and survival signals and mediating drug resistance, for the progression of MM. Targeting both MM cells and the microenvironmental interactions has already provided some promising results^{90;111}. The addition of bortezomib, thalidomide, and lenalidomide to the conventional cytotoxic chemotherapy based treatment of MM has changed treatment strategies during the last 5 years. Bortezomib, which inhibits the function of the 26S proteasome, induces apoptosis in drug-resistant MM cells, and inhibits both the production and the secretion of cytokines and the binding of MM cells in the BM microenvironment. Most of the therapeutic effects of thalidomide and its derivative lenalidomide have been assigned to their antiangiogenic potential and their ability to increase NK cell numbers and cytotoxic activity against MM^{91;111}. Although combining these drugs with the conventional drugs, such as dexamethasone and melphalan, increases the event-free and overall survival^{93;140}, MM is still not curable and additional strategies, targeting both tumor cells and the microenvironment, are needed. This thesis will focus on the role of some of the microenvironmental interactions, *i.e.* the hepatocyte growth factor (HGF), heparan sulphate proteoglycans (HSPGs), Wnts, and N-cadherin, in the pathogenesis of B and T cell malignancies.

Microenvironmental signals in the pathogenesis of multiple myeloma and malignant lymphoma

The HGF/Met signaling cascade

HGF, a pleiotropic cytokine, was originally identified as a growth factor for hepatocytes¹⁴¹. At the same time, a fibroblast-secreted molecule was identified that caused dissociation or “scattering” of epithelial cells and increases their motility, designated scatter factor (SF)¹⁴². Subsequent studies showed HGF and SF to be identical¹⁴³⁻¹⁴⁷. HGF is a heterodimeric protein consisting of an α and β -chain held by a disulfide bond (Figure 4A). The α -chain contains four kringle domains, structures that play a role in protein-protein interaction. The β -chain has homology to the catalytic domain of serine proteases, but lacks proteolytic activity, due to the lack of two crucial amino acids from the active site¹⁴⁸. Northern blotting revealed three HGF mRNA transcripts of 6, 3 and 1.5 kb. The 6 and 3 kb messages originate from differential polyadenylation¹⁴⁷, whereas the 1.5 kb message represents a splice variant encoding the N-terminal domain of HGF in combination with the first two kringle domains^{149;150}. This variant, NK2, functions as a HGF antagonist¹⁴⁹. Subsequently, a kringle domain variant, namely NK1, has been described, which acts as a partial HGF agonist^{151;152}. HGF is secreted as an inactive proform (pro-HGF), which can bind the HGF receptor MET with low affinity without initiating downstream activation^{153;154}. To activate MET and elicit biological responses, pro-HGF has to be cleaved at an Arg-Val cleavage site located in exon 13, converting it into HGF.

Proteolytic activation of HGF in the extracellular milieu is a critical limiting step in the activation of the HGF/MET signaling cascade¹⁵⁵. Several proteases, with a potential role in the activation of HGF, have been proposed, including coagulation factors XI and XII, kallikrein, urokinase-type and tissue-type plasminogen activators, matriptase, hepsin, and HGF activator (HGFA). Of which HGFA, matriptase, and hepsin show the highest processing activity, at least *in vitro*¹⁵⁶. HGFA belongs to the kringle serine protease superfamily, and shares great homology to coagulation factor XII¹⁵⁷. HGFA is primarily synthesized and

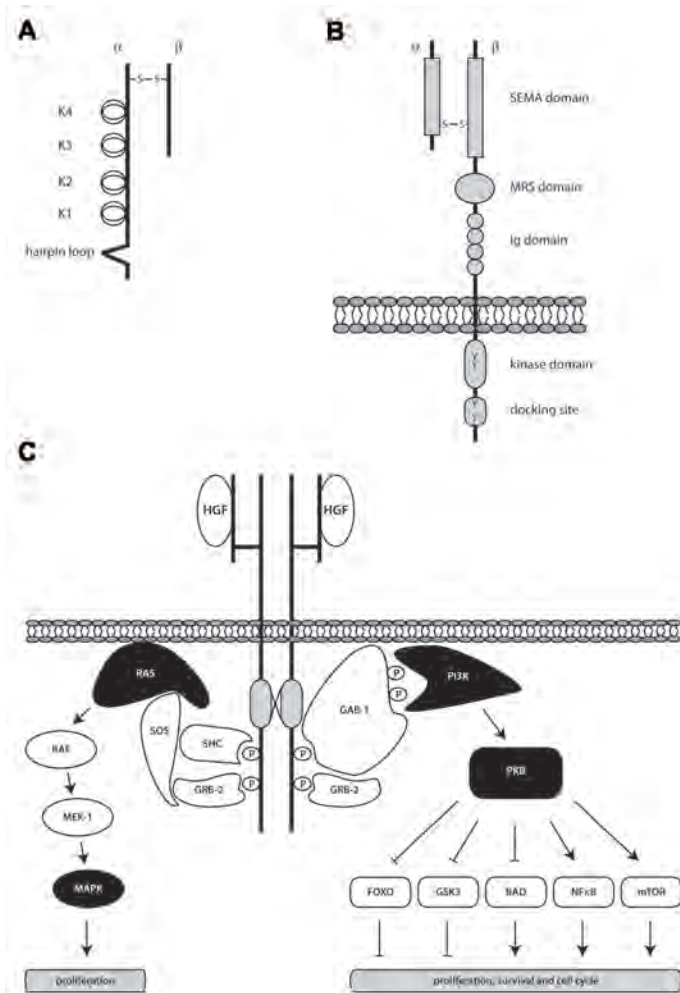


Figure 4. The HGF/MET signaling pathway.

(A) HGF, an α - β disulphide-linked heterodimer, contains a hairpin loop, followed by four kringle domains (K1–K4) and a serine protease domain devoid of proteolytic activity. **(B)** MET, an α - β disulphide-linked heterodimer, is a single-pass transmembrane receptor. The extracellular region contains a Sema domain, a Met-Related Sequence (MRS) domain and four Immunoglobulin-like structures (Ig domains). The intracellular portion of Met is composed of a catalytic site and a C-terminal regulatory portion. **(C)** Schematic representation of HGF-induced signaling. For reasons of clarity, only the RAS/MAPK, the PI3K/PKB pathway, and several additional important signal transducers are shown. Arrows indicate activation, blunted arrows point out inhibition. See text for further details.

secreted by hepatocytes as a zymogen (pro-HGFA). As significant activation of pro-HGFA is observed in injured tissues, it is reasonable to postulate that pro-HGFA is also activated in response to tissue injury. This makes thrombin a presumed activator of pro-HGFA, since activation of the coagulation cascade occurs in injured tissue^{156;158;159}. This activated form of HGFA can be further processed by plasma kallikrein, without loss of the activity of HGFA¹⁵⁸. Recently, another activating mechanism has been proposed for HGFA, *i.e.* kallikrein 1-related peptidase (KLK) proteins¹⁶⁰. These proteins form a family of serine proteases, of

which KLK4 and KLK5 activate pro-HGFA efficiently. The activity of KLK5 is comparable with that of thrombin, and requires a negatively charged substance as well. While KLK4 does not require a negatively charged substance for the activation, its specific activity is one-fifth that of KLK5¹⁶⁰. This machinery may be important for the generation of active HGF in the tumor microenvironment, since KLK4 and KLK5 are frequently upregulated in tumor cells^{156;160}. Once activated, HGFA activity is regulated by two serine-protease inhibitors, HGFA inhibitor type 1 (HAI-1) and HAI-2, in the pericellular microenvironment, and by protein C inhibitor (PCI) in the plasma and serum^{156;161}.

Mesenchymal-epithelial transition factor (MET, also known as c-Met), is a tyrosine kinase receptor for HGF. It was originally identified as the product of a chromosomal translocation, *TPR-MET*, fusing the intracellular domain of MET to that of TPR oncogene^{162;163}. This fusion protein is constitutively phosphorylated and bears kinase activity, with a strong transforming capacity^{162;164}. The MET-receptor, although synthesized as a single-chain, is a disulfide-linked heterodimer consisting of an α and β -chain (Figure 4B). The extracellular region of the β -chain contains a SEMA-domain to which semaphorin-type proteins can bind, a cysteine-rich Met-related sequence (MRS, or PSI domain also found in the plexins, semaphorins, and integrins), and four immunoglobulin-like structures^{165;166}. The intracellular part contains the tyrosine kinase domain, as well as a multisubstrate docking site, comprising tyrosine residues Y1349 and Y1356, capable of recruiting several downstream adaptors containing Src homology-2 (SH2) domains¹⁶⁷.

MET is expressed on a wide variety of epithelial cells, whereas its ligand HGF is expressed by mesenchymal cells. HGF and MET play an important role in the epithelial-mesenchymal interactions underlying differentiation of a wide variety of lumen-forming organs, such as lungs, kidney and mammary glands, leading to the formation of polarized epithelial cell layers and, depending on the type of tissue, tubulogenesis and branching morphogenesis^{168;169}. This important role in mammalian development is further strengthened by the embryonic lethality of both *HGF* and *MET* null mice, between E12.5 and E15.5¹⁷⁰⁻¹⁷². The HGF/MET pathway has also been implicated in hematopoiesis. Both HGF and MET are expressed in the human and rodent fetal liver, primordial sites of hematopoiesis¹⁷³. In the adult BM, MET is expressed by a subset of hematopoietic precursor cells, whereas HGF is expressed by the BMSCs, suggesting a paracrine interaction¹⁷⁴⁻¹⁷⁶. In B cells MET is expressed by centroblasts, and plasma cells, while HGF is produced by FDCs and tonsillar stromal cells^{177;178}. Here, HGF/MET signaling regulates integrin-mediated adhesion of B cells to FDCs via β 1-integrin to both VCAM-1 and fibronectin¹⁷⁷.

Activation of the HGF/MET signaling cascade requires binding of HGF to the receptor, inducing MET dimerization, and trans-phosphorylation of the tyrosine residues, *i.e.* Y1230, Y1234, and Y1235, within the activation loop of the tyrosine kinase domain, subsequently followed by the phosphorylation of the tyrosine residues, *i.e.* Y1349 and Y1356, which are essential for all biological responses¹⁷⁹⁻¹⁸¹. Upon phosphorylation, these latter tyrosines create a multisubstrate docking site where adaptor proteins can bind and become activated, enabling the activation of multiple downstream signaling cascades (Figure 4C). Mutational analysis of the multisubstrate docking site of MET revealed that Y1349 and Y1356 are both involved in the interactions with GAB-1, SRC, and SHC, while Y1356 is solely involved in the recruitment of GRB-2, PI3K, PLC γ , SHP2^{166;167;182;183}. Activation of the HGF/MET pathway results in a complex genetic program, consisting of a series of physiological processes, including proliferation, survival, invasion, and angiogenesis, that occur under normal physiological

conditions during embryogenesis and postnatal injury repair, and pathologically during oncogenesis¹⁸⁴. Growth and mitogenesis occurs through RAS-MAPK cascade, but also plays an important role in morphogenesis, the epithelial-to-mesenchymal transition that results from loss of intracellular adhesion via cadherins, focal adhesion kinase, and integrins, with change in cell shape¹⁸⁵. Furthermore, MET activation prevents apoptosis through PI3K and subsequent PKB activation^{120;186;187}. Crosstalk between the PI3K and the RAS-MAPK pathway has been implicated to promote survival^{188;189}. Besides downstream transducers, MET has also been shown to interact with several membrane receptors, including CD44, integrin $\alpha 6\beta 4$, plexin B1, and other receptor tyrosine kinases, *e.g.* RON and EGFR^{165;166;181;184}.

Under physiological conditions, HGF/MET activation is tightly regulated through paracrine ligand delivery, ligand activation at the target cell surface, and ligand-activated receptor internalisation and degradation¹⁹⁰. However, deregulation of this process has been implicated in the survival and progression of a variety of cancers, and can be due to genetic aberrations (*e.g.* translocation, gene amplification, point mutation), transcriptional upregulation, or ligand-dependent autocrine activation^{165;166;184;190}. Amplification of the *MET* gene, has been reported in a number of tumors, including gastric and oesophageal carcinomas, non-small-cell lung carcinomas, and medulloblastomas. In some patients with colorectal carcinomas, *MET* amplification was detected in a high percentage of liver metastasis, which was absent in the primary tumors¹⁹¹. Although uncommon, missense mutations, have also been identified as activating aberrations in the HGF/MET signaling cascade in sporadic and hereditary papillary renal cancer¹⁹²⁻¹⁹⁵, hepatocellular carcinoma¹⁹⁶, and gastric cancer¹⁹⁷. The effected regions of MET are the catalytic and the juxtamembrane domain, deregulating either the activation or the degradation of MET¹⁹⁰. Interestingly, the oncogenic potential of these mutations is still ligand dependent¹⁹⁸. The most frequent cause of MET activation is increased protein expression as a result of transcriptional upregulation, with cases found in virtually all types of carcinomas¹⁶⁵. Increased expression of MET on the cell surface apparently favors ligand-independent activation through spontaneous dimerization, but it is not generally sufficient to trigger activation. An additional signal, such as Met transactivation by other membrane receptors, may be required to activate signaling by these receptors¹⁹⁹. Furthermore, HGF can also aberrantly activate MET in an autocrine fashion, as described for glioblastoma, breast carcinoma, and osteosarcoma²⁰⁰⁻²⁰².

HGF/MET has also been implicated in the development and progression of B and T cell malignancies^{120;203-208}. Expression of Met in B cell malignancies was found in Burkitt lymphoma²⁰⁴, MM^{119;120;209}, primary effusion lymphoma (PEL)²¹⁰, Hodgkin lymphoma²¹¹, and DLBCL²¹². In the latter expression of MET has been associated with transformation of low-grade FLs into DLBCLs²¹³. In addition, overexpression of HGF/MET correlates with poor survival of patients with DLBCL²¹⁴. Furthermore, high serum HGF-levels are also reported to be correlated with poor prognosis in MM²¹⁵, HL²¹¹, as well as DLBCL^{212;216}. Moreover, concurrent expression of MET and HGF have been shown for MM^{119;209}, PEL²¹⁰, and HL²¹¹, whereas HGF can also be produced by stromal cells^{175;217}, suggesting a role for both para- and autocrine activation in B cell malignancies. Recently, a role for HGF/MET signaling in T cell lymphomas, *i.e.* adult T cell lymphoma/leukemia (ATLL) and AITL, has been identified²⁰⁶⁻²⁰⁸. In ATLL the expression of MET was associated with disease progression^{206;207}. Taken together, these data indicate an important role for the regulation of the HGF/MET pathway in the pathogenesis and progression of lymphoid malignancies.

Heparan sulfate proteoglycans

Heparan sulfate proteoglycans (HSPGs) are proteins with covalently attached, unbranched polysaccharide heparan sulfate (HS) chains, which consist of alternating *N*-acetylated glucosamine (GlcNAc) and *D*-glucuronic acid (GlcA) units²¹⁸⁻²²⁰. These macro-molecules are ubiquitously found at the cell surface and in the ECM in all mammalian tissues. The proteoglycan core proteins can be divided in three major families; the membrane spanning syndecans (syndecan1-4)²²¹, the glycosylphosphatidylinositol-linked glypicans (glypican1-6)²²², and the basement membrane proteoglycans perlecan, agrin, and collagen XVIII²²³⁻²²⁵. The cytoplasmic domain of HSPGs contains peptide sequences that can bind the cytoskeletal proteins, which can serve as substrates for cellular kinases. Thus, syndecans may act as signaling molecules²²⁶. Besides, HSPGs can bind and present proteins via their HS chains, of which the binding capacity and specificity is determined by enzymatic modifications^{219;220}. Hence, HSPGs act as multifunctional scaffolds regulating important biological processes, which include cell adhesion and migration, and angiogenesis^{220;227}. The synthesis of the heparan sulfate glucosaminoglycan side chains of proteoglycans proceeds in three steps; chain initiation, chain elongation or polymerization, and chain modification (Figure 5). The initiation starts after translation of a core protein and transfer of xylose from UDP-xylose by xylosyltransferase-I and/or -II to specific serine residues within the proteoglycan core protein. Subsequently, attachment of two *D*-galactose residues by galactosyltransferase-I and -II and GlcA by glucuronosyltransferase-I completes the formation of the core protein linkage tetrasaccharide^{219;220}. The second step can only take place once the tetrasaccharide linker is present²¹⁹. This polymerization reaction is carried out by enzymes from the exostin (EXT) family, including exostin-1 (EXT1) and EXT2²²⁸. These EXTs are thought to function as a hetero-oligomeric complex to polymerize the HS chain. Finally, the unbranched HS chains undergo a complex series of processing reactions involving GlcNAc deacetylation and sulfation by the *N*-deacetylase/*N*-sulfotransferases (NDST), epimerization of GlcA by glucuronyl C5-epimerase (GLCE), and subsequent *O*-sulfation by three different *O*-sulfotransferases (HS2ST, HS3ST and HS6ST)^{218;220}. In contrast to heparin, HS chains are only partly modified, with the modifications made in clusters, resulting in a polysaccharide chain having regions that are highly sulfated interspersed with nearly unmodified regions. These highly modified domains, which provide specific docking sites for a large number of bio-active molecules, are defined by their GlcNAc *N*-sulfation, indicated by NS, NS/NA, or NA, representing areas with (NS or NA/NS) or without (NA) *N*-sulfation (Figure 5). Binding of these ligands, such as growth factors and cytokines, serves a variety of functions, ranging from immobilization, protection, and concentration to distinct modulation of biological functions^{227;229;230}. After synthesis, HS glycosaminoglycan (GAG) chains are known to preferentially bind proteins containing the consensus sequences BBXB and BBBXXB, where B represents basic amino acids like Lys, Arg, or His, and X, hydrophobic (neutral or hydrophobic) residues²³¹. Many, if not all chemokines and growth factors contain such a consensus motif, including IL-6²³², CXCL12²³³, HGF^{234;235} and Wnts²³⁶. The important role of GAGs in hematopoiesis was first realized by the pioneer work of Dexter and Spooncer, who showed that hematopoiesis can be maintained in stromal cell co-cultures for several months without the addition exogenous growth factors²³⁷. Furthermore, they showed that growth factors, presumably produced by the stromal cells, are not released into the fluid phase of such cultures, but were retained by binding HS on stromal cell surfaces which could explain the dependence of hemopoietic cells on direct stromal cell contact for

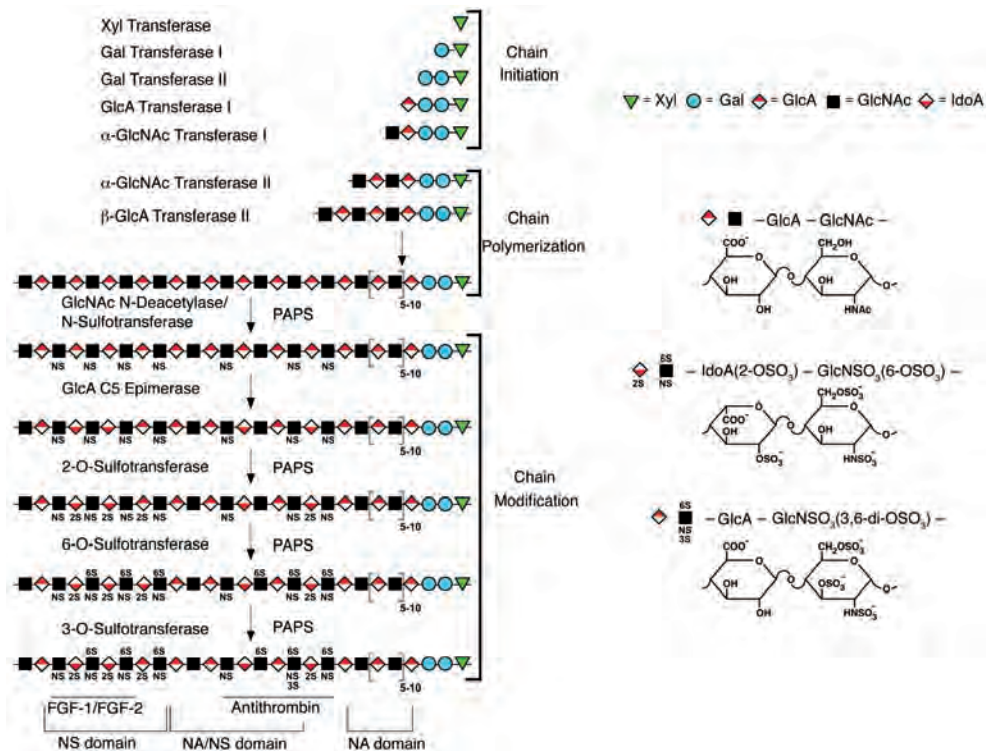


Figure 5. Schematic representation of heparan sulfate chain initiation, polymerization and modification.

The fine structure of the heparan sulfate chains ultimately depends on the regulated expression and action of multiple glycosyltransferases, sulfotransferases and one epimerase, which are arrayed in the lumen of the Golgi apparatus. In addition, a series of cytoplasmic enzymes are needed to catalyze nucleotide sugar (UDP-Xyl, UDP-Gal, UDP-GlcA, and UDP-GlcNAc) and nucleotide sulfate (PAPS). This eventually results in a highly modified HS chain. Shown are regions that have been implicated in binding of specific ligands, such as FGF-1/FGF-2 and antithrombin. Structural domains (NA, NA/NS, NS) are defined with regard to the distribution of GlcNAc and GlcNS, see text for more detail. At the right the (un)modified pyronase rings of GlcA, GlcNAc and IdoA are shown as disaccharides. Adapted and modified from Esko and Lindahl (2001) *J Clin Invest.* ²¹⁹.

their long-term proliferation and survival ^{237;238}. From later studies it has become apparent that HSPGs play a central role in the microenvironmental niches of the BM, suggested to be responsible for the juxtaposition of hematopoietic progenitor cells, stromal cells, cytokines and ECM proteins ²³⁹⁻²⁴². The fact that many growth factors, cytokines, and chemokines associated with lymphocyte growth, differentiation contain HS-binding domains, suggests that HSPGs could also play a key role in the control of lymphocyte function ^{243;244}. Consistent with this notion, it has been demonstrated that HSPGs expression by B lymphocytes is developmentally regulated and stimulation-dependent ^{243;245;246}. Specifically, activation by BCR and CD40-ligation showed a strong induction of cell surface CD44-HS, which acted as functional co-receptors promoting growth factor signaling ²⁴³. In addition, B cells acquire strong expression of the HSPG syndecan-1 upon their terminal differentiation into plasma cells. These observations indicate that regulation of HSPG expression by B cells might play a role in tuning their sensitivity to signals from the microenvironment, and could thus be crucial for B cell development.

In B cell malignancies, syndecan-1 is expressed by the malignant counterpart of plasma cells, MM^{247;248}, as well as the Reed Sternberg cells in Hodgkin's disease²⁴⁹, AIDS-related lymphoma's²⁴⁹, and a subset of CLL²⁵⁰. In MM syndecan-1 is the most abundant expressed HSPG on the surface of myeloma cells, promoting adhesion and inhibiting invasion *in vitro*²⁵¹. By contrast, syndecan-1 can be shed, resulting in high serum levels in MM patients. This shed syndecan-1 can get trapped within the BM ECM where it could enhance the growth and metastasis of MM cells within the bone. This is supported by the fact that increased soluble syndecan-1 expression by MM cells promotes tumor growth and metastasis^{252;253}. Moreover, syndecan-1 has shown to bind multiple growth factors, including IL-6, HGF, and APRIL, promoting the activation of several signaling pathways that induce survival and proliferation of MM cells^{248;254}. Interestingly, regulation of enzymes responsible for HS chain modification, *i.e.* HSulf-1, and HSulf-2²⁵⁵, and EXT1 (this thesis) leads to dramatically attenuated myeloma tumor growth *in vivo*. These observations outline an important role of HSPGs, particularly syndecan-1, in the pathogenesis of MM.

Wnt signaling

The name Wnt originates from combining the first two Wnt genes discovered, namely *Int1* in mammals and *wg* (wingless) in drosophila, which were found to be homologous²⁵⁶. *Int1* (Wnt1) was originally identified as an oncogene that, upon insertional activation by the mouse mammary tumor virus (MMTV), contributed to the formation of mammary carcinomas²⁵⁷. The Wnt signaling pathway is one of the fundamental mechanisms that direct cell proliferation, cell polarity, and cell fate during embryonic development and tissue homeostasis^{258;259}. The Wnt proteins comprise 19 highly conserved cysteine-rich, secreted glycoproteins, which can interact with the 10 different Frizzled (Fzd) receptors, or the receptor tyrosine kinases, Ryk and Ror^{260;261}. Currently, Wnt receptor activation is believed to be able to result in the activation of three different pathways: the canonical Wnt/ β -catenin cascade, the noncanonical planar cell polarity (PCP) pathway, and the Wnt/ Ca^{2+} pathway²⁶². Based on the initial studies on the effect of Wnt proteins, they are separated into "canonical" Wnts (including Wnt1, Wnt3A, and Wnt8) and "noncanonical" Wnts (including Wnt5A and Wnt11), which activate β -catenin-dependent and β -catenin-independent signaling pathways, respectively²⁶⁰. However, recent studies indicate that Wnts are not intrinsically canonical or noncanonical, and that Wnts from either class can elicit both β -catenin-dependent and β -catenin-independent responses determined by the receptors context on the cell surface^{261;263-265}.

By far the best understood pathway is the canonical, β -catenin-dependent, signaling pathway, which drives T cell factor (TCF)/ lymphoid enhancer factor (LEF)-mediated transcription. The key event within this signaling cascade is the stabilization/degradation of the β -catenin protein^{259;262;266}. In the absence of a Wnt ligand, β -catenin is actively degraded by a complex, also called the "destruction box", consisting of the proteins Axin, adenomatous polyposis coli (APC), casein-kinase 1 α (CK1 α), and glycogen synthase kinase 3 β (GSK3 β). Within this complex Axin and APC form a scaffold that facilitates the phosphorylation of β -catenin at specific serine (Ser) and threonine (Thr) residues. Phosphorylation of β -catenin at Ser45 by CK1 α will induce phosphorylation at Thr41, Ser37 and Ser33 by GSK3 β . This creates a binding site for E3 ubiquitin ligase β -TRCP, leading to β -catenin ubiquitination and proteasomal degradation. Due to the resulting low levels of free β -catenin, TCF/LEF proteins will now interact with transcriptional co-repressors to block gene expression in the nucleus

(Figure 6A)^{259;262;266}. Activation of the Wnt pathway by binding of a Wnt protein to the Fzd – low-density lipoprotein receptor-related protein (LRP) receptor complex results in the formation of Dishevelled (Dvl)–Fzd complexes and relocation of Axin from the destruction box to the cell membrane. Axin then facilitates the phosphorylation of the LRP5/6, which together with the subsequent accumulation of non-phosphorylated β -catenin will initiate downstream signaling. The non-phosphorylated β -catenin translocates to the nucleus, where it interacts with members of the TCF/LEF transcription family and converts these proteins into potent transcriptional activators by recruiting co-activators ensuring efficient activation of Wnt target genes (Figure 6B)^{259;262;266}.

The emerging list of Wnt target genes includes several Wnt signaling components, e.g. *Fzd*, *LRP6*, *Axin2*, *TCF*, *LEF*, *Naked* (a Dvl antagonist), and Dickkopf-1 (*DKK1*). Wnt induces expression of *Axin2*, *DKK1*, and *Naked* and suppression of *Fzd* and *LRP6*, forming negative feedback loops that dampen Wnt signaling²⁵⁹. Furthermore, several extracellular proteins have been identified to regulate the canonical Wnt signaling pathway. These secreted antagonists can be divided into two functional groups the secreted Frizzled related proteins (sFRP) class and the DKK class. The sFRP class, consisting of the sFRP-family, WIF-1, and Cerberus, bind directly to Wnts, thereby preventing the Wnt ligands to bind the receptor(-complex), whereas the DKK class, which comprises the DKK-family and sclerostin (SOST), interfere with the activation of the Wnt signaling pathway by binding to LRP5/6. Thus, in theory, the DKK class of antagonists specifically inhibits the canonical pathway, while the sFRP class will inhibit both canonical and noncanonical signaling²⁶⁷.

Given the crucial role of the Wnt signaling pathway in development and repair, it is not surprising that mutations of the Wnt pathway components are associated with hereditary disorders and other diseases, including osteoporosis and cancer^{259;262}. In adult live, the bone homeostasis is tightly regulated by balancing the activity of the osteoblasts, which produce bone matrix, and the osteoclasts, which resorb the old matrix. The crucial role for Wnt signaling in bone cells was first revealed by the occurrence of mutations in the *LRP5* gene, that give rise to bone abnormalities. Loss of function (lof) mutations have been identified in patients with osteoporosis pseudoglioma syndrome (OPPG), characterized by low bone mass²⁶⁸, while gain of function mutations (gof) are found in patients with autosomal dominant high bone mass diseases^{269;270}. These gof mutations cluster in the LRP5 extracellular domain and prevent binding of the Wnt signaling antagonists SOST^{271;272} and DKK1²⁷³. In addition, mutations in the *SOST* gene leads to sclerosteosis, a human disease characterized by high bone mass. Interestingly, alteration in the Wnt signaling pathway is one of the causative events of osteolytic lesions in MM, which will be discussed later. The Wnt pathway was first linked to cancer with the identification of a germline APC mutation as the driving force of the hereditary syndrome termed Familial Adenomatous Polyposis (FAP)^{274;275} and spontaneous forms of colon cancer. These patients inherit one defective APC allele and as a consequence develop large numbers of colon adenomas (also termed polyps), which frequently progress to invasive colon carcinoma following additional genetic mutations later in life. Besides APC mutations, accounting for 80% of the sporadic colon cancers²⁷⁶⁻²⁷⁹, mutation in *Axin2*²⁸⁰ and β -catenin^{281;282} have been found, although less frequent (Figure 6C). The mutations of APC or *Axin2* disrupt their function within the β -catenin destruction box complex, whereas mutation of the conserved phosphorylation sites of β -catenin blocks its targeted degradation by proteasome, all leading to unrestrained activation of the Wnt signaling pathway²⁶⁶. These genetic aberration have also been found

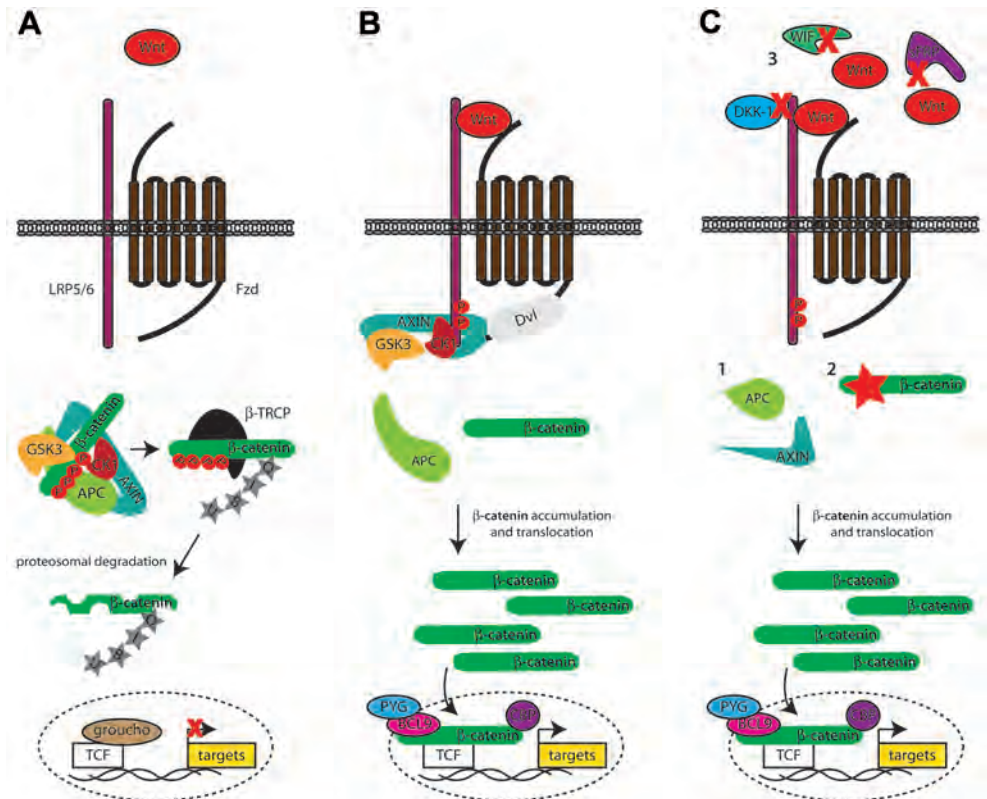


Figure 6. The canonical Wnt signaling pathway.

(A) In the absence of a Wnt signal, β -catenin is bound by APC and axin to form a degradation complex. These interactions facilitate the phosphorylation of a conserved set of serine and threonine residues at the amino terminus of β -catenin by the kinases CK1 α and GSK3 β . This will subsequently lead to binding of the β -TRCP, which mediates the ubiquitylation (UBIQ) and efficient proteasomal degradation of β -catenin. Due to the lack of free β -catenin the TCF/LEF transcription factor family (TCF1, TCF3, TCF4 and LEF1) actively repress target genes by recruiting transcriptional co-repressors (Groucho/TLE) to their promoters and/or enhancers. (B) In the presence of a Wnt ligand, Wnt forms a complex with a Frizzled family member and LRP5 or LRP6, which triggers the formation of Dvl–Fzd complexes and the phosphorylation of LRP by CK1. This induces the relocation of axin to the membrane and inactivation of the destruction complex, leading to the accumulation of β -catenin. β -catenin will translocate to the nucleus, where it interacts with members of the TCF/LEF family. In the nucleus, β -catenin converts the TCF proteins into potent transcriptional activators by displacing Groucho/TLE proteins and recruiting an array of coactivator proteins, activating the transcription of target genes. (C) In cancer the Wnt signaling pathway can be aberrantly activated by: 1) Mutations in APC or axin 1 genes that result in the production of truncated scaffold proteins lacking the capacity to bind β -catenin; 2) Mutation of the conserved serine/threonine phosphorylation sites at the amino terminus of β -catenin blocks its phosphorylation within the destruction complex, thereby preventing binding of β -TRCP; 3) Loss of natural Wnt inhibitors such as sFRP, DKK1, or WIF through epigenetic silencing of the corresponding genes allows Wnt proteins produced by the cancer cells to activate the pathway at the membrane. All these routes allow for accumulation of β -catenin and the formation of active transcription factor complexes with TCF/LEF proteins in the nucleus. In each case, the uncontrolled formation of TCF– β -catenin complexes in the nucleus causes chronic activation of the Wnt target gene program, driving cancer formation. APC, adenomatous polyposis coli; BCL9, B cell lymphoma 9; CBP, CREB-binding protein; CK1, casein kinase 1; Fzd, Frizzled; LRP, low-density lipoprotein receptor-related protein; PYG, Pygopus; sFRP, secreted Frizzled-related protein; TCF, T-cell factor; β -TRCP, β -transducin repeat-containing protein; WIF, Wnt inhibitory factor.

in other malignancies, although with lower frequency. Mutation of β -catenin seems to be the preferred route to chronic Wnt signaling dysfunction in cancers such as liver cancer (hepatocellular and hepatoblastoma), endometrial ovarian cancer, pilomatricoma skin cancer, prostate cancer, melanoma, Wilms tumor, and T cell lymphomas (this thesis) ²⁸³. Recent studies indicate that elevated levels of nuclear β -catenin, a hallmark of active Wnt signaling, without the existence of APC, β -catenin or Axin mutations, can be the result of epigenetic silencing of genes encoding natural Wnt pathway inhibitors (Figure 6C) such as sFRP ^{284;285}, WIF ^{286;287}, and DKK1 (this thesis) or increased expression of Wnt ligands (this thesis), Fzd receptors (this thesis), and Dvl family members.

TCF/LEF family transcription factors were initially identified in models of early lymphocyte development ²⁸⁸⁻²⁹⁰, whereas studies in TCF-1 and LEF1 knockout mice have shown that these factors are essential for the maintenance of progenitor T cell and B cell compartments ^{288;291}. These observations suggested a role for WNT signaling in the control of cell proliferation and survival during lymphocyte development. Indeed, recent studies have shown that WNT factors and β -catenin affect lymphocyte progenitor fate, as well as hematopoietic stem cell self-renewal ²⁹²⁻²⁹⁸. Since Wnt signaling plays an important role in the maintenance and expansion of lymphocyte progenitors, aberrant activation of this pathway might contribute to the pathogenesis of lymphoproliferative disease. Recent studies, including from our laboratory, have indeed established a role for the Wnt signaling pathway in the development and progression of B and T cell malignancies ^{123;299}. These studies also reveal that in different types of lymphoproliferative disease, distinct mechanisms of activation, including para/autocrine, viral, and mutational activation, may be involved. The first evidence for the involvement of the Wnt pathway in pathogenesis of human T cell lymphomas came from our laboratory. This study showed that the Wnt pathway can be activated by mutations (PTCLs), or autocrine stimulation (T-LBL/ALL) and controls cell growth (this thesis). These data are supported by the fact that stabilization of β -catenin in mouse thymocytes is oncogenic and results in malignant T-cell lymphomas ²⁹⁸. In addition to T cell lymphomas, the Wnt signaling pathway has been implicated in several different B cell malignancies, including B-LBL/ALL, CLL, MM, and immunodeficiency-related lymphoproliferative disease. In B-LBL/ALL, carrying a t(1;19)(q23:p13) translocation, *Wnt16* expression is induced by the fusion product of transcription factor E2A and pre-B-cell leukemia transcription factor 1 (PBX1) ³⁰⁰. This enhanced expression causes *Wnt16*-mediated autocrine growth, directly contributing to the development of this subset of B-LBL/ALL ³⁰¹. Overexpression of Wnt pathway genes, including *Wnt3*, *Wnt5b*, *Wnt6*, *Wnt10a*, *Wnt14*, and *Wnt16*, and LEF1 has been reported for CLL ³⁰². Furthermore, the expression of LEF1 is discriminative for CLL compared to other low-grade B cell lymphomas ³⁰³, and has recently been identified as a prosurvival factor in CLL, which is expressed in the preleukemic state of monoclonal B cell lymphocytosis ³⁰⁴. In addition, epigenetic dysregulation, *i.e.* hypermethylation, of soluble Wnt antagonists was found in over 50% of CLL patients and is associated with aberrant Wnt pathway activation in CLL ³⁰⁵. The gamma herpesviruses Epstein-Barr virus (EBV) and Kaposi's sarcoma-associated virus (KSHV) play a role in the pathogenesis of viral-induced lymphoproliferative disease ³⁰⁶⁻³⁰⁹. The KSHV-associated protein latency-associated nuclear antigen (LANA) was shown to stabilize β -catenin, presumably by interacting with GSK3 β , resulting in increased cell proliferation. This could promote cell growth in primary effusion lymphoma (PEL) ³¹⁰. In MM the Wnt signaling pathway plays an important role in the bipartite interaction with the BM microenvironment. Initial studies, including from our laboratory, have shown that

the para-/autocrine activation of the Wnt signaling pathway is involved in the proliferation¹²³ and migration^{311;312} of MM and on the other hand has a major influence on the bone homeostasis via the secreted Wnt antagonist DKK1¹³⁸. Subsequent studies confirmed the role of the Wnt signaling pathway in MM survival and proliferation³¹³⁻³¹⁷. The contribution of DKK1 to myeloma bone disease is now well established and subject to therapeutic intervention^{133;318;319}. Preclinical studies have shown that inhibition of DKK1 by antibody therapy results in the restoration of osteoblast function and could counteract the increased osteoclastogenesis observed in MM³²⁰⁻³²². Some of these studies show that inhibition of DKK1-induced osteolysis is accompanied by a reduction of tumor burden *in vivo*^{320;321}, although others did not³²². Fulcitini *et al.* show that this effect on tumor burden is indirect via the inhibition of IL-6 secretion by BMSCs³²¹, which might explain why not all patients react the same³²⁰. The direct effect of DKK1 on MM cells also remains controversial and needs to be investigated in more depth (this thesis). In addition to DKK1, sFRP-2 may also play a role in the dysregulation of osteoblast differentiation. sFRP-2 was often found in patients with advanced bone lesions, and could inhibit osteoblast differentiation *in vitro*³²³. Like in CLL, recent studies indicate an important role for epigenetic gene silencing of Wnt signaling antagonists in the aberrant activation of the Wnt pathway^{324;325}, driving the proliferation of MM cells³²⁴. All together, these data implicate a central role for Wnt signaling in the progression of MM and associated bone disease.

N-cadherin

Cadherins constitute a large family of transmembrane proteins, many of which participate in calcium-dependent cell-cell adhesion through homophilic interaction³²⁶⁻³²⁸. All classic cadherins contain 5 repeats of approximately 110 amino acids, called the extracellular cadherin (EC) domain, containing Ca²⁺-binding sites and in type I classic cadherins, such as E- and N-cadherin, a HAV (Histadine, Alanine, Valine respectively) sequence (Figure 7)^{326;328}. Two types of cadherin dimerization play an important role in cadherin-mediated adhesion, namely *cis*- and *trans*-dimerization. In *cis*-dimerization (between two molecules on the same cell), the EC1 domain of one molecule interacts with the EC2 domain of another, where in *trans*-dimerization (between adjacent cells) the tryptophan (W)-2 residue in EC1 of one cadherin-molecule interacts with a hydrophobic region in EC1 of the adhesive partner^{326;328-330}. Although the molecular mechanisms underlying *cis*- and *trans*-dimerization are still not fully understood, a widely-accepted model is that cadherin binding consist of three steps: (1) formation of *cis*-dimers; (2) formation of low-affinity *trans*-homodimers between cadherin *cis*-dimers; (3) lateral clustering of cadherin-molecules^{330;331}. Ca²⁺ plays an important role in these adhesive interaction, protecting the conformation of the cadherin-molecules. Withdrawal of calcium results in disordering of the interdomain orientation, increased proteolysis, and increased motion between successive domains^{328;329;332;333}. Classical cadherins, *i.e.* E- and N-cadherin, play a central role during embryonic development. During gastrulation, N-cadherin expression is first detected in cells of the primitive streak when they undergo an epithelial-mesenchymal transition (EMT), a process characterized by down-regulation of E-cadherin and up-regulation of N-cadherin, and form the mesoderm^{326;329;334}. In addition, N-cadherin is involved in mesenchymal condensation that leads to osteogenesis³³⁵⁻³³⁷. During osteogenesis, N-cadherin is expressed during all stages of bone formation and increases at the stages of nodule formation and mineralization^{326;338}. *In vitro* studies interfering with N-cadherin-mediated adhesion of osteoblasts, by the use of HAV-

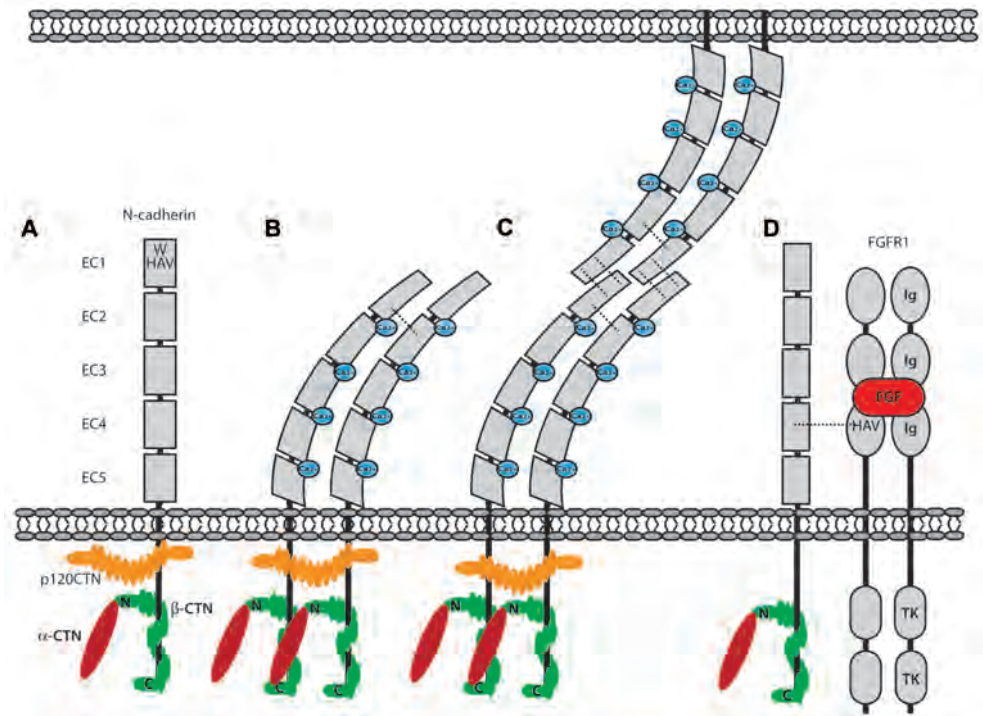


Figure 7. N-cadherin structure and protein interactions.

(A) N-cadherin consists of 5 extracellular repeats, extracellular cadherin (EC) domains, containing Ca^{2+} -binding sites and a HAV (Histidine, Alanine, Valine respectively) sequence. The cytoplasmic tail interacts with β -catenin and p120-catenin and is connected to the actin cytoskeleton via α -catenin. (B) In *cis*-dimerization, the EC1 domain of one cadherin-molecule interacts with the EC2 domain of another. Calcium is bound, which will give the conformation more stability. *Cis*-dimerization is thought to proceed *trans*-dimerization. (C) *Trans*-dimerization occurs between adjacent cells. Here the tryptophan (W)-2 residue in EC1 of one cadherin-molecule interacts with a hydrophobic region in EC1 of the adhesive partner N-cadherin. These interactions are the basis for the formation of adherens junctions. (D) In cancer, cross-talk of N-cadherin with other membrane proteins, e.g. FGFR1, has also been reported, leading to a more invasive phenotype.

peptides³³⁸, blocking antibodies³³⁹, antisense oligonucleotides³³⁹, and transfections with dominant negative N-cadherin³³⁸, revealed that N-cadherin interactions are important for osteoblast differentiation and function^{335;337}. Moreover, loss of cell-cell contact results in osteoblast apoptosis, which is suggested to be regulated by N-cadherin-mediated cell-cell adhesion^{335;340}. Besides its importance in osteogenesis, N-cadherin expression in osteoblasts might have an additional role in the BM, namely the formation of a supportive niche for the maintenance of HSCs. Zhang *et al.* showed that spindle shaped osteoblast and long term (LT)-HSCs interact via N-cadherin. Further, it was reported that there is a correlation between the number of spindle-shaped osteoblast lining the trabecular and cancellous bone and the size of the LT-HSC population³⁴¹. Although these data indicate a central role for N-cadherin in the endosteal stem cell niche, recent studies have resulted in some controversy about this issue, mainly regarding the role of N-cadherin in the interaction of hematopoietic stem cells with their niches, i.e. whether or not HSC themselves express N-cadherin³⁴²⁻³⁴⁸. Other adult tissues that have N-cadherin expression include amongst others neural tissue, myocytes,

as well as (venule) endothelial cells. In the latter N-cadherin is required for VE-cadherin expression³⁴⁹, both contributing to vessel stability and formation³⁵⁰.

In cancer, EMT is frequently observed and associated with an invasive phenotype and metastatic potential^{326;329;331;350}. Besides, aberrant expression of N-cadherin has shown to result in invasion and metastasis³⁵¹⁻³⁵³. One explanation for this invasive phenotype, is the interaction with the FGFR1 (Figure 7), preventing internalization that results in sustained MAPK activation and increased MMP-9 expression^{329;331;354}. In addition, the domain of N-cadherin that confers motility has been mapped to a region within EC4 that is also required for the interaction between N-cadherin and FGFR1³⁵⁵. Other molecules that have been reported to interact with N-cadherin, include integrins and S1P₁³²⁹. In malignant lymphomas not much is known about N-cadherin, although expression has been reported in T cell leukemia cell lines³⁵⁶⁻³⁵⁹, and t(1;19) translocated B-LBL/ALL³⁶⁰. These studies also showed that N-cadherin can mediate adhesion of lymphoma cells to stroma. These findings suggest a role for N-cadherin in lymphocyte development, as well as in malignant transformation.

1

Mouse models for multiple myeloma

To gain insight in the molecular and cellular mechanisms that control MM growth, suitable models are necessary. Cell lines offer many opportunities to investigate MM, however they also have their shortcomings. Most cell lines have been derived from extramedullary lesions of patients with advanced disease, while MM is typically characterized by its BM localization. Although the most common translocations, *e.g.* 11q13 (*CCND1*), 4p16 (*FGFR3* and *MMSET*), 16q23 (*MAF*), 6p21 (*CCND3*), and 20q12 (*MAFB*) are captured by the currently available cell lines, not all genetic backgrounds are represented. In addition, several cell lines have acquired abnormalities that are not found in MM patients³⁶¹. Furthermore, *in vitro* only two-dimensional interactions can be analyzed. Therefore, the last two decades, several mouse models have been developed for MM, including syngeneic, transgenic, and human xenograft models.

A widely used syngeneic mouse model is the 5TMM model. This model originates from the spontaneous development of MM in elderly mouse of the C57BL/KalwRij strain, and subsequent transfer to young syngeneic mice³⁶²⁻³⁶⁴. This has resulted in many different lines, of which the 5T2MM and 5T33MM are the best characterized. The clinical characteristics have been reported to be similar to human MM, and include preferential localization in the BM, measurable M-protein, osteolytic bone disease, and increased angiogenesis in the marrow^{361;364}. Another syngeneic model is based on the P3X63Ag8 mouse myeloma cell line, however its BM-independent growth makes it less representative for human MM³⁶⁵.

Besides syngeneic models, transgenic MM models have been established and used for therapeutic evaluation, as well as studying the biology of multiple myeloma. Most of these models involve the deregulation of the oncogene *MYC*^{366;367}, except for the E_μXBP1-model³⁶⁸. Although clonal expansion of malignant plasma cells is observed in these mice, the short latency of these highly aggressive tumors, and the predominant extramedullary localization of the disease do not really resemble the human situation. In contrast, a recently developed transgenic mouse, *i.e.* Vk**MYC*³⁶⁹, does result in a more indolent disease progression. In this model, the *MYC* transgene, containing a stopcodon, and flanked by Igκ regulatory sequences is activated by AID-dependent somatic hypermutation that reverts the stopcodon. The *MYC* activation in these mice results in a plasma cell tumor with a low proliferative rate localized

1

in the BM, and is accompanied by anemia and osteoporosis in most mice. The percentage of plasma cells in the BM is variable, consistent with MGUS in some but MM in most mice. Furthermore, approximately one-third of the MM mice develop extramedullary disease, *e.g.* in the spleen or other lymphoid tissues, and sometimes as ascitic fluid in the peritoneal cavity³⁶⁹.

In addition to mouse myeloma models, the generation of immunodeficient mice have enabled transplantation of human MM tumors or cell lines. This has resulted in numerous attempts to engraft human MM, from less successful attempts, by directly injecting primary MM cell in SCID³⁷⁰ and NOD/SCID-mice³⁷¹, to more successful attempts, the SCID-hu^{372;373}, the SCID-rab³⁷⁴, and the cell line-based NOD/SCID GFP model³⁷⁵. These xenograft models include localized disease, from subcutaneous implantations, and diffuse disease via intravenous injections with MM cells. The SCID-hu and SCID-rab models, either based on the implantation of a piece of fetal human bone or rabbit bone respectively, are two xenograft models that provide reproducible growth of primary myeloma cells. These models highly resemble human MM, with growth only in the bone implants, the induction of angiogenesis and resorption of the implanted bone. Interestingly, when SCID mice were implanted contralaterally with two rabbit bones, of which only one was injected with MM cells, myeloma cells migrated to and engrafted in the second bone, while they were not detected in the murine tissues³⁷⁴. Although these models are highly informative for primary human MM growth and the microenvironmental interaction, tumor growth can only be visualized by M-protein detection and post-mortem analysis. To this end, Mitsiades *et al.* developed a model, *i.e.* NOD/SCID GFP, where MM cells are gene-marked with green fluorescent protein (GFP) are intravenously introduced to NOD/SCID mice³⁷⁵. This cell line based model creates the opportunity to frequently monitor the mice in a non-invasive way by whole-body, real-time fluorescent imaging. The use of imaging techniques, together with cell lines, makes it possible to follow tumor outgrowth in time, and visualize the effect of molecular interference, *e.g.* by siRNA's, or drug treatment. However, the frequent extramedullary growth, especially the subcutaneous plasmacytomas of the tumor, is a drawback of this model. Thus, several models exist to study the pathogenesis of MM, however a representative (predominantly BM localized), quantifiable, and non-invasive human MM model (this thesis) is still highly desirable.

Aims and outline of this thesis

The studies described in this thesis investigated the contribution of the tumor microenvironment, in particularly the HGF/MET and Wnt signaling pathway, heparan sulfate proteoglycans (HSPGs), and N-cadherin, to lymphoma and myeloma growth and survival. Emerging data state the importance of the microenvironmental influences on tumor-pathobiology. In **chapter 2**, we examined a large panel of B cell malignancies for the expression of MET and screened for amplification and mutation of *MET*. This screening revealed that MET expression was largely restricted to DLBCL and MM. Furthermore, we defined the role of the HGF/MET pathway, including HGFA, in DLBCL (**chapter 2**). Another pathway involved in both development and cancer is the Wnt signaling pathway. This pathway was investigated in more detail in **chapter 3 and 4**. In **chapter 3**, an immunohistochemical screening for nuclear β -catenin was performed to visualize the incidence of aberrant Wnt pathway activation in

B and T cell lymphomas. This chapter shows that Wnt pathway activation, resulting from either gain-of function mutation in β -catenin or autocrine activation is more common in T cell lymphomas and induces cell growth. In **Chapter 4** we investigated the presence of a negative feedback loop in MM, in which DKK1 acts as a potential tumor suppressor. In line with this hypothesis, we show that expression of the Wnt antagonist DKK1 is lost in advanced MM, and correlates with Wnt pathway activation. This loss of DKK1 expression is due to promoter methylation. **Chapter 5** introduces a new mouse model based on luciferase-marked MM cell lines. This model enables quantitative measurements of the tumor in time, using bioluminescent imaging. Using this new MM mouse model, we studied the role of syndecan-1 on MM growth (**chapter 6**). In this chapter, we show that the HS chains attached to syndecan-1 are essential for the growth of MM, both *in vitro* and *in vivo*. This was demonstrated by applying inducible RNAi-mediated knockdown of EXT1, a co-polymerase indispensable for HS biosynthesis. One of the characteristic features of MM is osteolytic bone destruction. Although this is extensively studied, the biology underlying this phenomenon is still not fully understood. In **chapter 7**, we identified N-cadherin as a protein aberrantly expressed by malignant plasma cells of a subset of MM patients and explored its role in the pathogenesis of MM. We demonstrate that N-cadherin, which mediates homophilic adhesion, is involved in the BM localization of these malignant cells and that it contributes to the inhibition of osteoblast differentiation, thereby establishing a role for N-cadherin in myeloma bone disease. Finally, **chapter 8** and **chapter 9** discuss and summarize the results presented in this thesis, respectively.

References

1. Klein U, la-Favera R. Germinal centres: role in B-cell physiology and malignancy. *Nat.Rev.Immunol.* 2008;8:22-33.
2. Blom B, Spits H. Development of human lymphoid cells. *Annu.Rev.Immunol.* 2006;24:287-320.
3. Rajewsky K. Clonal selection and learning in the antibody system. *Nature* 1996;381:751-758.
4. Hardy RR, Hayakawa K. B cell development pathways. *Annu.Rev.Immunol.* 2001;19:595-621.
5. Liu YJ, Zhang J, Lane PJ, Chan EY, MacLennan IC. Sites of specific B cell activation in primary and secondary responses to T cell-dependent and T cell-independent antigens. *Eur.J.Immunol.* 1991;21:2951-2962.
6. Berek C, Berger A, Apel M. Maturation of the immune response in germinal centers. *Cell* 1991;67:1121-1129.
7. Jacob J, Kelsoe G, Rajewsky K, Weiss U. Intraclonal generation of antibody mutants in germinal centres. *Nature* 1991;354:389-392.
8. Kuppers R, Zhao M, Hansmann ML, Rajewsky K. Tracing B cell development in human germinal centres by molecular analysis of single cells picked from histological sections. *EMBO J.* 1993;12:4955-4967.
9. MacLennan IC. Germinal centers. *Annu.Rev.Immunol.* 1994;12:117-139.
10. Di Noia JM, Neuberger MS. Molecular mechanisms of antibody somatic hypermutation. *Annu.Rev.Biochem.* 2007;76:1-22.
11. Banchereau J, Steinman RM. Dendritic cells and the control of immunity. *Nature* 1998;392:245-252.
12. Liu YJ, de BO, Fugier-Vivier I. Mechanisms of selection and differentiation in germinal centers. *Curr.Opin.Immunol.* 1997;9:256-262.
13. Dubois B, Barthelemy C, Durand I et al. Toward a role of dendritic cells in the germinal center reaction: triggering of B cell proliferation and isotype switching. *J.Immunol.* 1999;162:3428-3436.

14. Fuller KA, Kanagawa O, Nahm MH. T cells within germinal centers are specific for the immunizing antigen. *J.Immunol.* 1993;151:4505-4512.
15. Cosgrove D, Gray D, Dierich A et al. Mice lacking MHC class II molecules. *Cell* 1991;66:1051-1066.
16. Kawabe T, Naka T, Yoshida K et al. The immune responses in CD40-deficient mice: impaired immunoglobulin class switching and germinal center formation. *Immunity.* 1994;1:167-178.
17. Renshaw BR, Fanslow WC, III, Armitage RJ et al. Humoral immune responses in CD40 ligand-deficient mice. *J.Exp.Med.* 1994;180:1889-1900.
18. Liu YJ, Arpin C. Germinal center development. *Immunol.Rev.* 1997;156:111-126.
19. Arpin C, Dechanet J, Van KC et al. Generation of memory B cells and plasma cells in vitro. *Science* 1995;268:720-722.
20. Miller JF. Immunological function of the thymus. *Lancet* 1961;2:748-749.
21. Miller JF, Osoba D. Current concepts of the immunological function of the thymus. *Physiol Rev.* 1967;47:437-520.
22. Scimone ML, Aifantis I, Apostolou I, von BH, von Andrian UH. A multistep adhesion cascade for lymphoid progenitor cell homing to the thymus. *Proc.Natl.Acad.Sci.U.S.A* 2006;103:7006-7011.
23. Petrie HT, Zuniga-Pflucker JC. Zoned out: functional mapping of stromal signaling microenvironments in the thymus. *Annu.Rev.Immunol.* 2007;25:649-679.
24. Haynes BF, Heinly CS. Early human T cell development: analysis of the human thymus at the time of initial entry of hematopoietic stem cells into the fetal thymic microenvironment. *J.Exp.Med.* 1995;181:1445-1458.
25. Bhandoola A, Sambandam A. From stem cell to T cell: one route or many? *Nat.Rev.Immunol.* 2006;6:117-126.
26. Takahama Y. Journey through the thymus: stromal guides for T-cell development and selection. *Nat.Rev.Immunol.* 2006;6:127-135.
27. Wurbel MA, Malissen M, Guy-Grand D et al. Mice lacking the CCR9 CC-chemokine receptor show a mild impairment of early T- and B-cell development and a reduction in T-cell receptor gamma delta(+) gut intraepithelial lymphocytes. *Blood* 2001;98:2626-2632.
28. Liu C, Ueno T, Kuse S et al. The role of CCL21 in recruitment of T-precursor cells to fetal thymus. *Blood* 2005;105:31-39.
29. Lesley J, Hyman R, Schulte R. Evidence that the Pgp-1 glycoprotein is expressed on thymus-homing progenitor cells of the thymus. *Cell Immunol.* 1985;91:397-403.
30. Rossi FM, Corbel SY, Merzaban JS et al. Recruitment of adult thymic progenitors is regulated by P-selectin and its ligand PSGL-1. *Nat.Immunol.* 2005;6:626-634.
31. Aifantis I, Raetz E, Buonamici S. Molecular pathogenesis of T-cell leukaemia and lymphoma. *Nat.Rev.Immunol.* 2008;8:380-390.
32. Lind EF, Prockop SE, Porritt HE, Petrie HT. Mapping precursor movement through the postnatal thymus reveals specific microenvironments supporting defined stages of early lymphoid development. *J.Exp.Med.* 2001;194:127-134.
33. Galy A, Verma S, Barcena A, Spits H. Precursors of CD3+CD4+CD8+ cells in the human thymus are defined by expression of CD34. Delineation of early events in human thymic development. *J.Exp.Med.* 1993;178:391-401.
34. Res P, Blom B, Hori T, Weijer K, Spits H. Downregulation of CD1 marks acquisition of functional maturation of human thymocytes and defines a control point in late stages of human T cell development. *J.Exp.Med.* 1997;185:141-151.
35. Kisielow P, Teh HS, Bluthmann H, von BH. Positive selection of antigen-specific T cells in thymus by restricting MHC molecules. *Nature* 1988;335:730-733.
36. Jameson SC, Hogquist KA, Bevan MJ. Positive selection of thymocytes. *Annu.Rev.Immunol.* 1995;13:93-126.
37. Egerton M, Scollay R, Shortman K. Kinetics of mature T-cell development in the thymus. *Proc.Natl.Acad.Sci.U.S.A* 1990;87:2579-2582.

38. Goldrath AW, Bevan MJ. Selecting and maintaining a diverse T-cell repertoire. *Nature* 1999;402:255-262.
39. Witt CM, Raychaudhuri S, Schaefer B, Chakraborty AK, Robey EA. Directed migration of positively selected thymocytes visualized in real time. *PLoS.Biol.* 2005;3:e160.
40. Reichert RA, Weissman IL, Butcher EC. Phenotypic analysis of thymocytes that express homing receptors for peripheral lymph nodes. *J.Immunol.* 1986;136:3521-3528.
41. Ramsdell F, Jenkins M, Dinh Q, Fowlkes BJ. The majority of CD4+8- thymocytes are functionally immature. *J.Immunol.* 1991;147:1779-1785.
42. Bendelac A, Matzinger P, Seder RA, Paul WE, Schwartz RH. Activation events during thymic selection. *J.Exp. Med.* 1992;175:731-742.
43. Staal FJ, Luis TC, Tiemessen MM. WNT signalling in the immune system: WNT is spreading its wings. *Nat.Rev. Immunol.* 2008;8:581-593.
44. Chaffin KE, Perlmutter RM. A pertussis toxin-sensitive process controls thymocyte emigration. *Eur.J.Immunol.* 1991;21:2565-2573.
45. Matloubian M, Lo CG, Cinamon G et al. Lymphocyte egress from thymus and peripheral lymphoid organs is dependent on S1P receptor 1. *Nature* 2004;427:355-360.
46. Ueno T, Hara K, Willis MS et al. Role for CCR7 ligands in the emigration of newly generated T lymphocytes from the neonatal thymus. *Immunity.* 2002;16:205-218.
47. Poznansky MC, Olszak IT, Evans RH et al. Thymocyte emigration is mediated by active movement away from stroma-derived factors. *J.Clin.Invest* 2002;109:1101-1110.
48. Kupperts R. The biology of Hodgkin's lymphoma. *Nat.Rev.Cancer* 2009;9:15-27.
49. Jaffe ES, Harris NL, Stein H, Vardiman JW. WHO Classification of Tumours. Pathology and Genetics of Tumours of Haematopoietic and Lymphoid Tissues. Lyon: IARC Press; 2001.
50. Fisher SG, Fisher RI. The epidemiology of non-Hodgkin's lymphoma. *Oncogene* 2004;23:6524-6534.
51. Kupperts R. Mechanisms of B-cell lymphoma pathogenesis. *Nat.Rev.Cancer* 2005;5:251-262.
52. Swerdlow SH, Campo E, Harris NL et al. WHO Classification of Tumours of Haematopoietic and Lymphoid Tissues. Lyon: IARC Press; 2008.
53. de Leval L, Bisig B, Thielen C, Boniver J, Gaulard P. Molecular classification of T-cell lymphomas. *Crit Rev. Oncol.Hematol.* 2009;72:125-143.
54. Staal FJ, Langerak AW. Signaling pathways involved in the development of T-cell acute lymphoblastic leukemia. *Haematologica* 2008;93:493-497.
55. Weng AP, Ferrando AA, Lee W et al. Activating mutations of NOTCH1 in human T cell acute lymphoblastic leukemia. *Science* 2004;306:269-271.
56. Flex E, Petrangeli V, Stella L et al. Somatically acquired JAK1 mutations in adult acute lymphoblastic leukemia. *J.Exp.Med.* 2008;205:751-758.
57. Raetz EA, Perkins SL, Bhojwani D et al. Gene expression profiling reveals intrinsic differences between T-cell acute lymphoblastic leukemia and T-cell lymphoblastic lymphoma. *Pediatr.Blood Cancer* 2006;47:130-140.
58. Uyttebroeck A, Vanhentenrijk V, Hagemeyer A et al. Is there a difference in childhood T-cell acute lymphoblastic leukaemia and T-cell lymphoblastic lymphoma? *Leuk.Lymphoma* 2007;48:1745-1754.
59. O'leary H, Savage KJ. The spectrum of peripheral T-cell lymphomas. *Curr.Opin.Hematol.* 2009;16:292-298.
60. Piccaluga PP, Agostinelli C, Califano A et al. Gene expression analysis of peripheral T cell lymphoma, unspecified, reveals distinct profiles and new potential therapeutic targets. *J.Clin.Invest* 2007;117:823-834.
61. Attygalle AD, Kyriakou C, Dupuis J et al. Histologic evolution of angioimmunoblastic T-cell lymphoma in consecutive biopsies: clinical correlation and insights into natural history and disease progression. *Am.J.Surg. Pathol.* 2007;31:1077-1088.
62. de Leval L, Rickman DS, Thielen C et al. The gene expression profile of nodal peripheral T-cell lymphoma demonstrates a molecular link between angioimmunoblastic T-cell lymphoma (AITL) and follicular helper T (TFH) cells. *Blood* 2007;109:4952-4963.

63. Mason DY, Bastard C, Rimokh R et al. CD30-positive large cell lymphomas ('Ki-1 lymphoma') are associated with a chromosomal translocation involving 5q35. *Br.J.Haematol.* 1990;74:161-168.
64. Morris SW, Kirstein MN, Valentine MB et al. Fusion of a kinase gene, ALK, to a nucleolar protein gene, NPM, in non-Hodgkin's lymphoma. *Science* 1994;263:1281-1284.
65. Lenz G, Staudt LM. Aggressive lymphomas. *N.Engl.J.Med.* 2010;362:1417-1429.
66. Kuppers R, la-Favera R. Mechanisms of chromosomal translocations in B cell lymphomas. *Oncogene* 2001;20:5580-5594.
67. Raghavan SC, Swanson PC, Wu X, Hsieh CL, Lieber MR. A non-B-DNA structure at the Bcl-2 major breakpoint region is cleaved by the RAG complex. *Nature* 2004;428:88-93.
68. Tsai AG, Lu H, Raghavan SC et al. Human chromosomal translocations at CpG sites and a theoretical basis for their lineage and stage specificity. *Cell* 2008;135:1130-1142.
69. Allen CD, Okada T, Cyster JG. Germinal-center organization and cellular dynamics. *Immunity.* 2007;27:190-202.
70. Bende RJ, Smit LA, van Noesel CJ. Molecular pathways in follicular lymphoma. *Leukemia* 2007;21:18-29.
71. Lo Coco F, Ye BH, Lista F et al. Rearrangements of the BCL6 gene in diffuse large cell non-Hodgkin's lymphoma. *Blood* 1994;83:1757-1759.
72. Bastard C, Deweindt C, Kerckaert JP et al. LAZ3 rearrangements in non-Hodgkin's lymphoma: correlation with histology, immunophenotype, karyotype, and clinical outcome in 217 patients. *Blood* 1994;83:2423-2427.
73. Bergsagel PL, Kuehl WM. Chromosome translocations in multiple myeloma. *Oncogene* 2001;20:5611-5622.
74. Pasqualucci L, Neumeister P, Goossens T et al. Hypermutation of multiple proto-oncogenes in B-cell diffuse large-cell lymphomas. *Nature* 2001;412:341-346.
75. Liu M, Duke JL, Richter DJ et al. Two levels of protection for the B cell genome during somatic hypermutation. *Nature* 2008;451:841-845.
76. Jaffe ES. The 2008 WHO classification of lymphomas: implications for clinical practice and translational research. *Hematology.Am.Soc.Hematol.Educ.Program.* 2009;523-531.
77. Hunt KE, Reichard KK. Diffuse large B-cell lymphoma. *Arch.Pathol.Lab Med.* 2008;132:118-124.
78. Said J. Diffuse aggressive B-cell lymphomas. *Adv.Anat.Pathol.* 2009;16:216-235.
79. Rao PH, Houldsworth J, Dyomina K et al. Chromosomal and gene amplification in diffuse large B-cell lymphoma. *Blood* 1998;92:234-240.
80. Alizadeh AA, Eisen MB, Davis RE et al. Distinct types of diffuse large B-cell lymphoma identified by gene expression profiling. *Nature* 2000;403:503-511.
81. Rosenwald A, Wright G, Chan WC et al. The use of molecular profiling to predict survival after chemotherapy for diffuse large-B-cell lymphoma. *N.Engl.J.Med.* 2002;346:1937-1947.
82. Lossos IS, Alizadeh AA, Eisen MB et al. Ongoing immunoglobulin somatic mutation in germinal center B cell-like but not in activated B cell-like diffuse large cell lymphomas. *Proc.Natl.Acad.Sci.U.S.A* 2000;97:10209-10213.
83. Wright G, Tan B, Rosenwald A et al. A gene expression-based method to diagnose clinically distinct subgroups of diffuse large B cell lymphoma. *Proc.Natl.Acad.Sci.U.S.A* 2003;100:9991-9996.
84. Lenz G, Nagel I, Siebert R et al. Aberrant immunoglobulin class switch recombination and switch translocations in activated B cell-like diffuse large B cell lymphoma. *J.Exp.Med.* 2007;204:633-643.
85. Davis RE, Brown KD, Siebenlist U, Staudt LM. Constitutive nuclear factor kappaB activity is required for survival of activated B cell-like diffuse large B cell lymphoma cells. *J.Exp.Med.* 2001;194:1861-1874.
86. Baldwin AS. Control of oncogenesis and cancer therapy resistance by the transcription factor NF-kappaB. *J.Clin.Invest* 2001;107:241-246.
87. Rawlings DJ, Sommer K, Moreno-Garcia ME. The CARMA1 signalosome links the signalling machinery of adaptive and innate immunity in lymphocytes. *Nat.Rev.Immunol.* 2006;6:799-812.
88. Lenz G, Davis RE, Ngo VN et al. Oncogenic CARD11 mutations in human diffuse large B cell lymphoma. *Science* 2008;319:1676-1679.

89. Davis RE, Ngo VN, Lenz G et al. Chronic active B-cell-receptor signalling in diffuse large B-cell lymphoma. *Nature* 2010;463:88-92.
90. Hideshima T, Mitsiades C, Tonon G, Richardson PG, Anderson KC. Understanding multiple myeloma pathogenesis in the bone marrow to identify new therapeutic targets. *Nat.Rev.Cancer* 2007;7:585-598.
91. Mitsiades CS, Mitsiades N, Munshi NC, Anderson KC. Focus on multiple myeloma. *Cancer Cell* 2004;6:439-444.
92. Kyle RA, Rajkumar SV. Multiple myeloma. *Blood* 2008;111:2962-2972.
93. Raab MS, Podar K, Breitkreutz I, Richardson PG, Anderson KC. Multiple myeloma. *Lancet* 2009;374:324-339.
94. Ferlay J, Shin H, Bray F et al. GLOBOCAN 2008, Cancer Incidence and Mortality Worldwide. Lyon, France: IARC CancerBase No. 10 [Internet]; International Agency for Research on Cancer; 2010.
95. Landgren O, Kyle RA, Pfeiffer RM et al. Monoclonal gammopathy of undetermined significance (MGUS) consistently precedes multiple myeloma: a prospective study. *Blood* 2009;113:5412-5417.
96. Weiss BM, Abadie J, Verma P, Howard RS, Kuehl WM. A monoclonal gammopathy precedes multiple myeloma in most patients. *Blood* 2009;113:5418-5422.
97. Kyle RA, Therneau TM, Rajkumar SV et al. Prevalence of monoclonal gammopathy of undetermined significance. *N.Engl.J.Med.* 2006;354:1362-1369.
98. Kyle RA, Rajkumar SV. Monoclonal gammopathy of undetermined significance and smouldering multiple myeloma: emphasis on risk factors for progression. *Br.J.Haematol.* 2007;139:730-743.
99. Bergsagel PL, Kuehl WM. Molecular pathogenesis and a consequent classification of multiple myeloma. *J.Clin.Oncol.* 2005;23:6333-6338.
100. Munshi NC. Plasma cell disorders: an historical perspective. *Hematology.Am.Soc.Hematol.Educ.Program.* 2008;297.
101. Kyle RA, Rajkumar SV. Criteria for diagnosis, staging, risk stratification and response assessment of multiple myeloma. *Leukemia* 2009;23:3-9.
102. Chng WJ, Glebov O, Bergsagel PL, Kuehl WM. Genetic events in the pathogenesis of multiple myeloma. *Best. Pract.Res.Clin.Haematol.* 2007;20:571-596.
103. Seidl S, Kaufmann H, Drach J. New insights into the pathophysiology of multiple myeloma. *Lancet Oncol.* 2003;4:557-564.
104. Zhan F, Huang Y, Colla S et al. The molecular classification of multiple myeloma. *Blood* 2006;108:2020-2028.
105. Zhou Y, Barlogie B, Shaughnessy JD, Jr. The molecular characterization and clinical management of multiple myeloma in the post-genome era. *Leukemia* 2009;23:1941-1956.
106. Annunziata CM, Davis RE, Demchenko Y et al. Frequent engagement of the classical and alternative NF-kappaB pathways by diverse genetic abnormalities in multiple myeloma. *Cancer Cell* 2007;12:115-130.
107. Shaffer AL, Emre NC, Lamy L et al. IRF4 addiction in multiple myeloma. *Nature* 2008;454:226-231.
108. Shaffer AL, Emre NC, Romesser PB, Staudt LM. IRF4: Immunity. Malignancy! Therapy? *Clin.Cancer Res.* 2009;15:2954-2961.
109. Paget S. THE DISTRIBUTION OF SECONDARY GROWTHS IN CANCER OF THE BREAST. *The Lancet* 1889;133:571-573.
110. Mitsiades CS, Mitsiades NS, Munshi NC, Richardson PG, Anderson KC. The role of the bone microenvironment in the pathophysiology and therapeutic management of multiple myeloma: interplay of growth factors, their receptors and stromal interactions. *Eur.J.Cancer* 2006;42:1564-1573.
111. Podar K, Chauhan D, Anderson KC. Bone marrow microenvironment and the identification of new targets for myeloma therapy. *Leukemia* 2009;23:10-24.
112. Hideshima T, Bergsagel PL, Kuehl WM, Anderson KC. Advances in biology of multiple myeloma: clinical applications. *Blood* 2004;104:607-618.
113. Yasui H, Hideshima T, Richardson PG, Anderson KC. Novel therapeutic strategies targeting growth factor signalling cascades in multiple myeloma. *Br.J.Haematol.* 2006;132:385-397.

114. Teoh G, Anderson KC. Interaction of tumor and host cells with adhesion and extracellular matrix molecules in the development of multiple myeloma. *Hematol.Oncol.Clin.North Am.* 1997;11:27-42.
115. Cozzolino F, Torcia M, Aldinucci D et al. Production of interleukin-1 by bone marrow myeloma cells. *Blood* 1989;74:380-387.
116. Ehrlich LA, Chung HY, Ghobrial I et al. IL-3 is a potential inhibitor of osteoblast differentiation in multiple myeloma. *Blood* 2005;106:1407-1414.
117. Kawano M, Hirano T, Matsuda T et al. Autocrine generation and requirement of BSF-2/IL-6 for human multiple myelomas. *Nature* 1988;332:83-85.
118. Kroning H, Tager M, Thiel U et al. Overproduction of IL-7, IL-10 and TGF-beta 1 in multiple myeloma. *Acta Haematol.* 1997;98:116-118.
119. Borset M, Lien E, Espevik T et al. Concomitant expression of hepatocyte growth factor/scatter factor and the receptor c-MET in human myeloma cell lines. *J.Biol.Chem.* 1996;271:24655-24661.
120. Derksen PWB, de Gorter DJJ, Meijer HP et al. The hepatocyte growth factor/Met pathway controls proliferation and apoptosis in multiple myeloma. *Leukemia* 2003;17:764-774.
121. Ferlin M, Noraz N, Hertogh C et al. Insulin-like growth factor induces the survival and proliferation of myeloma cells through an interleukin-6-independent transduction pathway. *Br.J.Haematol.* 2000;111:626-634.
122. Podar K, Anderson KC. The pathophysiologic role of VEGF in hematologic malignancies: therapeutic implications. *Blood* 2005;105:1383-1395.
123. Derksen PWB, Tjin E, Meijer HP et al. Illegitimate WNT signaling promotes proliferation of multiple myeloma cells. *Proc.Natl.Acad.Sci.U.S.A* 2004;101:6122-6127.
124. Urashima M, Ogata A, Chauhan D et al. Transforming growth factor-beta1: differential effects on multiple myeloma versus normal B cells. *Blood* 1996;87:1928-1938.
125. Hideshima T, Chauhan D, Hayashi T et al. The biological sequelae of stromal cell-derived factor-1alpha in multiple myeloma. *Mol.Cancer Ther.* 2002;1:539-544.
126. Vanderkerken K, Vande B, I, Eizirik DL et al. Monocyte chemoattractant protein-1 (MCP-1), secreted by bone marrow endothelial cells, induces chemoattraction of 5T multiple myeloma cells. *Clin.Exp.Metastasis* 2002;19:87-90.
127. Lentzsch S, Gries M, Janz M et al. Macrophage inflammatory protein 1-alpha (MIP-1 alpha) triggers migration and signaling cascades mediating survival and proliferation in multiple myeloma (MM) cells. *Blood* 2003;101:3568-3573.
128. Giuliani N, Colla S, Lazzaretti M et al. Proangiogenic properties of human myeloma cells: production of angiopoietin-1 and its potential relationship to myeloma-induced angiogenesis. *Blood* 2003;102:638-645.
129. Barille S, Akhoundi C, Collette M et al. Metalloproteinases in multiple myeloma: production of matrix metalloproteinase-9 (MMP-9), activation of proMMP-2, and induction of MMP-1 by myeloma cells. *Blood* 1997;90:1649-1655.
130. Vacca A, Ribatti D, Presta M et al. Bone marrow neovascularization, plasma cell angiogenic potential, and matrix metalloproteinase-2 secretion parallel progression of human multiple myeloma. *Blood* 1999;93:3064-3073.
131. Roodman GD. Pathogenesis of myeloma bone disease. *Leukemia* 2009;23:435-441.
132. Sanderson RD, Epstein J. Myeloma bone disease. *J.Bone Miner.Res.* 2009;24:1783-1788.
133. Yaccoby S. Osteoblastogenesis and tumor growth in myeloma. *Leuk.Lymphoma* 2010;51:213-220.
134. Bataille R, Chappard D, Marcelli C et al. Recruitment of new osteoblasts and osteoclasts is the earliest critical event in the pathogenesis of human multiple myeloma. *J.Clin.Invest* 1991;88:62-66.
135. Roux S, Meignin V, Quillard J et al. RANK (receptor activator of nuclear factor-kappaB) and RANKL expression in multiple myeloma. *Br.J.Haematol.* 2002;117:86-92.
136. Pearce RN, Sordillo EM, Yaccoby S et al. Multiple myeloma disrupts the TRANCE/ osteoprotegerin cytokine axis to trigger bone destruction and promote tumor progression. *Proc.Natl.Acad.Sci.U.S.A* 2001;98:11581-11586.

137. Seidel C, Hjertner O, Abildgaard N et al. Serum osteoprotegerin levels are reduced in patients with multiple myeloma with lytic bone disease. *Blood* 2001;98:2269-2271.
138. Tian E, Zhan F, Walker R et al. The role of the Wnt-signaling antagonist DKK1 in the development of osteolytic lesions in multiple myeloma. *N.Engl.J.Med.* 2003;349:2483-2494.
139. Qiang YW, Chen Y, Stephens O et al. Myeloma-derived Dickkopf-1 disrupts Wnt-regulated osteoprotegerin and RANKL production by osteoblasts: a potential mechanism underlying osteolytic bone lesions in multiple myeloma. *Blood* 2008;112:196-207.
140. Richardson PG, Weller E, Lonial S et al. Lenalidomide, bortezomib, and dexamethasone combination therapy in patients with newly diagnosed multiple myeloma. *Blood* 2010;116:679-686.
141. Zarnegar R, DeFrances MC, Oliver L, Michalopoulos G. Identification and partial characterization of receptor binding sites for HGF on rat hepatocytes. *Biochem.Biophys.Res.Commun.* 1990;173:1179-1185.
142. Stoker M, Perryman M. An epithelial scatter factor released by embryo fibroblasts. *J.Cell Sci.* 1985;77:209-223.
143. Furlong RA, Takehara T, Taylor WG, Nakamura T, Rubin JS. Comparison of biological and immunochemical properties indicates that scatter factor and hepatocyte growth factor are indistinguishable. *J.Cell Sci.* 1991;100 (Pt 1):173-177.
144. Konishi T, Takehara T, Tsuji T et al. Scatter factor from human embryonic lung fibroblasts is probably identical to hepatocyte growth factor. *Biochem.Biophys.Res.Commun.* 1991;180:765-773.
145. Naldini L, Weidner KM, Vigna E et al. Scatter factor and hepatocyte growth factor are indistinguishable ligands for the MET receptor. *EMBO J.* 1991;10:2867-2878.
146. Rubin JS, Chan AM, Bottaro DP et al. A broad-spectrum human lung fibroblast-derived mitogen is a variant of hepatocyte growth factor. *Proc.Natl.Acad.Sci.U.S.A* 1991;88:415-419.
147. Weidner KM, Arakaki N, Hartmann G et al. Evidence for the identity of human scatter factor and human hepatocyte growth factor. *Proc.Natl.Acad.Sci.U.S.A* 1991;88:7001-7005.
148. Nakamura T, Nishizawa T, Hagiya M et al. Molecular cloning and expression of human hepatocyte growth factor. *Nature* 1989;342:440-443.
149. Chan AM, Rubin JS, Bottaro DP et al. Identification of a competitive HGF antagonist encoded by an alternative transcript. *Science* 1991;254:1382-1385.
150. Miyazawa K, Kitamura A, Naka D, Kitamura N. An alternatively processed mRNA generated from human hepatocyte growth factor gene. *Eur.J.Biochem.* 1991;197:15-22.
151. Cioce V, Csaky KG, Chan AM et al. Hepatocyte growth factor (HGF)/NK1 is a naturally occurring HGF/scatter factor variant with partial agonist/antagonist activity. *J.Biol.Chem.* 1996;271:13110-13115.
152. Jakubczak JL, LaRochelle WJ, Merlino G. NK1, a natural splice variant of hepatocyte growth factor/scatter factor, is a partial agonist in vivo. *Mol.Cell Biol.* 1998;18:1275-1283.
153. Hartmann G, Naldini L, Weidner KM et al. A functional domain in the heavy chain of scatter factor/hepatocyte growth factor binds the c-Met receptor and induces cell dissociation but not mitogenesis. *Proc.Natl.Acad.Sci.U.S.A* 1992;89:11574-11578.
154. Lokker NA, Mark MR, Luis EA et al. Structure-function analysis of hepatocyte growth factor: identification of variants that lack mitogenic activity yet retain high affinity receptor binding. *EMBO J.* 1992;11:2503-2510.
155. Naka D, Ishii T, Yoshiyama Y et al. Activation of hepatocyte growth factor by proteolytic conversion of a single chain form to a heterodimer. *J.Biol.Chem.* 1992;267:20114-20119.
156. Kataoka H, Kawaguchi M. Hepatocyte growth factor activator (HGFA): pathophysiological functions in vivo. *FEBS J.* 2010;277:2230-2237.
157. Miyazawa K, Shimomura T, Kitamura A et al. Molecular cloning and sequence analysis of the cDNA for a human serine protease responsible for activation of hepatocyte growth factor. Structural similarity of the protease precursor to blood coagulation factor XII. *J.Biol.Chem.* 1993;268:10024-10028.
158. Shimomura T, Kondo J, Ochiai M et al. Activation of the zymogen of hepatocyte growth factor activator by thrombin. *J.Biol.Chem.* 1993;268:22927-22932.

159. Kataoka H, Miyata S, Uchinokura S, Itoh H. Roles of hepatocyte growth factor (HGF) activator and HGF activator inhibitor in the pericellular activation of HGF/scatter factor. *Cancer Metastasis Rev.* 2003;22:223-236.
160. Mukai S, Fukushima T, Naka D et al. Activation of hepatocyte growth factor activator zymogen (pro-HGFA) by human kallikrein 1-related peptidases. *FEBS J.* 2008;275:1003-1017.
161. Suzuki K. Hepatocyte growth factor activator (HGFA): its regulation by protein C inhibitor. *FEBS J.* 2010;277:2223-2229.
162. Cooper CS, Park M, Blair DG et al. Molecular cloning of a new transforming gene from a chemically transformed human cell line. *Nature* 1984;311:29-33.
163. Park M, Dean M, Cooper CS et al. Mechanism of met oncogene activation. *Cell* 1986;45:895-904.
164. Gonzatti-Haces M, Seth A, Park M et al. Characterization of the TPR-MET oncogene p65 and the MET protooncogene p140 protein-tyrosine kinases. *Proc.Natl.Acad.Sci.U.S.A* 1988;85:21-25.
165. Comoglio PM, Giordano S, Trusolino L. Drug development of MET inhibitors: targeting oncogene addiction and expedience. *Nat.Rev.Drug Discov.* 2008;7:504-516.
166. Gentile A, Trusolino L, Comoglio PM. The Met tyrosine kinase receptor in development and cancer. *Cancer Metastasis Rev.* 2008;27:85-94.
167. Ponzetto C, Bardelli A, Zhen Z et al. A multifunctional docking site mediates signaling and transformation by the hepatocyte growth factor/scatter factor receptor family. *Cell* 1994;77:261-271.
168. Tsarfaty I, Resau JH, Rulong S et al. The met proto-oncogene receptor and lumen formation. *Science* 1992;257:1258-1261.
169. Brinkmann V, Foroutan H, Sachs M, Weidner KM, Birchmeier W. Hepatocyte growth factor/scatter factor induces a variety of tissue-specific morphogenic programs in epithelial cells. *J.Cell Biol.* 1995;131:1573-1586.
170. Bladt F, Riethmacher D, Isenmann S, Aguzzi A, Birchmeier C. Essential role for the c-met receptor in the migration of myogenic precursor cells into the limb bud. *Nature* 1995;376:768-771.
171. Schmidt C, Bladt F, Goedecke S et al. Scatter factor/hepatocyte growth factor is essential for liver development. *Nature* 1995;373:699-702.
172. Uehara Y, Minowa O, Mori C et al. Placental defect and embryonic lethality in mice lacking hepatocyte growth factor/scatter factor. *Nature* 1995;373:702-705.
173. Hu Z, Everts RP, Fujio K, Marsden ER, Thorgeirsson SS. Expression of hepatocyte growth factor and c-met genes during hepatic differentiation and liver development in the rat. *Am.J.Pathol.* 1993;142:1823-1830.
174. Kmiecik TE, Keller JR, Rosen E, Vande Woude GF. Hepatocyte growth factor is a synergistic factor for the growth of hematopoietic progenitor cells. *Blood* 1992;80:2454-2457.
175. Takai K, Hara J, Matsumoto K et al. Hepatocyte growth factor is constitutively produced by human bone marrow stromal cells and indirectly promotes hematopoiesis. *Blood* 1997;89:1560-1565.
176. Weimar IS, Miranda N, Muller EJ et al. Hepatocyte growth factor/scatter factor (HGF/SF) is produced by human bone marrow stromal cells and promotes proliferation, adhesion and survival of human hematopoietic progenitor cells (CD34+). *Exp.Hematol.* 1998;26:885-894.
177. van der Voort R, Taher TE, Keehnen RM et al. Paracrine regulation of germinal center B cell adhesion through the c-met-hepatocyte growth factor/scatter factor pathway. *J.Exp.Med.* 1997;185:2121-2131.
178. Tjin EP, Bende RJ, Derksen PW et al. Follicular dendritic cells catalyze hepatocyte growth factor (HGF) activation in the germinal center microenvironment by secreting the serine protease HGF activator. *J.Immunol.* 2005;175:2807-2813.
179. Kong-Beltran M, Stamos J, Wickramasinghe D. The Sema domain of Met is necessary for receptor dimerization and activation. *Cancer Cell* 2004;6:75-84.
180. Gherardi E, Sandin S, Petoukhov MV et al. Structural basis of hepatocyte growth factor/scatter factor and MET signalling. *Proc.Natl.Acad.Sci.U.S.A* 2006;103:4046-4051.
181. Lai AZ, Abella JV, Park M. Crosstalk in Met receptor oncogenesis. *Trends Cell Biol.* 2009;19:542-551.

182. Zhu H, Naujokas MA, Fixman ED, Torossian K, Park M. Tyrosine 1356 in the carboxyl-terminal tail of the HGF/SF receptor is essential for the transduction of signals for cell motility and morphogenesis. *J.Biol.Chem.* 1994;269:29943-29948.
183. Furge KA, Zhang YW, Vande Woude GF. Met receptor tyrosine kinase: enhanced signaling through adapter proteins. *Oncogene* 2000;19:5582-5589.
184. Eder JP, Vande Woude GF, Boerner SA, LoRusso PM. Novel therapeutic inhibitors of the c-Met signaling pathway in cancer. *Clin.Cancer Res.* 2009;15:2207-2214.
185. Boccaccio C, Comoglio PM. Invasive growth: a MET-driven genetic programme for cancer and stem cells. *Nat. Rev.Cancer* 2006;6:637-645.
186. Fan S, Ma YX, Wang JA et al. The cytokine hepatocyte growth factor/scatter factor inhibits apoptosis and enhances DNA repair by a common mechanism involving signaling through phosphatidylinositol 3' kinase. *Oncogene* 2000;19:2212-2223.
187. Xiao GH, Jeffers M, Bellacosa A et al. Anti-apoptotic signaling by hepatocyte growth factor/Met via the phosphatidylinositol 3-kinase/Akt and mitogen-activated protein kinase pathways. *Proc.Natl.Acad.Sci.U.S.A* 2001;98:247-252.
188. Zeng Q, Chen S, You Z et al. Hepatocyte growth factor inhibits anoikis in head and neck squamous cell carcinoma cells by activation of ERK and Akt signaling independent of NFKappa B. *J.Biol.Chem.* 2002;277:25203-25208.
189. Tulasne D, Foveau B. The shadow of death on the MET tyrosine kinase receptor. *Cell Death.Differ.* 2008;15:427-434.
190. Cecchi F, Rabe DC, Bottaro DP. Targeting the HGF/Met signalling pathway in cancer. *Eur.J.Cancer* 2010;46:1260-1270.
191. Di Renzo MF, Olivero M, Giacomini A et al. Overexpression and amplification of the met/HGF receptor gene during the progression of colorectal cancer. *Clin.Cancer Res.* 1995;1:147-154.
192. Schmidt L, Duh FM, Chen F et al. Germline and somatic mutations in the tyrosine kinase domain of the MET proto-oncogene in papillary renal carcinomas. *Nat.Genet.* 1997;16:68-73.
193. Fischer J, Palmado G, von KR et al. Duplication and overexpression of the mutant allele of the MET proto-oncogene in multiple hereditary papillary renal cell tumours. *Oncogene* 1998;17:733-739.
194. Olivero M, Valente G, Bardelli A et al. Novel mutation in the ATP-binding site of the MET oncogene tyrosine kinase in a HPRCC family. *Int.J.Cancer* 1999;82:640-643.
195. Schmidt L, Junker K, Nakaigawa N et al. Novel mutations of the MET proto-oncogene in papillary renal carcinomas. *Oncogene* 1999;18:2343-2350.
196. Park WS, Dong SM, Kim SY et al. Somatic mutations in the kinase domain of the Met/hepatocyte growth factor receptor gene in childhood hepatocellular carcinomas. *Cancer Res.* 1999;59:307-310.
197. Lee JH, Han SU, Cho H et al. A novel germ line juxtamembrane Met mutation in human gastric cancer. *Oncogene* 2000;19:4947-4953.
198. Michieli P, Basilico C, Pennacchietti S et al. Mutant Met-mediated transformation is ligand-dependent and can be inhibited by HGF antagonists. *Oncogene* 1999;18:5221-5231.
199. Danilkovitch-Miagkova A, Zbar B. Dysregulation of Met receptor tyrosine kinase activity in invasive tumors. *J.Clin.Invest* 2002;109:863-867.
200. Ferracini R, Di Renzo MF, Scotlandi K et al. The Met/HGF receptor is over-expressed in human osteosarcomas and is activated by either a paracrine or an autocrine circuit. *Oncogene* 1995;10:739-749.
201. Tuck AB, Park M, Sterns EE, Boag A, Elliott BE. Coexpression of hepatocyte growth factor and receptor (Met) in human breast carcinoma. *Am.J.Pathol.* 1996;148:225-232.
202. Koochekpour S, Jeffers M, Rulong S et al. Met and hepatocyte growth factor/scatter factor expression in human gliomas. *Cancer Res.* 1997;57:5391-5398.
203. Jucker M, Gunther A, Gradl G et al. The Met/hepatocyte growth factor receptor (HGFR) gene is overexpressed in some cases of human leukemia and lymphoma. *Leuk.Res.* 1994;18:7-16.

204. Weimar IS, de JD, Muller EJ et al. Hepatocyte growth factor/scatter factor promotes adhesion of lymphoma cells to extracellular matrix molecules via alpha 4 beta 1 and alpha 5 beta 1 integrins. *Blood* 1997;89:990-1000.
205. Tjin EP, Derksen PW, Kataoka H, Spaargaren M, Pals ST. Multiple myeloma cells catalyze hepatocyte growth factor (HGF) activation by secreting the serine protease HGF-activator. *Blood* 2004;104:2172-2175.
206. Choi YL, Tsukasaki K, O'Neill MC et al. A genomic analysis of adult T-cell leukemia. *Oncogene* 2007;26:1245-1255.
207. Onimaru Y, Tsukasaki K, Murata K et al. Autocrine and/or paracrine growth of aggressive ATLL cells caused by HGF and c-Met. *Int.J.Oncol.* 2008;33:697-703.
208. Konstantinou K, Yamamoto K, Ishibashi F et al. Angiogenic mediators of the angiopoietin system are highly expressed by CD10-positive lymphoma cells in angioimmunoblastic T-cell lymphoma. *Br.J.Haematol.* 2009;144:696-704.
209. Borsset M, Hjorth-Hansen H, Seidel C, Sundan A, Waage A. Hepatocyte growth factor and its receptor c-met in multiple myeloma. *Blood* 1996;88:3998-4004.
210. Capello D, Gaidano G, Gallicchio M et al. The tyrosine kinase receptor met and its ligand HGF are co-expressed and functionally active in HHV-8 positive primary effusion lymphoma. *Leukemia* 2000;14:285-291.
211. Teofili L, Di Febo AL, Pierconti F et al. Expression of the c-met proto-oncogene and its ligand, hepatocyte growth factor, in Hodgkin disease. *Blood* 2001;97:1063-1069.
212. Hsiao LT, Lin JT, Yu IT et al. High serum hepatocyte growth factor level in patients with non-Hodgkin's lymphoma. *Eur.J.Haematol.* 2003;70:282-289.
213. Elenitoba-Johnson KS, Jenson SD, Abbott RT et al. Involvement of multiple signaling pathways in follicular lymphoma transformation: p38-mitogen-activated protein kinase as a target for therapy. *Proc.Natl.Acad. Sci.U.S.A* 2003;100:7259-7264.
214. Kawano R, Ohshima K, Karube K et al. Prognostic significance of hepatocyte growth factor and c-MET expression in patients with diffuse large B-cell lymphoma. *Br.J.Haematol.* 2004;127:305-307.
215. Seidel C, Borsset M, Turesson I et al. Elevated serum concentrations of hepatocyte growth factor in patients with multiple myeloma. The Nordic Myeloma Study Group. *Blood* 1998;91:806-812.
216. Giles FJ, Vose JM, Do KA et al. Clinical relevance of circulating angiogenic factors in patients with non-Hodgkin's lymphoma or Hodgkin's lymphoma. *Leuk.Res.* 2004;28:595-604.
217. Skibinski G, Skibinska A, James K. The role of hepatocyte growth factor and its receptor c-met in interactions between lymphocytes and stromal cells in secondary human lymphoid organs. *Immunology* 2001;102:506-514.
218. Lindahl U, Kusche-Gullberg M, Kjellen L. Regulated diversity of heparan sulfate. *J.Biol.Chem.* 1998;273:24979-24982.
219. Esko JD, Lindahl U. Molecular diversity of heparan sulfate. *J.Clin.Invest* 2001;108:169-173.
220. Esko JD, Selleck SB. Order out of chaos: assembly of ligand binding sites in heparan sulfate. *Annu.Rev. Biochem.* 2002;71:435-471.
221. Bernfield M, Kokenyesi R, Kato M et al. Biology of the syndecans: a family of transmembrane heparan sulfate proteoglycans. *Annu.Rev.Cell Biol.* 1992;8:365-393.
222. Filmus J, Selleck SB. Glypicans: proteoglycans with a surprise. *J.Clin.Invest* 2001;108:497-501.
223. Iozzo RV, Cohen IR, Grassel S, Murdoch AD. The biology of perlecan: the multifaceted heparan sulphate proteoglycan of basement membranes and pericellular matrices. *Biochem.J.* 1994;302 (Pt 3):625-639.
224. Cole GJ, Halfter W. Agrin: an extracellular matrix heparan sulfate proteoglycan involved in cell interactions and synaptogenesis. *Perspect.Dev.Neurobiol.* 1996;3:359-371.
225. Iozzo RV. Basement membrane proteoglycans: from cellar to ceiling. *Nat.Rev.Mol.Cell Biol.* 2005;6:646-656.
226. Rapraeger AC. Syndecan-regulated receptor signaling. *J.Cell Biol.* 2000;149:995-998.
227. Bishop JR, Schuksz M, Esko JD. Heparan sulphate proteoglycans fine-tune mammalian physiology. *Nature* 2007;446:1030-1037.

228. Zak BM, Crawford BE, Esko JD. Hereditary multiple exostoses and heparan sulfate polymerization. *Biochim. Biophys. Acta* 2002;1573:346-355.
229. Ruoslahti E, Yamaguchi Y. Proteoglycans as modulators of growth factor activities. *Cell* 1991;64:867-869.
230. Belenkaya TY, Han C, Yan D et al. Drosophila Dpp morphogen movement is independent of dynamin-mediated endocytosis but regulated by the glypican members of heparan sulfate proteoglycans. *Cell* 2004;119:231-244.
231. Cardin AD, Weintraub HJ. Molecular modeling of protein-glycosaminoglycan interactions. *Arteriosclerosis* 1989;9:21-32.
232. Mummery RS, Rider CC. Characterization of the heparin-binding properties of IL-6. *J. Immunol.* 2000;165:5671-5679.
233. Murphy JW, Cho Y, Sachpatzidis A et al. Structural and functional basis of CXCL12 (stromal cell-derived factor-1 alpha) binding to heparin. *J. Biol. Chem.* 2007;282:10018-10027.
234. Zhou H, Mazzulla MJ, Kaufman JD et al. The solution structure of the N-terminal domain of hepatocyte growth factor reveals a potential heparin-binding site. *Structure.* 1998;6:109-116.
235. Zhou H, Casas-Finet JR, Heath CR et al. Identification and dynamics of a heparin-binding site in hepatocyte growth factor. *Biochemistry* 1999;38:14793-14802.
236. Capurro MI, Xiang YY, Lobe C, Filmus J. Glypican-3 promotes the growth of hepatocellular carcinoma by stimulating canonical Wnt signaling. *Cancer Res.* 2005;65:6245-6254.
237. Dexter TM, Spooncer E. Growth and differentiation in the hemopoietic system. *Annu. Rev. Cell Biol.* 1987;3:423-441.
238. Roberts R, Gallagher J, Spooncer E et al. Heparan sulphate bound growth factors: a mechanism for stromal cell mediated haemopoiesis. *Nature* 1988;332:376-378.
239. Bruno E, Luikart SD, Long MW, Hoffman R. Marrow-derived heparan sulfate proteoglycan mediates the adhesion of hematopoietic progenitor cells to cytokines. *Exp. Hematol.* 1995;23:1212-1217.
240. Coombe DR. The role of stromal cell heparan sulphate in regulating haemopoiesis. *Leuk. Lymphoma* 1996;21:399-406.
241. Gupta P, Oegema TR, Jr., Brazil JJ et al. Structurally specific heparan sulfates support primitive human hematopoiesis by formation of a multimolecular stem cell niche. *Blood* 1998;92:4641-4651.
242. Coombe DR. Biological implications of glycosaminoglycan interactions with haemopoietic cytokines. *Immunol. Cell Biol.* 2008;86:598-607.
243. van der Voort R, Keehnen RMJ, Beuling EA, Spaargaren M, Pals ST. Regulation of cytokine signaling by B cell antigen receptor and CD40-controlled expression of heparan sulfate proteoglycans. *J. Exp. Med.* 2000;192:1115-1124.
244. Handel TM, Johnson Z, Crown SE, Lau EK, Proudfoot AE. Regulation of protein function by glycosaminoglycans-as exemplified by chemokines. *Annu. Rev. Biochem.* 2005;74:385-410.
245. Sanderson RD, Lalor P, Bernfield M. B lymphocytes express and lose syndecan at specific stages of differentiation. *Cell Regul.* 1989;1:27-35.
246. Yamashita Y, Oritani K, Miyoshi EK et al. Syndecan-4 is expressed by B lineage lymphocytes and can transmit a signal for formation of dendritic processes. *J. Immunol.* 1999;162:5940-5948.
247. Wijdenes J, Vooijs WC, Clement C et al. A plasmacyte selective monoclonal antibody (B-B4) recognizes syndecan-1. *Br. J. Haematol.* 1996;94:318-323.
248. Derksen PWB, Keehnen RMJ, Evers LM et al. Cell surface proteoglycan syndecan-1 mediates hepatocyte growth factor binding and promotes Met signaling in multiple myeloma. *Blood* 2002;99:1405-1410.
249. Carbone A, Ghoghini A, Gattei V et al. Reed-Sternberg cells of classical Hodgkin's disease react with the plasma cell-specific monoclonal antibody B-B4 and express human syndecan-1. *Blood* 1997;89:3787-3794.
250. Sebestyen A, Berczi L, Mihalik R et al. Syndecan-1 (CD138) expression in human non-Hodgkin lymphomas. *Br. J. Haematol.* 1999;104:412-419.
251. Fux L, Ilan N, Sanderson RD, Vlodavsky I. Heparanase: busy at the cell surface. *Trends Biochem. Sci.* 2009;34:511-519.

252. Yang Y, Yaccoby S, Liu W et al. Soluble syndecan-1 promotes growth of myeloma tumors in vivo. *Blood* 2002;100:610-617.
253. Sanderson RD, Yang Y. Syndecan-1: a dynamic regulator of the myeloma microenvironment. *Clin.Exp. Metastasis* 2008;25:149-159.
254. Moreaux J, Sprynski AC, Dillon SR et al. APRIL and TACI interact with syndecan-1 on the surface of multiple myeloma cells to form an essential survival loop. *Eur.J.Haematol.* 2009;83:119-129.
255. Dai Y, Yang Y, MacLeod V et al. HSulf-1 and HSulf-2 are potent inhibitors of myeloma tumor growth in vivo. *J.Biol.Chem.* 2005;280:40066-40073.
256. Rijsewijk F, Schuermann M, Wagenaar E et al. The Drosophila homolog of the mouse mammary oncogene int-1 is identical to the segment polarity gene wingless. *Cell* 1987;50:649-657.
257. Nusse R, Varmus HE. Many tumors induced by the mouse mammary tumor virus contain a provirus integrated in the same region of the host genome. *Cell* 1982;31:99-109.
258. Logan CY, Nusse R. The Wnt signaling pathway in development and disease. *Annu.Rev.Cell Dev.Biol.* 2004;20:781-810.
259. MacDonald BT, Tamai K, He X. Wnt/beta-catenin signaling: components, mechanisms, and diseases. *Dev.Cell* 2009;17:9-26.
260. van Amerongen R., Mikels A, Nusse R. Alternative wnt signaling is initiated by distinct receptors. *Sci.Signal.* 2008;1:re9.
261. van Amerongen R., Nusse R. Towards an integrated view of Wnt signaling in development. *Development* 2009;136:3205-3214.
262. Clevers H. Wnt/beta-catenin signaling in development and disease. *Cell* 2006;127:469-480.
263. Holmen SL, Salic A, Zylstra CR, Kirschner MW, Williams BO. A novel set of Wnt-Frizzled fusion proteins identifies receptor components that activate beta -catenin-dependent signaling. *J.Biol.Chem.* 2002;277:34727-34735.
264. Tao Q, Yokota C, Puck H et al. Maternal wnt11 activates the canonical wnt signaling pathway required for axis formation in *Xenopus* embryos. *Cell* 2005;120:857-871.
265. Cha SW, Tadjuidje E, Tao Q, Wylie C, Heasman J. Wnt5a and Wnt11 interact in a maternal Dkk1-regulated fashion to activate both canonical and non-canonical signaling in *Xenopus* axis formation. *Development* 2008;135:3719-3729.
266. Barker N, Clevers H. Mining the Wnt pathway for cancer therapeutics. *Nat.Rev.Drug Discov.* 2006;5:997-1014.
267. Kawano Y, Kypta R. Secreted antagonists of the Wnt signalling pathway. *J.Cell Sci.* 2003;116:2627-2634.
268. Gong Y, Slee RB, Fukai N et al. LDL receptor-related protein 5 (LRP5) affects bone accrual and eye development. *Cell* 2001;107:513-523.
269. Boyden LM, Mao J, Belsky J et al. High bone density due to a mutation in LDL-receptor-related protein 5. *N.Engl.J.Med.* 2002;346:1513-1521.
270. Little RD, Carulli JP, Del Mastro RG et al. A mutation in the LDL receptor-related protein 5 gene results in the autosomal dominant high-bone-mass trait. *Am.J.Hum.Genet.* 2002;70:11-19.
271. Ellies DL, Viviano B, McCarthy J et al. Bone density ligand, Sclerostin, directly interacts with LRP5 but not LRP5G171V to modulate Wnt activity. *J.Bone Miner.Res.* 2006;21:1738-1749.
272. Semenov MV, He X. LRP5 mutations linked to high bone mass diseases cause reduced LRP5 binding and inhibition by SOST. *J.Biol.Chem.* 2006;281:38276-38284.
273. Ai M, Holmen SL, Van HW, Williams BO, Warman ML. Reduced affinity to and inhibition by DKK1 form a common mechanism by which high bone mass-associated missense mutations in LRP5 affect canonical Wnt signaling. *Mol.Cell Biol.* 2005;25:4946-4955.
274. Kinzler KW, Nilbert MC, Su LK et al. Identification of FAP locus genes from chromosome 5q21. *Science* 1991;253:661-665.
275. Nishisho I, Nakamura Y, Miyoshi Y et al. Mutations of chromosome 5q21 genes in FAP and colorectal cancer patients. *Science* 1991;253:665-669.

276. Korinek V, Barker N, Morin PJ et al. Constitutive transcriptional activation by a beta-catenin-Tcf complex in APC-/- colon carcinoma. *Science* 1997;275:1784-1787.
277. Miyoshi Y, Nagase H, Ando H et al. Somatic mutations of the APC gene in colorectal tumors: mutation cluster region in the APC gene. *Hum.Mol.Genet.* 1992;1:229-233.
278. Miyaki M, Konishi M, Kikuchi-Yanoshita R et al. Characteristics of somatic mutation of the adenomatous polyposis coli gene in colorectal tumors. *Cancer Res.* 1994;54:3011-3020.
279. Powell SM, Zilz N, Beazer-Barclay Y et al. APC mutations occur early during colorectal tumorigenesis. *Nature* 1992;359:235-237.
280. Liu W, Dong X, Mai M et al. Mutations in AXIN2 cause colorectal cancer with defective mismatch repair by activating beta-catenin/TCF signalling. *Nat.Genet.* 2000;26:146-147.
281. Morin PJ, Sparks AB, Korinek V et al. Activation of beta-catenin-Tcf signaling in colon cancer by mutations in beta-catenin or APC. *Science* 1997;275:1787-1790.
282. Polakis P. The many ways of Wnt in cancer. *Curr.Opin.Genet.Dev.* 2007;17:45-51.
283. Polakis P. Wnt signaling and cancer. *Genes Dev.* 2000;14:1837-1851.
284. Liu TH, Raval A, Chen SS et al. CpG island methylation and expression of the secreted frizzled-related protein gene family in chronic lymphocytic leukemia. *Cancer Res.* 2006;66:653-658.
285. Ugolini F, Charafe-Jauffret E, Bardou VJ et al. WNT pathway and mammary carcinogenesis: loss of expression of candidate tumor suppressor gene SFRP1 in most invasive carcinomas except of the medullary type. *Oncogene* 2001;20:5810-5817.
286. Mazieres J, He B, You L et al. Wnt inhibitory factor-1 is silenced by promoter hypermethylation in human lung cancer. *Cancer Res.* 2004;64:4717-4720.
287. Ai L, Tao Q, Zhong S et al. Inactivation of Wnt inhibitory factor-1 (WIF1) expression by epigenetic silencing is a common event in breast cancer. *Carcinogenesis* 2006;27:1341-1348.
288. Verbeek S, Izon D, Hofhuis F et al. An HMG-box-containing T-cell factor required for thymocyte differentiation. *Nature* 1995;374:70-74.
289. Travis A, Amsterdam A, Belanger C, Grosschedl R. LEF-1, a gene encoding a lymphoid-specific protein with an HMG domain, regulates T-cell receptor alpha enhancer function [corrected]. *Genes Dev.* 1991;5:880-894.
290. van de Wetering M, Oosterwegel M, Dooijes D, Clevers H. Identification and cloning of TCF-1, a T lymphocyte-specific transcription factor containing a sequence-specific HMG box. *EMBO J.* 1991;10:123-132.
291. Schilham MW, Wilson A, Moerer P et al. Critical involvement of Tcf-1 in expansion of thymocytes. *J.Immunol.* 1998;161:3984-3991.
292. Reya T, O'Riordan M, Okamura R et al. Wnt signaling regulates B lymphocyte proliferation through a LEF-1 dependent mechanism. *Immunity.* 2000;13:15-24.
293. Reya T, Duncan AW, Ailles L et al. A role for Wnt signalling in self-renewal of haematopoietic stem cells. *Nature* 2003;423:409-414.
294. Gounari F, Aifantis I, Khazaie K et al. Somatic activation of beta-catenin bypasses pre-TCR signaling and TCR selection in thymocyte development. *Nat.Immunol.* 2001;2:863-869.
295. Ioannidis V, Beermann F, Clevers H, Held W. The beta-catenin--TCF-1 pathway ensures CD4(+)/CD8(+) thymocyte survival. *Nat.Immunol.* 2001;2:691-697.
296. Kirstetter P, Anderson K, Porse BT, Jacobsen SE, Nerlov C. Activation of the canonical Wnt pathway leads to loss of hematopoietic stem cell repopulation and multilineage differentiation block. *Nat.Immunol.* 2006;7:1048-1056.
297. Scheller M, Huelsken J, Rosenbauer F et al. Hematopoietic stem cell and multilineage defects generated by constitutive beta-catenin activation. *Nat.Immunol.* 2006;7:1037-1047.
298. Guo Z, Dose M, Kovalovsky D et al. Beta-catenin stabilization stalls the transition from double-positive to single-positive stage and predisposes thymocytes to malignant transformation. *Blood* 2007;109:5463-5472.
299. Staal FJ, Clevers HC. WNT signalling and haematopoiesis: a WNT-WNT situation. *Nat.Rev.Immunol.* 2005;5:21-30.

- 1
300. McWhirter JR, Neuteboom ST, Wancewicz EV et al. Oncogenic homeodomain transcription factor E2A-Pbx1 activates a novel WNT gene in pre-B acute lymphoblastoid leukemia. *Proc.Natl.Acad.Sci.U.S.A* 1999;96:11464-11469.
 301. Mazieres J, You L, He B et al. Inhibition of Wnt16 in human acute lymphoblastoid leukemia cells containing the t(1;19) translocation induces apoptosis. *Oncogene* 2005;24:5396-5400.
 302. Lu D, Zhao Y, Tawatao R et al. Activation of the Wnt signaling pathway in chronic lymphocytic leukemia. *Proc. Natl.Acad.Sci.U.S.A* 2004;101:3118-3123.
 303. Howe D, Bromidge T. Variation of LEF-1 mRNA expression in low-grade B-cell non-Hodgkin's lymphoma. *Leuk. Res.* 2006;30:29-32.
 304. Gutierrez A, Jr., Tschumper RC, Wu X et al. LEF-1 is a prosurvival factor in chronic lymphocytic leukemia and is expressed in the preleukemic state of monoclonal B cell lymphocytosis. *Blood* 2010
 305. Chim CS, Pang R, Liang R. Epigenetic dysregulation of the Wnt signalling pathway in chronic lymphocytic leukaemia. *J.Clin.Pathol.* 2008;61:1214-1219.
 306. Everly DN, Jr., Kusano S, Raab-Traub N. Accumulation of cytoplasmic beta-catenin and nuclear glycogen synthase kinase 3beta in Epstein-Barr virus-infected cells. *J.Virol.* 2004;78:11648-11655.
 307. Morrison JA, Gulley ML, Pathmanathan R, Raab-Traub N. Differential signaling pathways are activated in the Epstein-Barr virus-associated malignancies nasopharyngeal carcinoma and Hodgkin lymphoma. *Cancer Res.* 2004;64:5251-5260.
 308. Hayward SD, Liu J, Fujimuro M. Notch and Wnt signaling: mimicry and manipulation by gamma herpesviruses. *Sci.STKE.* 2006;2006:re4.
 309. Kusano S, Eizuru Y. Human I-mfa domain proteins specifically interact with KSHV LANA and affect its regulation of Wnt signaling-dependent transcription. *Biochem.Biophys.Res.Commun.* 2010;396:608-613.
 310. Fujimuro M, Wu FY, ApRhyas C et al. A novel viral mechanism for dysregulation of beta-catenin in Kaposi's sarcoma-associated herpesvirus latency. *Nat.Med.* 2003;9:300-306.
 311. Qiang YW, Endo Y, Rubin JS, Rudikoff S. Wnt signaling in B-cell neoplasia. *Oncogene* 2003;22:1536-1545.
 312. Qiang YW, Walsh K, Yao L et al. Wnts induce migration and invasion of myeloma plasma cells. *Blood* 2005;106:1786-1793.
 313. Sukhdeo K, Mani M, Zhang Y et al. Targeting the beta-catenin/TCF transcriptional complex in the treatment of multiple myeloma. *Proc.Natl.Acad.Sci.U.S.A* 2007;104:7516-7521.
 314. Kobune M, Chiba H, Kato J et al. Wnt3/RhoA/ROCK signaling pathway is involved in adhesion-mediated drug resistance of multiple myeloma in an autocrine mechanism. *Mol.Cancer Ther.* 2007;6:1774-1784.
 315. Ashihara E, Kawata E, Nakagawa Y et al. beta-catenin small interfering RNA successfully suppressed progression of multiple myeloma in a mouse model. *Clin.Cancer Res.* 2009;15:2731-2738.
 316. Dutta-Simmons J, Zhang Y, Gorgun G et al. Aurora kinase A is a target of Wnt/beta-catenin involved in multiple myeloma disease progression. *Blood* 2009;114:2699-2708.
 317. Mani M, Carrasco DE, Zhang Y et al. BCL9 promotes tumor progression by conferring enhanced proliferative, metastatic, and angiogenic properties to cancer cells. *Cancer Res.* 2009;69:7577-7586.
 318. Gavriatopoulou M, Dimopoulos MA, Christoulas D et al. Dickkopf-1: a suitable target for the management of myeloma bone disease. *Expert.Opin.Ther.Targets.* 2009;13:839-848.
 319. Pinzone JJ, Hall BM, Thudi NK et al. The role of Dickkopf-1 in bone development, homeostasis, and disease. *Blood* 2009;113:517-525.
 320. Yaccoby S, Ling W, Zhan F et al. Antibody-based inhibition of DKK1 suppresses tumor-induced bone resorption and multiple myeloma growth in vivo. *Blood* 2007;109:2106-2111.
 321. Fulciniti M, Tassone P, Hideshima T et al. Anti-DKK1 mAb (BHQ880) as a potential therapeutic agent for multiple myeloma. *Blood* 2009;114:371-379.
 322. Heath DJ, Chantry AD, Buckle CH et al. Inhibiting Dickkopf-1 (Dkk1) removes suppression of bone formation and prevents the development of osteolytic bone disease in multiple myeloma. *J.Bone Miner.Res.* 2009;24:425-436.

323. Oshima T, Abe M, Asano J et al. Myeloma cells suppress bone formation by secreting a soluble Wnt inhibitor, sFRP-2. *Blood* 2005;106:3160-3165.
324. Chim CS, Pang R, Fung TK, Choi CL, Liang R. Epigenetic dysregulation of Wnt signaling pathway in multiple myeloma. *Leukemia* 2007;21:2527-2536.
325. Jost E, Gezer D, Wilop S et al. Epigenetic dysregulation of secreted Frizzled-related proteins in multiple myeloma. *Cancer Lett.* 2009;281:24-31.
326. Derycke LD, Bracke ME. N-cadherin in the spotlight of cell-cell adhesion, differentiation, embryogenesis, invasion and signalling. *Int.J.Dev.Biol.* 2004;48:463-476.
327. Gumbiner BM. Regulation of cadherin-mediated adhesion in morphogenesis. *Nat.Rev.Mol.Cell Biol.* 2005;6:622-634.
328. Shapiro L, Weis WI. Structure and biochemistry of cadherins and catenins. *Cold Spring Harb.Perspect.Biol.* 2009;1:a003053.
329. Mariotti A, Perotti A, Sessa C, Ruegg C. N-cadherin as a therapeutic target in cancer. *Expert.Opin.Investig. Drugs* 2007;16:451-465.
330. Zhang Y, Sivasankar S, Nelson WJ, Chu S. Resolving cadherin interactions and binding cooperativity at the single-molecule level. *Proc.Natl.Acad.Sci.U.S.A* 2009;106:109-114.
331. Stemmler MP. Cadherins in development and cancer. *Mol.Biosyst.* 2008;4:835-850.
332. Pokutta S, Herrenknecht K, Kemler R, Engel J. Conformational changes of the recombinant extracellular domain of E-cadherin upon calcium binding. *Eur.J.Biochem.* 1994;223:1019-1026.
333. Haussinger D, Ahrens T, Sass HJ et al. Calcium-dependent homoassociation of E-cadherin by NMR spectroscopy: changes in mobility, conformation and mapping of contact regions. *J.Mol.Biol.* 2002;324:823-839.
334. Hatta K, Takeichi M. Expression of N-cadherin adhesion molecules associated with early morphogenetic events in chick development. *Nature* 1986;320:447-449.
335. Marie PJ. Role of N-cadherin in bone formation. *J.Cell Physiol* 2002;190:297-305.
336. Tuan RS. Cellular signaling in developmental chondrogenesis: N-cadherin, Wnts, and BMP-2. *J.Bone Joint Surg.Am.* 2003;85-A Suppl 2:137-141.
337. Stains JP, Civitelli R. Cell-cell interactions in regulating osteogenesis and osteoblast function. *Birth Defects Res.C.Embryo.Today* 2005;75:72-80.
338. Ferrari SL, Traianedes K, Thorne M et al. A role for N-cadherin in the development of the differentiated osteoblastic phenotype. *J.Bone Miner.Res.* 2000;15:198-208.
339. Hay E, Lemonnier J, Modrowski D et al. N- and E-cadherin mediate early human calvaria osteoblast differentiation promoted by bone morphogenetic protein-2. *J.Cell Physiol* 2000;183:117-128.
340. Hunter I, McGregor D, Robins SP. Caspase-dependent cleavage of cadherins and catenins during osteoblast apoptosis. *J.Bone Miner.Res.* 2001;16:466-477.
341. Zhang J, Niu C, Ye L et al. Identification of the haematopoietic stem cell niche and control of the niche size. *Nature* 2003;425:836-841.
342. Hosokawa K, Arai F, Yoshihara H et al. Function of oxidative stress in the regulation of hematopoietic stem cell-niche interaction. *Biochem.Biophys.Res.Commun.* 2007;363:578-583.
343. Hosokawa K, Arai F, Yoshihara H et al. Cadherin-based adhesion is a potential target for niche manipulation to protect hematopoietic stem cells in adult bone marrow. *Cell Stem Cell* 2010;6:194-198.
344. Hooper AT, Butler J, Petit I, Rafii S. Does N-cadherin regulate interaction of hematopoietic stem cells with their niches? *Cell Stem Cell* 2007;1:127-129.
345. Haug JS, He XC, Grindley JC et al. N-cadherin expression level distinguishes reserved versus primed states of hematopoietic stem cells. *Cell Stem Cell* 2008;2:367-379.
346. Kiel MJ, Radice GL, Morrison SJ. Lack of evidence that hematopoietic stem cells depend on N-cadherin-mediated adhesion to osteoblasts for their maintenance. *Cell Stem Cell* 2007;1:204-217.

- 1
347. Kiel MJ, Acar M, Radice GL, Morrison SJ. Hematopoietic stem cells do not depend on N-cadherin to regulate their maintenance. *Cell Stem Cell* 2009;4:170-179.
 348. Li P, Zon LI. Resolving the controversy about N-cadherin and hematopoietic stem cells. *Cell Stem Cell* 2010;6:199-202.
 349. Luo Y, Radice GL. N-cadherin acts upstream of VE-cadherin in controlling vascular morphogenesis. *J.Cell Biol.* 2005;169:29-34.
 350. Blaschuk OW, Devery E. Cadherins as novel targets for anti-cancer therapy. *Eur.J.Pharmacol.* 2009;625:195-198.
 351. Islam S, Carey TE, Wolf GT, Wheelock MJ, Johnson KR. Expression of N-cadherin by human squamous carcinoma cells induces a scattered fibroblastic phenotype with disrupted cell-cell adhesion. *J.Cell Biol.* 1996;135:1643-1654.
 352. Nieman MT, Prudoff RS, Johnson KR, Wheelock MJ. N-cadherin promotes motility in human breast cancer cells regardless of their E-cadherin expression. *J.Cell Biol.* 1999;147:631-644.
 353. Hazan RB, Phillips GR, Qiao RF, Norton L, Aaronson SA. Exogenous expression of N-cadherin in breast cancer cells induces cell migration, invasion, and metastasis. *J.Cell Biol.* 2000;148:779-790.
 354. Suyama K, Shapiro I, Guttman M, Hazan RB. A signaling pathway leading to metastasis is controlled by N-cadherin and the FGF receptor. *Cancer Cell* 2002;2:301-314.
 355. Kim JB, Islam S, Kim YJ et al. N-Cadherin extracellular repeat 4 mediates epithelial to mesenchymal transition and increased motility. *J.Cell Biol.* 2000;151:1193-1206.
 356. Tsutsui J, Moriyama M, Arima N et al. Expression of cadherin-catenin complexes in human leukemia cell lines. *J.Biochem.* 1996;120:1034-1039.
 357. Matsuyoshi N, Toda K, Imamura S. N-cadherin expression in human adult T-cell leukemia cell line. *Arch.Dermatol. Res.* 1998;290:223-225.
 358. Kawamura-Kodama K, Tsutsui J, Suzuki ST, Kanzaki T, Ozawa M. N-cadherin expressed on malignant T cell lymphoma cells is functional, and promotes heterotypic adhesion between the lymphoma cells and mesenchymal cells expressing N-cadherin. *J.Invest Dermatol.* 1999;112:62-66.
 359. Makagiansar IT, Yusuf-Makagiansar H, Ikesue A et al. N-cadherin involvement in the heterotypic adherence of malignant T-cells to epithelia. *Mol.Cell Biochem.* 2002;233:1-8.
 360. Nygren MK, en-Dahl G, Stubberud H et al. beta-catenin is involved in N-cadherin-dependent adhesion, but not in canonical Wnt signaling in E2A-PBX1-positive B acute lymphoblastic leukemia cells. *Exp.Hematol.* 2009;37:225-233.
 361. Dalton W, Anderson KC. Synopsis of a roundtable on validating novel therapeutics for multiple myeloma. *Clin. Cancer Res.* 2006;12:6603-6610.
 362. Radl J, De Glopper ED, Schuit HR, Zurcher C. Idiopathic paraproteinemia. II. Transplantation of the paraprotein-producing clone from old to young C57BL/KaLwRij mice. *J.Immunol.* 1979;122:609-613.
 363. Radl J, Croese JW, Zurcher C, Van den Eenden-Vieveen MH, de Leeuw AM. Animal model of human disease. Multiple myeloma. *Am.J.Pathol.* 1988;132:593-597.
 364. Vanderkerken K, Asosingh K, Croucher P, Van CB. Multiple myeloma biology: lessons from the 5TMM models. *Immunol.Rev.* 2003;194:196-206.
 365. Sainz IM, Isordia-Salas I, Espinola RG et al. Multiple myeloma in a murine syngeneic model: modulation of growth and angiogenesis by a monoclonal antibody to kininogen. *Cancer Immunol.Immunother.* 2006;55:797-807.
 366. Cheung WC, Kim JS, Linden M et al. Novel targeted deregulation of c-Myc cooperates with Bcl-X(L) to cause plasma cell neoplasms in mice. *J.Clin.Invest* 2004;113:1763-1773.
 367. Linden M, Kirchhof N, Kvitrud M, Van NB. ABL-MYC retroviral infection elicits bone marrow plasma cell tumors in Bcl-X(L) transgenic mice. *Leuk.Res.* 2005;29:435-444.
 368. Carrasco DR, Sukhdeo K, Protopopova M et al. The differentiation and stress response factor XBP-1 drives multiple myeloma pathogenesis. *Cancer Cell* 2007;11:349-360.
 369. Chesi M, Robbani DF, Sebag M et al. AID-dependent activation of a MYC transgene induces multiple myeloma in a conditional mouse model of post-germinal center malignancies. *Cancer Cell* 2008;13:167-180.

370. Feo-Zuppari FJ, Taylor CW, Iwato K et al. Long-term engraftment of fresh human myeloma cells in SCID mice. *Blood* 1992;80:2843-2850.
371. Pilarski LM, Hipperson G, Seeberger K et al. Myeloma progenitors in the blood of patients with aggressive or minimal disease: engraftment and self-renewal of primary human myeloma in the bone marrow of NOD SCID mice. *Blood* 2000;95:1056-1065.
372. Urashima M, Chen BP, Chen S et al. The development of a model for the homing of multiple myeloma cells to human bone marrow. *Blood* 1997;90:754-765.
373. Yaccoby S, Barlogie B, Epstein J. Primary myeloma cells growing in SCID-hu mice: a model for studying the biology and treatment of myeloma and its manifestations. *Blood* 1998;92:2908-2913.
374. Yata K, Yaccoby S. The SCID-rab model: a novel in vivo system for primary human myeloma demonstrating growth of CD138-expressing malignant cells. *Leukemia* 2004;18:1891-1897.
375. Mitsiades CS, Mitsiades NS, Bronson RT et al. Fluorescence imaging of multiple myeloma cells in a clinically relevant SCID/NOD in vivo model: biologic and clinical implications. *Cancer Res.* 2003;63:6689-6696.

2

Functional analysis of HGF/MET signaling and aberrant HGF-activator expression in diffuse large B cell lymphoma

Esther P.M. Tjin, Richard W.J. Groen, Irma Vogelzang, Patrick W. B. Derksen, Melanie D. Klok, Helen P. Meijer, Susanne van Eeden, Steven T. Pals and Marcel Spaargaren.

Department of Pathology, Academic Medical Center, Amsterdam, The Netherlands.

Blood. 2006; 107(2): 760-8

Abstract

2 Inappropriate activation of MET, the receptor tyrosine kinase for hepatocyte growth factor (HGF), has been implicated in tumorigenesis. Although we have previously shown that HGF/MET signaling controls survival and proliferation of multiple myeloma (MM), its role in the pathogenesis of other B cell malignancies has remained largely unexplored. Here, we have examined a panel of 110 B cell malignancies for MET expression, which, apart from MM (48%), was found to be largely confined to diffuse large B cell lymphomas (DLBCL) (30%). No amplification of the MET gene was found, however, mutational analysis revealed two germline missense mutations: R1166Q in the tyrosine kinase domain in one patient, and R988C in the juxtamembrane domain in four patients. The R988C mutation has recently been shown to enhance tumorigenesis. In MET-positive DLBCL cells, HGF induces MEK-dependent activation of ERK and PI3K-dependent phosphorylation of PKB, GSK3 and FOXO3a. Furthermore, HGF induces PI3K-dependent $\alpha4\beta1$ integrin-mediated adhesion to VCAM-1 and fibronectin. Within the tumor-microenvironment of DLBCL, HGF is provided by macrophages, whereas DLBCL cells themselves produce the serine protease HGF activator (HGFA), which autocatalyzes HGF activation. Taken together, these data indicate that HGF/MET-signaling, and secretion of HGFA by DLBCL cells contributes to lymphomagenesis in DLBCL.

Introduction

B cell lymphomas represent the malignant counterparts of normal B cells, arrested at specific maturational stages. They are classified into distinct disease categories based on their stage-specific morphological features, molecular profile, and B cell receptor (BCR) configuration¹. The initial step in lymphomagenesis is the acquisition of a genetic aberration, most often a chromosomal translocation involving a proto-oncogene, causing an increased lifespan and/or enhanced proliferation². In general, this event per se is not tumorigenic but further (multiple) genetic alterations are required for the development of a fully malignant phenotype. In addition to these oncogenic events, B cell malignancies require signals from the microenvironment for their growth, survival and progression. These signals, which include B cell receptor (BCR) stimulation by antigen³, direct physical contact of (malignant) B cells with stromal cells via integrin adhesion receptors⁴⁻⁷, as well as a number of cytokine/growth factors⁸, activate intracellular signaling cascades and present potential targets for therapeutic intervention. One of the candidate growth factors in B cell malignancies is hepatocyte growth factor (HGF)⁹⁻¹¹.

HGF induces complex biological responses in target cells, including adhesion, motility, growth, survival and morphogenesis by activating the tyrosine kinase receptor MET. HGF/MET signaling is indispensable for mammalian development, while uncontrolled activation of MET is oncogenic, and has been implicated in the growth, invasion, and metastasis of a variety of tumors^{12,13}. Several distinct mechanisms may underlie uncontrolled MET activation. These include translocation, amplification or mutation of the MET gene^{12,14-19}, and autocrine- or paracrine HGF production^{14,20,21}.

In B cells, the HGF/MET pathway has been implicated in differentiation, specifically in the regulation of adhesion and migration^{13,22}. We have previously demonstrated that the MET protein is expressed on GC B cells²², whereas follicular dendritic cells (FDC) and stromal cells express HGF^{22,23}. Furthermore, we and others have identified the HGF/MET pathway as a potentially important signaling route in lymphomagenesis^{9,13,24,25}. In several B cell malignancies, including multiple myeloma (MM)^{24,26,27}, primary effusion lymphoma (PEL)²⁸ and Hodgkin's lymphoma (HL)⁹, co-expression of HGF and MET has been observed, suggesting autocrine activation of HGF/MET signaling. Furthermore, in MM, HL and diffuse large B cell lymphoma (DLBCL), elevated serum HGF levels correlate with unfavorable prognosis⁹⁻¹¹. Moreover, we have recently shown that HGF induces a potent proliferative and anti-apoptotic response in MM cell lines and primary MMs^{24,29}. Together with our observation that MM cells themselves produce the serine protease HGF activator (HGFA), and thereby are able to autocatalyze HGF activation³⁰, the above data suggest an important role for the HGF/MET pathway in the pathogenesis of MM. To examine the possible role of HGF/MET in the pathogenesis of other B cell malignancies, we have studied the expression of MET and HGF in a large panel of B cell malignancies, including all major B-cell non-Hodgkin lymphoma (B-NHL) subtypes, and we analyzed the MET gene in MET-positive lymphomas for the presence of amplification and mutations. Furthermore, we have defined the role of the HGF/MET pathway, including HGFA, in the most common type of B-NHL, *i.e.* DLBCL.

Materials and Methods

Antibodies and reagents

2

Mouse monoclonal antibodies used were: anti-CD68 (IgG1); anti-CD21L (DRC-1, IgM); FITC-conjugated anti-IgD (all DAKO, Carpinteria, CA); anti-MET, DO24 (IgG2a)(Upstate Biotechnology, Lake Placid, NY)(IgG1); APC-conjugated anti-CD38 (IgG1)(BD Biosciences, Erembodegem, Belgium); anti-HGFA A-1 (IgG1) and P1-4 (IgG1)³¹; anti-factor XIIa, OT-2 (IgG1) (Sanquin, Amsterdam, The Netherlands); anti-CD20 (L26) (DAKO, Glostrup, Denmark); fluorescein isothiocyanate (FITC)-conjugated anti-human IgD (DAKO); allophycocyanin (APC)-conjugated anti-human CD38 (IgG1) (BD Biosciences); phycoerythrin (PE)-conjugated anti-human CD20 (DAKO); and antibodies against the integrin subunit $\alpha 4$ (CD49d) (HP2/1, IgG1) (Immunotech, Marseille, France) and $\alpha 4\beta 7$ (Act-1, IgG1)³² (a gift from A. Lazarovits, University of Western Ontario, London, Canada). Polyclonal antibodies used were: goat anti-human HGF (R&D Systems, Abingdon, UK), rabbit anti-MET (C12), rabbit anti-PKB, rabbit anti-ERK1 and -2 (all from Santa Cruz, Biotechnology, Santa Cruz, CA); AP-conjugated goat anti-mouse; biotin-conjugated rabbit anti-mouse (both DAKO); RPE-conjugated rabbit anti-mouse IgG2a (BD Biosciences); AP-conjugated anti-digoxigenin (Roche, Almere, The Netherlands) HRP-conjugated swine anti-goat (Biosource, Camarillo, CA); HRP-conjugated rabbit anti-mouse (DAKO). Antibodies against phosphorylated MET pY^{1230/1234/1235} (Biosource, Camarillo, CA); phospho-FOXO3a (FKHRL1, Thr32) (Upstate, Charlottesville, Virginia); rabbit anti-phospho-GSK3 a/b (Ser21 and Ser9); rabbit anti-phospho PKB/AKT (Ser 473); rabbit anti-phospho p44/42 MAP kinase (Thr 202/Tyr 204) (all from Cell Signaling, Beverly, MA). Reagents used were: recombinant HGF (ReliaTech GmbH, Braunschweig, Germany); recombinant single chain HGF (R&D Systems); the PI3K inhibitors LY294002 and Wortmannin; the MEK inhibitor PD98059 (both Biomol, Plymouth Meeting, PA).

B cell tumors and DLBCL cell lines

Tissue samples of 89 cases of B-NHL and 21 cases of MM were obtained during standard diagnostic procedure at the Academic Medical Center Amsterdam, The Netherlands and the University Medical Center Utrecht (UMCU, Utrecht, The Netherlands), and frozen at -80°C until further use. Mononuclear cells from BM-derived MM samples were obtained by standard Ficoll-Paque density gradient centrifugation (Amersham Pharmacia, Uppsala, Sweden). All B cell malignancies were classified according to the WHO classification¹. DLBCLs cell lines OCI-LY-1, -3, -7 and -18 were cultured in Iscove's medium (Life Technologies, Breda, The Netherlands) supplemented with 10 % fetal calf serum (FCS) (Hyclone Laboratories, Logan, UT), penicillin (50 U/ml), streptomycin (50 mg/ml) (both from Life Technologies). DLBCLs cell line OCI-LY-10 was cultured in the presence of 20% FCS, penicillin, streptomycin and b-mercaptoethanol (55 mM). OCI-LY-1, -7 and -18 were kindly provided by Dr. U. Klein (Institute for Cancer Genetics, Colombia University, NY); OCI-LY-3 and -10 were kindly provided by Dr. R. Küppers (Institute for Genetics and Department of Internal Medicine, University of Cologne, Germany). B cells were purified from human tonsils obtained from children undergoing routine tonsillectomy as described⁷. Briefly, mononuclear cells were isolated by Ficoll-Isopaque density gradient centrifugation (Amersham Pharmacia, Uppsala,

Sweden). Monocytes and T cells were depleted by plastic adherence and sheep red blood cells rosetting, respectively. The B cell fraction was >97% pure and contained \approx 60% naïve B cells and \approx 35% GC B cells as determined by FACS analysis using FITC-conjugated anti-human IgD, PE-conjugated anti-human CD20 and APC-conjugated anti-CD38. To obtain GC B cells, total B cells were stained with FITC-conjugated anti-human IgD, PE-conjugated anti-human CD20 and APC-conjugated anti-CD38 and sorted using a FACS aria (BD).

Single stranded conformation polymorphism (SSCP)

High molecular weight genomic DNA was obtained employing standard methods by lysis in SDS, proteinase K digestion, phenol-chloroform extraction and ethanol precipitation (all Sigma, Bornem, Belgium). PCR was performed by amplifying exon 14, and 16 to 19 of MET, using intron-specific primers as described¹⁶. Integrity of the DNA was confirmed through amplification of the b-globin gene using primers pair GH20/PCO4. The radioactive PCR amplification was carried out in a 30 ml reaction mixture containing 200 ng of genomic DNA, 10 mM Tris-HCl (pH 8.3), 50 mM KCl, 1.5 mM MgCl₂, 10 mM of dATP, dTTP, and dGTP, 15 pmol of primer, 1.5 mCi [a³²P] dCTP (Amersham Pharmacia) and 0.3 U of Taq DNA polymerase (Life Technologies). Following PCR, samples were diluted 1:7 in loading buffer (10 mM EDTA, pH 8.0, 0.05% SDS, 95% de-ionized formamid, 0.25% bromophenolblue, and 0.25% xylene cyanodie FF (all Sigma), denatured for 3 min. at 95 °C, and slowly cooled to 4 °C (1 °C / sec). Samples were loaded onto a 8% non-denaturing, 1x TBE acrylamide:bisacrylamide gel (50:1) (Life Technologies), containing 10% glycerol (Sigma), and run in for 16 hours at 8 Watts. Aberrant migrating amplicons were excised from the gel, re-amplified using Pfu DNA polymerase (Stratagene, La Jolla, CA), cloned into EcoRV-digested pZerO (Life Technologies), and sequenced using M13 primers and big-dye terminators (Amersham Pharmacia). Nucleotide and amino-acid numbering of MET was done according to the MET sequence as described by Schmidt et al¹⁶.

Immunohisto- and cytochemistry

Immunohistochemical stainings were performed as described previously³³ on acetone-fixed cryostat sections (MET and DRC-1) or formalin fixed paraffin embedded sections (CD68). Substrate was developed with either 3,3-diaminobenzidine (Sigma) (anti-MET and CD68 staining), or fast blue BB (DAKO)(anti-CD21L, DRC-1) staining. Immunocytochemical stainings were performed on acetone-fixed cytopsins. The cytopsins were preincubated with 1% bovine serum albumin (BSA) (Sigma) in PBS for 15 minutes. After incubating with the primary antibody (overnight at 4 °C), endogenous peroxidase was blocked with 0.1% NaN₃ and 0.3% H₂O₂ in PBS for 10 minutes. Subsequently, the cytopsins were stained with post-antibody of Powervision (Immunovision Technologies, Duiven, The Netherlands) for 15 minutes, followed by poly-HRP conjugated goat anti-mouse/rabbit IgG for 30 minutes. Substrate was developed with 3,3-amino-9-ethylcarbazole. The immunohistochemical stainings were examined by use of an Olympus BX51 microscope (Olympus Optical, Hamburg, Germany) with a 40/0.85 objective. Images were acquired by an Olympus DP11 camera and processed with Adobe Photoshop 7.

Assay for HGF activation

HGF activation was assayed as described previously³⁴. Conditioned medium was obtained as described previously³⁵. In brief, 20 ml DLBCL conditioned medium was pretreated with 1 unit of thrombin (Sigma Aldrich Chemie GmbH, Germany) and added to 0.1 mg single chain HGF. Inhibitor studies were done in the presence of leupeptin (500 mg/ml) (Sigma), or neutralizing antibody against HGFA (P1-4) (40 mg/ml).

ELISA for HGF

Conditioned medium of DLBCL cell lines or, as positive controls, of MM cell line UM-3 and follicular dendritic cells was used to detect the production of HGF²². The ELISA kit for HGF was used according to the manufacturer's instructions (R&D Systems). The lower detection limit was 125 pg/ml.

Immunoblot analysis

Immunoblotting was performed as described³³. For signaling experiments, cells were serum-starved for 2 hours and lysed after the indicated treatments. The samples were analyzed by SDS-PAGE. The phosphorylation of MET, PKB, FOXO3a, GSK3 and ERK1 and -2 was examined by phosphorylation-state specific antibodies. After stripping, the same blot was restained with antibodies against MET, PKB and ERK. The samples of the HGF conversion assay or DLBCL cell lines were also analyzed by SDS-PAGE. The immunoblots were stained with anti-HGF or anti-HGFA (A-1) and detected with HRP-conjugated swine anti-goat and HRP-conjugated rabbit anti-mouse, respectively.

Cell adhesion assay

Adhesion assays were done essentially as described³⁶. Briefly, 96-well plates were coated with 1 mg/ml soluble vascular cell adhesion molecule-1 (VCAM-1) (R&D Systems) or 10 mg/ml foreskin fibronectin (FN) (Sigma). 1.5×10^5 cells were pre-incubated for 30 min at 4°C in the presence or absence of either 1 mg/ml anti- $\alpha 4\beta 1$ or 3 mg/ml anti- $\alpha 4\beta 7$ integrin antibodies, or at 37°C with inhibitors. Next, the cells were plated in the absence or presence of recombinant HGF (ReliaTech GmbH) or phorbol-12-myristate-13-acetate (PMA) (Sigma) in 100 μ l/well, and incubated at 37 °C for 30 minutes. The adherent cells were stained with crystal violet, washed, the dye was eluted and absorbance was measured on a spectrophotometer (Microplate Reader 450, Biorad). Background absorbance (no cells added) was subtracted. Maximal adhesion (= 100%) was determined by measuring non-specific adhesion to poly L-lysine-coated wells.

RNA isolation, cDNA synthesis and reverse transcriptase-PCR

RNA isolation and cDNA synthesis was done as described previously²². Primers used were: HGFA forward (5'-AGGACACAAGTGCCAGATTG-3'); HGFA reverse (5'-GTTGATCCAGTCCACACATAGT-3'); MET forward (5'-GAGACTCATAATCCAACCTG-3'); MET reverse (5'-AGCATACAGTTTCTTGCAG-3'); HGF forward (5'-CAGCATGTCCTCCTGCATCTCC-3') and HGF reverse (5'-TCGTGTGGTATCATGGAACCTCC-3').

HGF mRNA in situ hybridization

Snap-frozen tissues were collected and frozen at -80°C until further use. 10 mm thick sections were cut, recovered on silianized slides, fixed for 15 minutes in 4% paraformaldehyde in PBS, dehydrated using ethanol, dried overnight and stored at -20°C . Before use, tissue sections were re-hydrated, washed in PBS and incubated for 10 minutes in PBS containing 0.1 M glycine (Sigma). Sections were permeabilized for 15 minutes in 10 $\mu\text{g}/\text{ml}$ proteinase K (Roche), after which the sections were washed three times with PBS, treated with 4% PFA/PBS for 10 minutes and washed with 4x SSC. Acetylation was done using acetic acid anhydride and triethanolamidehydrochlorid for 15 minutes and pre-hybridized in hybridization mixture (50% formamid, 5x SSC, 5x Denhardt's, 25 $\mu\text{g}/\text{ml}$ baker's yeast tRNA, 500 $\mu\text{g}/\text{ml}$ herring sperm DNA) for 1 hour. cRNA probes were synthesized as run-off transcripts using either T3 or T7 RNA polymerase and a digoxigenin RNA labeling kit (Roche). Probes were made from an 847 bp human HGF EcoR1 cDNA fragment (nt 186-1033, kindly provided by Dr W. Birchmeier, MDC, Berlin, Germany) in pBSSK⁺. Overnight hybridization was done at 58°C . After hybridization, the slides were rinsed with 4x SSC/50% formamid, and subsequently washed in 4x SSC and 1x SSC, respectively. Sections were treated with 1% PFA/PBS for 30 minutes, washed in 0.1M glycine/PBS and equilibrated in TRIC buffer (100 mM Tris, 150 mM NaCl, pH 7.5). Blocking of non-specific binding was performed in TRICB buffer (TRIC buffer containing 1% blocking reagent (Roche)). Slides were incubated with AP-conjugated antidigoxigenin antibody in TRICB buffer. Color development was done using nitro blue tetrazolium-5-bromo-4-chloro-3-indolyl phosphate (NBT/BCIP)(Roche) in color buffer (100 mM Tris, 100 mM NaCl, 50 mM MgCl_2 , pH 9.5) containing 2.4 mg/ml levamisole (Sigma).

Table 1. Expression and mutational analysis of MET in B cell tumors.

<i>WHO classification</i>	<i>n</i>	<i>% positive (n)</i>	<i>Intensity*</i>	<i># mutated/examined</i>
Precursor B lymphoblastic	3	0 (0)	-	0/3
Mantle cell	5	0 (0)	-	0/3
Follicular	15	7 (1)	2	1/15
Burkitt's	12	8 (1)	3	1/12
DLBCL	43	30 (13)	2-3	2/39
Marginal zone	3	0 (0)	-	ND
B-CLL	8	25 (2)	1	1/8
Multiple myeloma	21	48 (10)	NA (Φ)	0/21

* 1=weak, 2=moderate, 3=strong staining with a monoclonal anti-MET antibody. N=number of samples; B-CLL=B cell chronic lymphocytic leukemia; DLBCL=diffuse large B cell lymphoma. NA=non applicable. (Φ)=expression of MET by multiple myeloma was determined by western blot analysis using a polyclonal anti-MET antibody. ND=not done.

Results

MET expression in B cell malignancies

To investigate the expression of MET in B cell malignancies, a panel of 110 B cell tumors of different subtypes, representing a broad spectrum of differentiation stages ranging from precursor-B cell to plasma cell was analyzed by immunohistochemistry and/or immunoblotting. A few cases of follicular- (FL), Burkitt's- (BL), and chronic lymphocytic lymphoma (CLL) showed MET expression (Table 1), whereas MET was not detected on precursor-B cell lymphomas, mantle cell lymphomas and marginal zone lymphomas (Table 1). MET expression was largely confined to MMs (48%) and DLBCLs (30%) (Table 1). In several cases of DLBCL, which is the most common type of B cell non-Hodgkin lymphoma (B-NHL) (30-40% of cases), staining of MET was very strong (Figure 1A, right panel), indicating overexpression relative to the expression levels in normal GCs (Figure 1A, left panel).

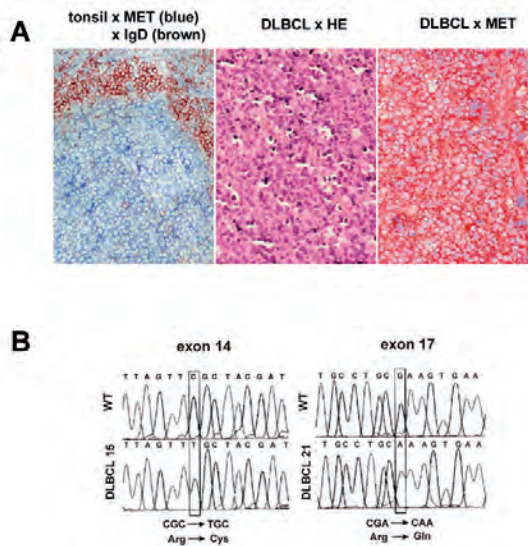


Figure 1. MET expression and missense germline MET mutations in DLBCL.

(A) MET expression in normal lymphoid tissue and primary DLBCL. Immunohistochemical double staining of tonsillar sections for MET (blue) and IgD (brown), showing MET expression on germinal center B cells (left panel). Frozen tissue sections of DLBCL were stained with haematoxylin-eosin (HE) (middle panel) or with haematoxylin and anti-MET (brown, right panel). Image magnification: 200x. **(B)** Sequence analysis showing mutational transitions. PCR products were excised, re-amplified, cloned and sequenced. Shown are wild type (WT) and mutant sequences. Mutational transitions are boxed.

MET mutations in B cell lymphomas

Amplification of the MET gene resulting in MET overexpression has been described in several types of cancer^{14,20,37}. However, Southern blot analysis using a MET-specific cDNA probe did not reveal MET gene amplification in the MET-positive lymphomas (data not shown). Furthermore, missense germline or somatic MET mutations have been found in HPRC^{16,17}, and in several other types of cancer^{18,19,38}. The affected regions

of MET are the catalytic- or the juxtamembrane (JM) domain, resulting in deregulated activation or degradation of MET, respectively^{19,39,40}. Upon HGF stimulation, cells with MET mutations in these regions display enhanced or prolonged kinase activity, resulting in transformation, invasive growth and enhanced tumor cell survival³⁹⁻⁴¹. To investigate whether MET mutations may also contribute to lymphomagenesis, we screened the tumor samples listed in table 1 for mutations in exon 14, encoding the JM region, and exon 16 to 19, encoding the tyrosine kinase and docking site regions of MET, by means of SSCP analysis. Using this approach, two distinct missense mutations were detected in MET (Figure 1B). The first was at position 2961 (C to T) in exon 14, resulting in a nonconservative transition from arginine to cysteine at position 988 (R988C), and was found in 4 individual cases of CLL, FL, BL, and DLBCL. The second mutation (3496 G to A) in exon 17, resulting in a transition from arginine to glutamine at position 1166 (R1166Q), was detected in one case of DLBCL. Analysis of normal tissues from the affected individuals revealed that these mutations were germline mutations. Noteworthy, in none of the 5 DLBCL cell lines these mutations were found (data not shown). During the course of our study, the R988C mutation was also reported in several (non-) small cell lung cancer ((N)SCLC) cell lines^{42,43}, and in 2 lung cancer patients^{42,44}. Interestingly, these studies revealed that R988C conveys enhanced *in vitro* tumorigenicity as well as lung tumor susceptibility in mice^{43,44}, indicating that R988C is a gain-of-function mutation.

2

HGF/MET signaling in DLBCL cells

Apart from MM, MET expression was largely restricted to DLBCLs (Table 1). Interestingly, in DLBCL high serum HGF levels were previously found, which were shown to be correlated with unfavorable prognosis^{10,45}. In addition, a gene-profiling study showed significantly enhanced expression of MET upon transformation of low-grade FLs into DLBCLs⁴⁶, suggesting a pathogenic role for HGF/MET signaling in tumor progression. Therefore, we decided to explore the functionality of MET signaling in DLBCL cells and to examine which signaling pathways become activated upon HGF stimulation. For this purpose, we analyzed a panel of DLBCL cell lines for MET expression. In a subset of DLBCL cell lines (3/5), expression of MET was observed at mRNA (Figure 2A) and protein level (Figure 2B). HGF stimulation resulted in enhanced phosphorylation of MET in the strongly MET-positive DLBCL cell lines OCI-LY-3 and LY-10, whereas the weakly MET-positive cell line OCI-LY-1 showed a weak response (Figure 2C). Moreover, HGF stimulation of the MET-positive cells leads to phosphorylation of the mitogen activated protein kinases ERK1 and -2, as well as to phosphorylation of PKB and of the PKB substrates GSK3 and the forkhead transcription factor FOXO3a (FKHRL1) (Figure 2C). The unrelated PI3K inhibitors Wortmannin (WM) or LY294002 (LY) both completely abrogated the HGF-induced phosphorylation of PKB, GSK3 and FOXO3a, but hardly affected the phosphorylation of ERK-1/2 (Figure 2D). *Vise versa*, the HGF-stimulated activation of ERK-1/2 was specifically blocked by the MEK inhibitor PD98059 (PD), which did not affect phosphorylation of PKB, GSK3 or FOXO3a (Figure 2D). The RAS downstream effector components MEK and ERK-1/2 have been directly linked to the regulation of cell proliferation^{47,48}, whereas PKB, GSK3 and FOXOs, targets of PI3K-derived signals, have been implicated in the both proliferation and survival^{49,50}.

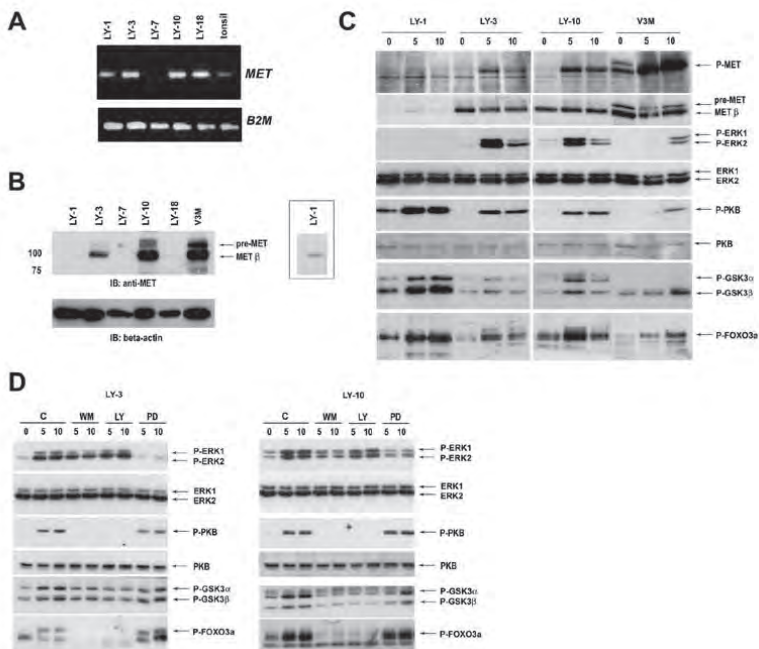


Figure 2. HGF induces phosphorylation of MET in DLBCL cells, and activates the RAS/MAPK and PI3K/PKB pathway.

(A) mRNA expression of MET in DLBCL cell lines. After RNA isolation and cDNA synthesis, RT-PCR for MET was performed. b2-microglobulin was used as housekeeping gene control. (B) MET protein expression in DLBCL cell lines. DLBCL cell lines were analyzed by immunoblotting for the expression of MET. The (weak) expression of MET by OCI-LY-1 cells is clearly demonstrated by means of a 3 times longer exposure (see inset). Staining with anti- β -actin represents the loading control. (C) HGF induces tyrosine phosphorylation of MET, PKB, FOXO3a, GSK3 and ERK. The DLBCL cells OCI-LY-1, -3 and -10 and MET transfected Namalwa cells (V3M) were stimulated with HGF for the indicated time periods. Cell lysates were immunoblotted with phosphorylation-specific antibodies against MET, FOXO3a, GSK3, PKB and ERK. The blots were stripped and restained with antibodies against MET, PKB and ERK. (D) HGF-induced phosphorylation of FOXO3a and GSK3 requires PI3K activity, whereas phosphorylation of ERK1 and -2 is MEK dependent. OCI-LY-3 and -10 cells were pretreated with the PI3K inhibitors wortmannin (WM) (50 mM) or LY294002 (LY) (20 mM), the MEK inhibitor PD98059 (PD) (50 mM), or DMSO (C) for 30 minutes, prior to incubation with HGF (200 ng/ml). Phosphorylation of ERK-1 and -2, PKB, GSK3 and FOXO3a was determined by immunoblotting with phosphorylation-specific antibodies. The blots were stripped and restained for ERK1 and -2, and PKB.

HGF induces integrin-mediated adhesion of DLBCL cells in a PI3K-dependent fashion

Previous studies, including from our laboratory, revealed that HGF/MET signaling induces survival and proliferation of MM cells^{24,29}, and can control integrin-mediated adhesion of Burkitt's lymphoma cells^{6,22} and MM cells⁵¹. Despite the activation of several survival- and proliferation-regulatory signaling proteins (Figure 2C), we did not observe an effect of HGF on the survival or proliferation of DLBCL cells (data not shown). To further define the role of HGF/MET signaling in DLBCLs, we examined whether HGF may be able to control integrin-mediated adhesion. HGF stimulation of both OCI-LY-1 and LY-10 cells strongly augmented adhesion to both VCAM-1 (Figure 3A) and FN (data not shown). In contrast,

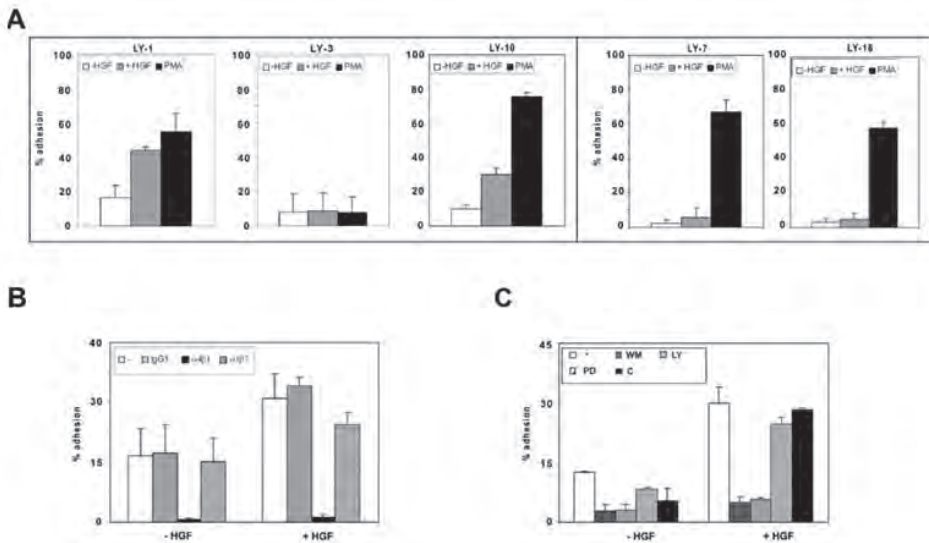


Figure 3. HGF induces $\alpha 4\beta 1$ -mediated adhesion of DLBCL cells in a PI3K-dependent fashion.

(A) HGF induces adhesion of DLBCL cell line OCI-LY-1 and LY-10 to VCAM-1. Cells were stimulated with 200 ng/ml HGF or 50 ng/ml PMA followed by adhesion to VCAM-1. The OCI-LY-3 cells displayed extensive (constitutive) cell aggregation. Neither HGF nor PMA could enhance adhesion of OCI-LY-3 (left panel). MET-negative OCI-LY-7 and LY-18 cells were used as negative controls (right panel). The results are expressed as a percentage of maximal adhesion. The bars represent the means \pm the standard deviation of a triplicate experiment representative of at least three independent experiments. **(B)** HGF-induced adhesion involves $\alpha 4\beta 1$ integrin. The effect of pre-incubation with anti- $\alpha 4\beta 1$ (HP2/1) and anti- $\alpha 4\beta 7$ (Act-1) integrin antibodies on the HGF-induced binding of DLBCL cell lines OCI-LY-10 to VCAM-1 was established. Cells were pre-incubated for 30 minutes at 4°C in the presence or absence of anti-integrin monoclonal antibodies or isotype control antibody, as indicated. Next, adhesion to VCAM-1 in the presence of 200 ng/ml HGF was measured. Error bars represent the means standard deviation of a triplicate experiment representative of two independent experiments. **(C)** HGF-induced adhesion requires PI3K activity. HGF-induced adhesion of OCI-LY-10 was determined after pretreatment with the PI3K inhibitors wortmannin (WM) (100 nM) and LY294002 (LY) (20 mM), the MEK inhibitor PD98059 (PD) (50 mM), or DMSO (C) for 30 minutes at 37°C, followed by adhesion to VCAM-1 in the presence of 200 ng/ml HGF. The bars represent the means standard deviation of a triplicate experiment representative of two independent experiments.

as expected, the MET-negative DLBCL cell lines OCI-LY-7 and -18 did not exhibit any HGF-induced adhesion (Figure 3A). Noteworthy, the OCI-LY-3 cells displayed extensive (constitutive) cell aggregation. As a consequence neither HGF nor PMA could enhance adhesion of OCI-LY-3, thus rendering this cell line useless for adhesion analysis (Figure 3A). To identify the adhesion receptors on the DLBCL cell lines responsible for the enhanced VCAM-1 binding, integrin expression analysis and antibody blocking experiments were performed. OCI-LY-1, -3 and -10 showed high expression of integrin $\alpha 4\beta 1$ but do not express $\alpha 4\beta 7$, as established by FACS analysis (data not shown). Notably, HGF treatment did not enhance $\alpha 4\beta 1$ or $\alpha 4\beta 7$ expression during the course of the adhesion assay (data not shown). The adhesion to VCAM-1 was completely blocked by the $\alpha 4\beta 1$ -blocking antibody HP2/1, whereas the $\alpha 4\beta 7$ -blocking antibody Act-1 or an isotype control antibody had no effect (Figure 3B). To investigate the functional importance of PI3K and MEK/MAPK in the HGF-induced

adhesion of DLBCL cells, we analyzed the effect of the PI3K inhibitors WM or LY, and the MEK inhibitor PD. The specificity and effectivity of these inhibitors in DLBCL cells is shown in figure 2D. Both WM and LY completely abolished the HGF-induced adhesion of OCI-LY-10 cells, whereas hardly any effect by PD was observed (Figure 3C). Hence, HGF-induced adhesion of DLBCL cells is dependent on PI3K, but not on MEK or MAPK activity. Taken together, these results show that the HGF/MET pathway controls $\alpha 4\beta 1$ integrin-mediated adhesion of DLBCL cells in a PI3K-dependent manner.

2

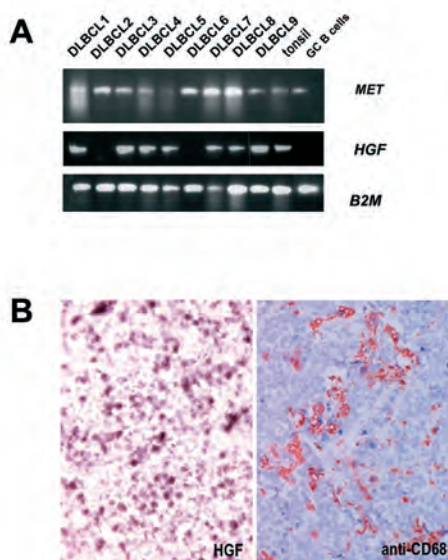


Figure 4. HGF expression in DLBCL.

(A) MET-positive primary DLBCLs were analyzed for HGF mRNA expression. After RNA isolation and cDNA synthesis, RT-PCR for MET and HGF was performed. $\beta 2$ -microglobulin was used as housekeeping gene control. (B) Frozen sections of DLBCL cases were analyzed for the presence of expression of HGF by mRNA in situ hybridization, using DIG-labeled anti-sense cRNA run-off transcripts. Serial sections were stained with anti-CD68 to identify macrophages. The section was counterstained with haematoxylin. The result shown is a representative of 8 tested DLBCL cases. Image magnification: 200x.

HGF expression in the DLBCL microenvironment

In several epithelial tumors as well as in MM, autocrine HGF secretion by tumor cells as well as paracrine HGF production by fibroblasts and macrophages in the tumor stroma is crucial for the growth and invasion of MET-positive tumor cells¹³. To investigate whether autocrine or paracrine stimulation of MET by HGF takes place in DLBCLs and is responsible for the signaling and adhesion effects observed in the DLBCL cell lines, we first studied the expression of HGF mRNA in a number of primary MET-positive DLBCL samples. RT-PCR showed HGF mRNA expression in most of the MET-positive primary DLBCL tumors (7/9) (Figure 4A). By mRNA in situ hybridization, we found that HGF was localized in single cells and small cell clusters within the DLBCLs (n=8). Staining of serial sections with anti-CD68 showed a similar staining pattern, suggesting that these cells were (activated) macrophages (Figure 4B). Furthermore, analysis of the conditioned medium of the DLBCL cell lines by

means of HGF ELISA did not reveal any autocrine production of HGF (data not shown). Our findings suggest that DLBCL cells are stimulated via a paracrine rather than via an autocrine mechanism.

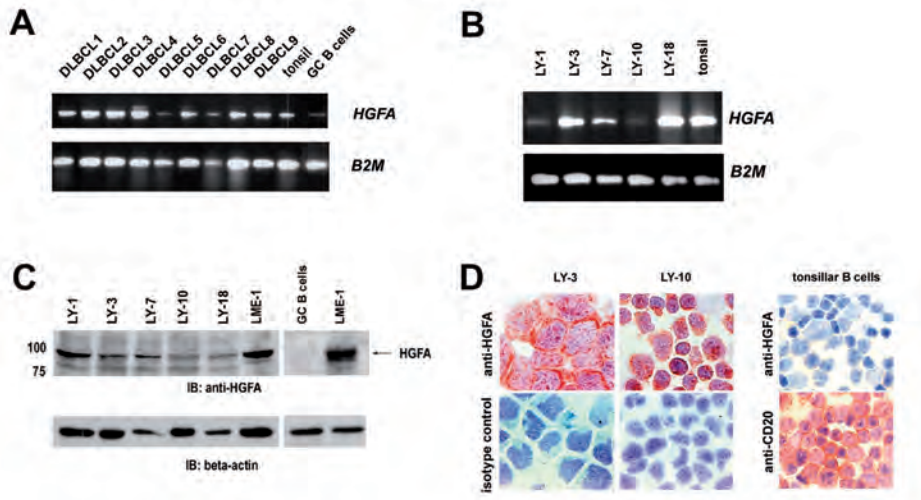


Figure 5. HGFA expression in DLBCL cells.

(A) Expression of HGFA in GC B cells and primary DLBCLs at mRNA level. After RNA isolation and cDNA synthesis, RT-PCR for MET was performed. β 2-microglobulin was used as housekeeping gene control. (B) mRNA expression of HGFA in DLBCL cell lines. (C) HGFA protein is expressed in DLBCL cell lines, but not in GC B cells. Cell lysates were immunoblotted using a monoclonal anti-HGFA antibody (A-1). MM cell line LME-1 was used as positive control. β -actin was used as loading control. (D) Expression of HGFA protein in DLBCL lines and tonsillar B cells by immunocytochemical staining. DLBCL- and tonsillar B cells were immunocytochemically stained with mAb A-1 against HGFA (A-1), CD20 (L26) or isotype control, as indicated. Image magnification: 400x.

DLBCL cells activate HGF by secretion of HGFA

The serine protease HGFA has been shown to mediate proteolytic conversion of single-chain HGF (scHGF, HGF precursor) to its active heterodimeric form³¹, which is essential for the activation and biological function of HGF⁵². HGFA, a factor Xlla-related serine protease has been identified as the most potent activator of HGF³¹. We have previously demonstrated that MM plasma cells produce HGFA, and in this way may activate HGF in the bone marrow microenvironment³⁰. To assess whether HGFA is expressed and mediates HGF conversion in DLBCLs, we evaluated the expression of HGFA in MET-positive DLBCLs and cell lines. Interestingly, all primary DLBCLs and cell lines expressed HGFA mRNA (Figure 5A and B). Moreover, contrary to normal tonsillar naïve-, GC- or memory B cells, which do not or very weakly express HGFA⁵³ (Figure 5C), the DLBCL cells express HGFA protein (Figure 5C and D). Subsequently, we examined whether DLBCL cells are able to process scHGF (precursor of HGF) to its active form. Indeed, we observed processing of scHGF to its a-chain by conditioned media from the DLBCL cell lines. This conversion was completely inhibited by addition of the serine protease inhibitor leupeptin (Figure 6). Since proteases other than HGFA are, although with low efficiency, capable of activating scHGF in vitro, we explored

whether the conversion of scHGF by DLBCLs could be specifically inhibited by interfering with HGFA activity. Indeed, we observed that the anti-HGFA monoclonal P1-4, which blocks HGFA function, effectively inhibits scHGF conversion by DLBCLs (Figure 6). These findings demonstrate that HGFA is the serine protease responsible for the conversion of scHGF in DLBCLs and identifies the DLBCL cells themselves as an important source of HGFA, thereby regulating HGF activity within the tumor microenvironment.

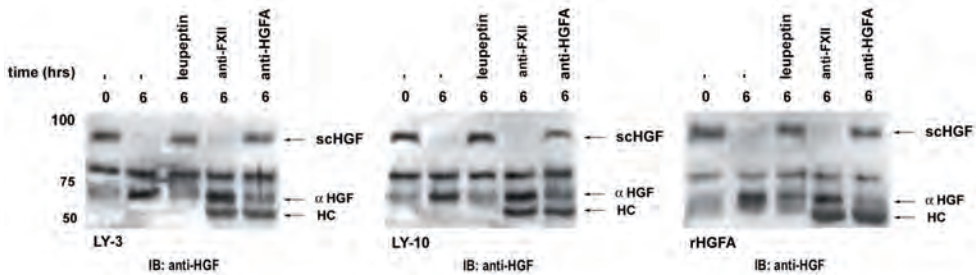


Figure 6. DLBCL cells autocatalyze HGF activation by producing HGFA.

Conditioned medium of DLBCL cell lines LY-3 (left panel) and LY-10 (middle panel) was incubated with scHGF for 6 hours in the presence of thrombin, combined with either the serine protease inhibitor leupeptin, neutralizing antibody against HGFA (P1-4) or factor XIIa (OT-2), as indicated. As positive control, HGF conversion by recombinant HGFA is shown (right panel). HGF conversion was determined by immunoblotting with anti-HGF. αHGF= active, a heavy chain of HGF; scHGF= inactive, single chain of HGF; HC= heavy chain of immunoglobulin.

Discussion

Uncontrolled activation of HGF/MET signaling pathway has been implicated in tumor growth, invasion and metastasis in both mice and human¹³. Here, we have investigated the expression of MET protein on a large panel of B cell malignancies. We have found that MET is frequently expressed on MM (48%) and DLBCL (30%) (Table 1), and that MET is occasionally mutated in B cell malignancies, including DLBCL (Figure 1). Furthermore, we have demonstrated that HGF is produced within the DLBCL microenvironment (Figure 4), that DLBCL cells themselves produce HGFA thereby activating HGF (Figure 5 and 6), and that HGF/MET signaling in DLBCL cells is functional and controls integrin-mediated adhesion (Figures 2 and 3). Previously, overexpression of either HGF or MET in DLBCL tumor sections, as well as high levels of HGF in the serum of DLBCL patients, has been found to associate with poor prognosis^{10,45,54}. Notably, the treatment response was associated with changes in serum HGF levels¹⁰. More recently, a gene-profiling study showed significantly enhanced expression of MET upon transformation of low-grade FLs into DLBCLs within the same patients⁴⁶. Combined, these data strongly suggest a pathogenic role for HGF/MET signaling in DLBCL. Overexpression of MET in tumor cells may be due to MET amplification, defective transcriptional regulation of the MET gene, or mutations affecting MET protein stability¹⁴. Although amplification of MET has been reported in several types of human cancer, this was not found in any of the MET-expressing lymphomas studied (data not shown). Importantly, however, the high MET-expressing cell lines OCI-LY-3 and 10 are so-called activated B cell (ABC)-like DLBCL. These ABC-like DLBCLs are characterized by a nuclear factor- κ B (NF- κ B) expression profile,

and indeed OCI-LY-3 and LY-10 exhibit constitutive NF- κ B activation⁵⁵. This is particularly interesting, since the MET promoter contains several putative NF- κ B responsive elements. Thus far, no MET mutations have been described for B cell malignancies. However, here we found two distinct germline missense mutations in MET: R1166Q in the kinase domain in one DLBCL patient; and R988C in the JM domain in four patients with either DLBCL, CLL, FL or BL (Figure 2). Notably, no mutations in MET were found in the DLBCL cell lines (data not shown). In hereditary and sporadic papillary renal cell cancer, most missense mutations are located in the tyrosine kinase domain of MET, causing constitutive activity and/or a lower threshold for HGF-induced activation of the tyrosine kinase^{39,41,56,57}. Thus, the R1166Q mutant may have a similar effect. Since the JM region of MET harbors important negative regulatory sites involved in receptor ubiquitination, degradation and inhibition of kinase activity⁵⁸⁻⁶¹, the R988C MET mutation may affect these processes, leading to aberrant MET signaling. Recently, the R988C mutation has also been reported in 2 SCLC cell lines⁴³, and, during the preparation of this manuscript, in a NSCLC cell line and in 2 lung cancer patients^{42,44}. Interestingly, upon transfection the R988C mutant promoted proliferation, motility and overall tyrosine phosphorylation of the pre-B cell line BaF3⁴³. Moreover, expression of the R988C mutant in a SCLC cell line resulted in enhanced focus-formation and soft-agar colony-formation⁴³. These observations, combined with the recent demonstration that a mouse MET mutation homologous to R988C plays an important role in lung tumor susceptibility⁴⁴, strongly suggest that the R988C mutation is a true gain-of-function mutation. Since a recent study has shown that mice expressing oncogenic MET mutants develop lymphomas⁶², it is conceivable that the R988C MET mutation can convey B cell lymphoma susceptibility in humans. Within the DLBCL microenvironment, we found that HGF was localized in single cells and small cell clusters, most likely representing (activated) macrophages (Figure 4B). This, combined with the lack of HGF expression by the DLBCL cell lines as measured in conditioned medium (data not shown), indicates a paracrine rather than an autocrine mechanism of MET activation in DLBCL. Noteworthy, since HGF itself has angiogenic properties⁶³, and has been demonstrated to induce expression of vascular endothelial growth factor (VEGF) as well^{64,65}, HGF might also stimulate angiogenesis in DLBCL, thereby promoting tumor growth. Proteolytic activation of HGF in the extracellular milieu is a critical limiting step in HGF/MET signaling. Here we have demonstrated that DLBCLs and cell lines express HGFA and are able to process scHGF to its active form (Figure 6). This is in sharp contrast to tonsillar naïve-, GC or memory B cells, which do not or very weakly express HGFA⁵³ (Figure 5C). Hence, autocrine production of HGFA by DLBCL cells may support tumorigenesis via autocatalyzation of HGF conversion, consequently providing a constant source of active HGF in the tumor microenvironment. HGF-induced activation of MET in DLBCL cells resulted in MEK-dependent phosphorylation of the MAP kinases ERK-1 and -2 (Figure 2C). The consecutive activation of MEK-1 and ERK-1/2, the phosphorylation of the transcription factors ELK1 and ETS2, and the expression of immediate early genes such as FOS, has been directly linked to regulation of cell proliferation^{47,48}. Furthermore, upon HGF stimulation of DLBCL cells, we observed PI3K-dependent phosphorylation of PKB/Akt and its substrates GSK3 and FOXO3a (Figure 2D). By direct phosphorylation, PKB can inhibit BAD and caspase 9, activate IKK α resulting in activation of NF- κ B, and inhibit GSK3 and forkhead transcription factors of the FOXO subfamily, including FOXO3a (FKHRL1), all of which contributes to its anti-apoptotic function⁶⁶. Inhibition of GSK3 and FOXOs by PKB can also induce cell proliferation through enhanced cyclin D1 stabilization and transcription, respectively^{66,67}. Noteworthy, overexpression of

cyclin D1, often as a consequence of chromosomal translocations, is frequently observed in lymphomas⁶⁸. Phosphorylation of FOXOs by PKB prevents their nuclear translocation and thereby the expression of FOXO target genes, which include the pro-apoptotic genes FasL and Bim, and the anti-proliferative genes p27^{KIP} and Rb2⁶⁹. Indirectly, FOXOs can suppress expression of the anti-apoptotic gene FLIP⁷⁰ and the pro-proliferative genes cyclin D1 and D2⁶⁶. Recently, PI3K/PKB-mediated inactivation of FOXO3a was shown to be important for B cell proliferation⁷¹. The observed low expression of p27kip1 in GC B-type DLBCL, as well as the constitutive activation of NF- κ B and high expression of FLIP and cyclin D2 in ABC-type DLBCL^{1,55}, illustrates the relevance of these HGF/MET-controlled signaling cascades for DLBCL. Similar to our previous studies with the GC B cell-like Burkitt's lymphoma cell line Namalwa²², we have shown that HGF induces integrin-mediated adhesion of DLBCL cells to VCAM-1 and FN (Figure 3A and data not shown). Furthermore, this HGF-induced adhesion involved α 4 β 1 integrin (Figure 3B) and required activation of PI3K (Figure 3C). The HGF-induced integrin activation can control the interaction of the DLBCL cells with extracellular matrix, stromal cells and FDCs within the tumor microenvironment. By analogy to B cell antigen-receptor-controlled adhesion of GC B cells^{7,36,72}, this may provide important integrin-mediated outside-in, as well as paracrine, growth and survival signals.

A better understanding of the biology of B cell malignancies is needed in the development of potential therapeutic agents that target specific intracellular pathways and the crosstalk that occurs between malignant B cells and the microenvironment. Our data indicate that aberrant HGF/MET-signaling and conversion of HGF by DLBCL cell-secreted HGFA can play an important role in the control of adhesion, survival and proliferation of DLBCL cells, and thereby in the maintenance of DLBCL in the tumor microenvironment (Figure 7). Thus, our data provide new insights into the pathogenesis of DLBCL and identify the HGF/MET pathway as a potential novel therapeutic target for the treatment of DLBCL.

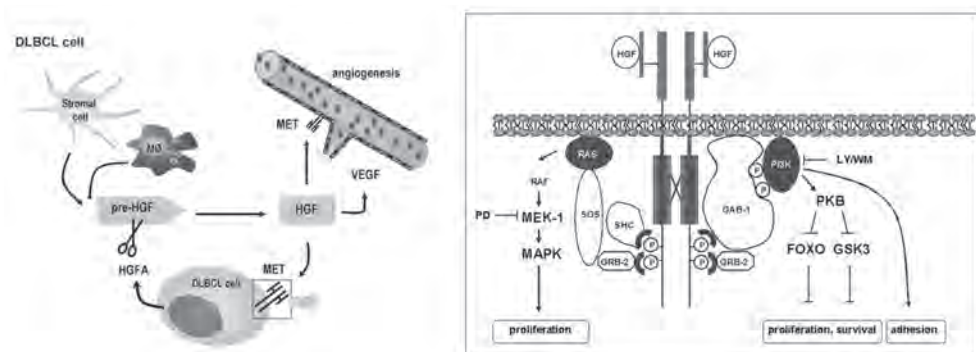


Figure 7. Activation and biological actions of HGF in the DLBCL microenvironment.

HGF is produced by macrophages (M ϕ) and/or stromal cells. Expression and secretion of HGFA by DLBCL cells regulates the bioavailability of active HGF in the DLBCL microenvironment. Catalyzation of HGF activation by DLBCL cells can directly stimulate HGF/MET signaling (insert), promoting DLBCL adhesion, growth and survival. In addition, HGF can directly or indirectly stimulate angiogenesis. Insert: Schematic representation of the HGF-induced signaling events in DLBCL cells. HGF-induced activation of MAPK and PKB is mediated by Grb2/SOS coupling to RAS and GAB-1 coupling to PI3K, respectively⁷³. Activation of RAS/MAPK may lead to proliferation of DLBCL cells. Activation of PI3K/PKB leads to phosphorylation of FOXO3a and GSK3, which may control proliferation and survival (see Discussion for further details). Furthermore, PI3K mediates HGF-induced adhesion of DLBCL cells. pre-HGF= inactive, precursor of HGF.

Acknowledgements

The authors would like to thank Prof. dr. H. Kataoka for the antibodies against HGFA and recombinant active HGFA.

References

1. Shaffer AL, Rosenwald A, Staudt LM. Lymphoid malignancies: the dark side of B-cell differentiation. *Nat Rev Immunol.* 2002;2:920-932.
2. Kuppers R, Klein U, Hansmann ML, Rajewsky K. Cellular origin of human B-cell lymphomas. *N Engl J Med.* 1999;341:1520-1529.
3. Bende RJ, Aarts WM, Riedl RG et al. Among B cell non-Hodgkin's lymphomas, MALT lymphomas express a unique antibody repertoire with frequent rheumatoid factor reactivity. *J Exp Med.* 2005;201:1229-1241.
4. Patrick CW, Jr., Juneja HS, Lee S, Schmalstieg FC, McIntire LV. Heterotypic adherence between human B-lymphoblastic and pre-B-lymphoblastic cells and marrow stromal cells is a biphasic event: integrin very late antigen-4 alpha mediates only the early phase of the heterotypic adhesion. *Blood.* 1995;85:168-178.
5. Lindhout E, Koopman G, Pals ST, de Groot C. Triple check for antigen specificity of B cells during germinal centre reactions. *Immunol Today.* 1997;18:573-577.
6. Weimar IS, de Jong D, Muller EJ et al. Hepatocyte growth factor/scatter factor promotes adhesion of lymphoma cells to extracellular matrix molecules via alpha 4 beta 1 and alpha 5 beta 1 integrins. *Blood.* 1997;89:990-1000.
7. Koopman G, Keehnen RM, Lindhout E et al. Adhesion through the LFA-1 (CD11a/CD18)-ICAM-1 (CD54) and the VLA-4 (CD49d)-VCAM-1 (CD106) pathways prevents apoptosis of germinal center B cells. *J Immunol.* 1994;152:3760-3767.
8. Klein B, Tarte K, Jourdan M et al. Survival and proliferation factors of normal and malignant plasma cells. *Int J Hematol.* 2003;78:106-113.
9. Teofili L, Di Febo AL, Pierconti F et al. Expression of the c-met proto-oncogene and its ligand, hepatocyte growth factor, in Hodgkin disease. *Blood.* 2001;97:1063-1069.
10. Hsiao LT, Lin JT, Yu IT et al. High serum hepatocyte growth factor level in patients with non-Hodgkin's lymphoma. *Eur J Haematol.* 2003;70:282-289.
11. Seidel C, Borset M, Turesson I et al. Elevated serum concentrations of hepatocyte growth factor in patients with multiple myeloma. The Nordic Myeloma Study Group. *Blood.* 1998;91:806-812.
12. Trusolino L, Comoglio PM. Scatter-factor and semaphorin receptors: cell signalling for invasive growth. *Nat Rev Cancer.* 2002;2:289-300.
13. van der Voort R, Taher TE, Derksen PW et al. The hepatocyte growth factor/Met pathway in development, tumorigenesis, and B-cell differentiation. *Adv Cancer Res.* 2000;79:39-90.
14. Birchmeier C, Birchmeier W, Gherardi E, Vande Woude GF. Met, metastasis, motility and more. *Nat Rev Mol Cell Biol.* 2003;4:915-925.
15. Fischer J, Palmado G, von Knobloch R et al. Duplication and overexpression of the mutant allele of the MET proto-oncogene in multiple hereditary papillary renal cell tumours. *Oncogene.* 1998;17:733-739.
16. Schmidt L, Duh FM, Chen F et al. Germline and somatic mutations in the tyrosine kinase domain of the MET proto-oncogene in papillary renal carcinomas. *Nat Genet.* 1997;16:68-73.
17. Schmidt L, Junker K, Nakaigawa N et al. Novel mutations of the MET proto-oncogene in papillary renal carcinomas. *Oncogene.* 1999;18:2343-2350.

18. Park WS, Dong SM, Kim SY et al. Somatic mutations in the kinase domain of the Met/hepatocyte growth factor receptor gene in childhood hepatocellular carcinomas. *Cancer Res.* 1999;59:307-310.
19. Lee JH, Han SU, Cho H et al. A novel germ line juxtamembrane Met mutation in human gastric cancer. *Oncogene.* 2000;19:4947-4953.
20. Ma PC, Maulik G, Christensen J, Salgia R. c-Met: structure, functions and potential for therapeutic inhibition. *Cancer Metastasis Rev.* 2003;22:309-325.
21. Takayama H, LaRochelle WJ, Sharp R et al. Diverse tumorigenesis associated with aberrant development in mice overexpressing hepatocyte growth factor/scatter factor. *Proc Natl Acad Sci U S A.* 1997;94:701-706.
22. van der Voort R, Taher TE, Keehnen RM et al. Paracrine regulation of germinal center B cell adhesion through the c-met-hepatocyte growth factor/scatter factor pathway. *J Exp Med.* 1997;185:2121-2131.
23. Skibinski G, Skibinska A, James K. The role of hepatocyte growth factor and its receptor c-met in interactions between lymphocytes and stromal cells in secondary human lymphoid organs. *Immunology.* 2001;102:506-514.
24. Derksen PW, de Gorter DJ, Meijer HP et al. The hepatocyte growth factor/Met pathway controls proliferation and apoptosis in multiple myeloma. *Leukemia.* 2003;17:764-774.
25. Jucker M, Gunther A, Gradl G et al. The Met/hepatocyte growth factor receptor (HGFR) gene is overexpressed in some cases of human leukemia and lymphoma. *Leuk Res.* 1994;18:7-16.
26. Borset M, Lien E, Espevik T et al. Concomitant expression of hepatocyte growth factor/scatter factor and the receptor c-MET in human myeloma cell lines. *J Biol Chem.* 1996;271:24655-24661.
27. Borset M, Hjorth-Hansen H, Seidel C, Sundan A, Waage A. Hepatocyte growth factor and its receptor c-met in multiple myeloma. *Blood.* 1996;88:3998-4004.
28. Capello D, Gaidano G, Gallicchio M et al. The tyrosine kinase receptor met and its ligand HGF are co-expressed and functionally active in HHV-8 positive primary effusion lymphoma. *Leukemia.* 2000;14:285-291.
29. Derksen PW, Keehnen RM, Evers LM et al. Cell surface proteoglycan syndecan-1 mediates hepatocyte growth factor binding and promotes Met signaling in multiple myeloma. *Blood.* 2002;99:1405-1410.
30. Tjin EP, Derksen PW, Kataoka H, Spaargaren M, Pals ST. Multiple myeloma cells catalyze hepatocyte growth factor (HGF) activation by secreting the serine protease HGF-activator. *Blood.* 2004;104:2172-2175.
31. Shimomura T, Miyazawa K, Komiya Y et al. Activation of hepatocyte growth factor by two homologous proteases, blood-coagulation factor XIIIa and hepatocyte growth factor activator. *Eur J Biochem.* 1995;229:257-261.
32. Lazarovits AI, Moscicki RA, Kurnick JT et al. Lymphocyte activation antigens. I. A monoclonal antibody, anti-Act I, defines a new late lymphocyte activation antigen. *J Immunol.* 1984;133:1857-1862.
33. van der Voort R, Taher TE, Wielenga VJ et al. Heparan sulfate-modified CD44 promotes hepatocyte growth factor/scatter factor-induced signal transduction through the receptor tyrosine kinase c-Met. *J Biol Chem.* 1999;274:6499-6506.
34. Kataoka H, Hamasuna R, Itoh H, Kitamura N, Koono M. Activation of hepatocyte growth factor/scatter factor in colorectal carcinoma. *Cancer Res.* 2000;60:6148-6159.
35. van Adelsberg J, Sehgal S, Kukes A et al. Activation of hepatocyte growth factor (HGF) by endogenous HGF activator is required for metanephric kidney morphogenesis in vitro. *J Biol Chem.* 2001;276:15099-15106.
36. Spaargaren M, Beuling EA, Rurup ML et al. The B cell antigen receptor controls integrin activity through Btk and PLCgamma2. *J Exp Med.* 2003;198:1539-1550.
37. Kuniyasu H, Yasui W, Kitadai Y et al. Frequent amplification of the c-met gene in scirrhous type stomach cancer. *Biochem Biophys Res Commun.* 1992;189:227-232.
38. Lorenzato A, Olivero M, Patane S et al. Novel somatic mutations of the MET oncogene in human carcinoma metastases activating cell motility and invasion. *Cancer Res.* 2002;62:7025-7030.
39. Jeffers M, Fiscella M, Webb CP et al. The mutationally activated Met receptor mediates motility and metastasis. *Proc Natl Acad Sci U S A.* 1998;95:14417-14422.

40. Jeffers M, Schmidt L, Nakaigawa N et al. Activating mutations for the met tyrosine kinase receptor in human cancer. *Proc Natl Acad Sci U S A*. 1997;94:11445-11450.
41. Michieli P, Basilico C, Pennacchietti S et al. Mutant Met-mediated transformation is ligand-dependent and can be inhibited by HGF antagonists. *Oncogene*. 1999;18:5221-5231.
42. Ma PC, Jagadeeswaran R, Jagadeesh S et al. Functional expression and mutations of c-Met and its therapeutic inhibition with SU11274 and small interfering RNA in non-small cell lung cancer. *Cancer Res*. 2005;65:1479-1488.
43. Ma PC, Kijima T, Maulik G et al. c-MET mutational analysis in small cell lung cancer: novel juxtamembrane domain mutations regulating cytoskeletal functions. *Cancer Res*. 2003;63:6272-6281
44. Zaffaroni D, Spinola M, Galvan A et al. Met proto-oncogene juxtamembrane rare variations in mouse and humans: differential effects of Arg and Cys alleles on mouse lung tumorigenesis. *Oncogene*. 2005;24:1084-1090.
45. Giles FJ, Vose JM, Do KA et al. Clinical relevance of circulating angiogenic factors in patients with non-Hodgkin's lymphoma or Hodgkin's lymphoma. *Leuk Res*. 2004;28:595-604.
46. Elenitoba-Johnson KS, Jenson SD, Abbott RT et al. Involvement of multiple signaling pathways in follicular lymphoma transformation: p38-mitogen-activated protein kinase as a target for therapy. *Proc Natl Acad Sci U S A*. 2003;100:7259-7264.
47. Downward J. Targeting RAS signalling pathways in cancer therapy. *Nat Rev Cancer*. 2003;3:11-22.
48. Wasylyk B, Hagman J, Gutierrez-Hartmann A. Ets transcription factors: nuclear effectors of the Ras-MAP-kinase signaling pathway. *Trends Biochem Sci*. 1998;23:213-216.
49. Okkenhaug K, Vanhaesebroeck B. PI3K in lymphocyte development, differentiation and activation. *Nat Rev Immunol*. 2003;3:317-330.
50. Accili D, Arden KC. FoxOs at the crossroads of cellular metabolism, differentiation, and transformation. *Cell*. 2004;117:421-426.
51. Hov H, Holt RU, Ro TB et al. A selective c-met inhibitor blocks an autocrine hepatocyte growth factor growth loop in ANBL-6 cells and prevents migration and adhesion of myeloma cells. *Clin Cancer Res*. 2004;10:6686-6694.
52. Naka D, Ishii T, Yoshiyama Y et al. Activation of hepatocyte growth factor by proteolytic conversion of a single chain form to a heterodimer. *J Biol Chem*. 1992;267:20114-20119.
53. Tjin EP, Bende RJ, Derksen PW et al. Follicular Dendritic Cells Catalyze Hepatocyte Growth Factor (HGF) Activation in the Germinal Center Microenvironment by Secreting the Serine Protease HGF Activator. *J Immunol*. 2005;175:2807-2813.
54. Kawano R, Ohshima K, Karube K et al. Prognostic significance of hepatocyte growth factor and c-MET expression in patients with diffuse large B-cell lymphoma. *Br J Haematol*. 2004;127:305-307.
55. Davis RE, Brown KD, Siebenlist U, Staudt LM. Constitutive nuclear factor kappaB activity is required for survival of activated B cell-like diffuse large B cell lymphoma cells. *J Exp Med*. 2001;194:1861-1874.
56. Jeffers MF. Activating mutations in the Met receptor overcome the requirement for autophosphorylation of tyrosines crucial for wild type signaling. *Oncogene*. 1999;18:5120-5125.
57. Chiara F, Michieli P, Pugliese L, Comoglio PM. Mutations in the MET oncogene unveil a 'dual switch' mechanism controlling tyrosine kinase activity. *J Biol Chem*. 2003.
58. Gandino L, Longati P, Medico E, Prat M, Comoglio PM. Phosphorylation of serine 985 negatively regulates the hepatocyte growth factor receptor kinase. *J Biol Chem*. 1994;269:1815-1820.
59. Villa-Moruzzi E, Puntoni F, Bardelli A et al. Protein tyrosine phosphatase PTP-S binds to the juxtamembrane region of the hepatocyte growth factor receptor Met. *Biochem J*. 1998;336 (Pt 1):235-239.
60. Peschard P, Fournier TM, Lamorte L et al. Mutation of the c-Cbl TKB domain binding site on the Met receptor tyrosine kinase converts it into a transforming protein. *Mol Cell*. 2001;8:995-1004.
61. Taher TE, Tjin EP, Beuling EA et al. c-Cbl is involved in Met signaling in B cells and mediates hepatocyte growth factor-induced receptor ubiquitination. *J Immunol*. 2002;169:3793-3800.

62. Graveel C, Su Y, Koeman J et al. Activating Met mutations produce unique tumor profiles in mice with selective duplication of the mutant allele. *Proc Natl Acad Sci U S A*. 2004;101:17198-17203. 63 .
Jiang W, Hiscox S, Matsumoto K, Nakamura T. Hepatocyte growth factor/scatter factor, its molecular, cellular and clinical implications in cancer. *Crit Rev Oncol Hematol*. 1999;29:209-248.
64. Wojta J, Kaun C, Breuss JM et al. Hepatocyte growth factor increases expression of vascular endothelial growth factor and plasminogen activator inhibitor-1 in human keratinocytes and the vascular endothelial growth factor receptor flk-1 in human endothelial cells. *Lab Invest*. 1999;79:427-438.
65. Xin X, Yang S, Ingle G et al. Hepatocyte growth factor enhances vascular endothelial growth factor-induced angiogenesis in vitro and in vivo. *Am J Pathol*. 2001;158:1111-1120.
66. Vivanco I, Sawyers CL. The phosphatidylinositol 3-Kinase AKT pathway in human cancer. *Nat Rev Cancer*. 2002;2:489-501.
67. Diehl JA, Cheng M, Roussel MF, Sherr CJ. Glycogen synthase kinase-3beta regulates cyclin D1 proteolysis and subcellular localization. *Genes Dev*. 1998;12:3499-3511.
68. Nakamura S, Yatabe Y, Seto M. Cyclin D1 overexpression in malignant lymphomas. *Pathol Int*. 1997;47:421-429.
69. Coffey PJ, Burgering BM. Forkhead-box transcription factors and their role in the immune system. *Nat Rev Immunol*. 2004;4:889-899.
70. Skurk C, Maatz H, Kim HS et al. The Akt-regulated forkhead transcription factor FOXO3a controls endothelial cell viability through modulation of the caspase-8 inhibitor FLIP. *J Biol Chem*. 2004;279:1513-1525.
71. Yusuf I, Zhu X, Kharas MG, Chen J, Fruman DA. Optimal B-cell proliferation requires phosphoinositide 3-kinase-dependent inactivation of FOXO transcription factors. *Blood*. 2004;104:784-787.
72. Koopman G, Parmentier HK, Schuurman HJ et al. Adhesion of human B cells to follicular dendritic cells involves both the lymphocyte function-associated antigen 1/intercellular adhesion molecule 1 and very late antigen 4/vascular cell adhesion molecule 1 pathways. *J Exp Med*. 1991;173:1297-1304.
73. Zhang YW, Vande Woude GF. HGF/SF-met signaling in the control of branching morphogenesis and invasion. *J Cell Biochem*. 2003;88:408-417.

3

Illegitimate Wnt pathway activation by β -catenin mutation or autocrine stimulation in T cell malignancies

Richard W.J. Groen¹, Monique E.C.M. Oud¹, Esther J.M. Schilder-Tol¹, Marije B. Overdijk¹, Derk ten Berge², Roel Nusse², Marcel Spaargaren¹ and Steven T. Pals¹.

¹Department of Pathology, Academic Medical Center, University of Amsterdam, Amsterdam, The Netherlands; and ²Howard Hughes Medical Institute and Department of Developmental Biology, Stanford University, Stanford, CA 94305-5323.

Cancer Res. 2008; 68(17): 6969-77

Abstract

Recent studies in mice have demonstrated a role for the canonical Wnt pathway in lymphocyte development. Since cancers often arise as a result of aberrant activation of signaling cascades that normally promote the self-renewal and expansion of their progenitor cells, we hypothesized that activation of the Wnt pathway might contribute to the pathogenesis of lymphoproliferative disease. Therefore, we screened a large panel (n=162) of non Hodgkin lymphomas (NHLs), including all major WHO categories, for nuclear expression of β -catenin, a hallmark of “active” Wnt signaling. In 16 lymphomas, mostly of T-lineage origin, nuclear localization of β -catenin was detected. Interestingly, some of these tumors contained established gain-of-function mutations in the gene encoding β -catenin (*CTNNB1*), however, in the majority mutations in either *CTNNB1* or *APC* were not detected. Functional analysis of Wnt signaling in precursor T-lymphoblastic lymphomas/leukemias (T-LBL/ALLs), the NHL subset in which β -catenin accumulation was most prevalent (33% positive), revealed a constitutively activated but still responsive Wnt pathway, which controlled TCF-mediated gene transcription and cell growth. Our data indicate that activation of the Wnt pathway, either by *CTNNB1* mutation or autocrine stimulation, plays a role in the pathogenesis of a subset of NHLs, in particular those of T cell origin.

3

Introduction

Non Hodgkin lymphomas (NHLs) represent a heterogeneous group of malignancies originating from lymphocytes arrested at specific stages of differentiation ¹. The transition of a lymphocyte to a fully transformed aggressive lymphoma is a multistep process, which requires the activation of proto-oncogenes as well as the disruption of tumor suppressor genes ¹⁻³. In spite of their genetic defects, most lymphomas do not replicate spontaneously *in vitro*, implying that they are still dependent on environmental stimuli for their growth. To date these external factors are ill defined ². Wnt signals form one class of paracrine growth factors that could act to influence lymphoma growth. Wnt proteins are able to promote the proliferation of progenitor- or stem cells ⁴⁻⁶, and their sustained overexpression can cause cancer ^{7,8}. Wnt genes encode a family of 19 secreted glycoproteins, which promiscuously interact with several Frizzled (Fzd) receptors. This leads to intracellular signals that control gene expression, cell behavior, cell adhesion, and cell polarity, during both embryonic development and postnatal life ^{9,10}. The key event in the Wnt signaling pathway is the stabilization of β -catenin. In the absence of Wnt signals, a complex of proteins, including the tumor suppressor gene product APC, axin, and glycogen synthase kinase-3 β (GSK3 β), controls phosphorylation of specific serine and threonine residues in the N-terminal region of β -catenin. This phosphorylation marks β -catenin for ubiquitination and degradation by the proteasome. Signaling by Wnt proteins blocks GSK3 β activity, resulting in the accumulation of β -catenin, which will translocate to the nucleus. Here it interacts with T cell factor (TCF) transcription factors ^{11,12} to drive transcription of target genes ¹³⁻¹⁵. Mutations of the phosphorylation sites in the N-terminal domain of β -catenin or mutations of the APC tumor suppressor, leading to the formation of constitutive nuclear β -catenin/TCF complexes and altered expression of target genes, have been found in many types of cancer ^{8,16,17}. Target genes which presumably cooperate in neoplastic transformation include *CCND1* (cyclin D1) ¹³, *MYC* ¹⁴, *CD44* ¹⁸ and *MET* ¹⁹. TCF/LEF family transcription factors were initially identified in models of early lymphocyte development ^{4,20,21}, whereas studies in TCF-1 and LEF1 knockout mice have demonstrated that these factors are essential for the maintenance of progenitor T- and B cell compartments ^{4,22}. These observations suggested a role for Wnt signaling in the control of cell proliferation and survival during lymphocyte development. Indeed, recent studies, have demonstrated that Wnt factors and β -catenin affect lymphocyte progenitor fate as well as hematopoietic stem cell self-renewal ^{5,6,23-27}. These observations, combined with the key oncogenic role of Wnt signaling in several non-lymphoid tumors, and our recent finding that the Wnt pathway is illegitimately activated in multiple myeloma ²⁸, prompted us to explore whether deregulation of Wnt signaling contributes to lymphoid neoplasia. While the specificity of Wnt signals with respect to target cells is relatively unknown, there is now a powerful method to examine whether cells are activated by a Wnt signal, *i.e.* detection of accumulation and nuclear localization of β -catenin. Here, we show that canonical Wnt signaling is active in a substantial subset of precursor T-lymphoblastic lymphomas/leukemias (T-LBL/ALL) and peripheral (mature) T cell lymphomas (pTL) and that Wnt signals are involved in the control of lymphoma growth.

Materials and Methods

Case selection and classification

A panel of NHLs was selected from the files of the Department of Pathology, Academic Medical Center, University of Amsterdam, Amsterdam, The Netherlands. All tumors were classified according to the WHO classification, using standard histological, immunohistochemical, and molecular criteria.

Immunohistochemistry

Immunohistochemical staining was performed on formalin-fixed paraffin-embedded tissue sections or cell lines. Endogenous peroxidase activity was blocked with 0.1% NaN₃ and 1.5% H₂O₂ in a 20 mM citrate buffer. For detection of β -catenin, we used an antigen-retrieval protocol, which allows effective and specific detection of nuclear β -catenin in formalin-fixed paraffin-embedded tissue sections²⁹. In brief, the sections were gently boiled for 50 minutes in a Tris/EDTA buffer (respectively 40 mM/1 mM) pH 8, after which they were blocked with 1% BSA in PBS and incubated for 2 hour with anti- β -catenin monoclonal antibody clone 14 (BD Biosciences, Erembodegem, Belgium). Binding of the antibody was visualized using the Envision⁺ detection system and DAB⁺ (DAKO, Carpinteria, CA). The sections were counterstained with hematoxylin (Merck, Darmstadt, Germany). Slides were analyzed with a BX51 microscope (Olympus, Hamburg, Germany) and images were captured, using Olympus software and a DP70 camera (Olympus).

Mutation analysis

DNA for PCR amplification was extracted and purified from representative tumor tissue, using the QIAamp DNA Mini Kit (Qiagen, Hilden, Germany) for paraffin-embedded material or DNAzol (Invitrogen Life technologies, Breda, The Netherlands) for snap-frozen material. Of CTNNB1, we analyzed exon 3 encoding amino acids (AA) 25-65, for gain of function mutations. This domain, containing the phosphorylation sites important for ubiquitination and degradation of β -catenin was screened, using the following primers: forward: 5' ATGGAACCAGACAGAAAAGC 3' and reverse: 5' GCTACTTGTCTTGAGTGAAG 3'. The PCR mixture contained: 100 ng of genomic DNA, 1x PCR Rxn buffer (Invitrogen Life technologies), 0.2 mmol/L dNTP, 2 mmol/L MgCl₂, 0.2 mg/ml Bovine Serum Albumin (Roche, Basel, Switzerland), 0.2 μ mol/L of each primer, and 1U platinum Taq polymerase (Invitrogen Life technologies). PCR conditions were: denaturing at 95°C for 5 minutes, followed by 35 cycles of 45 seconds at 95°C, 45 seconds at 52°C and 1 minute and 30 seconds at 72°C. The reaction was completed for 10 minutes at 72°C. The PCR products were cloned into pCR2.1-TOPO (Invitrogen Life technologies), and several clones were sequenced to determine specificity of the amplified products using a big-dye terminator kit (Amersham Biosciences, Roosendaal, The Netherlands) and the T7 primer. For APC, we analyzed four overlapping regions spanning the mutation cluster region (MCR), located between codons 1286 and 1513 in exon 15. Mutations in this region lead to a truncated APC protein, which has lost its ability to bind axin and to regulate β -catenin. Nonradioactive PCR-SSCP analysis was performed to screen the MCR of APC for mutations. Four overlapping regions were amplified spanning the MCR, using the following primers: for fragment I, 5' GAAATAGGATGTAATCAGACG 3' and 5' CGCTCCTGAAGAAAATTCAAC 3';

for fragment II, 5' AGACTGCAGGGTTCTAGTTTATC 3' and 5' GAGCTGGCAATCGAACGACT 3'; for fragment III, 5' TACTTCTGTCACTTCACTTGAT 3' and 5' ATTTTATAGGACTTCTCGCTTG 3'; for fragment IV, 5' AAACACCTCCACCACCTCT 3' and 5' GCATTATTCTTAATCCACATC 3'. PCR conditions were: denaturing at 96°C for 7 minutes, followed by 35 cycles of 50 seconds at 96°C, 50 seconds at 56°C, 50 seconds at 72°C and a final elongation step at 72°C, for 10 minutes. The PCR mixture contained: 100 ng of genomic DNA, 1x PCR Rxn buffer (Invitrogen Life technologies), 0.2 mmol/L dNTP, 2 mmol/L MgCl₂, 0.2 μmol/L of each primer, and 0.5U platinum Taq polymerase (Invitrogen Life technologies). SSCP was performed using the GeneGel Excel 12.5/24 Kit (Amersham Biosciences). 7 μl PCR mixture was diluted with 7 μl a denaturing solution, consisting of 23.75 ml formamide (95%), 1.25 ml xylene cyanol (1%) and 10 mg bromophenol blue. Samples were denatured at 95°C for 5 minutes and directly placed on ice, 5 μl sample was applied to the gel. Samples were run at two different temperatures, 5°C and 15°C, at a GenePhor Electrophoresis unit. Gels were stained according to manufacturer's protocol using the PlusOne DNA Silver Staining Kit (Amersham Biosciences). For NOTCH1, exon 26, 27 and 34 were analyzed with nonradioactive PCR-SSCP analysis, using primers as described by Weng et al.³⁰ and the above mentioned PCR conditions. PCR amplicons exhibiting aberrant migration patterns during SSCP, were ligated into pCR2.1-TOPO (Invitrogen Life technologies), and several clones were sequenced to determine specificity of the amplified products using a big-dye terminator kit (Amersham Biosciences) and the T7 primer. Images were captured using a Imacon digital back (Hasselblad, Ahrensburg, Germany) and processed with Adobe Photoshop. All primers were manufactured by Sigma-Aldrich (Haverhill, UK).

3

Cell culture and transfections

T-LBL/ALL cell lines, Molt4, CCRF-CEM and SupT1, were cultured in Iscove's medium (Invitrogen Life technologies) supplemented with 10% fetal calf serum (FCS), penicillin (50U/ml) and streptomycin (50 μg/ml) (both from Invitrogen Life Technologies). L-cells stably transfected with the TOPFLASH and LacZ reporter plasmids ("LSL cells")³¹, were cultured in Dulbecco's Modified Eagle's Medium (Invitrogen Life technologies) supplemented with 10% fetal calf serum (FCS), penicillin (50U/ml) and streptomycin (50 μg/ml). Transient transfections were performed by electroporation using the BioRad GenePulser (BioRad, Hercules, CA) at 250 V and 960 μF. Conditioned medium was obtained from cells being seeded at a density of 8x10⁵/ml and cultured for 48 hours in fully supplemented medium. As control the fully supplemented medium was incubated for 48 hours without cells.

Western blot analysis

Cells were lysed with a NP-40 lysis buffer, containing 20 mM Tris-HCl (pH8), 300 mM NaCl, 2% NP-40, 20% glycerol, 10 mM EDTA, 4 mM Na₃VO₄, 10 mM NaF and protease inhibitors. Equal amounts of protein (25μg/lane) were loaded. Samples were separated by 10% SDS-polyacrylamide gel electrophoresis and subsequently blotted. Equal loading was confirmed by staining the lower part of the blot (< 50 kDa) with anti-β-actin monoclonal antibody (clone AC-15, Sigma-Aldrich, St Louis, MO). The upper part (> 50 kDa) was stained for β-catenin (clone 14; BD Biosciences) or non-phosphorylated β-catenin (clone 8E4; Alexis Biochemicals, Lausen, Switzerland). Primary antibodies were detected by a HRP-conjugated rabbit anti-mouse, followed by detection using Lumi-LightPLUS western blotting substrate (Roche).

Luciferase assay

Cells were transfected with either the TOPFLASH or the FOPFLASH reporter construct alone or in combination with constructs expressing $S_{33}Y$ - β -catenin, DKK1, dnTCF4, or a control plasmid without insert. If indicated, stimuli were added 24 hours after transfection or plating. After 48 hours, cells were harvested, lysed and luciferase activity was determined using the Dual-Luciferase Reporter assay (Promega, Madison, WI). Luciferase activity in LSL cells was determined using the Dual-Light system for combined detection of luciferase and β -galactosidase (Applied Biosystems, Bedford, MA).

Growth analysis

3 Cells were co-transfected with pEGFP-N3 (Invitrogen Life technologies) and either a construct expressing $S_{33}Y$ - β -catenin or an empty vector. 24 hours after transfection, viable GFP-positive cells were sorted using a FACS aria (BD Biosciences). Sorted cells were plated in 96-wells flat bottom tissue culture plates (Costar, Cambridge, MA) at a density of 10^4 cells/200 μ l and cultured for 4 days. At day two and four cells were analyzed for viability by means of a trypan blue staining (Sigma-Aldrich). Results are expressed as total number of viable cells.

Wnt signaling pathway gene array

Total RNA was isolated using Trizol according to the manufacturer (Invitrogen Life technologies). The RNA was further purified using iso-propanol precipitation and was concentrated using the RNeasy MinElute Cleanup kit (Qiagen). The quantity of total RNA was measured using a NanoDrop ND-1000 Spectrophotometer (NanoDrop Technologies, Wilmington, DE) and the RNA quality was examined using the Agilent 2100 bioanalyser (Agilent Technologies, Santa Clara, CA). 3 μ g of total RNA was used for cDNA synthesis, labeling, amplification, and subsequently hybridized to a Wnt signaling pathway Oligo GEArray membrane (OHS-043) according to manufacturer's protocol (SuperArray, Frederick, MD). After chemiluminescent detection, images were analyzed using manufacturer's software (SuperArray).

Results

Aberrant activation of the canonical Wnt signaling pathway in non-Hodgkin lymphomas

To explore whether the Wnt signaling pathway activation might play a role in the pathogenesis of lymphoid malignancies, we screened a large panel of NHLs for a key feature of active canonical Wnt signaling, i.e., the presence of nuclear β -catenin, by employing a staining protocol that allows effective and specific detection of nuclear β -catenin in formalin-fixed paraffin-embedded tissue sections²⁹. As expected, this method revealed a strong nuclear β -catenin staining in colorectal carcinoma tissue from patients with familial adenomatous polyposis (FAP), in which β -catenin is stabilized as a consequence of loss of APC function (Figure 1A left panel). By contrast, the B- and T cells in normal lymph nodes, thymus, tonsils, and spleen, were devoid of detectable nuclear β -catenin expression (Figure 1A middle and right panel, and data not shown).

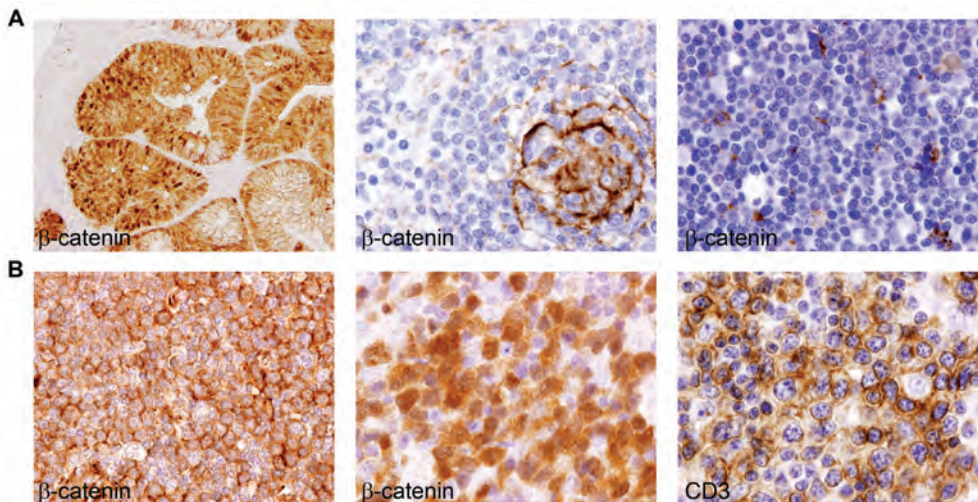


Figure 1. Nuclear localization of β -catenin in malignant lymphomas.

(A) Left panel. Positive control: Colorectal cancer specimen of a familial adenomatous polyposis (FAP) patient, showing strong nuclear β -catenin expression in part of the tumor cells, as well as cytoplasmic and membrane staining. Middle panel. Normal lymph node: β -catenin expression was not detectable in T or B lymphocytes. Follicular dendritic cells show positive (membrane) staining for β -catenin. Right panel. Normal thymus, showing the absence of (nuclear) β -catenin expression in precursor T cells. **(B)** Left panel. T-LBL/ALL showing membrane and nuclear expression of β -catenin. In this tumor a S₃₃Y mutation was found. Middle panel. Peripheral (mature) T cell lymphoma (pTL), showing a strong nuclear accumulation of β -catenin. In this tumor a S₃₃F mutation was found. Right panel. Consecutive section of (B middle panel) stained for CD3. Original magnifications x20 (A left panel) and x64 (A middle-B right panel).

Of the 162 NHLs studied, 110 were of B-lineage origin. Of these tumors, only 3 (3%) showed nuclear β -catenin expression (Table 1). One of these three tumors was a precursor-B lymphoblastic lymphoma. Notably, this tumor carried a t(1;19)(q23;p13), which results in expression of a E2A-Pbx1 fusion protein³². This fusion protein was shown to cause Wnt16 overexpression, resulting in constitutive Wnt signaling^{32,33}. Furthermore, 2 of the 54 (4%)

diffuse large B cell lymphomas (DLBCLs) showed nuclear expression of β -catenin. Nuclear β -catenin staining in this clinically and biologically heterogeneous group of tumors was neither associated with the presence of a germinal center (GC), activated B cell (ABC), or plasmablastic phenotype, nor with the presence of a preexisting immunodeficiency, viz. infection with Epstein-Barr virus (EBV) and/or Kaposi sarcoma associated herpes virus (KSHV) (data not shown). Nuclear β -catenin was not detected in mantle cell lymphomas (MCLs), Burkitt lymphomas (BLs), follicular lymphomas (FLs), chronic lymphocytic leukemia/small lymphocytic lymphomas (CLLs/SLLs), and marginal zone lymphomas (MZLs).

Table 1. Nuclear β -catenin expression in NHLs.

Lymphoma subtype (WHO)	tested (n)	positive (n)	%
<i>B cell neoplasms</i>			
Precursor B cell lymphoblastic	16	1	6
Chronic lymphocytic leukemia	7	0	0
Mantle cell lymphoma	6	0	0
Marginal zone lymphoma	8	0	0
Burkitt lymphoma	7	0	0
Follicular lymphoma	12	0	0
Diffuse large B cell lymphoma	54	2	4
<i>T cell neoplasms</i>			
Precursor T cell lymphoblastic	27	9	33
Anaplastic large cell lymphoma	10	0	0
Angioimmunoblastic T cell lymphoma	3	0	0
NK/T cell lymphoma	2	0	0
Mature T cell lymphomas, other	10	4	40

Of the 52 T-lineage lymphomas studied, 13 (25%) showed nuclear expression of β -catenin (Table 1). Nuclear β -catenin was present in 9 of 27 (33%) precursor T-lymphoblastic lymphomas/leukemias (T-LBL/ALL) (Figure 1B left panel). In addition, 4 peripheral (mature) T cell lymphomas (pTL) showed a distinct nuclear β -catenin expression (Figure 1B middle panel). Notably, 3 of these cases represented advanced cutaneous T cell lymphoma (CTCL) localized to regional lymph nodes. The tumor cells at the (primary) cutaneous site in these patients did not show nuclear β -catenin expression (data not shown). The fourth pTL showing nuclear β -catenin expression represented a nodal pTL-unspecified. Nuclear β -catenin was not detected in anaplastic large cell lymphoma (ALCL), angioimmunoblastic T cell lymphoma (AITL), or NK/T cell lymphoma (Table 1). Taken together, our observations indicate that aberrant activation of the canonical Wnt pathway is present in a subset of the lymphomas within several distinct NHL-subcategories and is relatively common (33%) in T-LBL/ALL.

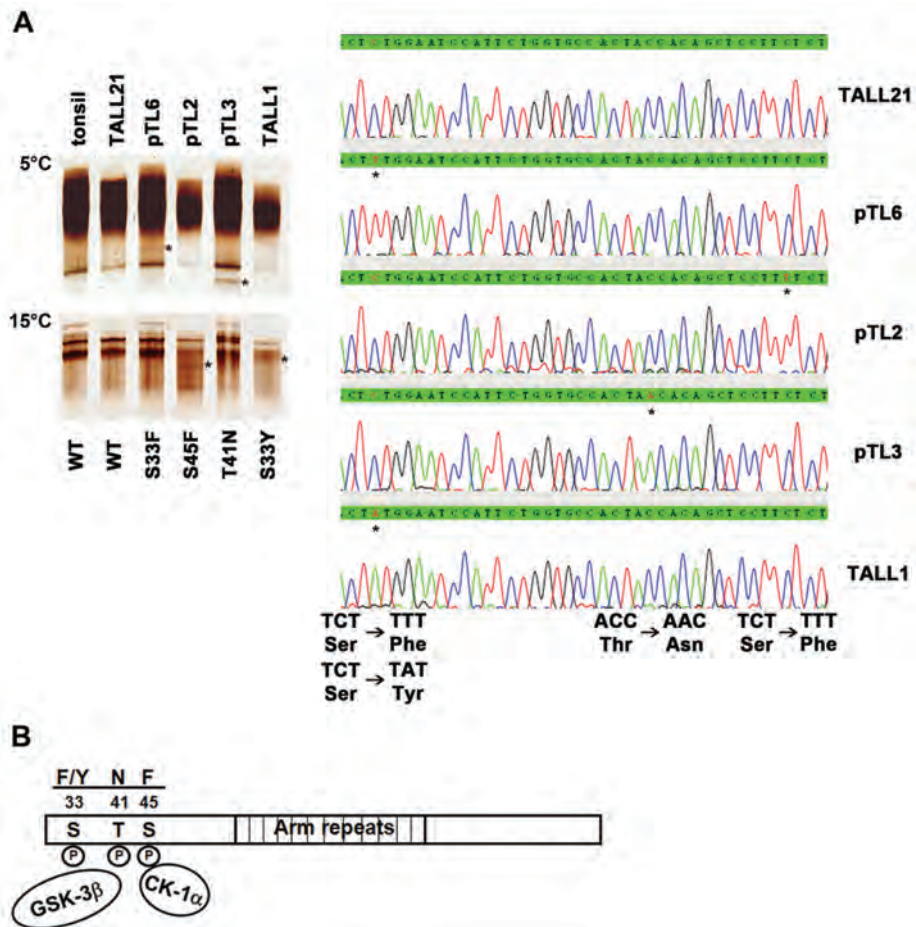


Figure 2. Missense mutations of β -catenin in T cell lymphomas.

(A) Mutational analysis of exon3 of *CTNNB1*. Left panel. Mutational transitions were visualized as aberrant migrating amplicons by SSCP analysis at either 5°C or 15°C (asterisks). Shown are the migration patterns of a non-mutated lymphoma (TALL21) and the four T cell lymphomas carrying a mutational transition in *CTNNB1* compared to a non-mutated control (tonsil). Right panel. Sequence analysis of *CTNNB1* confirmed the mutational transitions in T cell lymphomas (asterisks). Shown are a non-mutated lymphoma (TALL21) and the four T cell lymphomas carrying a mutation in the gene encoding β -catenin. (B) Schematic representation of the β -catenin protein with the mutated phosphorylation sites ($S_{33}F/Y$, $T_{41}N$ and $S_{45}F$) identified in T cell lymphomas.

Activation of Wnt signaling in T-NHLs by gain of function mutations in *CTNNB1* (β -catenin)

Mutations in Wnt pathway components, specifically in the genes encoding β -catenin (*CTNNB1*) or *APC*, often underlie the accumulation of β -catenin and aberrant activation of TCF-mediated transcription in cancer. To explore whether mutational activation of the Wnt pathway also takes place in non Hodgkin lymphomas, we studied the tumors with nuclear β -catenin expression for the presence of mutations in *CTNNB1* or *APC*. This analysis

identified four lymphomas containing a point mutation in the mutational hotspot region in exon 3 of *CTNNB1* (Figure 2A). All four mutations were established gain-of-function mutations resulting in an amino acid substitution at a specific phosphorylation site (Figure 2B), required for targeting β -catenin for ubiquitination and degradation. Three mutations were found in pTLs, *i.e.* two lymph nodes involved by CTCL and one nodal pTL-unspecified ($S_{33}F$; $S_{45}F$; $T_{41}N$), whereas one mutation was found in a T-LBL/ALL ($S_{33}Y$). PCR-SSCP and sequence analysis of the mutation cluster region (MCR) of APC identified several known single nucleotide polymorphisms (SNPs) but no loss-of-function *APC* mutations (data not shown). Our data identify gain-of-function mutation of *CTNNB1* as one of the mechanisms of β -catenin deregulation in T cell malignancies.

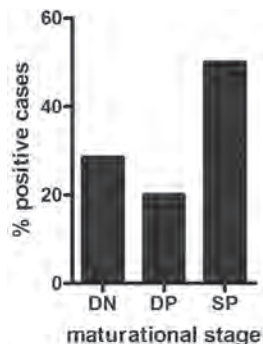


Figure 3. Frequent nuclear accumulation of β -catenin in T-LBL/ALL.

Nuclear localization of β -catenin in T-LBL/ALLs, subdivided by stage of maturation arrest as being double negative (DN; n=7), double positive (DP; n=10), or single positive (SP; n=10). Although the accumulation of β -catenin was more often found in T-LBL/ALL derived from more mature (SP) T cells, it was not restricted to a single stage of maturation arrest.

Nuclear β -catenin expression in T-LBL/ALL is not restricted to a specific stage of maturation arrest

T cell maturation in the thymus proceeds through a number of developmental checkpoints, marked by distinct phenotypic changes. In the human, thymocytes are successively double negative (DN, CD4⁻CD8⁻), immature single positive (ISP, CD4⁺CD3⁻), double positive (DP, CD4⁺CD8⁺) and single positive (SP, CD3⁺CD4⁺ or CD3⁺CD8⁺). This maturation is tightly controlled by various signaling pathways, including the NOTCH, Wnt, and HEDGEHOG pathways^{34,35}. To assess whether aberrant Wnt signaling in T-LBL/ALL is associated with arrest at a specific developmental stage, the relation between nuclear β -catenin expression and T-LBL/ALL phenotype was studied. As shown in figure 3, nuclear β -catenin expression was not restricted to a single stage of maturation arrest but was present in several DN, DP, as well as a SP tumors (Figure 3; Supplementary Table S1). However, the incidence was higher (5/10) in late stage (SP) than in the early stage (DN and DP) tumors (4/17). Since aberrant activation of NOTCH signaling contributes to tumor development in a majority of patients with T-LBL/ALL³⁰, the presence of mutations in NOTCH1 was examined in a subset of T-LBL/ALL patients (Supplementary Table S2). In line with previous studies^{30,36}, more than half of the T-LBL/ALL carried mutations in NOTCH1, dispersed over the heterodimerization and PEST domains. However, no correlation between the absence or presence of NOTCH1 mutations and nuclear β -catenin expression was observed (Supplementary Table S2).

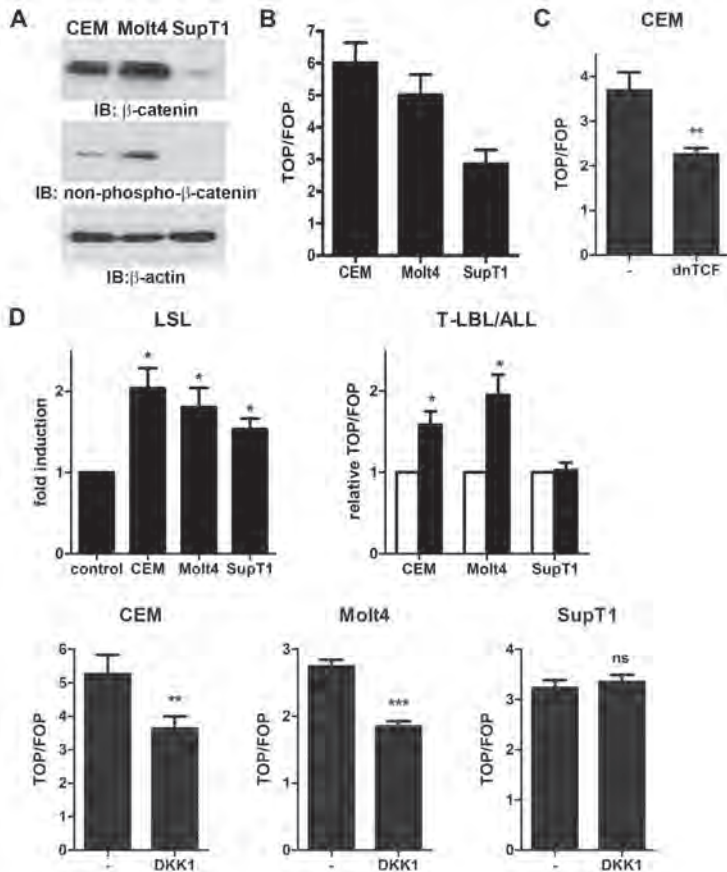


Figure 4. Autocrine Wnt signaling controls constitutive TCF-mediated gene transcription in T-LBL/ALL cells.

(A) β -catenin expression in T-LBL/ALL cell lines. To monitor the β -catenin protein levels, cells were lysed and immunoblotted using a monoclonal anti- β -catenin antibody (top panel), or an antibody recognizing non-phosphorylated β -catenin (middle panel). The bottom part of the blot was stained with anti- β -actin to verify equal loading (lower panel). **(B)** T-LBL/ALL cell lines have basal TCF-mediated transcription, as depicted by the TOPFLASH over FOPFLASH ratio. Cell lines were either transfected with the TOPFLASH reporter or the FOPFLASH reporter, and assayed for luciferase activity. The mean TOP/FOPFLASH ratio of 10 independent experiments (+/-SEM) is shown. **(C)** dnTCF4 suppresses the constitutive TCF-mediated transcription in T-LBL/ALL, indicating constitutive TCF-mediated transcription. CEM was transfected with the TOPFLASH reporter or the FOPFLASH reporter, either alone or in combination with dnTCF4. The mean TOP/FOPFLASH ratio of 3 independent (+/-SEM) is shown. ** $P < 0.01$ by student's t-test. **(D)** Conditioned medium of T-LBL/ALL cells activates TCF-mediated transcription. Upper left panel. LSL cells were either incubated with control medium (control), or with the conditioned medium harvested from 48 hours cultured T-LBL/ALL cells. The mean fold induction of 5 independent experiments (+/-SEM) is shown. * $P < 0.05$ by student's t-test. Upper right panel. T-LBL/ALL cell lines were either transfected with the TOPFLASH reporter or the FOPFLASH reporter. 24 Hours after transfection, the cells were extensively washed and incubated for 24 hours with control medium (white bars), or with conditioned medium harvested from 48 hours cultured T-LBL/ALL cells (black bars). The TOPFLASH over FOPFLASH ratio of the target cells incubated with control medium was normalized to 1. The mean fold induction of 3 independent experiments (+/-SEM) is shown. * $P < 0.05$ by student's t-test. Lower panel. DKK1 expression reduces TCF-mediated transcription in T-LBL/ALL. Cell lines were transfected with the TOPFLASH reporter or the FOPFLASH reporter alone, or in combination with DKK1. The mean TOP/FOPFLASH ratio of 3 independent experiments (+/-SEM) is shown. ** $P < 0.01$; *** $P < 0.001$; ns: not significant, by student's t-test.

Constitutive TCF-mediated gene transcription in T-LBL/ALL cells by autocrine Wnt signaling

As demonstrated above, nuclear accumulation of β -catenin is relatively common in T-LBL/ALL suggesting activation of the canonical Wnt signaling pathway. However, with the exception of a single tumor having a *CTNNB1* mutation, the T-LBL/ALLs with nuclear β -catenin had no mutations in either *CTNNB1* or *APC*. In these tumors, the Wnt signaling pathway is presumably intact and activation could be caused by autocrine stimulation. To explore this hypothesis, we employed the T-LBL/ALL cell lines CEM, Molt4 and SupT1. Similar to the primary T-LBL/ALLs, CEM and Molt4 strongly express β -catenin, including the active non-phosphorylated form of the protein (Figure 4A). To monitor the TCF transcriptional activity in the T-LBL/ALL cell lines, we transfected a TCF reporter (pTOPFLASH); as a control, we used a reporter containing scrambled TCF binding sites (pFOPFLASH). All three cell lines showed constitutive activation of the TCF reporter (Figure 4B). Transfection of a dominant negative form of TCF4 (dnTCF4) to CEM, the cell line with the highest TOP/FOPFLASH ratio, caused a significant reduction of the basal TCF-mediated transcriptional activity (Figure 4C), confirming the specificity of the detected reporter activity. Since the T-LBL/ALL cell lines do not carry any *CTNNB1* or *APC* mutations (data not shown), our results suggest the possible existence of an autocrine stimulatory loop. Therefore, we assessed the expression of Wnts and their receptors (Fzd) by means of a Wnt signaling pathway gene expression array. The cell lines as well as a primary T-LBL/ALL revealed predominant expression of the ligands Wnt16 and Wnt10A and the receptors Fzd1 and Fzd2 (Supplementary Table S3), thus allowing for autocrine activation. Accordingly, incubation of an established Wnt reporter cell line (LSL)³¹ with conditioned media harvested from the T-LBL/ALL cell lines, resulted in enhanced TCF-mediated reporter activity (Figure 4D). Moreover, applying the conditioned media to the corresponding T-LBL/ALL cell lines themselves, previously transfected with pTOPFLASH and deprived of any autocrine-produced ligands, resulted in enhanced reporter activity in CEM and Molt4 (Figure 4D). Importantly, transfection of Dickkopf-1 (DKK1), a secreted antagonist that prevents Wnt signaling by preventing binding of Wnt ligands to Wnt-signaling coreceptors LRP5/6, led to reduced TCF-reporter activity in both CEM and Molt4 (Figure 4D). Notably, SupT1, which did not respond to either conditioned medium or DKK1 expression, showed lower expression of Fzd1 (and Wnt16) (Supplementary Table S3). Taken together, these results demonstrate that the Wnt signaling pathway is constitutively active in the T-LBL/ALL cell lines CEM and Molt4 and support the presence of an autocrine activation loop.

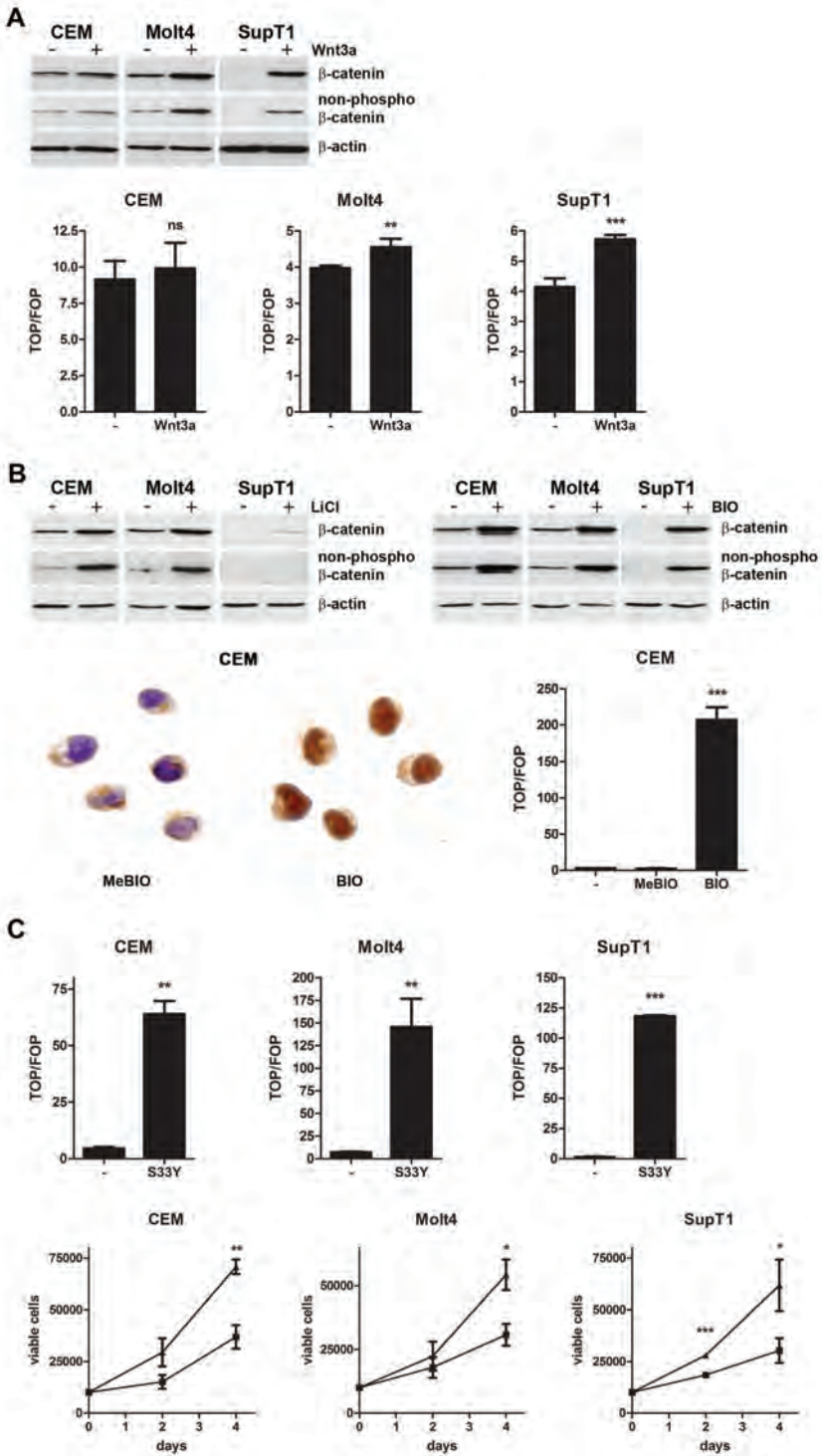
Stimulation of the Wnt-signaling pathway promotes TCF-mediated gene transcription and growth of T-LBL/ALL cells

To further explore the integrity and functionality of the Wnt signaling pathway in the T-LBL/ALL cells, we tested β -catenin levels and TCF transcriptional activity after applying a number of stimuli that activate the Wnt signaling at different levels. Initially, we tested the effect of stimulation at the level of the receptor by purified Wnt3a³⁷. In Molt4 and SupT1, stimulation with Wnt3a resulted in a pronounced accumulation of β -catenin, including accumulation of non-phosphorylated β -catenin, and a significant increase of the TCF-reporter activity (Figure 5A). By contrast, CEM hardly responded to Wnt3a (Figure 5A); in these cells receptor

binding/stimulation may have already been saturated/optimal as a result of autocrine produced Wnts (see Figure 4D).

Stimulation of Wnt signaling at the intracellular level, by lithium chloride (LiCl), or the pharmacological inhibitor BIO, which both mimics Wnt signaling by inhibition of GSK3 β ³⁸, resulted in additional β -catenin accumulation in all three ALL cell lines (Figure 5B; top panel). GSK3 β inhibition also affected β -catenin localization; prior to inhibitor treatment, low amounts of β -catenin were detected in the cytoplasm of the T-LBL/ALL cells, after treatment, an increase in the total amount of β -catenin and its nuclear translocation was observed (Figure 5B and data not shown). This was accompanied by a strongly increased TCF-reporter activity in all three cell lines (Figure 5B and data not shown).

Finally, we also studied the impact of transfection of the β -catenin mutant S₃₃Y, which was found in one of the primary T-LBL/ALLs described in this study (Figure 2). Notably, this is an established gain of function mutation, also found in e.g. colorectal cancer, resulting in β -catenin stabilization. Interestingly, apart from strongly enhancing TCF-mediated transcription (Figure 5C; top panel), transfection of this β -catenin mutant markedly enhanced the growth of all three ALL-cell lines (Figure 5C; bottom panel). Taken together, our observations indicate that the canonical Wnt pathway in T-LBL/ALL is constitutively activated, but still sensitive to regulation, and induces the growth of T-LBL/ALL cells.



3

Figure 5. Stimulation of the Wnt signaling pathway increases TCF-mediated gene transcription and growth of T-LBL/ALL cells.

(A) Accumulation of β -catenin and enhanced TCF-mediated transcription in response to purified Wnt3a. Top panel. Cells were incubated for 6 hours in the presence or absence of purified Wnt3a (200 ng/ml). Cells were lysed and immunoblotted using a monoclonal anti- β -catenin antibody, or an antibody recognizing non-phosphorylated β -catenin. The bottom part of the blot was stained with anti- β -actin to verify equal loading. Bottom panel. Cells were transfected with either the TOPFLASH or the FOPFLASH reporter construct, 24 hours after transfection the cells were stimulated for 24 hours with purified Wnt3a, as indicated (bottom panel). The mean TOP/FOPFLASH ratio of 3 independent experiments (+/-SEM) is shown. ** $P < 0.01$; *** $P < 0.001$; ns: not significant, by student's t-test. **(B)** Activation of the Wnt signaling pathway by inhibition of GSK-3 β results in accumulation and nuclear translocation of β -catenin, as well as enhanced TCF-mediated transcription. Top panel. Cells were incubated for 24 hours in the presence of 20 mM LiCl or KCl as a control (left panel), or in the presence or absence of 5 μ M BIO (right panel), after which they were lysed and immunoblotted as described above. Bottom left panel. To visualize nuclear translocation of β -catenin, CEM was cultured in the presence of 5 μ M MeBIO as a control (left panel) or BIO (right panel) for 24 hours. Nuclear localization was visualized by immunohistochemistry using a monoclonal anti- β -catenin antibody. Bottom right panel. Enhanced basal TCF-mediated transcriptional activity in CEM in response to GSK-3 β inhibition. CEM was transfected with the TOPFLASH reporter or the FOPFLASH reporter, 24 hours after transfection, the cells were incubated for another 24 hours in the presence of 5 μ M BIO or a control, MeBIO. The mean TOP/FOPFLASH ratio of 3 independent experiments (+/-SEM) is shown. *** $P < 0.001$ by student's t-test. **(C)** Activation of the Wnt signaling pathway by a constitutive active mutant β -catenin ($S_{33}Y$ β -catenin) leads to enhanced TCF-mediated transcription and growth. Top panel. T-LBL/ALL cell lines were transfected with the TOPFLASH reporter or the FOPFLASH reporter, either alone or in combination with $S_{33}Y$ β -catenin. The mean TOP/FOPFLASH ratio of 3 independent experiments (+/-SEM) is shown. ** $P < 0.01$; *** $P < 0.001$, by student's t-test. Bottom panel. To monitor the effect of $S_{33}Y$ β -catenin on the growth of the T-LBL/ALL cell lines, cells were transfected with pEGFP in combination with either pcDNA3.1 (■) as a control, or $S_{33}Y$ β -catenin (▲). After overnight recovery viable GFP-positive cells were FACS-sorted and cultured at a density of 5×10^4 cells/ml. Viability was measured after two and four days of culture. The mean of 3 independent experiments (+/-SEM) of the three T-LBL/ALL cell lines CEM, Molt4 and SupT1 is shown. * $P < 0.05$; ** $P < 0.01$; *** $P < 0.001$, by student's t-test.

Discussion

3 In the present study, we have explored the role of the Wnt signaling pathway in NHLs and show that a significant subset of T cell lymphomas and some B cell lymphomas display evidence of active Wnt signaling. This aberrant Wnt pathway activation was caused by *CTNNB1* mutations or, in lymphomas with mutations in neither *CTNNB1* nor *APC*, by the presence of an autocrine activation loop. Functional studies indicate that the Wnt signaling pathway may promote lymphoma growth. Our findings imply that the Wnt pathway, which is essential for early T and B cell development^{4,22} and plays a role in the self-renewal of hematopoietic stem cells, is aberrantly activated in a substantial subgroup of NHLs and contributes to lymphomagenesis. Regulation of β -catenin levels plays a central role in Wnt signaling. Our immunohistochemical screening of a large panel of NHLs revealed that a substantial subset of T cell lymphomas (25%) and occasional B cell lymphomas (3%) showed nuclear accumulation of β -catenin, a hallmark of active canonical Wnt signaling (Table 1 and Figure 1). Compared to the undetectable β -catenin expression in the lymphocytes in tissue sections of normal lymphoid organs, β -catenin was vastly overexpressed in these tumors, implying aberrant Wnt signaling activation. Indeed, mutational analysis of *CTNNB1* and *APC* revealed that several of the lymphomas identified by our screening contained missense mutations in *CTNNB1* (Figure 2). In contrast to the mutations of unknown functional significance previously reported in NK/T cell lymphomas^{39,40}, the current mutations all represented established gain-of-function mutations, involving phosphorylation sites important for ubiquitination and degradation of β -catenin, and have previously been reported in hepatocellular, prostate, and colorectal cancer⁸. In addition, a B-LBL/ALL with nuclear β -catenin accumulation was found to contain a t(1;19)(q23;p13) translocation with consequent expression of a E2A-Pbx1 fusion protein. This fusion protein causes Wnt16 overexpression and constitutive autocrine Wnt signaling^{32;33}. These observations clearly illustrate the power of our screening protocol to identify NHL with deregulated Wnt signaling.

Of the 110 primary B cell NHLs studied only three showed nuclear β -catenin expression. Apart from the B-LBL/ALL with the t(1;19)(q23;p13), two DLBCLs were β -catenin positive. Neither of these tumors showed evidence of infection with KSHV or EBV, viruses that have been suggested to induce Wnt pathway activation in B lymphocytes^{41;42}. Vice versa, DLBCLs with a proven infection by these gamma-herpes viruses⁴³, did not show nuclear β -catenin accumulation (data not shown). Recent studies have suggested a role for uncontrolled Wnt signaling in the pathogenesis of B-LBL/ALL and B-CLL^{32;44;45}, involving either epigenetic silencing of Wnt inhibitors⁴⁶ or deregulated expression of Wnts and/or other Wnt pathway components. However, in line with our current findings (Table 1), these studies did not reveal constitutive nuclear β -catenin expression in B-CLL⁴⁴ and in the large majority of LBL/ALLs⁴⁵. Although we cannot formally exclude the possibility that low levels of nuclear β -catenin, sufficient to support TCF-mediated transcription, escape detection by our method, we conclude that the currently available data do not support a major role for the Wnt pathway in these lymphoid malignancies.

Of the 52 T cell lymphomas studied, 13 (25%) showed marked nuclear β -catenin expression (Table 1 and Figure 1). These included precursor T-LBL/ALLs as well as mature T-lineage lymphomas. Among these tumors, one T-LBL/ALL and three pTLs showed classical gain-of-function mutations in *CTNNB1*, a finding that constitutes 'proof of principle' for the

oncogenic potential of the Wnt pathway in both precursor- and mature T cells. Two of the pTLs with *CTNNB1* mutations were lymph nodes involved by CTCL. In the primary cutaneous tumors of these patients neither a *CTNNB1* mutation nor β -catenin expression was detected, implying that the Wnt pathway activation in these lymphomas was acquired during tumor progression. Notably, nuclear β -catenin expression was most prevalent in lymphomas of the precursor T-LBL/ALLs subgroup (33%). This expression was not restricted to tumors showing an early maturation arrest and, hence, does not reflect the Wnt signaling activity present during early thymocyte development⁴⁷. By contrast, nuclear β -catenin expression appears to be more common in T-LBL/ALLs with a relatively mature (single positive) phenotype, implying aberrant Wnt pathway activation (Figure 3 and Supplementary Table S1). In addition, no correlation was found between Wnt pathway activation and the absence or presence of mutations in *NOTCH1*, a gene mutated in the majority of T-LBL/ALLs³⁰.

In agreement with our current findings in human T-LBL/ALL, it was recently shown that stabilization of β -catenin in mouse thymocytes is oncogenic, and results in malignant T cell lymphomas²⁷. Except in one of the T-LBL/ALLs, this activation was not caused by mutations in either *CTNNB1* or *APC*, suggesting that the Wnt pathway is intact and might be activated in situ by autocrine or paracrine Wnts. Consistent with this hypothesis, Wnts have been reported to be expressed by thymocytes as well as by thymic epithelial cells^{47;48}, and several studies have demonstrated overexpression of Wnts by ALL cells^{32;33;45}. Our studies in T-LBL/ALL cell lines strongly support this autocrine activation scenario: They show that these cells contain active β -catenin and display constitutive TCF-mediated transcriptional activity (Figure 4B), which is inhibited by *DKK1*, an extracellular Wnt signaling antagonist that blocks Wnt-induced receptor activation by binding to the co-receptor *LRP5/6* (Figure 4D). In line with this observation, we found expression of several Wnt and *Fzd* genes in these cells (Supplementary Table S3), and demonstrated that the conditioned media have Wnt signaling inducing capacity (Figure 4D). Notably, *Wnt16*, which has been found to be overexpressed in B-LBL/ALL carrying a *t(1;19)(q23;p13)* translocation^{32;33}, was among the two most prominently expressed Wnts identified (Supplementary Table S3). Furthermore, our results show that the Wnt pathway in T-LBL/ALL cells, although constitutively active, can still be regulated by exogenous stimuli like *LiCl*, *BIO*, *Wnt3a*, conditioned media, by the Wnt signaling inhibitor *DKK1*, or by an active β -catenin mutant (*S33Y*). This regulability by stimuli that act at distinct levels, including at the receptor level, implies that the pathway is basically intact (Figure 4, 5A and B). Our observation that the activating β -catenin mutation (*S33Y*), which we identified in one of our primary T-LBL/ALLs, enhances the growth of all three T-LBL/ALL cell lines tested (Figure 5C), suggest that aberrant Wnt pathway activation may indeed contribute to tumor growth in human precursor T-LBL/ALLs.

In conclusion, our data indicate that Wnt signaling, which normally controls lymphocyte progenitor fate as well as the self-renewal of hematopoietic stem cells, is illegitimately activated in a distinct subset of NHL, particularly in precursor T cell lymphomas, and contributes to the pathogenesis of these tumors. Targeting Wnt signaling components with recently developed small-molecule drugs may prove a successful novel means of therapeutic intervention in lymphoma patients displaying active Wnt signaling.

Acknowledgements

The authors would like to thank Dr. J.J. Oudejans for kindly providing us with primary patient material, Dr. C.H.M. Mellink for the cytogenetic data of the T-LBL/ALL patients, H.P. Meijer and B. Hooibrink for technical assistance, and Dr. E.J.W. Redeker for helping us with the PCR-SSCP.

References

1. Evans LS, Hancock BW. Non-Hodgkin lymphoma. *Lancet* 2003;362:139-146.
2. Kupperts R. Mechanisms of B-cell lymphoma pathogenesis. *Nat.Rev.Cancer* 2005;5:251-262.
3. Rizvi MA, Evens AM, Tallman MS, Nelson BP, Rosen ST. T-cell non-Hodgkin lymphoma. *Blood* 2006;107:1255-1264.
4. Verbeek S, Izon D, Hofhuis F et al. An HMG-box-containing T-cell factor required for thymocyte differentiation. *Nature* 1995;374:70-74.
5. Reya T, O’Riordan M, Okamura R et al. Wnt signaling regulates B lymphocyte proliferation through a LEF-1 dependent mechanism. *Immunity*. 2000;13:15-24.
6. Reya T, Duncan AW, Ailles L et al. A role for Wnt signalling in self-renewal of haematopoietic stem cells. *Nature* 2003;423:409-414.
7. Nusse R, Varmus HE. Wnt genes. *Cell* 1992;69:1073-1087.
8. Polakis P. Wnt signaling and cancer. *Genes Dev.* 2000;14:1837-1851.
9. Wodarz A, Nusse R. Mechanisms of Wnt signaling in development. *Annu.Rev.Cell Dev.Biol.* 1998;14:59-88.
10. Moon RT, Bowerman B, Boutros M, Perrimon N. The promise and perils of Wnt signaling through beta-catenin. *Science* 2002;296:1644-1646.
11. Molenaar M, van de WM, Oosterwegel M et al. XTcf-3 transcription factor mediates beta-catenin-induced axis formation in *Xenopus* embryos. *Cell* 1996;86:391-399.
12. Behrens J, von Kries JP, Kuhl M et al. Functional interaction of beta-catenin with the transcription factor LEF-1. *Nature* 1996;382:638-642.
13. Tetsu O, McCormick F. Beta-catenin regulates expression of cyclin D1 in colon carcinoma cells. *Nature* 1999;398:422-426.
14. He TC, Sparks AB, Rago C et al. Identification of c-MYC as a target of the APC pathway. *Science* 1998;281:1509-1512.
15. van de Wetering M, Sancho E, Verweij C et al. The beta-catenin/TCF-4 complex imposes a crypt progenitor phenotype on colorectal cancer cells. *Cell* 2002;111:241-250.
16. Bienz M, Clevers H. Linking colorectal cancer to Wnt signaling. *Cell* 2000;103:311-320.
17. Kinzler KW, Vogelstein B. Lessons from hereditary colorectal cancer. *Cell* 1996;87:159-170.
18. Wielenga VJ, Smits R, Korinek V et al. Expression of CD44 in *Apc* and *Tcf* mutant mice implies regulation by the WNT pathway. *Am.J.Pathol.* 1999;154:515-523.
19. Boon EMJ, van der Neut R, van de Wetering M, Clevers H, Pals ST. Wnt signaling regulates expression of the receptor tyrosine kinase *Met* in colorectal cancer. *Cancer Res.* 2002;62:5126-5128.
20. Travis A, Amsterdam A, Belanger C, Grosschedl R. LEF-1, a gene encoding a lymphoid-specific protein with an HMG domain, regulates T-cell receptor alpha enhancer function [corrected]. *Genes Dev.* 1991;5:880-894.
21. van de Wetering M, Oosterwegel M, Dooijes D, Clevers H. Identification and cloning of TCF-1, a T lymphocyte-specific transcription factor containing a sequence-specific HMG box. *EMBO J.* 1991;10:123-132.
22. Schilham MW, Wilson A, Moerer P et al. Critical involvement of Tcf-1 in expansion of thymocytes. *J.Immunol.* 1998;161:3984-3991.

23. Gounari F, Aifantis I, Khazaie K et al. Somatic activation of beta-catenin bypasses pre-TCR signaling and TCR selection in thymocyte development. *Nat.Immunol.* 2001;2:863-869.
24. Ioannidis V, Beermann F, Clevers H, Held W. The beta-catenin--TCF-1 pathway ensures CD4(+)CD8(+) thymocyte survival. *Nat.Immunol.* 2001;2:691-697.
25. Kirstetter P, Anderson K, Porse BT, Jacobsen SE, Nerlov C. Activation of the canonical Wnt pathway leads to loss of hematopoietic stem cell repopulation and multilineage differentiation block. *Nat.Immunol.* 2006;7:1048-1056.
26. Scheller M, Huelsken J, Rosenbauer F et al. Hematopoietic stem cell and multilineage defects generated by constitutive beta-catenin activation. *Nat.Immunol.* 2006;7:1037-1047.
27. Guo Z, Dose M, Kovalovsky D et al. Beta-catenin stabilization stalls the transition from double-positive to single-positive stage and predisposes thymocytes to malignant transformation. *Blood* 2007;109:5463-5472.
28. Derksen PWB, Tjin E, Meijer HP et al. Illegitimate WNT signaling promotes proliferation of multiple myeloma cells. *Proc.Natl.Acad.Sci.U.S.A* 2004;101:6122-6127.
29. Battle E, Henderson JT, Beghtel H et al. Beta-catenin and TCF mediate cell positioning in the intestinal epithelium by controlling the expression of EphB/ephrinB. *Cell* 2002;111:251-263.
30. Weng AP, Ferrando AA, Lee W et al. Activating mutations of NOTCH1 in human T cell acute lymphoblastic leukemia. *Science* 2004;306:269-271.
31. Blitzer JT, Nusse R. A critical role for endocytosis in Wnt signaling. *BMC.Cell Biol.* 2006;7:28.
32. McWhirter JR, Neuteboom ST, Wancewicz EV et al. Oncogenic homeodomain transcription factor E2A-Pbx1 activates a novel WNT gene in pre-B acute lymphoblastoid leukemia. *Proc.Natl.Acad.Sci.U.S.A* 1999;96:11464-11469.
33. Mazieres J, You L, He B et al. Inhibition of Wnt16 in human acute lymphoblastoid leukemia cells containing the t(1;19) translocation induces apoptosis. *Oncogene* 2005;24:5396-5400.
34. Staal FJ, Clevers HC. Wnt signaling in the thymus. *Curr.Opin.Immunol.* 2003;15:204-208.
35. Weerkamp F, van Dongen JJ, Staal FJ. Notch and Wnt signaling in T-lymphocyte development and acute lymphoblastic leukemia. *Leukemia* 2006;20:1197-1205.
36. Mansour MR, Linch DC, Feroni L, Goldstone AH, Gale RE. High incidence of Notch-1 mutations in adult patients with T-cell acute lymphoblastic leukemia. *Leukemia* 2006;20:537-539.
37. Willert K, Brown JD, Danenberg E et al. Wnt proteins are lipid-modified and can act as stem cell growth factors. *Nature* 2003;423:448-452.
38. Meijer L, Skaltsounis AL, Magiatis P et al. GSK-3-selective inhibitors derived from Tyrian purple indirubins. *Chem.Biol.* 2003;10:1255-1266.
39. Hoshida Y, Hongyo T, Jia X et al. Analysis of p53, K-ras, c-kit, and beta-catenin gene mutations in sinonasal NK/T cell lymphoma in northeast district of China. *Cancer Sci.* 2003;94:297-301.
40. Takahara M, Kishibe K, Bandoh N, Nonaka S, Harabuchi Y. P53, N- and K-Ras, and beta-catenin gene mutations and prognostic factors in nasal NK/T-cell lymphoma from Hokkaido, Japan. *Hum.Pathol.* 2004;35:86-95.
41. Fujimuro M, Hayward SD. The latency-associated nuclear antigen of Kaposi's sarcoma-associated herpesvirus manipulates the activity of glycogen synthase kinase-3beta. *J.Virol.* 2003;77:8019-8030.
42. Morrison JA, Klingelhutz AJ, Raab-Traub N. Epstein-Barr virus latent membrane protein 2A activates beta-catenin signaling in epithelial cells. *J.Virol.* 2003;77:12276-12284.
43. Delooste ST, Smit LA, Pals FT et al. High incidence of Kaposi sarcoma-associated herpesvirus infection in HIV-related solid immunoblastic/plasmablastic diffuse large B-cell lymphoma. *Leukemia* 2005;19:851-855.
44. Lu D, Zhao Y, Tawatao R et al. Activation of the Wnt signaling pathway in chronic lymphocytic leukemia. *Proc. Natl.Acad.Sci.U.S.A* 2004;101:3118-3123.
45. Khan NI, Bradstock KF, Bendall LJ. Activation of Wnt/beta-catenin pathway mediates growth and survival in B-cell progenitor acute lymphoblastic leukaemia. *Br.J.Haematol.* 2007;138:338-348.
46. Roman-Gomez J, Cordeu L, Agirre X et al. Epigenetic regulation of Wnt-signaling pathway in acute lymphoblastic leukemia. *Blood* 2007;109:3462-3469.

47. Weerkamp F, Baert MR, Naber BA et al. Wnt signaling in the thymus is regulated by differential expression of intracellular signaling molecules. *Proc.Natl.Acad.Sci.U.S.A* 2006;103:3322-3326.
48. Pongracz J, Hare K, Harman B, Anderson G, Jenkinson EJ. Thymic epithelial cells provide WNT signals to developing thymocytes. *Eur.J.Immunol.* 2003;33:1949-1956.

Supplementary Data

Table S1. Characteristics of the T-LBL/ALL patients.

Case	Sex/ Age	Localization	Immunophenotype				
			CD3	CD4	CD8	TdT	β-catenin
1	M/15	lymph node	+	-	-	+	+
2	M/6	testis	+	-	-	+	-
3	M/46	bone marrow	+	-	-	+	+
4	M/39	bone marrow	+	-	-	-	-
5	M/8	lymph node	w	-	-	+	-
6	M/35	lymph node	w	-	-	w	-
7	M/22	skin	+	-	-	+	-
<hr/>							
8	F/54	lymph node	+	+	+	+	-
9	M/4	lymph node	+	+	+	+	-
10	F/7mth	mediastinum	+	+	+	+	-
11	M/9	lymph node	+	+	+	+	-
12	M/4	lymph node	+	+	+	+	-
13	M/15	lymph node	+	+	+	+	+
14	M/10	mediastinum	+	+	+	+	+
15	M/16	mediastinum	+	+	+	+	-
16	M/17	bone marrow	+	+	+	+	-
17	F/21	lymph node	+	+	+	+	-
<hr/>							
18	M/38	testis	+	+	-	+	-
19	M/26	lymph node	w	+	-	+	+
20	M/10	skin	+	+	-	+	-
21	M/14	lymph node	+	w	-	+	+
22	M/12	lymph node	+	+	-	w	-
23	F/5	skin	+	w	-	+	+
24	M/26	lymph node	+	+	-	+	-
25	F/6	lymph node	+	w	-	+	-
26	F/29	lymph node	+	-	+	+	+
27	M/18	bone marrow	+	-	+	-	+

Staining was evaluated as follows: +: positive; -: negative; w: weak.

mth = month

Table S2. NOTCH1 mutations in T-LBL/ALL.

Case	Heterodimerization domain	PEST-domain	β-catenin expression
2	-	-	-
7	-	2515 RVP*stop; T2484A	-
9	-	<i>delP2416</i>	-
12	-	<i>P2414L</i>	-
20	-	<i>delP2416; A2425V</i>	-
22	-	-	-
25	delV1579	<i>V2444A</i>	-
<hr/>			
13	-	<i>A2357T; S2358N</i>	+
14	-	-	+
19	delV1579	-	+
21	delFP1618/19; G1647S	-	+
23	-	-	+

Published mutations in bold, newly identified mutations in italics.

del = deletion

Nuclear staining of β-catenin was evaluated as follows: +: positive; -: negative.

Table S3. WNT signaling pathway related gene-expression in a T-LBL/ALL patient and cell lines.

	CEM	Molt4	SupT1	T-LBL/ALL #21
WNT1	+	+	+	+
WNT2	-	-	-	-
WNT2B	-	-	-	-
WNT3	+	+	+	+
WNT3A	-	-	-	-
WNT4	-	-	-	-
WNT5A	-	-	-	-
WNT5B	-	-	-	-
WNT6	-	-	-	-
WNT7A	-	-	-	-
WNT7B	-	-	-	-
WNT8A	-	-	-	-
WNT8B	-	-	-	-
WNT9A	-	-	-	-
WNT9B	-	-	-	-
WNT10A	++	+	+	+++
WNT10B	-	-	-	-
WNT11	-	-	-	-
WNT16	+++	+++	++	+++
FZD1	++	++	+	+++
FZD2	+	++	+++	++
FZD3	-	-	-	-
FZD4	-	-	-	-
FZD5	+	+	+	-
FZD6	+	+	-	+
FZD7	-	-	-	-
FZD8	-	-	-	-
FZD9	+	+	+	+
FZD10	-	-	-	-
LRP5	-	-	-	-
LRP6	+	+	+	+
CTNNB1	+	+	+	+
APC	-	-	-	-
APC2	+	+	+	+
AXIN1	+	+	+	++
AXIN2	+	+	+	++
DVL1	+++	+++	++	+++
DVL2	-	-	-	-
DVL3	++	+	+	++
GSK3A	+++	+++	+++	+++
GSK3B	+	+	+	+
LEF1	+++	++	+++	++
TCF1	+++	+++	+++	+++
TCF3	+	++	++	+++
TCF4	+	+	+	+

Expression was evaluated as follows: +: low expression; ++ intermediate expression; +++ high expression.

4

Transcriptional silencing of the Wnt-antagonist Dickkopf-1 by promoter methylation unleashes aberrant Wnt signaling in advanced multiple myeloma

Richard W.J. Groen^{1,3}, Kinga A. Kocemba^{1,3}, Harmen van Andel¹, Marie José Kersten², Karène Mahtouk¹, Marcel Spaargaren¹ and Steven T. Pals¹.

¹Department of Pathology and ²Hematology, Academic Medical Center, University of Amsterdam, Amsterdam, The Netherlands. ³These authors contributed equally to this work.

Manuscript in preparation

Abstract

Aberrant activation of the Wnt/ β -catenin pathway is implicated in driving the formation of various human cancers. Recent studies indicate that the pathway plays at least two distinct roles in the pathogenesis of multiple myeloma (MM): i) Aberrant, presumably autocrine, activation of canonical Wnt signaling in MM cells promotes tumor proliferation and metastasis; ii) Overexpression of the Wnt inhibitor Dickkopf1 (DKK1), contributes to osteolytic bone disease by inhibiting osteoblast differentiation. Since DKK1 itself is a target of TCF/ β -catenin mediated transcription, these findings suggests the presence of a negative feedback loop in MM, in which DKK1 acts as a potential tumor suppressor. In line with this hypothesis, we show here that DKK1 expression is lost in most MM cell lines and in a subset of patients with advanced MM. This loss is correlated with activation of the Wnt pathway, as demonstrated by increased nuclear accumulation of β -catenin. Analysis of the *DKK1* promoter revealed CpG island methylation in several MM cell lines as well as in MM cells from patients with advanced MM. Moreover, demethylation of the *DKK1* promoter restores *DKK1* expression, which results in inhibition of β -catenin/TCF-mediated gene transcription in MM cell lines. Taken together, our data identify aberrant methylation of the *DKK1* promoter as a cause of *DKK1* silencing in advanced stage MM, which may play an important role in the progression of MM by unleashing Wnt signaling.

Introduction

Multiple myeloma (MM), one of the most common hematological malignancies in adults, is characterized by a clonal expansion of malignant plasma cells in the bone marrow (BM), associated with suppression of normal hematopoiesis, renal failure, and osteolytic bone lesions^{1,2}. These bone lesions have been shown to be the result of uncoupled or imbalanced bone remodeling with decreased formation and increased resorption of bone tissue, due to impaired osteoblast differentiation and aberrant osteoclast activation³. Recent studies have identified canonical Wnt signaling as a key signal pathway in both normal bone homeostasis and in the pathogenesis of MM bone disease⁴⁻⁶. The canonical Wnt/ β -catenin signaling pathway plays a central role in modulating the delicate balance between stemness and differentiation in several adult stem cell niches, including the intestinal crypt and the hematopoietic stem cell niche in the BM⁷⁻⁹. Wnt genes encode a family of 19 secreted glycoproteins, which promiscuously interact with several Frizzled (Fzd) receptors and the low-density lipoprotein receptor-related protein 5/6 (LRP5/6). The key event in the Wnt signaling pathway is the stabilization of β -catenin. Signaling by Wnt proteins results in inhibition of glycogen synthase kinase-3 β (GSK3 β) activity and dissociation of the adenomatous polyposis coli (APC)/axin complex, resulting in accumulation of β -catenin, which translocates to the nucleus. Here, β -catenin interacts with T cell factor (TCF) transcription factors to drive transcription of target genes¹⁰. The Wnt pathway is regulated by a large number of antagonists, including the secreted frizzled-related proteins (sFRPs) and the Dickkopf (DKK) family proteins. These two classes of antagonists either act by direct binding to the Wnt ligands (the sFRPs) or by interacting with the LRP5/6 coreceptors, preventing binding of the Wnt proteins to the Fzd/LRP receptor complex (the DKKs)¹¹. Recent studies indicate that the Wnt signaling pathway plays at least two distinct but divergent roles in the pathogenesis of MM. On the one hand, studies by our own laboratory¹² as well as by the Anderson laboratory¹³ have demonstrated that MMs can display aberrant activation of the canonical Wnt signaling pathway. This Wnt pathway activation presumably results from auto- and/or paracrine stimulation by Wnts, and promotes tumor proliferation and metastasis^{12;13}. On the other hand, as first shown by Tian and colleagues⁴, MMs overexpress and secrete the Wnt signaling inhibitor Dickkopf-1 (DKK1), which contributes to osteolytic bone disease by inhibiting osteoblast differentiation¹⁴⁻¹⁷. Similar to DKK1, secretion of the Wnt inhibitor sFRP2 by MM cells may also promote myeloma bone disease⁵. Since both DKK1 and sFRP2 are established targets of TCF/ β -catenin mediated transcription that can act as feedback suppressors of Wnt signaling¹⁸⁻²⁰, these findings suggests the presence of a negative feedback loop in MM in which DKK1 and sFRP2 act as potential tumor suppressors. In line with this hypothesis, we show here that DKK1 expression is often lost in advanced myeloma and is absent in MM cell lines, which are generally from advanced extramedullary myeloma. This loss of DKK1 unleashes β -catenin/TCF mediated transcription and is caused by methylation of the *DKK1* promotor.

Materials and methods

Case selection and classification

A panel of BM biopsy specimen from 41 MM and 7 MGUS patients, obtained at clinical diagnosis, was selected from the files of the Department of Pathology, Academic Medical Center, University of Amsterdam, Amsterdam, The Netherlands. All patients were staged according to the Salmon–Durie system. For statistical analysis patients with stage I and II disease were grouped together (n=16) and classified as early MM, whereas patients with stage III disease (n=25) were classified as having advanced MM.

Microarray analysis

For the analysis of expression of Wnt family members in MM patients, expression data publically available and deposited in the NIH Gene Expression Omnibus (GEO; National Center for Biotechnology Information [NCBI], <http://www.ncbi.nlm.nih.gov/geo/>) were used. These concerned the U133 Plus2.0 affymetrix oligonucleotide microarray data from 559 newly diagnosed MM patients included in total therapy 2/3 (TT2, TT3), provided by the University of Arkansas for Medical Sciences, GSE2658²¹.

Immunohistochemistry/Immunocytochemistry

Immunohistochemical staining was performed on formalin-fixed, plastic-embedded BM sections as described previously²². Sections were deplastified in acetone, after which endogenous peroxidase was blocked with a 0.3% solution of H₂O₂ in methanol and followed by antigen retrieval for 10 minutes in TRIS/EDTA buffer (respectively 10mM/1mM) pH 9.0 at 100°C. After blocking with serum free blocker (DAKO, Carpinteria, CA), the slides were either incubated for one hour at room temperature with anti-CD138 (IQP-153; IQ Products, Groningen, The Netherlands) or overnight at 4°C with anti-DKK1 (Abcam, Cambridge, MA), or anti-β-catenin (clone 14; BD Biosciences, Erembodegem, Belgium). For CD138 and β-catenin, binding of the antibody was visualized using the PowerVision plus detection system (Immunovision Technologies, Duiven, The Netherlands) and 3, 3'-diaminobenzidine (Sigma-Aldrich, St Louis, MO). Whereas binding of the DKK1-antibody was visualized with a biotinylated rabbit anti-goat antibody, followed by horseradish peroxidase (HRP)-conjugated streptavidin (DAKO) and DAB⁺ (DAKO). The sections were counterstained with hematoxylin (Merck, Darmstadt, Germany), washed and subsequently dehydrated through graded alcohol, cleared in xylene, and coverslipped. Immunocytochemical staining was performed on formalin-fixed cells. Briefly, slides were incubated for 30 minutes with PBS 0.3% Triton X-100 followed by blocking with serum free blocker (DAKO, Carpinteria, CA), the slides were then incubated overnight at 4°C with anti-DKK1 (goat polyclonal R&D). Binding of the DKK1-antibody was visualized with a biotinylated rabbit anti-goat antibody, followed by horseradish peroxidase (HRP)-conjugated streptavidin (DAKO) and 3-amino-9-ethyl carbazole (AEC). The biopsies were analyzed for DKK1 and β-catenin expression by two independent observers (RWJG and STP). DKK1 expression was scored in three semi-quantitative categories, i.e., low (0-25%), intermediate (25-75%) and high (75-100%), with the percentages indicating the number of DKK1 positive MM plasma cells. For β-catenin expression the intensity of nuclear staining was scored as negative/low, intermediate or high. For statistical analysis, the cases scored as negative/low and intermediate were grouped together as low β-catenin.

Methylation analysis

Genomic DNA was extracted and purified from MM BM suspensions and cell lines using DNAzol (Invitrogen Life technologies, Breda, The Netherlands) according to the manufacturer's protocol. The extracted DNA was modified by treatment with sodium bisulfite using the EpiTect Bisulfite Kit (Qiagen, Hilden, Germany). The methylation status of the DKK1 gene was assessed using both methylation specific PCR (MSP) and bisulfate sequencing, as described by Aquilera *et al.*²³.

Cell culture and demethylation treatment

MM cell lines L363, UM-1, OPM-1, RPMI 8226, and PC-3 were cultured in RPMI medium 1640 (Invitrogen Life technologies) containing 10% clone I serum (HyClone), 100 units/ml penicillin, and 100 µg/ml streptomycin. XG-1 and LME-1 cell lines were cultured in IMDM medium (Invitrogen Life technologies) supplemented with transferrin (20 mg/ml) and b-mercaptoethanol (50 mM). For XG-1, medium was additionally supplemented with IL-6 (500 pg/ml). 293T cells were cultured in DMEM medium containing 10% clone I serum (HyClone), 100 units/ml penicillin, and 100 µg/ml streptomycin. The PC-3 cell line was kindly provided by Christopher Hall. Cells were treated for 72h with 5-aza-2'-deoxycytidine (5-aza-CdR; Sigma-Aldrich) at a final concentration of 5 µM in PBS, after which they were harvested and lysed in Trizol (Invitrogen Life technologies).

RT-PCR

Total RNA was isolated using Trizol according to the manufacturer's protocol (Invitrogen Life technologies). The RNA was further purified using iso-propanol precipitation and was concentrated using the RNeasy MinElute Cleanup kit (Qiagen). The quantity of total RNA was measured using a NanoDrop ND-1000 Spectrophotometer (NanoDrop Technologies, Wilmington, DE). 5 µg of total RNA was used for cDNA synthesis as described previously. The PCR mixture contained: 100 ng of cDNA, 1x PCR Rxn buffer (Invitrogen Life technologies), 0.2 mmol/L dNTP, 2 mmol/L MgCl₂, 0.2 µmol/L of each primer, and 1U platinum Taq polymerase (Invitrogen Life technologies). PCR conditions were: denaturing at 95°C for 5 minutes, followed by 30 cycles of 30 s at 95°C, 30 s at 65°C (DKK1), 55°C (β-actin) and 30 s at 72°C. The reaction was completed for 10 minutes at 72°C. Primers used were: DKK1 forward (5'-GATCATAGCACCTTGGATGGG-3'); DKK1 reverse (5'-CAGTCTGATGACCGG-3'); β-actin forward (5'-GGATGCAGAAGGAGATCACTG-3'); β-actin reverse (5'-TCCACACGGAGTACTTG-3'). All primers were manufactured by Sigma-Aldrich (Haverhill, UK).

Western blot analysis

Conditioned medium was directly lysed in sample buffer, separated by SDS/10% PAGE, and blotted. Primary goat anti-DKK1 antibody (R&D) was detected by a horseradish peroxidase-conjugated swine anti-goat antibody, followed by detection using Lumi-Light PLUS western blotting substrate (Roche).

Co-culture assay

293T cells were plated in 6cm dish with 30% confluency and transfected by use of Fugene with DKK1 pcDNA3.1 or empty pcDNA3.1 construct. Co-cultures with MM cells transfected with Topflash/Fopflash reporter construct and pRL-TK were initiated 24h upon transfection of 293T cells and subsequently maintained for 48h. After 48h of co-culture, MM cells were harvested, lysed and luciferase activity was determined using the Dual-Luciferase Reporter assay (Promega).

Luciferase assay

MM cells (10mln) were transfected with TOPFLASH/FOPFLASH reporter construct (5ug) and pRL-TK (1ug) in 500ul serum-free medium. After 48h cells were lysed in 100ul passive lysis buffer (Promega) and firefly luciferase activity and Renilla luciferase activity were measured using the dual luciferase assay kit (Promega) following the manufacturers instruction. Renilla luciferase activity served as an internal control for transfection efficiency.

4

Statistical analysis

The chi-square (χ^2) test was used to test the correlation between the DKK1 expression and the stage of disease, the relation between expression of nuclear β -catenin and the stage of disease and the correlation between expression of DKK1 and nuclear β -catenin.

Results

Decreased expression of the DKK1 protein is associated with advanced stage MM

To gain insight into the expression of the DKK1 protein in primary MM samples, we studied DKK1 expression in a panel of BM biopsies of 41 MM and 7 MGUS patients by immunohistochemistry. All biopsies were obtained at first diagnosis. Although DKK1 was detected in most (81%) samples, it was restricted to a subfraction of the malignant plasma cells or entirely lost in a significant proportion of the biopsies (Figure 1A). Interestingly, (partial) loss of DKK1 expression was found to be related to disease stage: Whereas all MGUS patients and the majority (63%) of early (stage I/II) MM patients demonstrated high DKK1 expression, DKK1 expression was either partially or completely absent in 68 % of the patients with advanced MM (Figure 1B). Moreover, we did not detect DKK1 protein expression in any of the studied MM cell lines (Figure 1B and C), which are generally derived from late stage extra-medullary MMs. Our results demonstrate a correlation between DKK1 expression and MM progression with a (partial) loss of DKK1 in advanced stage MM ($p < 0.05$).

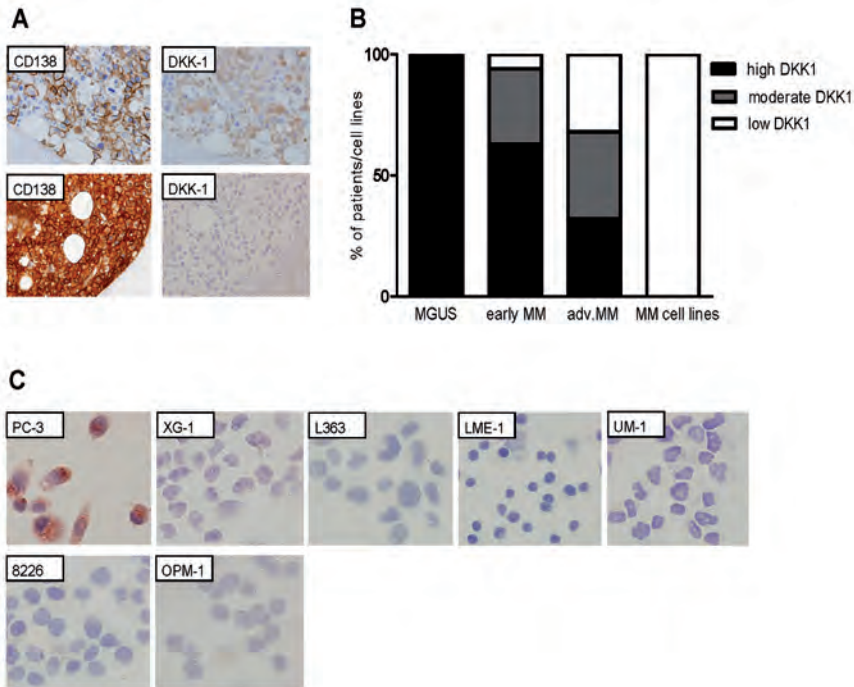


Figure 1. Loss of DKK1 is associated with advanced stage MM.

(A) Representative pictures of immunohistochemical staining of a multiple myeloma patient displaying either high DKK1 expression or DKK1 loss. Immunohistochemical stainings are shown for CD138 (left column), DKK1 (right column). (B) Quantification of the DKK1 staining performed on MM-derived plastic-embedded BM sections. DKK1 expression was scored in three semi-quantitative categories, i.e., low (0-25%), moderate (25-75%) and high (75-100%), with the percentages indicating the number of DKK1 positive MM plasma cells. (C) DKK1 protein expression was visualized on MM cell lines cytopspins stained with goat polyclonal anti-DKK1 antibody (magnification: 400×).

Loss of DKK1 expression unleashes autocrine Wnt pathway activation in MM

Previous studies have demonstrated that MMs can display increased proliferation due to aberrant Wnt pathway activation, which is most likely caused by autocrine production of Wnt ligands^{12,13}. Consistent with such an autocrine activation scenario, analysis of publicly available gene expression profiling data of the malignant plasma cells of 345 MM patients (<http://www.ncbi.nlm.nih.gov/geo/> accession number GSE2658) revealed frequent (co-) expression of various Frizzleds (*e.g.* Fzd 1, 3, 6, 7 and 8) and the co-receptor LRP6, (LRP5 could not be studied because of defective probe sets), as well as various Wnts (*e.g.* Wnt 4, 5A, 5B 6, 10A and 16). Moreover, in 51% of the primary MM co-expression of the co-receptor LRP6 and at least one of the Frizzled genes in combination with expression of at least one of the Wnt genes was demonstrated (Supplementary table 1). Thus, in the majority of MM patients the malignant plasma cells appear to be well equipped to evoke autocrine activation of the Wnt pathway. Since DKK1 is an antagonist of the

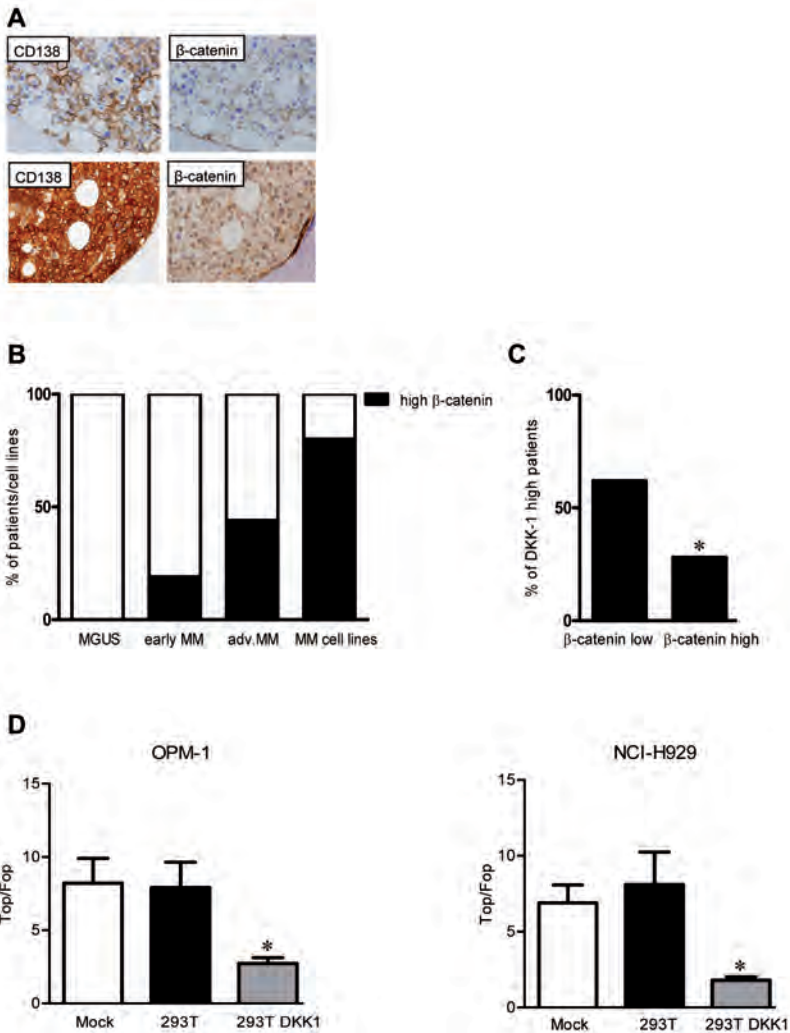


Figure 2. Loss of DKK1 expression unleashes autocrine Wnt pathway activation in MM.

(A) Representative pictures of immunohistochemical staining of a multiple myeloma patient displaying either high or low β -catenin expression. Immunohistochemical stainings are shown for CD138 (left column) and β -catenin (right column). **(B)** Nuclear β -catenin expression in relation to multiple myeloma progression ($p < 0.05$). **(C)** Relation between the loss of DKK-1 expression and nuclear localization of β -catenin. A significant correlation ($p < 0.05$) between expression of nuclear β -catenin and DKK-1 was observed in the two extreme groups identified based on DKK-1 expression. * indicates p value < 0.05 . **(D)** NCI-H929 and OPM-1 cells were either transfected with the TOPFLASH reporter or the FOPFLASH reporter and after co-cultured for 48h with 293T cells transfected with either the empty pcDNA3.1 vector (control) or the pcDNA3.1 DKK1 vector (DKK1). Transfection of 293T cells was performed 24h before the initiation of co-culture. NCI-H929 and OPM-1 cells have basal TCF-mediated transcription, as depicted by TOPFLASH over FOPFLASH ratio (mock). The mean \pm SEM of 3 independent experiments is shown. * indicates p value < 0.05

Wnt pathway, which binds to LRP5/6 thereby preventing activation of the pathway by (autocrine) Wnt ligands, we hypothesized that loss of DKK1 might lead to enhanced Wnt signaling. To explore this notion, we analyzed our panel of MM BM biopsies for a key feature of active canonical Wnt signaling, *i.e.* nuclear expression of β -catenin. Overall, immunohistochemical studies revealed strong β -catenin staining in the malignant plasma cells of 34% of the MM patients (Figure 2A and B). Interestingly, as shown in figure 2B, β -catenin expression increased during disease progression, with high levels of nuclear β -catenin in none of the MGUS patients, 19% of the stage I/II patients, 44% of the patients with advanced MM, and 80% of the MM cell lines ($p < 0.05$). Direct comparison between the level of DKK1 and nuclear β -catenin expression in individual patients indeed revealed a significant inverse correlation between these parameters ($p < 0.05$) (Figure 2C). The above data suggest that the high levels of nuclear β -catenin in MM patients could be the direct consequence of the reduced DKK1 expression, allowing unrestrained autocrine activation of the canonical Wnt pathway. To directly address the functional link between DKK1 loss and (autocrine) Wnt pathway activation, we restored the DKK1 activity in the MM cell lines OPM-1 and NCI-H929, which display constitutively active β -catenin/TCF-dependent transcription¹². Since these MM cells lack mutations in Wnt pathway components and co-express Frizzleds, the co-receptor LRP6, and Wnts^{12;24;25}, restoration of DKK1 expression should inhibit Wnt signaling, provided it is indeed controlled by an autocrine mechanism. As shown in figure 2D, co-culture of OPM-1 and NCI-H929 with DKK1-secreting 293T cells (Supplementary Figure 1) indeed resulted in a strong inhibition of β -catenin/TCF-dependent transcription, as measured by Wnt reporter activity. The basal Wnt reporter activity in the MM cell lines was not affected by the control co-culture system, thereby confirming the specificity of the DKK1 effect. Thus, these findings show that aberrant activation of the Wnt pathway in these MM cells is the consequence of autocrine Wnt signaling and unleashed by DKK1 loss.

4

DKK1 promoter hypermethylation in MM cell lines and primary tumors

To further analyze the loss of DKK1 expression in MM, we examined MM cell lines for DKK1 mRNA expression. In MM cell lines, which all lack detectable levels of DKK1 protein (Figure 1C), the DKK1 transcript was either undetectable (UM-1, RPMI 8226 and OPM-1), or weakly expressed (XG-1, L363 and LME-1) in comparison to the DKK1 expression in the (positive control) prostate cancer cell line PC-3 (Figure 3A)²⁶. Since it has been reported that *DKK1* is a target for epigenetic inactivation by CpG island promoter hypermethylation in several forms of cancer^{23;27-30}, we hypothesized that epigenetic silencing could also be responsible for the lack of DKK1 in primary MM cells and cell lines. Hence, we studied the *DKK1* promoter region, including the CpG island encompassing the transcriptional start site for methylation using a methylation specific PCR (MSP) and a bisulphate-sequencing PCR (BSP) (Figure 3B). DNA isolated from the colon cancer cell lines HT-29 and DLD-1, previously reported to be unmethylated and methylated, respectively²³, was used to validate our experimental set-up (Figure 3C). The combined MSP and BSP analysis revealed that four of the 6 MM cell lines tested, *i.e.* L363, LME-1, UM-1, and OPM-1, showed hypermethylation of the *DKK1* promoter, while XG-1 and RPMI8226 were unmethylated (Figure 3D and E). Notably, the BSP analysis of OPM-1 revealed a methylation pattern that was not detected by the MSP primers, thus

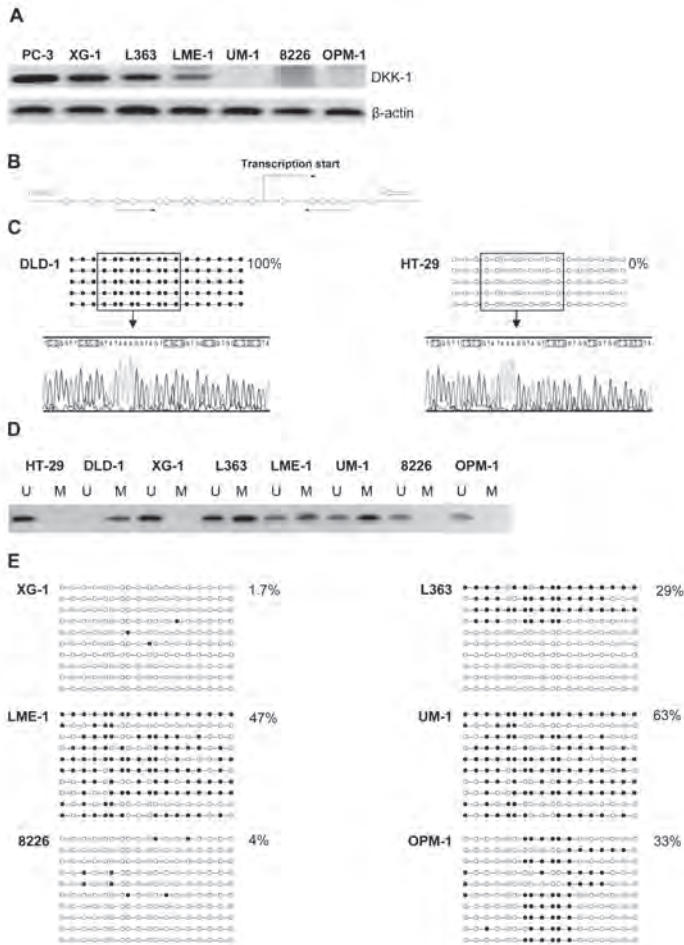


Figure 3. *DKK1* promoter methylation in MM cell lines.

(A) Total RNA was isolated and RT-PCR analyses were performed with the specific primers indicated. Complementary DNA from prostate cancer cell line (PC-3) was used as positive control for *DKK1* expression. The β -actin expression was used as a loading control. **(B)** Schematic representation of the promoter area analyzed for *DKK1*, containing a CpG island. White arrows indicate the positions of primers used for bisulfite sequencing, and black arrows indicate the positions of primers used for methylation specific PCR. Each of the CpG dinucleotides is presented as open circle. **(C)** Upper panel. Representation of bisulfite genomic sequencing results of 5 clones of the *DKK1* promoter region in HT-29 and DLD-1 colon cell lines used as unmethylated and methylated control, respectively. The amplified 326 bp product corresponds to the *DKK1* promoter region from -193 to +122. In total, 18 CpG dinucleotides (CpGs) within the CpG island were analyzed and are represented as open and closed circles, which indicate unmethylated and methylated CpG sites, respectively. Lower panel. Electropherograms of bisulfite modified DNA from *DKK1* CpG island in HT-29 and DLD-1 cells. **(D)** Methylation specific PCR of the CpG island of the *DKK1* promoter region in MM cell lines. DNA bands in lanes labeled with U indicate PCR products amplified with primers recognizing unmethylated promoter sequences, whereas DNA bands in lanes labeled with M represent amplified products with primers designed for the methylated template. **(E)** Bisulfite sequencing analysis of the *DKK1* promoter region in multiple myeloma cell lines, open circles indicating unmethylated CpG sites, and closed circles representing methylated CpG sites. Percentages indicate the fraction of methylated CpG dinucleotides of the total CpG sites analyzed.

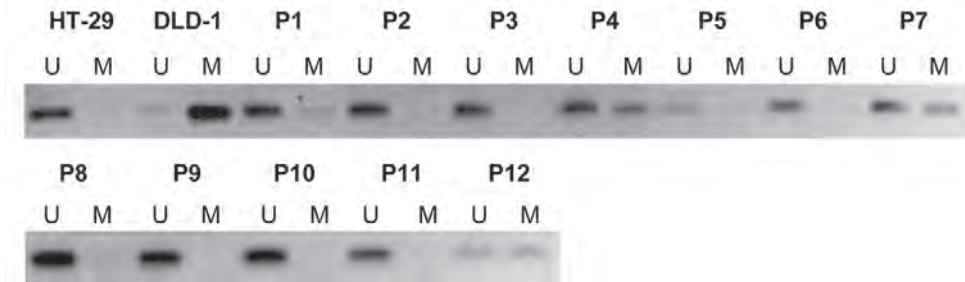


Figure 4. Analysis of *DKK1* promoter methylation in MM bone marrow samples.

Methylation specific PCR of the CpG island of the *DKK1* promoter region in the BM samples of twelve patients with multiple myeloma (P1-P12), HT-29 and DLD-1 colon cell lines were used as unmethylated and methylated control, respectively. DNA bands in lanes labeled with U and M indicate PCR products amplified with primers recognizing unmethylated and methylated promoter sequences, respectively.

showing the necessity of using both techniques to adequately perform methylation studies. Interestingly, in the L363 cell line four out of ten sequenced clones displayed extensive CpG methylation, suggesting that either a subset of cells shows methylation or that there is partial monoallelic methylation within individual cells. The lack of *DKK1* expression despite the absence of promoter methylation in RPMI 8226 cells indicates either the mere lack of transcriptional activation or an alternative mechanism of *DKK1* silencing. Since *DKK1* expression appears to be decreased in MM cells isolated from patients with advanced stage MM, we next investigated the *DKK1* promoter associated CpG island in the bone marrow mononuclear cells (BM-MNC) of patients with MM and compared this to BM-MNC from healthy donors. The *DKK1* promoter was hypermethylated in 33% (4 out of 12) of the primary MM specimen studied, as determined by BSP (Supplementary Figure 2) and MSP analysis (Figure 4). In accordance with a previous study²⁸, none of the healthy donor BM samples tested displayed methylation of the *DKK1* promoter (data not shown).

Promoter methylation silences *DKK1* expression

To assess whether *DKK1* promoter methylation indeed plays a causative role in the transcriptional silencing of *DKK1* in MM, we investigated whether *DKK1* expression could be restored or enhanced in the MM cell lines by means of treatment with the demethylating agent 5-aza-2-deoxycytidine. Analysis by BSP of the genomic DNA isolated from OPM-1 and UM-1 cells, which combine a lack of *DKK1* expression with hypermethylation of its promoter (Figures 1 and 3), confirmed that treatment results in a decrease in methylation of the *DKK1* promoter (Figure 5A). Importantly, treatment of these cell lines results in restoration of *DKK1* expression (Figure 5B). In addition, in LME-1, a cell line with a hypermethylated *DKK1* promoter and low *DKK1* expression, *DKK1* expression was increased upon 5-aza-2-deoxycytidine treatment. As expected, treatment of XG-1 and RPMI 8226, the two cell lines that lack methylation of the *DKK1* promoter, did not affect expression (Figure 5B). Taken together, these data establish a direct role for CpG island methylation in epigenetic silencing of *DKK1* expression in MM.

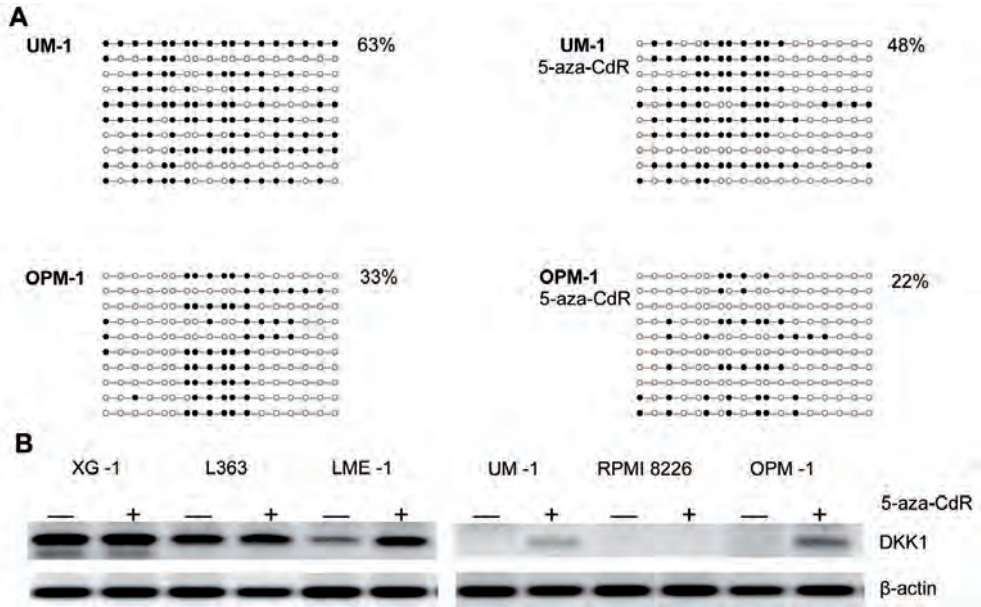


Figure 5. Restoration of *DKK1* expression in MM cell lines by 5-aza-2-deoxycytidine treatment. (A) Bisulfite genomic sequencing on DNA isolated from 5-aza-2-deoxycytidine treated (5-aza-CdR) and untreated (PBS) MM cell lines UM-1 and OPM-1. With open circles representing unmethylated CpG sites, and closed circles representing methylated CpG sites. Percentages indicate the fraction of methylated CpG dinucleotides of the total CpG sites analyzed. (B) Reverse transcriptase-PCR analysis for *DKK1* gene expression in multiple myeloma cell lines in the absence and presence of the demethylating agent 5-aza-2-deoxycytidine. β-actin expression is shown as input control.

Discussion

We have previously demonstrated that the Wnt pathway, which is essential for normal T and B cell development^{7;31} and plays a key role in the development of several types of cancer^{32;33}, is aberrantly activated in MM and can promote MM tumor growth¹². Subsequent studies have confirmed the oncogenic potential of the Wnt pathway in MM by demonstrating that targeting the Wnt pathway by drugs or siRNAs leads to inhibition of MM growth^{13;34-36}. In addition, by knocking down β-catenin, Dutta-Simmons *et al.* revealed new potential Wnt/β-catenin transcriptional targets involved in various aspects of cell-cycle progression, such as CDC25A/B, cyclins, cyclin-dependent kinases, and AurKA/B. Among the genes significantly downregulated upon β-catenin knock down, a significant proportion had LEF/TCF4 (GCTTTGT/A) binding sites in their promoters, identifying them as putative direct Wnt target genes¹³. Although the exact cause(s) of aberrant Wnt pathway activation in MM has not yet been established, the absence of detectable Wnt pathway mutations¹² as well as the (over) expression of Wnt ligands in the BM microenvironment by both stromal cells and by the MM cells themselves^{12;25} (Supplementary table 1) suggests a key role for auto- and/or paracrine stimulation. As a consequence, loss of secreted Wnt pathway antagonists, like DKKs and sFRPs, could have a major impact on the pathogenesis of MM. Indeed, we observed that

whereas the DKK1 protein is strongly expressed in most primary MMs, the expression of this Wnt antagonist is down-regulated or even completely lost in a subgroup of advanced (stage III) MMs (Figure 1A and B). In addition, the DKK1 protein was undetectable in MM cell lines, which represent the ultimate, microenvironment independent, phase of MM tumor progression and are almost invariably derived from extramedullary MMs (Figure 1B and C). Interestingly, the loss of DKK1 protein expression in BM samples of MM patients was correlated with an increased nuclear expression of β -catenin, a hallmark of canonical Wnt signaling (Figure 2C). DKK1 is a major Wnt pathway antagonist which acts by interfering with the binding of Wnt ligands to the LRP5/6 coreceptor³⁷. Importantly, the *DKK1* gene itself is a direct target of β -catenin/TCF-mediated transcription¹⁸⁻²⁰, and DKK1 has been implicated in the feed-back regulation of Wnt signaling in several biological systems³⁸⁻⁴⁰. Consistent with a tumor suppressor function, *DKK1* silencing during tumor progression has been reported in several types of cancer^{23;27;28;30}. Our observation, that DKK1 expression can be lost in advanced MM and that its restoration inhibits β -catenin/TCF transcriptional activity (Figure 2D), suggests that silencing of *DKK1* may contribute to activation of the canonical Wnt pathway during MM progression.

Like loss of function mutations, aberrant methylation of the promoter of tumor suppressor genes can provide a selective advantage to neoplastic cells⁴¹⁻⁴⁵. We identified *DKK1* promoter hypermethylation as a mechanism underlying the loss of DKK1 expression in MM (Figures 3-5). In four of the 6 MM cell lines tested, *i.e.* L363, LME-1, UM-1, and OPM-1, we showed hypermethylation of the *DKK1* promoter (Figure 3). The CpG island analyzed encompasses the first exon of the *DKK1* gene, which encodes the transcriptional and translational start sites as well as a significant part of the region upstream of the coding sequence, an organization characteristic of genes targeted by epigenetic silencing⁴². Indeed, this CpG island has previously been implicated in *DKK1* silencing in several types of cancer, including colorectal cancer, gastric cancer, breast cancer, medulloblastoma and leukaemia^{23;27;28;30}. Importantly, the promoter methylation was significantly reduced and *DKK1* expression was either restored and/or markedly increased by the DNA demethylating agent 5-aza-2-deoxycytidine (Figure 5A and B), confirming that the observed aberrant methylation indeed was instrumental in the silencing of *DKK1* expression (Figure 5B). In primary MM, we also observed dense methylation of the DKK1-associated CpG island (Figure 4 and Supplementary Figure 2). Since methylation of the *DKK1* promoter was not observed in normal BM samples²⁸, this methylation can be considered aberrant and disease-related. In addition to *DKK1* loss, silencing of other Wnt antagonists could also contribute to the enhanced Wnt signaling in advanced MM. Consistent with this notion, Chim *et al.*, have reported that constitutive Wnt signaling in MM cell lines is associated with methylation dependent silencing of several Wnt inhibitors, including the sFRP1, 2, 4 and 5. Methylation of at least one of these soluble Wnt inhibitors was observed in most primary MM BM samples⁴⁶. Our finding that the *DKK1* promoter is methylated and the Wnt pathway is hyperactivated in advanced multiple myeloma, strongly suggests the presence of autocrine Wnt signaling in malignant plasma cells. In accordance with this hypothesis we observed strong inhibition of Wnt reporter activity upon restoration of DKK1 in MM cells (Figure 2D). Importantly, MM cell lines used in this experiment have dense methylation of the *DKK1* promoter around the transcription start region and lack detectable *DKK1* transcript (Figure 1C, 3A and Supplementary Figure 3). Taken together, these data suggest that activation of Wnt signaling in these cell lines is the consequence of *DKK1* silencing and could reflect

4

the progression-dependent Wnt pathway activation in patients with advanced MM. Our current study, in conjunction with work of others, points to a multi-faceted role of DKK1 in the pathogenesis of MM. Studies by Shaughnessy and colleagues have previously also reported that DKK1 is strongly expressed by the malignant plasma cells of most MM patients⁴. It was shown that secretion of the DKK1 can contribute to MM bone disease by inhibiting Wnt signaling in osteoblasts, thereby interfering with their differentiation¹⁴⁻¹⁷. Furthermore, in line with our current findings, which suggests that DKK1 may act as a feedback tumor suppressor, these authors also reported loss of DKK1 protein expression in a subgroup of patients with advanced MM⁴. In addition to causing bone disease, inhibition of osteoblast differentiation by DKK1 may also promote MM growth, since mature osteoblasts can suppress myeloma growth, whereas immature osteoblasts express high levels of IL-6, a central growth and survival factor for myeloma plasma cells⁴⁷. Furthermore, DKK1 enhances the expression of receptor activator of NF- κ B ligand (RANKL) and downregulates the expression of osteoprotegerin (OPG) in immature osteoblast¹⁶. The resulting increased RANKL/OPG ratio leads to osteoclast activation promoting osteolytic bone disease. Osteoclasts may also support the growth of myeloma cells through secretion of IL-6 and osteopontin, and by adhesive interactions, stimulating the proliferation of malignant plasma cells⁴⁸. Thus, like several other soluble factors expressed by MM cells, for example vascular endothelial growth factor (VEGF) and hepatocyte growth factor (HGF)⁴⁹⁻⁵¹, DKK1 can both exercise paracrine effects on the BM microenvironment and affect the MM cells in an autocrine fashion; the net effect could be either enhanced or reduced tumor growth. Consistent with this hypothesis, by employing a MM SCID/rab mouse model, Yaccoby *et al.* showed that treatment with anti-human DKK1-neutralizing antibody stimulates osteoblast activity, reduces osteoclastogenesis, and promotes bone formation in myelomatous and nonmyelomatous bones⁵². MM burden was also reduced, but notably, not in all mice bearing human myeloma cells⁵². Similar results were also obtained in a SCID/hu mouse model by Fulciniti *et al.*⁵³. Together, these studies suggest that MM bone disease and tumor growth are interdependent, at least at the intramedullary stage, and that increased bone formation as a consequence of neutralization of DKK1, may also control MM growth^{52,53}. However, in a 5T2MM murine myeloma model treatment with the anti-DKK1 antibody BHQ880 also caused a reduction of osteolytic bone lesions but did not have any effect on tumor burden⁵⁴. Given our current finding that DKK1 inhibits autocrine canonical Wnt signaling in MM cells, inhibition of DKK1 could hyperactivate the Wnt pathway and thereby promote tumor growth, especially at extramedullary sites. Indeed, stimulation of the Wnt signaling pathway in a 5TGM1 mouse myeloma model significantly increased subcutaneous tumor growth⁵⁵. In patients, extramedullary presentation is associated with aggressive disease, occurring subsequent to the osteolytic bone disease, often resulting in plasma cell leukemia. Importantly, in a human-mouse xenograft MM model, Dutta-Simmons *et al.* demonstrated that the Wnt pathway not only controls the proliferation of MM plasma cells but also their metastatic potential¹³. Hence, although blocking DKK1 inhibits osteolytic bone disease *in vivo*, the data presented here suggest that targeting DKK1 in MM patients could enhance Wnt pathway activation in MM plasma cells, increasing in the metastatic potential and extramedullary growth of the tumor. In conclusion, our study establishes for the first time a relation between the loss of DKK1 expression and Wnt pathway activation during MM progression. Moreover, we demonstrate the presence of a functional autocrine Wnt signaling loop in MM cells and identify methylation of the DKK1 promoter as a mechanism underlying the loss of DKK1 expression

in advanced stage MM. These data strongly suggests that epigenetic silencing of DKK1 unleashes Wnt signaling in a subset of advanced myelomas, promoting disease progression.

Acknowledgements

Grant support: Dutch Cancer Society (M. Spaargaren and S.T. Pals).
We thank Dr. Christopher Hall for kindly providing the PC-3 cell line.

References

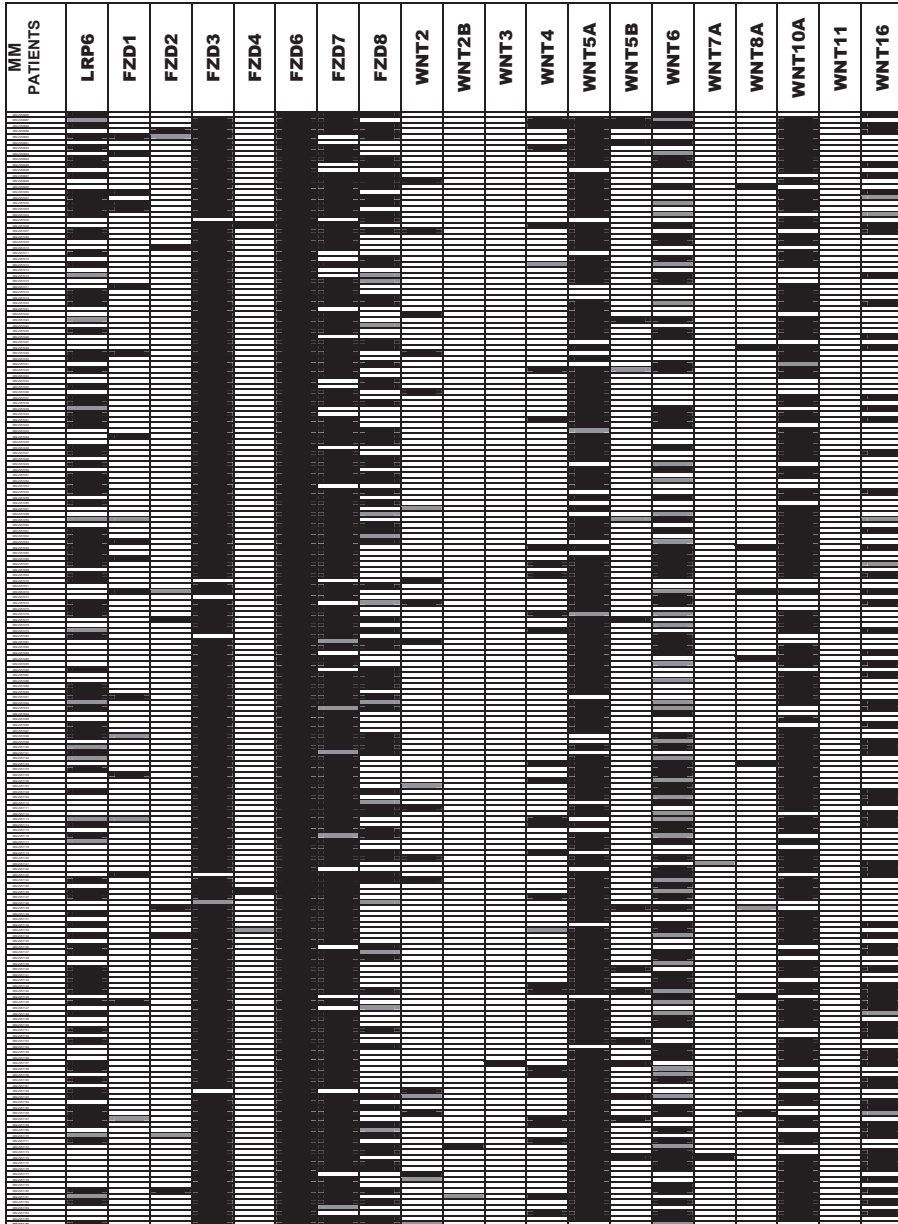
1. Podar K, Chauhan D, Anderson KC. Bone marrow microenvironment and the identification of new targets for myeloma therapy. *Leukemia* 2009;23:10-24.
2. Raab MS, Podar K, Breitkreutz I, Richardson PG, Anderson KC. Multiple myeloma. *Lancet* 2009;374:324-339.
3. Edwards CM, Zhuang J, Mundy GR. The pathogenesis of the bone disease of multiple myeloma. *Bone* 2008;42:1007-1013.
4. Tian E, Zhan F, Walker R et al. The role of the Wnt-signaling antagonist DKK1 in the development of osteolytic lesions in multiple myeloma. *N.Engl.J.Med.* 2003;349:2483-2494.
5. Oshima T, Abe M, Asano J et al. Myeloma cells suppress bone formation by secreting a soluble Wnt inhibitor, sFRP-2. *Blood* 2005;106:3160-3165.
6. Giuliani N, Morandi F, Tagliaferri S et al. Production of Wnt inhibitors by myeloma cells: potential effects on canonical Wnt pathway in the bone microenvironment. *Cancer Res.* 2007;67:7665-7674.
7. Staal FJ, Clevers HC. WNT signalling and haematopoiesis: a WNT-WNT situation. *Nat.Rev.Immunol.* 2005;5:21-30.
8. Staal FJ, Sen JM. The canonical Wnt signaling pathway plays an important role in lymphopoiesis and hematopoiesis. *Eur.J.Immunol.* 2008;38:1788-1794.
9. Malhotra S, Kincade PW. Wnt-related molecules and signaling pathway equilibrium in hematopoiesis. *Cell Stem Cell* 2009;4:27-36.
10. van de Wetering M, Cavallo R, Dooijes D et al. Armadillo coactivates transcription driven by the product of the *Drosophila* segment polarity gene dTCF. *Cell* 1997;88:789-799.
11. Kawano Y, Kypta R. Secreted antagonists of the Wnt signalling pathway. *J.Cell Sci.* 2003;116:2627-2634.
12. Derksen PWB, Tjin E, Meijer HP et al. Illegitimate WNT signaling promotes proliferation of multiple myeloma cells. *Proc.Natl.Acad.Sci.U.S.A* 2004;101:6122-6127.
13. Dutta-Simmons J, Zhang Y, Gorgun G et al. Aurora kinase A is a target of Wnt/beta-catenin involved in multiple myeloma disease progression. *Blood* 2009;114:2699-2708.
14. Haaber J, Abildgaard N, Knudsen LM et al. Myeloma cell expression of 10 candidate genes for osteolytic bone disease. Only overexpression of DKK1 correlates with clinical bone involvement at diagnosis. *Br.J.Haematol.* 2008;140:25-35.
15. Qiang YW, Barlogie B, Rudikoff S, Shaughnessy JD, Jr. Dkk1-induced inhibition of Wnt signaling in osteoblast differentiation is an underlying mechanism of bone loss in multiple myeloma. *Bone* 2008;42:669-680.
16. Qiang YW, Chen Y, Stephens O et al. Myeloma-derived Dickkopf-1 disrupts Wnt-regulated osteoprotegerin and RANKL production by osteoblasts: a potential mechanism underlying osteolytic bone lesions in multiple myeloma. *Blood* 2008;112:196-207.
17. Pinzone JJ, Hall BM, Thudi NK et al. The role of Dickkopf-1 in bone development, homeostasis, and disease. *Blood* 2009;113:517-525.

18. Lescher B, Haenig B, Kispert A. sFRP-2 is a target of the Wnt-4 signaling pathway in the developing metanephric kidney. *Dev.Dyn.* 1998;213:440-451.
19. Niida A, Hiroko T, Kasai M et al. DKK1, a negative regulator of Wnt signaling, is a target of the beta-catenin/TCF pathway. *Oncogene* 2004;23:8520-8526.
20. Chamorro MN, Schwartz DR, Vonica A et al. FGF-20 and DKK1 are transcriptional targets of beta-catenin and FGF-20 is implicated in cancer and development. *EMBO J.* 2005;24:73-84.
21. Zhan F, Barlogie B, Arzoumanian V et al. Gene-expression signature of benign monoclonal gammopathy evident in multiple myeloma is linked to good prognosis. *Blood* 2007;109:1692-1700.
22. Groen RW, Oud ME, Schilder-Tol EJ et al. Illegitimate WNT pathway activation by beta-catenin mutation or autocrine stimulation in T-cell malignancies. *Cancer Res.* 2008;68:6969-6977.
23. Aguilera O, Fraga MF, Ballestar E et al. Epigenetic inactivation of the Wnt antagonist DICKKOPF-1 (DKK-1) gene in human colorectal cancer. *Oncogene* 2006;25:4116-4121.
24. Qiang YW, Endo Y, Rubin JS, Rudikoff S. Wnt signaling in B-cell neoplasia. *Oncogene* 2003;22:1536-1545.
25. Qiang YW, Walsh K, Yao L et al. Wnts induce migration and invasion of myeloma plasma cells. *Blood* 2005;106:1786-1793.
26. Hall CL, Bafico A, Dai J, Aaronson SA, Keller ET. Prostate cancer cells promote osteoblastic bone metastases through Wnts. *Cancer Res.* 2005;65:7554-7560.
27. Sato H, Suzuki H, Toyota M et al. Frequent epigenetic inactivation of DICKKOPF family genes in human gastrointestinal tumors. *Carcinogenesis* 2007;28:2459-2466.
28. Suzuki R, Onizuka M, Kojima M et al. Preferential hypermethylation of the Dickkopf-1 promoter in core-binding factor leukaemia. *Br.J.Haematol.* 2007;138:624-631.
29. Vibhakar R, Foltz G, Yoon JG et al. Dickkopf-1 is an epigenetically silenced candidate tumor suppressor gene in medulloblastoma. *Neuro.Oncol.* 2007;9:135-144.
30. Suzuki H, Toyota M, Carraway H et al. Frequent epigenetic inactivation of Wnt antagonist genes in breast cancer. *Br.J.Cancer* 2008;98:1147-1156.
31. Timm A, Grosschedl R. Wnt signaling in lymphopoiesis. *Curr.Top.Microbiol.Immunol.* 2005;290:225-252.
32. Clevers H. Wnt/beta-catenin signaling in development and disease. *Cell* 2006;127:469-480.
33. Polakis P. Wnt signaling and cancer. *Genes Dev.* 2000;14:1837-1851.
34. Sukhdeo K, Mani M, Zhang Y et al. Targeting the beta-catenin/TCF transcriptional complex in the treatment of multiple myeloma. *Proc.Natl.Acad.Sci.U.S.A* 2007;104:7516-7521.
35. Ashihara E, Kawata E, Nakagawa Y et al. beta-catenin small interfering RNA successfully suppressed progression of multiple myeloma in a mouse model. *Clin.Cancer Res.* 2009;15:2731-2738.
36. Schmidt M, Sievers E, Endo T et al. Targeting Wnt pathway in lymphoma and myeloma cells. *Br.J.Haematol.* 2009;144:796-798.
37. Semenov MV, Tamai K, Brott BK et al. Head inducer Dickkopf-1 is a ligand for Wnt coreceptor LRP6. *Curr.Biol.* 2001;11:951-961.
38. Sick S, Reinker S, Timmer J, Schlake T. WNT and DKK determine hair follicle spacing through a reaction-diffusion mechanism. *Science* 2006;314:1447-1450.
39. Lewis SL, Khoo PL, De Young RA et al. Dkk1 and Wnt3 interact to control head morphogenesis in the mouse. *Development* 2008;135:1791-1801.
40. Yamaguchi Y, Passeron T, Hoashi T et al. Dickkopf 1 (DKK1) regulates skin pigmentation and thickness by affecting Wnt/beta-catenin signaling in keratinocytes. *FASEB J.* 2008;22:1009-1020.
41. Esteller M, Fraga MF, Paz MF et al. Cancer epigenetics and methylation. *Science* 2002;297:1807-1808.
42. Feltus FA, Lee EK, Costello JF, Plass C, Vertino PM. Predicting aberrant CpG island methylation. *Proc.Natl.Acad.Sci.U.S.A* 2003;100:12253-12258.
43. Egger G, Liang G, Aparicio A, Jones PA. Epigenetics in human disease and prospects for epigenetic therapy. *Nature* 2004;429:457-463.

44. Herman JG. Epigenetic changes in cancer and preneoplasia. *Cold Spring Harb. Symp. Quant. Biol.* 2005;70:329-333.
45. Klein G. Epigenetics: surveillance team against cancer. *Nature* 2005;434:150.
46. Chim CS, Pang R, Fung TK, Choi CL, Liang R. Epigenetic dysregulation of Wnt signaling pathway in multiple myeloma. *Leukemia* 2007;21:2527-2536.
47. Klein B, Zhang XG, Jourdan M et al. Paracrine rather than autocrine regulation of myeloma-cell growth and differentiation by interleukin-6. *Blood* 1989;73:517-526.
48. Abe M, Hiura K, Wilde J et al. Osteoclasts enhance myeloma cell growth and survival via cell-cell contact: a vicious cycle between bone destruction and myeloma expansion. *Blood* 2004;104:2484-2491.
49. Le Gouill S, Podar K, Amiot M et al. VEGF induces Mcl-1 up-regulation and protects multiple myeloma cells against apoptosis. *Blood* 2004;104:2886-2892.
50. Derksen PWB, Keehnen RMJ, Evers LM et al. Cell surface proteoglycan syndecan-1 mediates hepatocyte growth factor binding and promotes Met signaling in multiple myeloma. *Blood* 2002;99:1405-1410.
51. Standal T, Abildgaard N, Fagerli UM et al. HGF inhibits BMP-induced osteoblastogenesis: possible implications for the bone disease of multiple myeloma. *Blood* 2007;109:3024-3030.
52. Yaccoby S, Ling W, Zhan F et al. Antibody-based inhibition of DKK1 suppresses tumor-induced bone resorption and multiple myeloma growth in vivo. *Blood* 2007;109:2106-2111.
53. Fulciniti M, Tassone P, Hideshima T et al. Anti-DKK1 mAb (BHQ880) as a potential therapeutic agent for multiple myeloma. *Blood* 2009;114:371-379.
54. Heath DJ, Chantry AD, Buckle CH et al. Inhibiting Dickkopf-1 (Dkk1) removes suppression of bone formation and prevents the development of osteolytic bone disease in multiple myeloma. *J. Bone Miner. Res.* 2009;24:425-436.
55. Edwards CM, Edwards JR, Lwin ST et al. Increasing Wnt signaling in the bone marrow microenvironment inhibits the development of myeloma bone disease and reduces tumor burden in bone in vivo. *Blood* 2008;111:2833-2842.

Supplementary Data

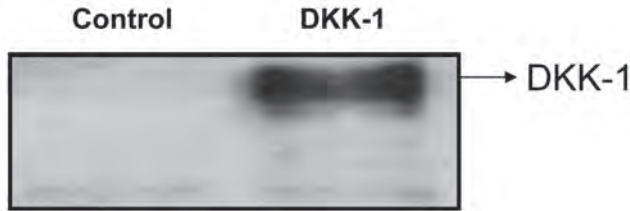
Supplementary Table 1. Expression of Wnt family members in 345 MM patients from total therapy 2 (TT2) patients set.



Legend:

- transcript is not detected (Absent)
- transcript is marginally detected (Marginal)
- transcript is detected (Present)

HEK 293T cells



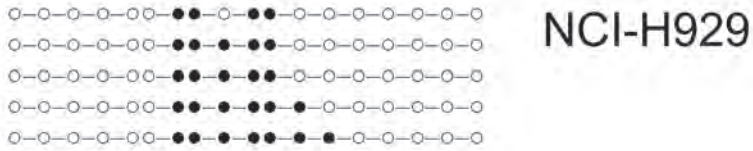
Supplementary Figure 1. Western blot analysis of DKK-1 expression.

293T cells were either transfected with the empty pcDNA3.1 vector (control) or the pcDNA3.1 DKK-1 vector (DKK-1). At 72 h after transfection, the conditioned medium was harvested, lysed and immunoblotted using a goat polyclonal anti-DKK-1 antibody. Representative immunoblot analysis confirms the expression of DKK-1 in conditioned medium of 293T cells transfected with the pcDNA3.1 DKK-1 vector.



Supplementary Figure 2. Bisulfite genomic sequencing of the *DKK-1* promoter in MM bone marrow samples.

Bisulfite sequencing analysis was performed on DNA isolated from total bone marrow samples of twelve MM patients (P1-P12). For individual patient 5 clones of the *DKK-1* promoter region are presented. Open circles indicate unmethylated CpG sites; closed circles represent methylated CpG sites.



Supplementary Figure 3. Bisulfite genomic sequencing of the *DKK-1* promoter in MM cell line.

Bisulfite genomic sequencing on DNA isolated from NCI-H929 MM cell line. 5 clones of the *DKK-1* promoter region are presented. Open circles indicate unmethylated CpG sites; closed circles represent methylated CpG sites.

5

A bioluminescence imaging based in vivo model for preclinical testing of novel cellular immunotherapy strategies to improve Graft versus Myeloma

Henk Rozemuller^{1,5}, Ellen van der Spek^{2,5}, Lijnie H. Bogers-Boer², Mieke C. Zwart¹, Vivienne Verweij¹, Maarten Emmelot³, Richard W.J. Groen⁴, Robbert Spaapen³, Andries C. Bloem¹, Henk M. Lokhorst², Tuna Mutis³ and Anton C. Martens¹.

¹Department of Immunology, ²Haematology and ³Clinical Chemistry and Haematology, University Medical Center Utrecht, Utrecht, The Netherlands; ⁴Department of Pathology, Amsterdam Medical Center, University of Amsterdam, Amsterdam, The Netherlands;

⁵Both authors contributed equally to this work.

Haematologica. 2008; 93(7): 1049-57

Abstract

Background and objective: Development and preclinical testing of novel immuno-therapy strategies for multiple myeloma (MM) can substantially benefit from a humanized animal model that permits quantitative real-time monitoring of tumour progression. Here we have explored the feasibility of establishing such a model in immuno-deficient RAG2^{-/-}γC^{-/-} mice, by utilizing non-invasive bioluminescent imaging (BLI) for real-time monitoring of MM cell growth.

Design and methods: Seven MM cell lines, marked with a GFP-Firefly Luciferase fusion gene, were intravenously injected in RAG2^{-/-}γC^{-/-} mice. Tumour localization and outgrowth was monitored by BLI. The sensitivity of BLI was compared to that of free Ig light chain (FLC)-based myeloma monitoring. Established tumours were treated with radiotherapy or with allogeneic PBMC infusions to evaluate the application areas of the model.

Results: Five out of seven tested MM cell lines progressed as myeloma-like tumours predominantly in the bone marrow; the two other lines showed additional growth in soft tissues. In our model BLI appeared superior to FLC-based monitoring and also allowed semi-quantitative monitoring of individual MM foci. Tumours treated with radiotherapy showed temporary regression. However, infusion of allogeneic PBMC resulted in the development of xenogeneic GvHD and a powerful cell dose-dependent graft-vs-myeloma effect, resulting in complete eradication of tumours, depending on the in vitro immunogenicity of inoculated MM cells.

Interpretations and conclusions: Our results indicate that this new model allows convenient and sensitive real-time monitoring of cellular approaches for immunotherapy of MM-like tumours with different immunogenicities. Thus this model allows comprehensive preclinical evaluation of novel combination therapies for MM.

Introduction

Multiple myeloma (MM) is a neoplastic disease, characterized by the outgrowth of monoclonal plasma cells in the bone marrow (BM). Over the past decade, treatment of MM has undergone significant change by the introduction of several novel agents such as Bortezomib, Thalidomide and Lenalidomide¹. Furthermore, with the success of non-myeloablative conditioning in reducing transplant-related mortality, allogeneic stem cell transplantation (allo-SCT) may become a realistic and attractive therapeutical option for chemotherapy-resistant MM patients². Despite these promising achievements, MM still remains incurable, indicating the necessity for novel combination therapies. Unfortunately, clinical testing of several potentially promising drugs with or without the combination with allo-SCT is cumbersome and requires large controlled studies, emphasizing once again the necessity of useful and convenient animal models that permit preclinical testing of novel immunological and pharmacological combination therapy strategies against MM. To date, three xenograft models of human myeloma, SCID-Hu³⁻⁵, NOD/SCID⁶⁻¹⁰, or SCID-Rab¹¹ have been developed. While these models offer several opportunities to test therapeutics *in vivo* against human myeloma, each of them has also reported limitations, in particular for reproducible, convenient and sensitive monitoring of cellular immunological therapies in combination with immunomodulatory agents¹². To develop a model that offers an optimal platform for preclinical evaluation of cellular immunotherapies, we here tested the feasibility of using the immuno-deficient RAG2^{-/-}γc^{-/-} mice for this purpose because these mice completely lack B, T and NK cells¹³ and are far more suitable than NOD/SCID mice for reproducible engraftment of human T and B cells¹⁴⁻¹⁵. To this end we transduced seven different human MM cell lines with a retroviral vector encoding a green fluorescent protein-luciferase (GFP-LUC) fusion protein and injected them in the RAG2^{-/-}γc^{-/-} mice. Bioluminescence imaging (BLI) was used to (semi-) quantitatively monitor the *in vivo* engraftment, outgrowth and distribution of MM cell lines. Subsequently, radiotherapy and allogeneic lymphocyte infusions were used to eradicate established tumours. Our results demonstrate that five out of seven GFP-LUC transduced MM cell lines established invasive tumours in the RAG2^{-/-}γc^{-/-} mice with an *in vivo* distribution highly similar to human MM. The growth kinetics and *in vivo* distribution of these tumours can be easily and quantitatively monitored by BLI, which appeared in our model, much more sensitive to the free light chain (FLC-Ig)-based myeloma monitoring. Finally, we found that established tumours, depending on their immunogenicity, can be effectively eradicated by infusion of allogeneic human peripheral blood mononucleated cells (PBMC) in a dose dependent manner. This illustrates the utility of this model for evaluating the novel immunopharmacological treatment strategies to improve the graft-versus-myeloma (GvM) effects after allo-SCT.

Design and Methods

Animals

The animals used in this study are the RAG2^{-/-}γc^{-/-} mice¹³ that were bred and housed in the specified pathogen-free (SPF) breeding unit of the Central Animal Facility of the University of Utrecht. The animals were supplied with autoclaved sterilized food pellets and distilled water ad libitum. All animal experiments were conducted according to Institutional Guidelines after acquiring permission from the local Ethical Committee for Animal Experimentation and in accordance with current Dutch laws on Animal Experiments.

Cell lines and cell culturing

The human MM cell lines that we studied were U266, RPMI-8226/S (both obtained from the American Tissue Culture Collection (ATCC)), UM-9 (generated in our institute)¹⁶, LME-1¹⁷, XG-1¹⁸ OPM-1¹⁹, and L363²⁰. All MM cell lines were cultured in RPMI-1640 (Gibco, Breda, The Netherlands) supplemented with 10% FCS (Integro, Zaandam, The Netherlands), 100 U/ml penicillin (Gibco), 100 µg/ml streptomycin (Gibco), and 10 µM β-mercaptoethanol (Merck, Darmstadt, Germany). The amphotropic packaging cell line Phoenix (a kind gift from Dr. G. Nolan), PG13 cell line (ATCC) and NIH-3T3 fibroblasts (ATCC) were cultured in DMEM (Gibco) supplemented with 10% FCS, 100 U/ml penicillin and 100 µg/ml streptomycin. The cultures were maintained at 37°C and 5% CO₂ in a humidified atmosphere.

5

Retroviral vector production

The GFP-LUC retroviral vector encoding a fusion gene of GFP and luciferase was generated by inserting the luciferase gene from pBSSKGFP-luc²¹ (kindly provided by Dr. R. Day) into the XhoI-NotI sites of LZRSpBMN-IRES-EGFP (S-001-AB provided by Dr. G. Nolan). The amphotropic Phoenix packaging cell line and the gibbon ape leukemia virus (GALV) pseudotyped cell line PG13 were transfected with the GFP-LUC plasmid using calcium phosphate precipitation. The viral titer was 10⁵ infectious virus particles per ml, as determined on 3T3 cells by FACS analyses of GFP expression.

Retroviral transduction of the MM cell lines.

For retroviral transduction of MM cell lines we used Retronectin coated tissue culture plates (CH-296, Takara Shuzo, Otsu, Japan) as described previously²². Transduction efficiencies, as assessed by FACS analysis of GFP expression, were 11-17% with or GALV pseudotyped viruses (RPMI-8226/S) or amphotropic pseudotyped viruses (rest of MM cell lines). The percentage of GFP-luc expressing cells was increased to 85% by FACS sorting of the transduced cells. Luciferase activity was confirmed according to manufacturer's protocol (Promega, Madison, WI, USA). FACS-sorted MM cells were expanded to required amounts to use in the assays. Before in vivo transfer, the cells were analyzed for the expression of CD45, CD38, CD86 and CD138 by labeling with phycoerythrin conjugated antibodies (Becton, Dickinson Biosciences, San Jose, CA, USA).

Transplantation of MM cells into the RAG2^{-/-}γc^{-/-} mice.

RAG2^{-/-}γc^{-/-} mice (age 9-14 weeks) were used in the experiments. Twenty-four hours before the injection of the freshly cultured MM, mice received a total body irradiation (TBI; 3.0 Gy X-rays). Between 5-20x10⁶ MM cells, suspended in 200 μl PBS containing 0.1% BSA (Gibco) were injected intravenous (i.v.) via the lateral tail vein. The tumour load in the mice was determined by weekly BLI measurements as described. In case of paralysis of the hind limbs or when the mice became moribund, mice were sacrificed by cervical dislocation. Cell isolates from various skeletal parts and soft tissues were analyzed using flow cytometry (FACS) for the presence of GFP⁺ MM cells in the total nucleated cell fraction. BM was obtained by flushing the bones with RPMI1640. Single cell suspensions from the soft tissues were produced by passing through 70 mm cell strainers (Becton Dickinson). The cell concentration was determined by adding a fixed number of 4 μm beads to the single cell suspensions just prior to flow cytometry (FACS). Ten thousand events were analyzed for blood and bone marrow (BM) samples, whereas 100,000 events from the soft tissue cell suspensions were analyzed. From some the mice organs were isolated and fixed in 4% formalin and used for further immuno-histochemical analysis.

Bioluminescent Imaging (BLI)

A few minutes before BLI, the mice were anesthetized by intramuscular (i.m.) injection of 50 μl of Ketamine-Xylazine-Atropine. One minute before imaging, the mice received an intraperitoneal (i.p.) injection of 100 μl 7.5 mM D-luciferine (*i.e.* 125 mg/kg) (Synchem Chemie, Kassel, Germany) and were placed in a light-tight chamber. Bioluminescence images were taken from both the ventral and the dorsal side of the mice using a cooled charge-coupled device (CCCD) camera (Roper Scientific, Princeton instrument, Trenton, NJ, USA), fitted to a light-tight chamber and mounted with a 50 mm F1.2 Nikon lens, controlled by the Metavue Software package software (Universal Imaging Corporation, Downingtown, PA, USA). The instrument is especially designed for photon counting. The integrated light intensity of a stack of 10 sequential 1-minute exposures was used to quantify the amount of light emitted by the MM cells. A low intensity visible light image was made and used to produce “overlay” images. The images were analyzed with Metamorph Imaging System software (Universal Imaging Corporation).

Histochemical analysis

Femurs were fixed and decalcified in saturated EDTA for 7 days and embedded in paraffin. Five-μm thick sections were stained with H&E for histological examination. For detection of human MM cells the sections were labelled with anti CD138 (Labvision, Fremont, USA). As secondary antibody PowerVision Poly HRP-anti Rabbit IgG (ImmunoLogic/Klinpath, Duiven, The Netherlands) was used followed by the peroxidase enzymatic reaction.

Determination of free Ig light chain levels

The levels of human free light chains (FLC) were determined in undiluted cell culture supernatants and in urine samples using automated immunoassays as described previously²³.

Tumour-load reduction by radiotherapy

To induce a temporary tumour load reduction, mice bearing MM tumours were subjected to a total body irradiation (TBI) of 6.0 Gy X-rays, in week 5 after injection with 5×10^6 U266 cells i.v. To rescue the irradiated mice from bone marrow failure, 5×10^6 syngeneic bone marrow cells were injected i.v. The effect of the TBI on the total tumour load per mouse as well as on individual foci of MM growth was monitored with BLI.

Human Peripheral Blood Mononuclear Cells (PBMC) and Mixed Lymphocyte Reaction (MLR)

Human Peripheral Blood Mononuclear Cells (PBMC) isolated from buffy-coats of healthy blood bank donors, were thawed. The percentages of CD3⁺ cells were determined by FACS analysis and then suspended in PBS/0.1% human serum albumin (HSA) at $5-40 \times 10^6$ T cells that were injected in a volume of 0.2 ml as effector cells into the mice. To determine the reactivity against the MM cell lines, irradiated U266 and RPMI-8226/S cells were used as target cells in a ratio of 1:1. Briefly, 40,000 effector and 40,000 target cells were cultured in round-bottom 96-well plates for 6 days and pulsed with [³H] thymidine for the last 18 hours.

5

Tumour load reduction by immunotherapy (the Graft-versus-Myeloma effect)

To induce a GvM effect, mice bearing MM tumours were injected with various doses of human PBMC at week 5, in which the BLI signal was clearly visible in the image analysis (approximately 2 fold above the lower BLI baseline). To facilitate the engraftment of human cells, resident murine macrophage function was suppressed by i.v. injection of 2-chloromethyl biphosphonate liposomes, one day prior to the PBMC injection. The effect of the PBMC infusions on the MM tumour load was monitored with BLI. Mice were also monitored for the development of xenogeneic GvHD (x-GvHD) as described previously¹⁴. x-GvHD diagnosis was based on a combination of poor physical condition of the mice, hunched posture, ruffled fur and a body weight loss above 20%, and a high human T cell engraftment of >50%.

Table 1. Outgrowth of different MM cell lines after i.v. injection in RAG2^{-/-}γc^{-/-} mice.

cell line	# cells (i.v.)	location	experiment termination *	time of death mean (wks)
U266	5×10^6	skeleton	paralysis	13
UM-9	20×10^6	skeleton	paralysis	12
RPMI-8226/S	5×10^6	skeleton	paralysis	8
XG-1	15×10^6	skeleton	paralysis	8
L-363	5×10^6	skeleton	paralysis	8
OPM-1	5×10^6	skeleton, liver	weight loss	4
LME-1	5×10^6	skeleton, intestinal tract	weight loss	5

Seven cell lines were transduced with the GFP-LUC gene and selected for GFP⁺ cells and injected intravenously in RAG2^{-/-}γc^{-/-} mice. The location of MM growth was determined by BLI during the terminal stage of MM development.* reason to sacrifice the animals; hind leg paralysis or loss of >20% of body weight

Results

Engraftment and tumour outgrowth of MM cell lines in RAG2^{-/-}γc^{-/-} mice.

To test the suitability of RAG2^{-/-}γc^{-/-} mice for generating a useful MM murine model, seven different MM cell lines, U266, RPMI-8226/S, XG-1, L363, UM-9, LME-1 and OPM-1 were transduced with GFP-LUC and inoculated in RAG2^{-/-}γc^{-/-} mice. The U266, RPMI-8226/S, XG-1, L363, and UM-9 cell lines revealed similar results in terms of selective growth (survival time 7-12 weeks) in the bone marrow compartment only. The LME-1 and OPM-1 lines also showed growth in soft tissues, such as liver and intestines (Table 1). Detailed results for the two cell lines, U266 and RPMI-8226/S are depicted in Figures 1 and 2. After the i.v. injection of the mice with 5x10⁶ transduced MM cells the first signs of tumour growth, i.e. areas of luciferase activity, in the mice were detectable in the femur and/or tibia after 2 weeks, followed by additional foci of luciferase activity in the pelvic region, skull, limbs, sternum,

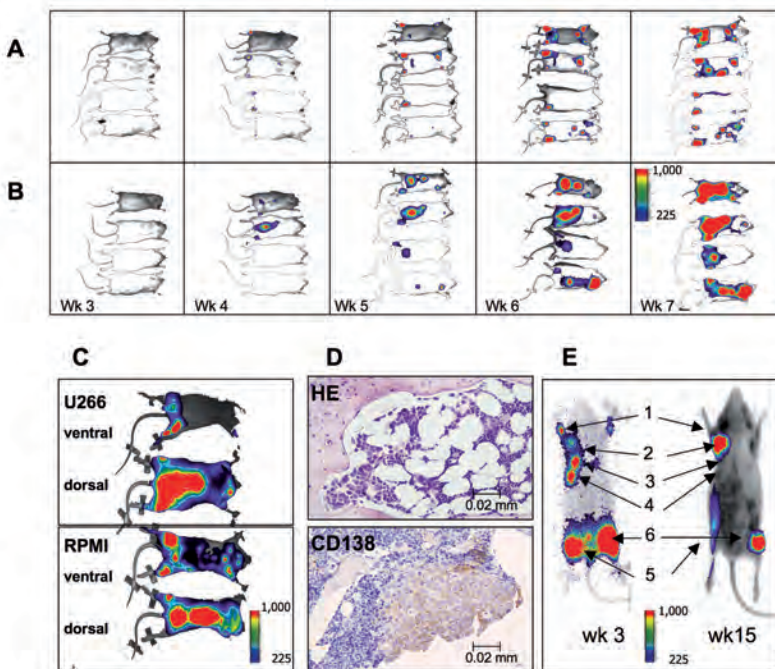


Figure 1. In vivo growth dynamics of luciferase gene marked RPMI-8226/S and U266 Multiple Myeloma. Bioluminescence images (BLI) taken from the ventral side (A) or from the dorsal side (B) of the mice at 5 sequential time points from week 3 to 7, with one week interval, after i.v. injection with GFP-LUC transduced RPMI-8226/S MM cells. (C) Higher magnification images taken from the dorsal and ventral side showing distinct foci of MM growth at various sites in the BM compartment of the mice inoculated with U266 or with RPMI-8226/S. (D) Presence of MM cells in the bone marrow of a mouse injected with U266 shown by hematoxylin-eosin (HE) staining and by immuno-staining for expression of CD138. (E) Location of various foci of U266 MM growth before total body irradiation (week 3) and after MM re-growth measured at week 15. All images are depicted in false colour, blue is at least 225 a.u./pixel and red is a maximal light intensity of 1,000 a.u./pixel.

ribs and the spinal vertebrae (Figure 1A and B). On average 5-15 foci of MM growth were detected per mouse but the pattern of distribution was different, but for each mouse specific (Figure 1A-C). MM growth in the vertebrae resulted in the development of hind leg paralysis in late-stage disease in about 70% of the animals, which was a reason to sacrifice the mice. The non-paralyzed mice also became moribund and were sacrificed when they lost 20% of their body weight. BLI revealed no MM lesions in soft tissues as spleen, lung liver, and kidneys (Figure 1C).

In the terminal stage of U266 MM growth, mice were sacrificed and from several bone and soft tissue samples cell suspensions were prepared and analyzed by FACS (10,000-100,000 cells per sample) for the presence of MM cells. All bone marrow specimens that were positive for BLI *in vivo*, contained large numbers of MM cells. Very few or no MM cells were found in specimens that did not reveal BLI signals. The expression pattern of GFP, CD45, CD38, CD138 and CD86 was not changed after the *in vivo* passage (data not shown). For the U266-derived tumours we examined the presence of MM cells in soft tissues (Table 2). Using flow cytometry as a read-out system with a lower threshold of 0.005% we did not detect any GFP positive cells (Table 2). Although these results do not completely exclude the presence of MM in soft tissues, they indicate that soft tissues were not the primary site for MM growth for five out of the seven cell lines that we studied". This predominant medullary outgrowth was also observed for RPMI-8226/S, XG-1, L363, and UM-9 (data not shown), indicating that in this model MM cell homing and growth strongly resembles human MM. Two other lines LME-1 and OPM-1 appeared to show not only medullary but also extramedullary growth (data not shown).

Table 2. Localization of MM lesions in RAG2^{-/-}γc^{-/-} mice detected by bioluminescence imaging confirmed by FACS analysis.

location	BLI (a.u.) range	FACS GFP ⁺ cells	MM cells detected	correlation between FACS and BLI
<i>skeletal parts</i>				
femur	1.4x10 ⁵ -1.5x10 ⁷	1.0-12.3	14/14	yes
tibia	5.0x10 ⁴ -1.2x10 ⁷	0.8-21.8	14/14	yes
humerus	1.2x10 ⁵ -9.0x10 ⁶	0.9-10.2	14/14	yes
sternum	below BDL	< 0.01	6/7*	yes
<i>soft tissues*</i>				
spleen	below BDL [†]	<0.005	0/7	yes
lungs	below BDL	<0.005	0/7	yes
liver	below BDL	<0.005	0/7	yes
kidney	below BDL	<0.005	0/7	yes
brain	below BDL	<0.005	0/7	yes
blood		<0.01	—	—

Data are pooled from four independent experiments with PBMC of four different individuals.

Treatment: day 0: 5x10⁶ MM cells; day 35: Cl₂MDP-liposomes (iv); day 36 PBMC iv (on the basis of % huCD3⁺) as indicated. TRM: treatment related mortality (death within 2 weeks after treatment, not GvH or MM related)

x-GvHD: Graft-versus-Host Disease, i.e. severe weight loss, ruffled fur, plus high huCD45 chimerism in blood.

MM: high multiple myeloma associated luciferase signal plus hind leg paralysis

MM free: no MM associated luciferase signal (BLI)

*: on the basis of BLI 20 animals were MM free and 6 had substantially reduced BLI signal at time of death.

The growth curves of U266 and RPMI-8226/S that are based on sequential BLI measurements, show an exponential increase of the myeloma tumour cell load in time, for the whole mouse (Figure 2A and B) as well as for individual foci of MM scattered throughout the bone marrow compartment (Figure 2C and D). The MM tumour growth could be monitored over a range of 4 log (factor of 10,000). The survival time of the mice inoculated with U266-tumours was 13.6 ± 2.4 weeks. The RPMI-8226/S tumours appeared to develop a little more rapid with a mean survival time = 7.9 ± 0.8 weeks. The medullary and extramedullary growing cell lines LME-1 and OPM-1 behaved as more aggressive growing tumours. The survival time was approximately 4 to 5 weeks. In these mice the initial signs of tumour growth was in the femur and tibia areas, soon thereafter fast growing MM tumours were observed in liver (OPM-1) or in the abdominal (intestinal tract) region (LME-1) and in the rest of the skeleton.

Comparison of BLI-based and Free Light Chain (FLC)-based tumour monitoring

A sensitive parameter that has been recognized as an indicator of the MM burden is the concentration of free light chain (FLC) in the urine or plasma. In vitro U266 cells produce high concentrations of FLC in culture medium. We therefore compared the sensitivity of tumour monitoring either with BLI or with urine FLC measurements in 12 mice that were inoculated with U266 cells. Whilst in all mice clearly increasing BLI-signals were observed starting from week 2 onwards, in six out of nine mice the FLC measurements remained negative until week 8 (Figure 2D), indicating that in our model BLI is a more sensitive method to monitor the tumor load. At all time points the plasma creatine levels remained normal (data not shown), indicating that the measured FLC concentrations were not confounded by renal dysfunction.

5

Suitability of BLI for tumour monitoring after therapeutic intervention

To evaluate whether the newly developed MM model was suitable for sensitive tumour monitoring after therapeutic intervention, we first subjected mice bearing U266-tumours to a dose of 6.0 Gy X-rays total body irradiation (TBI), which is the maximum tolerated dose for this mouse strain²². At the time of TBI (week 5), the BLI signals were approximately 10-20 times higher than baseline level. As depicted in figure 3A, the BLI signals in treated mice were significantly reduced to baseline levels within 2 weeks. In the meantime, the controls showed a 10-fold increase in signal. Thus, at the nadir there was a 100-fold (2 log) difference in tumour load between the treated mice and the control mice. However, BLI measurements beyond the second week post treatment revealed that, similar to the human situation, TBI was not sufficient to eradicate the MM tumours. This was evident from the steady increase of BLI signals with kinetics similar to that of the non-treated control group. These experiments demonstrated that the intervention in tumour growth in the new model was possible and that the tumour regression and progression could be easily and sensitively monitored by BLI. Furthermore BLI appeared also suitable for the monitoring of individual tumour foci. A representative mouse depicted in figure 3B and figure 1E illustrates that, before TBI, two of the total 6 MM foci detected in this mouse displayed weak BLI signals. Following treatment,

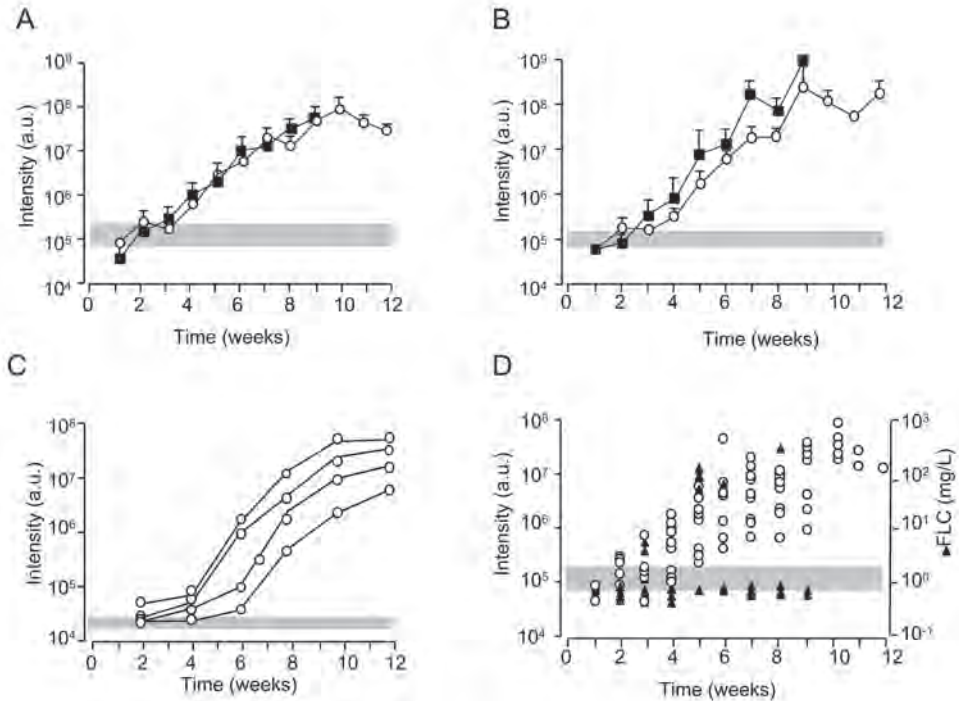


Figure 2. BLI based growth kinetics of RPMI-8226/S and U266 MM in RAG2^{-/-}γc^{-/-} mice.

MM growth curves on the basis of bioluminescence photon emission measurements and shown as mean ± SD (n=8). The curves reflect the increase in photon emission measured for the whole mouse inoculated with RPMI-8226/S (■) or U266 MM cells (O) and imaged from the ventral side (A) as well as from the dorsal side (B) at various time intervals after inoculation of the MM cells. (C) Growth curves for several individual foci of bioluminescence from RPMI-8226/S in a single mouse imaged from the ventral side. (D) Comparison between levels of bioluminescence (O) and Free-light-chain (FLC) concentrations that are recorded on several time points during Multiple Myeloma (U266) growth FLC is measured in the urine. The grey area at the bottom of the graphs represents the mean photon emission count from an identical sized control region in the same image over the 15 weeks.

these two foci disappeared completely indicating eradication of MM in the affected bones. The foci with high BLI signals, however, showed only temporary regression by TBI treatment, but eventually showed progression (Figure 3B and 1E).

Induction of GvM effect in the RAG2^{-/-}γc^{-/-} based human myeloma model

One of our most important goals was to develop a MM model suitable for evaluation of cellular immunotherapy approaches, such as donor lymphocyte infusions (DLI). To this end, we first explored whether infusion of human PBMC in U266-bearing mice would induce a GvM effect. Human PBMC containing either 10x10⁶ or 40x10⁶ T cells were injected in mice at week 5, when the U266-tumours were clearly detectable by BLI (Figure 3C). Another group received PBMC containing 10x10⁶ T cells, one day after preconditioning of the mice with clodronate containing liposomes. Preconditioning with clodronate liposomes depletes

murine macrophages and in our experience this improves the engraftment of human cells in the $RAG2^{-/}\gamma c^{-/}$ mice^{14,22}. In a control group, liposomes had no anti tumour effect (Figure 3C). As expected, all animals treated with human PBMC developed, from week 7 onwards, a cell-dose-dependent x-GVHD (data not shown). In mice treated with 40×10^6 T cells, the BLI signals started to drop for all tumour locations one week after the onset of x-GVHD. BLI signals decreased below the lower threshold levels within two weeks (Figure 3C). All mice were free of MM, but eventually died from lethal x-GvHD between week 8-12 (Table 3). At the T cell

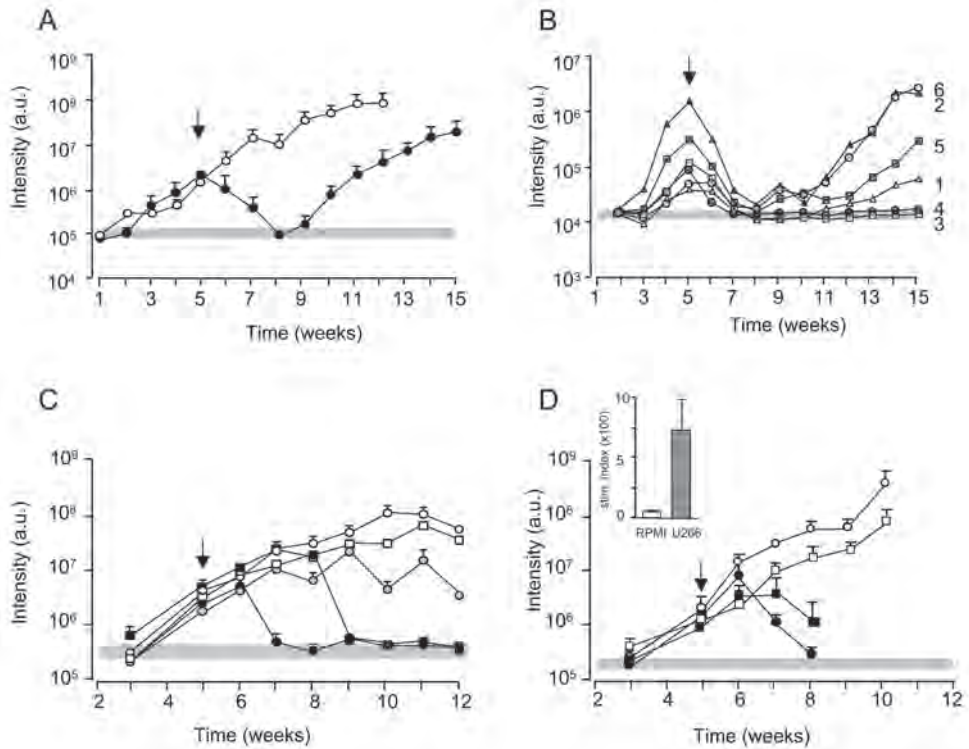


Figure 3. BLI based monitoring of MM tumor reduction after radiotherapy (total body irradiation) or the Graft-versus-Myeloma effect by cellular immunotherapy with human PBMC.

(A) $RAG2^{-/}\gamma c^{-/}$ mice were inoculated i.v. with U266 cells and subjected to a total body irradiation in week 5 (indicated by the arrow). The MM tumor load in treated mice (●) and in non-irradiated control mice (○) was weekly monitored with BLI. The curves show the bioluminescence photon emission in a.u. for the whole mouse \pm SD ($n=4$). **(B)** Individual foci of MM growth (1 through 6) in one representative mouse. The BLI images of this mouse is shown in Figure 1E and the corresponding foci of MM 1 through 6 are indicated. **(C)** GvM effect in mice with U266 MM cells after inoculation of 40×10^6 T cells (●) and 10×10^6 T cells (○) in week 5 (indicated by the arrow) compared to a non-treated group of mice (○). The GvM effect is also evident after inoculation of 10×10^6 T cells in CL₂MDP liposome pretreated mice (■) and is compared with only liposome treated animals (□). **(D)** $RAG2^{-/}\gamma c^{-/}$ mice were inoculated with 5×10^6 RPMI-8226/S or 5×10^6 U266 MM cells. At week 5 all mice were pretreated with CL₂MDP liposomes followed by inoculation of 10×10^6 T cells the next day (indicated by the arrow). The GvM effect is shown in the RPMI-8226/S (■) and the U266 mice (●) compared with the non-treated RPMI-8226/S (□) and U266 mice (○). The bar graph inset shows the results of the in vitro mixed lymphocyte reaction analysis to RPMI-8226/S and U266 MM cells respectively. The grey area at the bottom of the graphs represents the mean photon emission count from an identical sized control region in the same image over the 12 weeks

dose of 10×10^6 (without liposome pretreatment) the x-GvHD and GvM effects were merely sufficient to stabilize the tumour progression but did not lead to tumour clearance. Only 1 out of 6 mice developed a clear x-GvH reaction. However, when combined with liposome pretreatment, 10×10^6 T cells mediated strong x-GvH and GvM effects and similar results as for the 40×10^6 T cell group were observed. In total a 31 mice were treated with PBMC from 3 different donors. Five animals died early from treatment related toxicity. The remaining 26 mice all developed x-GvHD, although less rapid than the group of mice receiving 40×10^6 T cells; 6 mice died within 3 weeks, however, already with significantly reduced tumour load. The remaining 20 mice survived longer, but ultimately all mice died from x-GvHD between week 8 and week 12, however, these mice were all free of MM (Figure 3C and Table 3) In our in vitro mixed lymphocyte reactions, the RPMI-8226/S cell line consistently fails to induce a significant T cell proliferation from PBMC of 5 different donors, while the U266 cell line is highly immunogenic (Figure 3D inset). The stimulation index is 697 ± 581 for the U266 versus 30 ± 48 for the RPMI. This suggested that RPMI-8226/S-derived tumours could represent, less immunogenic, MM tumours in our new model. To test this we compared the development of GvM effects against U266- or RPMI-8226/S-derived tumours in a separate experiment. Mice bearing either U266- or RPMI-8226/S tumours received PBMC containing 10×10^6 T cells 1 day after the liposome conditioning at week 5 after inoculation of the MM cells. All mice developed severe x-GvHD, and died between week 8 and 9. BLI measurements performed within this short period revealed that the GvM effect was more pronounced for the U266-tumours as compared to the RPMI-8226/S-tumours (figure 3D). The tumour load reduction started in the U266 group at week 7, one week earlier than seen in the RPMI-8226/S group. At week 9, when the experiments were terminated due to severe x-GvHD, the tumour load in the U266 group was almost at baseline levels ($10 \pm 9\%$ of starting signal), whereas the tumour load in the RPMI-8226/S group was higher ($91 \pm 53\%$), which was significantly different ($p < 0.05$). These results indeed suggested that RPMI-8226/S-tumours might be used as a model for nonimmunogenic or DLI-resistant tumours when testing the efficacy of new combination therapies.

5

Discussion

In this study we present a convenient and reproducible in vivo model for human myeloma that can facilitate preclinical testing of cellular therapy strategies in combination with immuno-modulatory agents to improve the GvM effects after allo-SCT. Since we aimed at convenient and sensitive immunomonitoring of tumour load, the model was established by intravenous transfer of GFP-luc transduced MM cell lines in RAG2^{-/-}γc^{-/-} mice.

Despite the use of MM cell lines, five out of 7 tested MM cell lines developed tumours with phenotype, dissemination, and growth pattern highly similar to human MM. In particular, the multifocal-growth predominantly in the BM, production of FLC, and expression of MM-associated molecule CD138 of the established tumors, are the most striking similarities with human MM. Furthermore, the differences in the in vivo growth kinetics and immunogenicity of the used MM cell lines enables us a comprehensive evaluation of novel strategies on various predefined conditions.

Previously, other investigators also developed MM models by injecting MM cell lines into SCID-NOD mice³⁻¹¹. A recently developed model also exploited the advantages of fluorescence

Table 3. Development of x-GvHD and GvM effects in the PBMC-treated mice bearing U266-tumors.

group	n	TRM	x-GvHD symptoms	cause of death		MM-free ^c
				x-GvHD ^a	MM ^b	
Untreated MM controls	35	0	0	0	35	0
40x10 ⁶ T cells	7	0	7	7	0	7
10x10 ⁶ T cells	6	1	5	0	5	0
Liposomes only controls	16	6	0	0	10	0
Liposomes +10x10 ⁶ PBMC	31	5	26	26*	0	20
Liposomes + 5x10 ⁶ PBMC	6	1	5	4	1	0

The overall distribution of MM cells was assessed by bioluminescence imaging (BLI) in 7 mice, 9 weeks after inoculation of 5x10⁶ U266 MM cells i.v. Cell isolates from various skeletal parts and soft tissues were analyzed by flow cytometry (FACS) for the presence of GFP⁺ cells in the total nucleated cell fraction; 100,000 cells were analyzed per sample (10,000 for the blood). BLI is expressed as arbitrary light units (a.u.)/10 minutes per mouse. BDL: below detection limit (in region not covered by skeletal parts)

*: one sternum showed a small BLI signal not confirmed by FACS analysis.

based optical imaging, which has a high resolution for GFP imaging and also allows frequent and serial non-invasive monitoring^{28,29}. While highly useful and convenient, an important drawback of this recent model was the extramedullary growth of tumours, which is not a typical feature of MM. The mechanisms that are controlling the homing behaviour of MM cells to the bone marrow are not yet elucidated but it is believed that chemokines and their respective receptor counterparts involved in lymphocyte trafficking also play a role in MM homing. Differential expression of chemokine receptors has been reported for primary MM²⁴ as well as for MM cell lines²⁵. It was also shown that SDF-1/CXCL12 is a critical regulator of MM homing²⁶. Murine SDF-1, expressed by the stromal elements in mouse bone marrow, can interact with human hematopoietic cells²⁷, may play an important role in this process. Whatever the reason extramedullary growth may introduce a significant bias, if the model is aimed at testing the efficacy of cellular immunotherapy strategies. Furthermore, outgrowth of human T cells in the SCID/NOD mice is far less reproducible as compared to the RAG2^{-/-}γc^{-/-} mice¹⁴. Thus, in our view, our model offers several advantages above the NOD-SCID model and therefore it may be better suited for preclinical testing of cellular immunotherapeutic approaches. Furthermore the availability of cell lines with different growth kinetics and with medullary or extramedullary outgrowth in our model, gives us the possibility to compare the efficacy of combination therapies in more detail. Nevertheless, it should be noted that our model, as the tumor cells are not primary, may be less suitable for studying a number of the biological aspects of myeloma such as stroma-myeloma interactions or natural growth kinetics. Thus far we have not tested whether RAG2^{-/-}γc^{-/-} immune deficient mice facilitate the outgrowth of primary human MM cells after intravenous transfer in a similar way as has been described by other investigators who showed that primary MM cells can only engraft when injected in combination with previously implanted human fetal bone^{3,10} or rabbit bone¹¹ fragments. In our study, an important reason to prefer MM cell lines above primary MM cells was to exploit the advantages of BLI technology as a sensitive and non-invasive technology for tumor monitoring. In our model BLI appeared superior to FLC-based monitoring and also allowed semi-quantitative monitoring of individual MM foci. Indeed, BLI appeared not only suitable for quantitative detection of the tumour load in the whole body, but it was also highly useful for visualization and quantitative analysis of individual

foci of myeloma growth throughout the marrow compartment. Bioluminescence is very sensitive for the detection of low levels of marker gene expression³⁰, allowing even the detection of small size tumours, which becomes relevant when monitoring small tumours after therapy. Obviously, the location of the tumour (depth inside the animals) influences the lower detection limits of BLI. This is clearly seen in panel 2C for the individual foci of growth. However, once that the light signals coming from a tumour at a given location reach levels beyond the base line the doubling times are similar indicating that the growth kinetics are not effected by the location. A positive correlation between tumour burden and BLI signal intensity has been shown in a variety of in vivo studies of animal tumour models³⁰⁻³⁴. We show here that this correlation also applies to human MM cell lines that we studied and confirms reports with human MM by others³⁵⁻³⁷. This unique advantage provides us the opportunity to evaluate the effects of therapeutic interventions on individual tumour foci, which often differed in size.

To evaluate the application areas of our model we treated established full-blown tumours with radiotherapy as well as with allogeneic cellular immunotherapy. Radiotherapy resulted in a slow decay in tumour load, initially diminishing the tumour load under the detection limits of the BLI. Based on the whole body BLI measurements we calculated that an approximate 2 log tumour reduction was achieved by radiotherapy, which is in agreement with the radiosensitivity of the clonogenic MM cells³⁸. While for small individual lesions radiotherapy seemed to be sufficient for tumour eradication (there was no reappearance of the tumour), this was clearly not the case for the larger tumour foci. Tumours in these latter foci eventually progressed with the same pace, providing only a six weeks delay in overall survival. Hence, these results once again emphasized the necessity of additional therapies after radiotherapy. Most important, however, the radiotherapy experiments illustrated the feasibility to use BLI as a sensitive tumour monitoring technology. Finally, the results of allo-immune therapy experiments demonstrated that the MM model developed in RAG2^{-/-}γc^{-/-} mice is very useful for preclinical testing of cellular immune therapies, as the mice easily permits the engraftment and outgrowth of human T cells. The potent GvM effect obtained by infusion of allogeneic, thus MHC mismatched human T cells reveals first of all the proof of principle that it may be possible to eradicate full-blown MM by potent allo-immune cellular therapies. Secondly, the results obtained so far suggest that the cell dose and immunogenicity of myeloma cells are important parameters determining the chances for cure. While the U266-derived tumours could be completely eradicated by allo-immune treatment containing 10x10⁶ T cells, the RPMI-8226/S-based tumours appeared less susceptible to the same treatment dose. Also in in vitro assays, the RPMI-8226/S cell line evoked little or poor responses from several HLA-mismatched PBMC. Taken together these results suggest that RPMI-8226/S-based tumors are less immunogenic as compared to U266-derived tumors, providing us a unique opportunity to compare and optimize the efficacy of cellular immunotherapy approaches. While at this stage we used HLA-mismatched PBMC to develop the model, it is obviously quite interesting to evaluate the GvM effects of 3 locus HLA-matched PBMC which can be selected among HLA-typed blood-bank donors. Such a model will be obviously more comparable to the HLA identical matched unrelated donor (MUD) transplantation. As the mice also develops x-GvHD after infusion of human PBMC, effects on x-GvHD can be used as a control for all therapeutic interventions in combination with infusion of allogeneic lymphocytes. In this respect, we think that one of the interesting application areas of our current model will be the evaluation of the impact of regulatory T cells (Tregs) on the GvM

effect, since we have recently shown in this model that co-infusion of human PBMC with autologous Tregs effectively down regulates the lethal x-GvHD¹⁵.

In conclusion, we present here a model of human MM growth in an immunodeficient mouse, strongly resembling human MM that can be used to monitor non-invasively and quantitatively the outgrowth of MM cells. This model offers the possibility for preclinical evaluation of several treatment strategies and therefore may facilitate the design of optimal protocols for multiple myeloma treatment.

References

- 1 Richardson PG, Mitsiades C, Schlossman R, Munshi N, Anderson K. New drugs for myeloma. *Oncologist*. 2007;12:664-89.
- 2 Badros A, Barlogie B, Morris C, Desikan R, Martin SR, Munshi N et al. High response rate in refractory and poor-risk multiple myeloma after allotransplantation using a nonmyeloablative conditioning regimen and donor lymphocyte infusions. *Blood* 2001;97:2574-9.
- 3 Yaccoby S, Barlogie B, Epstein J. Primary myeloma cells growing in SCID-hu mice: a model for studying the biology and treatment of myeloma and its manifestations. *Blood* 1998;92:2908-13.
- 4 Pilarski LM, Hipperson G, Seeberger K, Pruski E, Coupland RW, Belch AR. Myeloma progenitors in the blood of patients with aggressive or minimal disease: engraftment and self-renewal of primary human myeloma in the bone marrow of NOD SCID mice. *Blood* 2000;95:1056-65.
- 5 Bellamy WT, Odeleye A, Finley P, Huizenga B, Dalton WS, Weinstein RS, et al. An in vivo model of human multidrug-resistant multiple myeloma in SCID mice. *Am J Pathol* 1993;142:691-8.
- 6 Urashima M, Chen BP, Chen S, et al. The development of a model for the homing of multiple myeloma cells to human bone marrow. *Blood* 1997;90:754-65
- 7 Reme T, Gueydon E, Jacquet C, Klein B, Brochier J. Growth and immortalization of human myeloma cells in immunodeficient severe combined immunodeficiency mice: a preclinical model. *Br J Haematol* 2001;114: 406-13.
- 8 Mitsiades C, Mitsiades N, Munshi N, Anderson KC. Focus on multiple myeloma. *Cancer Cell*, 2004;6:5,439-44.
- 9 Huang SY, Tien HF, Su FH, Hsu SM. Nonirradiated NOD/SCID-human chimeric animal model for primary human multiple myeloma: a potential in vivo culture system. *Am J Pathol* 2004;164:747-56.
- 10 Tassone P, Neri P, Carrasco DR, Burger R, Goldmacher VS, Fram R, et al. A clinically relevant SCID-hu in vivo model of human multiple myeloma. *Blood* 2005;106:713-6.
- 11 Yata K, Yaccoby S. The SCID-rab model: a novel in vivo system for primary human myeloma demonstrating growth of CD138-expressing malignant cells. *Leukemia* 2004;18:1891-7.
- 12 Dalton W, Anderson KC. Synopsis of a roundtable on validating novel therapeutics for multiple myeloma. *Clin Cancer Res*. 2006;12:6603-10. Review.
13. Weijer K, Uittenbogaart CH, Voordouw A, Couwenberg F, Seppen J, Blom B, et al. Intrathymic and extrathymic development of human plasmacytoid dendritic cell precursors in vivo. *Blood* 2002;99:2752-9.
14. van Rijn RS, Simonetti ER, Hagenbeek A, Bonyhadi M, Storm G, Martens AC, et al. A new xenograft model for graft-versus-host disease by intravenous transfer of human peripheral blood mononuclear cells in RAG2-/-gammac-/- double-mutant mice. *Blood* 2003;102:2522-31.
- 15 Mutis T, van Rijn RS, Simonetti ER, Aarts-Riemens T, Emmelot ME, van Bloois L, et al. Human regulatory T cells control xenogeneic graft-versus-host disease induced by autologous T cells in RAG2-/-gammac-/- immunodeficient mice. *Clin Cancer Res* 2006;12:5520-5.
16. Kuipers J, Vaandrager JW, Weghuis DO, Pearson PL, Scheres J, Lokhorst HM, et al. Fluorescence in situ hybridization analysis shows the frequent occurrence of 14q32.3 rearrangements with involvement of immunoglobulin switch re-gions in myeloma cell lines. *Cancer Genetics and Cytogenetics*, 1999;109:99-107.
- 17 Derksen PW, Keehnen RM, Evers LM, van Oers MH, Spaargaren M, Pals ST. Cell surface proteoglycan syndecan-1 mediates hepatocyte growth factor binding and promotes Met signaling in multiple myeloma. *Blood* 2002;99:1405-10.
- 18 Zhang XG, Gaillard JP, Robillard N, Lu ZY, Gu ZJ, Jourdan M, et al. Reproducible obtaining of human myeloma cell lines as a for tumor stem cell study in human multiple myeloma. *Blood* 1994;83:3654-63.
- 19 Katagiri S, Yonezawa T, Kuyama J, Kanayama Y, Nishida K, Abe T, et al. Two distinct human myeloma cell lines originating from one patient with myeloma. *Int J Cancer* 1985;36:241-6.
- 20 Diehl V, Schaadt M, Kirchner H, Hellriegel KP, Gudat F, Fonatsch C, et al. Long-term cultivation of plasma cell leukemia cells and autologous lymphoblasts (LCL) in vitro: a comparative study. *Blut* 1978;36:331-8.
- 21 Day RN, Kawecki M, Berry D. Dual-function reporter protein for analysis of gene expression in living cells. *Biotechniques* 1998;25:848-56.

22. Rozemuller H, Knaan-Shanzer S, Hagenbeek A, van Bloois L, Storm G, Martens AC. Enhanced engraftment of human cells in RAG2/gammac double-knockout mice after treatment with CL2MDP liposomes. *Exp Hematol* 2004;32:1118-25.
23. Abraham RS, Clark RJ, Bryant SC, Lymp JF, Larson T, Kyle RA, et al. Correlation of serum immunoglobulin free light chain quantification with urinary Bence Jones protein in light chain myeloma. *Clin Chem* 2002;48:655-57
24. Möller C, Strömberg T, Juremalm M, Nilsson K, Nilsson G. Expression and function of chemokine receptors in human multiple myeloma. *Leukemia*. 2003 Jan;17(1):203-10.
25. Dürig J, Schmücker U, Dührsen U. Differential expression of chemokine receptors in B cell malignancies. *Leukemia*. 2001 May;15(5):752-6.
26. Alsayed Y, Ngo H, Runnels J, Leleu X, Singha UK, Pitsillides CM, et al., Mechanisms of regulation of CXCR4/SDF-1 (CXCL12)-dependent migration and homing in multiple myeloma. *Blood*. 2007 Apr 1;109(7):2708-17.
27. Broxmeyer HE, Mejia JA, Hangoc G, Barese C, Dinauer M, Cooper S. SDF-1/CXCL12 enhances in vitro replating capacity of murine and human multipotential and macrophage progenitor cells. *Stem Cells Dev*. 2007 Aug;16(4):589-96.
28. Mitsiades CS, Mitsiades NS, Bronson RT, Chauhan D, Munshi N, Treon SP, et al. Fluorescence imaging of multiple myeloma cells in a clinically relevant SCID/NOD in vivo model: biologic and clinical implications. *Cancer Res* 2003;63:6689-96.
29. Oyajobi BO, Muñoz S, Kakonen R, Williams PJ, Gupta A, Wideman CL, et al. Detection of myeloma in skeleton of mice by whole-body optical fluorescence imaging. *Mol Cancer Ther* 2007;6:1701-8. Epub 2007 May 31.
30. Caceres G, Zhu XY, Jiao JA, Zankina R, Aller A, Andreotti P. Imaging of luciferase and GFP-transfected human tumours in nude mice. *Luminescence* 2003;18:218-23.
31. Jenkins DE, Oei Y, Hornig YS, Yu SF, Dusich J, Purchio T, Contag PR. Bioluminescent imaging (BLI) to improve and refine traditional murine models of tumor growth and metastasis. *Clin Exp Metastasis* 2003;20:733-44
32. Smakman N, Martens A, Kranenburg O, Borel Rinkes IH. Validation of bioluminescence imaging of colorectal liver metastases in the mouse. *J Surg Res* 2004;122:225-30
33. Paroo Z, Bollinger RA, Braasch DA, Richer E, Corey DR, Antich PP, et al., Validating bioluminescence imaging as a high-throughput, quantitative modality for assessing tumor burden. *Mol Imaging* 2004;3:117-12
34. Nogawa M, Yuasa T, Kimura S, Kuroda J, Sato K, Segawa H, et al. Monitoring luciferase-labeled cancer cell growth and metastasis in different in vivo models. *Cancer Lett* 2005;21:243-5
35. Mitsiades CS, Mitsiades NS, McMullan CJ, Poulaki V, Shringarpure R, Akiyama M, et al. Inhibition of the insulin-like growth factor receptor-1 tyrosine kinase activity as a therapeutic strategy for multiple myeloma, other hematologic malignancies, and solid tumors. *Cancer Cell*. 2004;5:221-30.
36. Wu KD, Cho YS, Katz J, Ponomarev V, Chen-Kiang S, Danishefsky SJ, et al. Investigation of antitumor effects of synthetic ephothilone analogs in human myeloma models in vitro and in vivo. *PNAS* 2005;102:10640-5. Epub 2005 Jul 1
37. Xin X, Abrams TJ, Hollenbach PW, Rendahl KG, Tang Y, Oei YA, et al. CHIR-258 is efficacious in a newly developed fibroblast growth factor receptor 3-expressing orthotopic multiple myeloma model in mice. *Clin Cancer Res* 2006;12:4908-15.
38. Gluck S, Van DJ, Messner HA. Radiosensitivity of human clonogenic myeloma cells and normal bone marrow precursors: effect of different dose rates and fractionation. *Int J Radiat Oncol Biol Phys* 1994;28:877-82.

5

6

Targeting EXT1 reveals a crucial role for heparan sulfate in the growth of multiple myeloma

Richard W. J. Groen,^{1,2,3} Rogier M. Reijmers,^{1,3} Henk Rozemuller,² Annemieke Kuil,¹ Anneke de Haan-Kramer,¹ Tamás Csikós,¹ Anton C. M. Martens,² Marcel Spaargaren,^{1,4} and Steven T. Pals^{1,4,5}

¹Department of Pathology, Academic Medical Center, Meibergdreef 9, 1105 AZ Amsterdam, The Netherlands; ²Department of Immunology, University Medical Center Utrecht, Lundlaan 6, 3584 EA Utrecht, The Netherlands; ³These authors contributed equally to this work; ⁴These authors share last authorship.

Blood. 2010; 115(3): 601-4

Abstract

Expression of the heparan sulfate proteoglycan (HSPG) syndecan-1 is a hallmark of both normal and multiple myeloma (MM) plasma cells. Syndecan-1 could affect plasma cell fate by strengthening integrin-mediated adhesion via its core protein and/or by accommodating and presenting soluble factors via its HS side-chains. Here, we show that inducible RNAi-mediated knockdown of syndecan-1 in human MM cells leads to reduced growth rates and a strong increase of apoptosis. Importantly, knockdown of EXT1, a co-polymerase critical for HS-chain biosynthesis, had similar effects. By employing an innovative myeloma xenotransplant model in RAG2^{-/-}γc^{-/-} mice, we demonstrate that induction of EXT1 knockdown in vivo dramatically suppresses the growth of bone marrow localized myeloma. Our findings provide direct evidence that the HS-chains of syndecan-1 are crucial for the growth and survival of MM cells within the bone marrow environment, and indicate the HS biosynthesis machinery as a potential treatment target in MM.

Introduction

Within the lymphoid system, expression of the heparan sulfate proteoglycan (HSPG) syndecan-1 is characteristic for terminally differentiated B cells, i.e. plasma cells, and their malignant counterpart multiple myeloma (MM),¹ a plasma cell neoplasm, which expands in the bone marrow.^{2,3} HSPGs are proteins with covalently attached HS-chains, which consist of alternating N-acetylated glucosamine and D-glucuronic acid units. To exert their function, the HS-chains undergo a complex series of processing reactions involving deacetylation, epimerization, and (de)sulfation.^{4,5} This endows HS-chains with highly modified domains that provide specific docking sites for many bio-active molecules. Binding of these ligands serves a variety of functions, ranging from immobilization and concentration to distinct modulation of biological functions. HSPGs are widely expressed in mammalian tissues as extracellular matrix components or cell-membrane-bound proteins. These membrane-localized HSPGs can also function independent of their HS side chains, for example by the ability of their core protein to interact with signaling molecules or cytoskeletal proteins.⁶⁻⁸ Thus, HSPGs act as multifunctional scaffolds regulating important biological processes including cell adhesion and migration, tissue morphogenesis and angiogenesis.^{4,6,7,9} Studies from several laboratories, including our own, point to a versatile role of the transmembrane HSPG syndecan-1 in the interaction of MM plasma cells with the BM microenvironment.¹⁰⁻¹³ Various growth factors have been implicated in controlling MM survival and growth, including hepatocyte growth factor (HGF), epidermal growth factor (EGF)-family members, and WNTs.^{10-12,14-16} Most of these factors can bind to the HS-chains of syndecan-1,^{11,12,17} which promotes their ability to stimulate MM cell growth and survival in vitro.^{11,12} Independent of HS-chains, the syndecan-1 core protein can interact with, and regulate the activity of, integrin adhesion molecules.^{7,18} Thus, both the HS-chains and the syndecan-1 core protein could contribute to the dynamic interaction of tumor with the BM milieu and influence tumor behavior.^{13,19} This notion prompted us to specifically study the impact of targeting of EXT1, an enzyme indispensable for HS-chain synthesis,^{20,21} on MM growth, both in vitro and in vivo.

6

Materials and methods

Cell lines and culture.

The human MM cell lines RPMI-8226 and L363 were cultured as described.²² Generation of inducible cell lines. Doxycycline-inducible cell lines were generated using theT-REx™ System (Invitrogen Life technologies). L363 and RPMI-8226 were transfected by electroporation (Gene Pulser Apparatus, BioRad, USA) with the pTER construct alone (TetR), or in combination with a construct containing an shRNA directed against either syndecan-1 (shSYN1) or EXT1 (shEXT1a, b, or c). shRNA sequences are given in the supplemental methods and the position of the target sites is shown in supplemental Figure 1A. To induce shRNA expression, 1 µg/ml doxycycline (Sigma-Aldrich, St Louis, MO) was used. In vitro growth and apoptosis measurements. Cells were plated (1×10^4) in 96-wells plates.

Cells were quantified by FACS (BD Biosciences, Erembodegem, Belgium), employing TO-PRO-3-iodide to exclude dead cells. Apoptotic cells were identified by AnnexinV and TO-PRO-3-iodide. Transplantation of MM cells in mice. RAG2^{-/-}γc^{-/-} mice (9-14 weeks) were bred and housed as described.²² Transplantation of GFP-luciferase transduced L363 or RPMI-8226 cells into RAG2^{-/-}γc^{-/-} mice was performed essentially as described,²² except that 1x10⁶ MM cells were injected intracardially. During the experiment, the mice were supplied with water ad libitum, containing 5% sucrose with or without 1 mg/ml doxycycline (Sigma-Aldrich). In addition, mice receiving doxycycline were injected i.p., twice a week, with 125 mg doxycycline to sustain adequate serum levels. Bioluminescent imaging. Mice were anesthetized by isoflurane inhalation before they received an i.p. injection of 100 μl 7.5 mM D-luciferine (Synchem Chemie, Kassel, Germany). Bioluminescence images were acquired using a third generation cooled GaAs intensified charge-coupled device (ICCD) camera, controlled by the Photo Vision software and analyzed with M³Vision software (all from Photon Imager; Biospace lab, Paris, France).

Statistical analysis.

The unpaired two-tailed Student's-t test was used to determine the significance of differences between means, unless stated otherwise.

Results and discussion

6

In this study, we have directly explored the impact of HS-modification of syndecan-1 on MM growth in vivo, by using a recently developed, innovative, xenotransplant model.²² Key features of this model are that it employs immunodeficient RAG2^{-/-}γc^{-/-} mice as recipients of human MM cells transduced with GFP-luciferase to allow non-invasive real-time monitoring of MM cell growth in vivo. RAG2^{-/-}γc^{-/-} mice completely lack B, T, and NK cells, and therefore permit highly reproducible engraftment of human lymphocytes.²³⁻²⁵ As we recently demonstrated, these RAG2^{-/-}γc^{-/-} mice are also highly permissive to grafting of human MM cell lines, several of which displayed a strikingly selective tumor outgrowth in recipient's bone marrow compartment upon i.v. injection.²² For our current studies, two of these MM cell lines (L363 and RPMI-8226) were selected and stably transfected with doxycycline-inducible shRNAs against either the syndecan-1 core protein or the HS co-polymerase EXT1 (shSYN1 and shEXT1 respectively). To rule out off-target effects of the shRNAs, three different L363-shEXT1 lines, each containing a different non-overlapping targeting sequence for EXT1, were generated (shEXT1a, b and c), (see Supplemental Methods and Supplemental Figure 1A and B). Doxycycline treatment of L363-shSYN1 cells led to a ~75% reduction of syndecan-1 expression (Figure 1A), while treatment of L363-shEXT1a, b, or c or RPMI-shEXT1a cells was even more effective and reduced cell-surface HS expression by ~90% (Figure 1B). In control (TetR) cells, doxycycline did not affect syndecan-1 or HS levels (Figure 1A and B). Interestingly, the doxycycline induced knockdown of either syndecan-1 or EXT1 led to a marked reduction of the in vitro growth rate of the myeloma cells (Figure 1C and D), which was accompanied by a prominent increase in apoptosis (Figure 1E), as well as a minor increase in the percentage of cells in phase G₁/G₀ of the cell cycle (data not shown). Importantly, the expression of the syndecan-1 core protein was unaffected by EXT1 knockdown

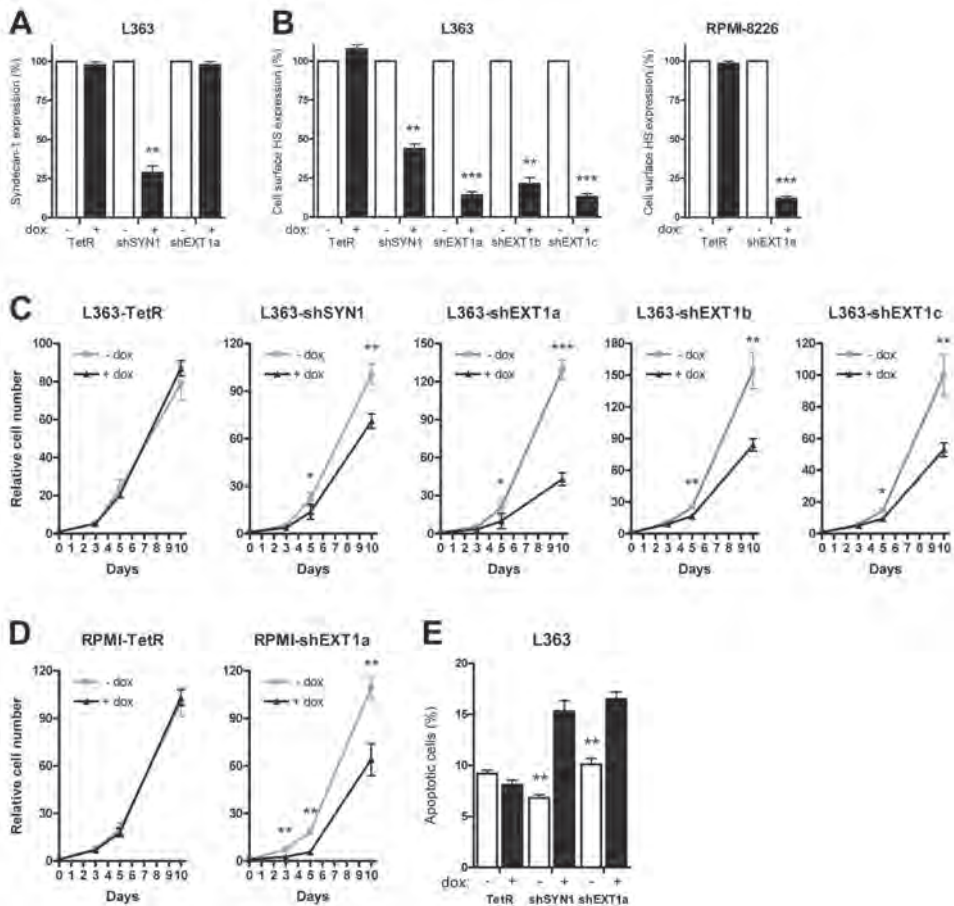


Figure 1. Loss of syndecan-1 and cell surface HS reduces the in vitro growth of MM due to increased apoptosis. L363 and RPMI-8226 MM control cells (TetR) and L363 and RPMI-8226 MM cells containing inducible shRNA, targeting either syndecan-1 (shSYN1) or EXT1 (shEXT1a, b and c), were incubated with (+dox) or without doxycycline (-dox) for 5 days prior to each experiment to allow for optimal knockdown of the target genes. **(A)**, **(B)** Expression of syndecan-1 **(A)** or cell surface HS **(B)** measured by FACS using antibodies BB4 (Serotec, Bicester, United Kingdom) and 10E4 (Seikagaku America, Rockville, MD), respectively. The expression level of the untreated samples was normalized to 100%, and the bars represent the means \pm SD of at least 5 independent experiments. **(C, D)** The growth rate of L363-TetR, -shSYN1 and -shEXT1a, b and c MM cells **(C)** or RPMI-TetR and -shEXT1a MM cells **(D)** was analyzed over a 10 day culture period in the presence of 10% FCS. The growth curves represent the means \pm SD of 3-5 independent experiments (in triplicate). **(E)** The percentages of apoptotic cells were measured for the different L363 MM cell lines after 3 days of culture. Apoptotic cells were determined as AnnexinV⁺/TO-PRO⁻. Necrotic, TO-PRO single positive cells, were excluded. *, $p < 0.05$; **, $p < 0.01$; ***, $p < 0.001$.

(Figure 1A). Therefore, our results underscore the importance of HS side-chains, rather than the proteoglycan core protein per se, in the growth and survival of MM cells in vitro. To directly assess the role of HS on tumor growth in vivo, the L363-shEXT1a and RPMI-shEXT1a MM cells were retrovirally transduced to express a GFP-luciferase fusion protein and injected intracardially into irradiated RAG2^{-/-} γ c^{-/-} mice. Consistent with our previous observations using untransfected L363 cells,²² mice that did not receive doxycycline

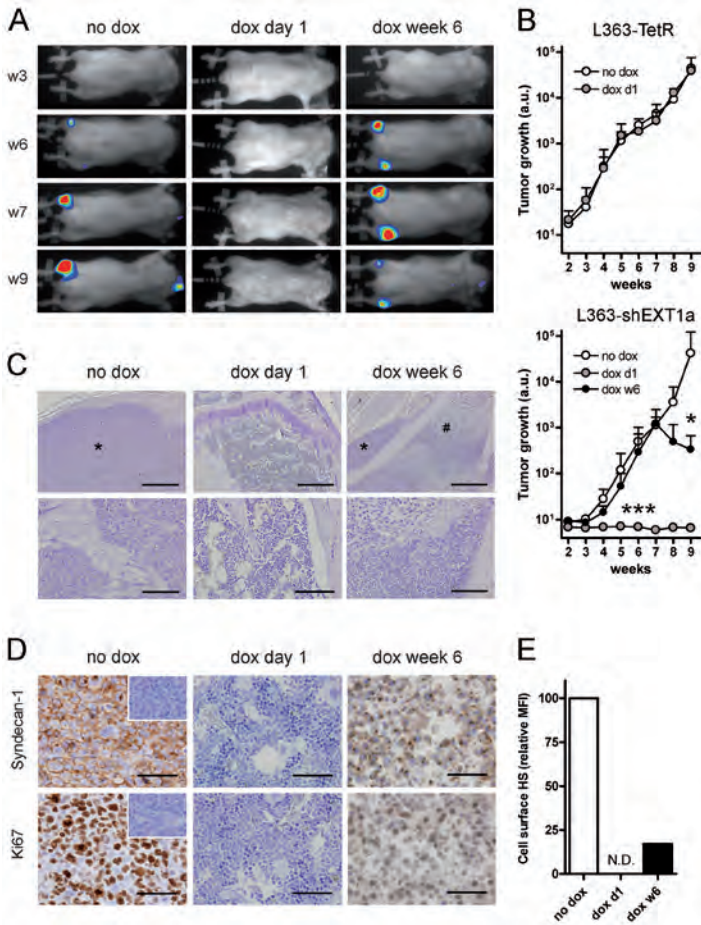


Figure 2. In vivo growth of MM requires EXT-1.

L363-TetR or L363-shEXT1a MM cells, transduced to express a GFP-Luciferase fusion protein, were injected intracardially into RAG2^{-/-}γc^{-/-} mice. Subsequently, the mice were divided into two (L363-TetR) or three (L363-shEXT1a) groups; the first group did not receive doxycycline (no dox), the second group was treated with doxycycline throughout the entire experiment (dox day 1), and the third group (L363-shEXT1a only) received doxycycline after 6 weeks (dox week 6). Bones were collected after 9 weeks, fixed in normal buffered formalin, decalcified, and embedded in paraffin. **(A)** Bioluminescence images of the ventral side of mice injected with L363-shEXT1a MM cells, taken at week 3 (w3), w6, w7 and w9. Representative mice are shown for each group. **(B)** Tumor growth in mice injected with L363-TetR or L363-shEXT1a MM cells, as determined by the average photon emission intensity (arbitrary units) measured for the total body, data shown as the mean ± SD (n=5 per group). A Mann-Whitney test (two-tailed) was applied to determine significance (*, p<0.05; **, p<0.01; ***, p<0.001) **(C)** Hematoxylin-stained femur sections of representative mice. Within the femurs of the no dox and dox week 6 mice, myeloma tumors (indicated with asterisks) were found. Bars are 500 μm and 100 μm for upper and lower panels respectively. #, necrotic MM cells; *, MM cells. **(D)** To visualize the tumors and their proliferation, anti-human syndecan-1 (clone MI-15, Dako, Glostrup, Denmark) and anti-human Ki67 (M7240, Dako) immunostainings were performed. The no dox and dox week 6 mice had tumors with ~87% and ~34% Ki67⁺ MM cells, respectively (data not shown). In the dox week 6 mice, areas of necrosis with weak and diffuse syndecan-1 and Ki67 staining were found. Representative areas are shown. Bars are 50 μm. Insets, isotype controls. **(E)** Cell surface HS expression of GFP⁺ L363-shEXT1a MM cells harvested from the bones of no dox and dox week 6 mice, as determined by FACS. The mean fluorescence intensity (MFI) of the untreated mice was normalized to 100%. N.D., not determined (no tumor).

displayed a rapid exponential tumor growth (Figure 2A and B and Supplemental Figure 3A), localized in various parts of the skeleton, preferentially in the large bones, including the femurs (Figure 2A), and the lower spinal cord (Supplemental Figure 2). Immunohistochemical analysis of the isolated bones confirmed the presence of highly proliferative tumor-foci (Figure 2C and D). In striking contrast, mice injected with L363-shEXT1a that received doxycycline from the first day remained completely tumor free throughout the entire experiment (Figure 2A-D). Interestingly, in mice in which these tumors were allowed to form prior to doxycycline treatment, doxycycline administration from week 6 onwards led to either growth arrest or even a reduction in tumor size. Histological studies revealed the presence of areas of extensive necrosis within these tumors, which were found to be devoid of HS expression (Figure 2E), confirming EXT1 knockdown in vivo. In line with these findings, knockdown of EXT1 in RPMI-8226 cells also markedly inhibited the in vivo MM tumor growth, resulting in a significantly extended survival (Supplemental Figure 3A and B). Importantly, doxycycline did not influence the tumor growth of L363-TetR or RPMI-TetR control cells in vivo (Figure 2B and Supplemental Figure 3A). In conclusion, although mutations in essential growth control genes underlies MM development, signals from the BM microenvironment are also essential for driving tumor growth.^{2,3} As targets for intervention, these signals may be equally important as are mutated oncogene products. Our current study demonstrates that the HS-chains decorating syndecan-1 are crucial for the growth and survival of MM cells within the bone marrow environment and indicates these HS-chains and their biosynthesis machinery⁵ as potential treatment targets in MM.

Acknowledgements

The authors would like to thank Gerard Geelen and Kiki Hesp for excellent animal care in the Central Animal Facility of the University of Utrecht, Berend Hooibrink for FACS-sorting, Dr. Guido David for kindly providing the 10E4 antibody, and Dr. Hans Clevers for the generous gift of the Tet repressor expression plasmid (pTetR). This work was supported by a grant from the Dutch Cancer Society to M.S. and S.T.P. and by a TOP grant from the Netherlands Organization for Health Research and Development (ZonMw/NWO) to M.S. and S.T.P. Conflict-of-interest disclosure: The authors declare no competing financial interests.

References

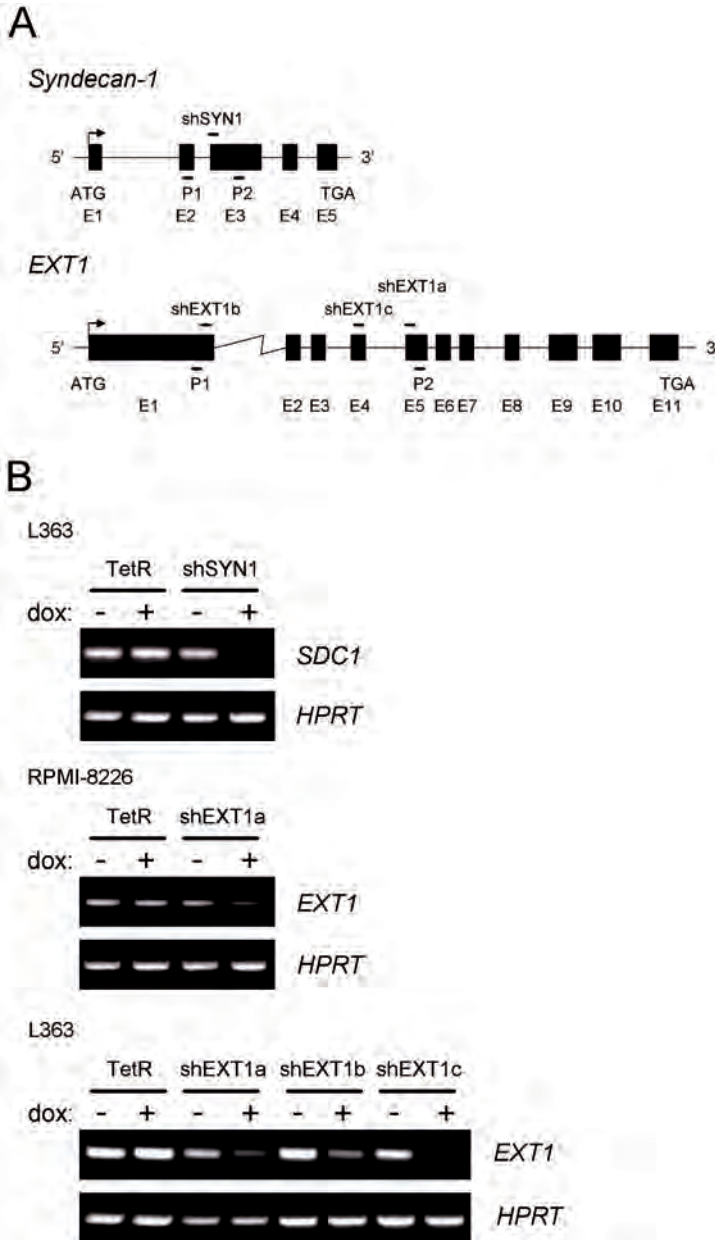
1. Wijdenes J, Vooijs WC, Clément C, et al. A plasmocyte selective monoclonal antibody (B-B4) recognizes syndecan-1. *Br J Haematol.* 1996;94(2):318-323.
2. Hideshima T, Mitsiades C, Tonon G, Richardson PG, Anderson KC. Understanding multiple myeloma pathogenesis in the bone marrow to identify new therapeutic targets. *Nat Rev Cancer.* 2007;7(8):585-598.
3. Kuehl WM, Bergsagel PL. Multiple myeloma: evolving genetic events and host interactions. *Nat Rev Cancer.* 2002;2(3):175-187.
4. Esko JD, Selleck SB. Order out of chaos: assembly of ligand binding sites of heparan sulfate. *Ann Rev Biochem.* 2002;71:435-471.
5. Lindahl U. Heparan sulfate-protein interactions—a concept for drug design? *Thromb Haemost.* 2007;98(1):109-115.
6. Kramer KL, Yost HJ. Heparan sulfate core proteins in cell-cell signaling. *Annu Rev Genet.* 2003;37:461-484.
7. Morgan MR, Humphries MJ, Bass MD. Synergistic control of cell adhesion by integrins and syndecans. *Nat Rev Mol Cell Biol.* 2007;8(12):957-969.
8. Yoneda A, Couchman JR. Regulation of cytoskeletal organization by syndecan transmembrane proteoglycans. *Matrix Biol.* 2003;22(1):25-33.
9. Bishop JR, Schuksz M, Esko JD. Heparan sulphate proteoglycans fine-tune mammalian physiology. *Nature.* 2007;446(7139):1030-1037.
10. Børset M, Hjertner O, Yaccoby S, Epstein J, Sanderson RD. Syndecan-1 is targeted to the uropods of polarized myeloma cells where it promotes adhesion and sequesters heparin-binding proteins. *Blood.* 2000;96(7):2528-2536.
11. Derksen PW, Keehnen RM, Evers LM, van Oers MH, Spaargaren M, Pals ST. Cell surface proteoglycan syndecan-1 mediates hepatocyte growth factor binding and promotes Met signaling in multiple myeloma. *Blood.* 2002;99(4):1405-1410.
12. Mahtouk K, Cremer FW, Rème T, et al. Heparan sulphate proteoglycans are essential for the myeloma cell growth activity of EGF-family ligands in multiple myeloma. *Oncogene.* 2006;25(54):7180-7191.
13. Yang Y, MacLeod V, Dai Y, et al. The syndecan-1 heparan sulfate proteoglycan is a viable target for myeloma therapy. *Blood.* 2007;110(6):2041-2048.
14. Derksen PW, de Gorter DJ, Meijer HP, et al. The hepatocyte growth factor/Met pathway controls proliferation and apoptosis in multiple myeloma. *Leukemia.* 2003;17(4):764-774.
15. Derksen PW, Tjin E, Meijer HP, et al. Illegitimate WNT signaling promotes proliferation of multiple myeloma cells. *Proc Natl Acad Sci U S A.* 2004;101(16):6122-6127.
16. Tjin EP, Derksen PW, Kataoka H, Spaargaren M, Pals ST. Multiple myeloma cells catalyze hepatocyte growth factor (HGF) activation by secreting the serine protease HGF-activator. *Blood.* 2004;104(7):2172-2175.
17. Alexander CM, Reichsman F, Hinkes MT, et al. Syndecan-1 is required for Wnt-1-induced mammary tumorigenesis in mice. *Nat Genet.* 2000;25(3):329-332.
18. Beauvais DM, Burbach BJ, Rapraeger AC. The syndecan-1 ectodomain regulates alphavbeta3 integrin activity in human mammary carcinoma cells. *J Cell Biol.* 2004;167(1):171-181.
19. Sasisekharan R, Shriver Z, Venkataraman G, Narayanasami U. Roles of heparan-sulphate glycosaminoglycans in cancer. *Nat Rev Cancer.* 2002;2(7):521-528.
20. Lind T, Tufaro F, McCormick C, Lindahl U, Lidholt K. The putative tumor suppressors EXT1 and EXT2 are glycosyltransferases required for the biosynthesis of heparan sulfate. *J Biol Chem.* 1998;273(41):26265-26268.
21. McCormick C, Leduc Y, Martindale D, et al. The putative tumour suppressor EXT1 alters the expression of cell-surface heparan sulfate. *Nat Genet.* 1998;19(2):158-161.
22. Rozemuller H, van der Spek E, Bogers-Boer LH, et al. A bioluminescence imaging based in vivo model for preclinical testing of novel cellular immunotherapy strategies to improve the graft-versus-myeloma effect. *Haematologica.* 2008;93(7):1049-1057.

23. Legrand N, Weijer K, Spits H. Experimental model for the study of the human immune system: production and monitoring of "human immune system" Rag2^{-/-}gamma c^{-/-} mice. *Methods Mol Biol.* 2008;415:65-82.
24. van Rijn RS, Simonetti ER, Hagenbeek A, et al. A new xenograft model for graft-versus-host disease by intravenous transfer of human peripheral blood mononuclear cells in RAG2^{-/-} gammac^{-/-} double-mutant mice. *Blood.* 2003;102(7):2522-2531.
25. Traggiai E, Chicha L, Mazzucchelli L, et al. Development of a human adaptive immune system in cord blood cell-transplanted mice. *Science.* 2004;304(5667):104-107.

Supplementary Data

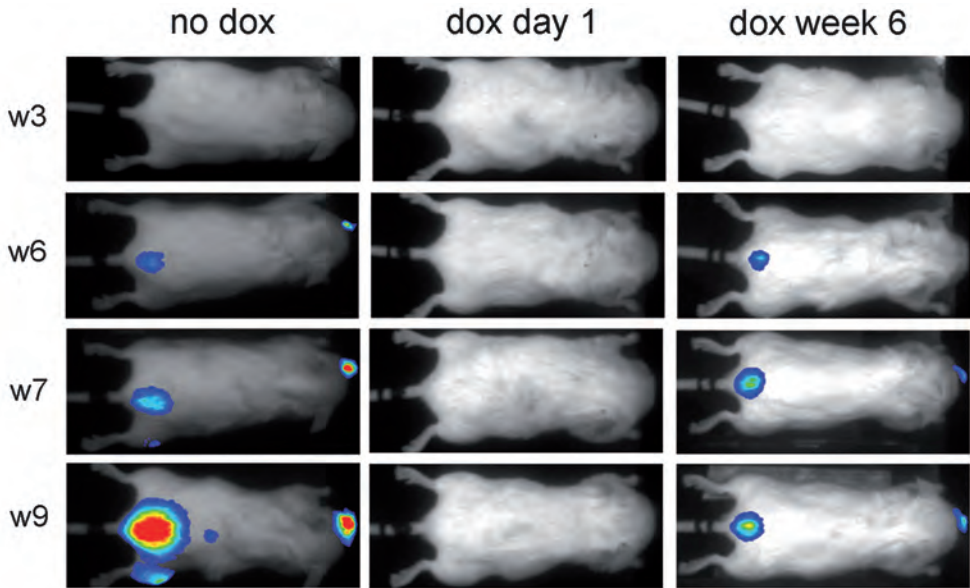
Generation of inducible cell lines. Doxycycline-inducible cell lines were generated using theT-REx™ System (Invitrogen Life technologies). L363 and RPMI-8226 were transfected by electroporation (Gene Pulser Apparatus, BioRad, USA) with the pTER construct alone (L363-TetR and RPMI-TetR), or in combination with a construct containing an shRNA directed against syndecan-1 or EXT1. For targeting of syndecan-1 we designed one shRNA (shSYN1) and for EXT1 three different shRNAs (shEXT1a, shEXT1b, and shEXT1c) with non-overlapping target sequences. For a schematic overview see supplemental Figure 1A. shSYN1: 5'-GGTGCTTTGCAAGATATCA-3'; shEXT1a: 5'-GCACATATCACGTAACAGT-3'; shEXT1b: 5'-GACAACACCGAGTATGAGA-3'; shEXT1c: 5'-CCTAGCACTTAGACAGCAGAC-3'. To induce shRNA expression, 1 µg/ml doxycycline (Sigma-Aldrich, St Louis, MO) was used.

RT-PCR. For mRNA, transcripts were quantified by semi-quantitative reverse transcriptase polymerase chain reaction (RT-PCR) and compared to the amount of hypoxanthine-guanine phosphoribosyltransferase (HPRT) mRNA expressed (see supplemental Figure 1B). The PCR products were separated on a 1% agarose gel by electrophoresis and bands were visualized by ethidium bromide staining. PCR product sizes were 310 bp for syndecan-1, 435 bp for EXT1 and 752 bp for HPRT. Forward and reverse primers used were: Syndecan-1, 5'-GCTCTGGGGATGACTCTGAC-3' and 5'-ACCACTCATCTGGCCTCAAC-3'; EXT1, 5'-CACAAGGATTCTCGCTGTGA-3' and 3'-GGAACAAACATCCTGGAGGA-3'; HPRT, 5'-TTCCTCCTCTGAGCAGTCAGC-3' and 5'-CATCTGGAGTCCTATTGACATCGC-3'.



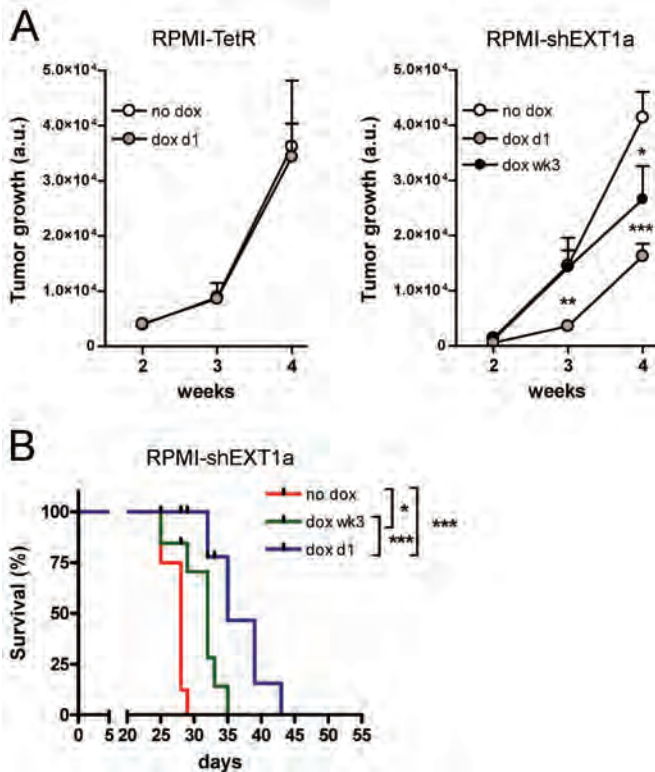
Supplementary Figure 1. shRNA-mediated targeting of Syndecan-1 and EXT1.

(A) Schematic overview of the Syndecan-1 (*SDC1*) and *EXT1* genes. The shRNA target sites (shSYN1, shEXT1a, b, c) and the locations of the primers used for the RT-PCR are depicted. P1, primer 1; P2, primer 2; E, exon; ATG, translation start; TGA, translation stop. shEXT1a was used for both L363 and RPMI-8226 myeloma cells. (B) *SDC1* and *EXT1* mRNA expression in L363 and RPMI-8226 cell lines containing the different inducible shRNAs depicted in A. The cells were treated for 5 days without (-) or with (+) doxycycline to obtain optimal knockdown of *SDC1* (shSYN1) or *EXT1* (shEXT1a, -b, -c). The *HPRT* gene was used as an mRNA input control. dox, doxycycline.



Supplementary Figure 2. In vivo growth of MM requires EXT-1 expression (dorsal images).

L363-shEXT1a MM cells, transduced to express a GFP-Luciferase fusion protein, were injected intracardially into $RAG2^{-/}\gamma c^{-/}$ mice ($n=15$). Subsequently, the mice were divided into three groups of five mice; the first group did not receive doxycycline (no dox), the second group was treated with doxycycline throughout the entire experiment (dox day 1), and in the third group the mice received doxycycline after 6 weeks (dox week 6), all until the end of the experiment. Bioluminescence images of the dorsal side of mice injected with L363-shEXT1a MM cells, taken at week 3 (w3), w6, w7 and w9. Representative mice are shown for each group ($n=5$).



Supplementary Figure 3. EXT1 knockdown inhibits the in vivo growth of RPMI-8226 MM cells and extends survival.

(A,B) RPMI-TetR or RPMI-shEXT1a MM cells, transduced to express a GFP-Luciferase fusion protein, were injected intracardially into RAG2^{-/-}γc^{-/-} mice (n=10 and n=24 respectively). Subsequently, the mice were divided into two (n=5 for RPMI-TetR) or three groups (n=8 for RPMI-shEXT1a); the first group did not receive doxycycline (no dox), the second group was treated with doxycycline throughout the entire experiment (dox day 1), and in the third group (RPMI-shEXT1a only) the mice received doxycycline after 3 weeks (dox w3), all until the end of the experiment. **(A)** Tumor growth was monitored by measuring bioluminescence photon emission; data shown represent means ± SD of photon emission intensity (arbitrary units) measured for the total body (dorsal and ventral sides). **(B)** Kaplan-Meier survival plot showing the survival of the mice injected with RPMI-shEXT1a MM cells treated either with doxycycline (dox d1 or dox w3) or untreated. Significance was determined by a Logrank test; *, p<0.05; **, p<0.01; ***, p<0.001.

6

7

N-cadherin-mediated adhesion of multiple myeloma cells inhibits osteoblast differentiation

Richard W.J. Groen¹, Kinga A. Kocemba¹, Martin F.M. de Rooij¹, Rogier M. Reijmers¹, Anneke de Haan-Kramer¹, Marije B. Overdijk¹, Henk Rozemuller², Anton C.M. Martens², P. Leif Bergsagel³, Marie José Kersten⁴, Steven T. Pals^{1,5}, and Marcel Spaargaren^{1,5}.

¹Department of Pathology, Academic Medical Center, University of Amsterdam, Amsterdam, The Netherlands, ²Department of Immunology, University Medical Center Utrecht, Utrecht, The Netherlands, ³Comprehensive Cancer Center, Mayo Clinic Arizona, Scottsdale, Arizona 85259, USA, ⁴Department of Hematology, Academic Medical Center, University of Amsterdam, Amsterdam, The Netherlands. ⁵These authors share last authorship.

Submitted

Abstract

Multiple myeloma (MM) is a hematologic malignancy characterized by a clonal expansion of malignant plasma cells in the bone marrow (BM), which is accompanied by the development of osteolytic lesions and/or diffuse osteopenia. The intricate bi-directional interaction with the BM microenvironment plays a critical role in sustaining the growth and survival of MM cells during tumor progression. Here we show that the malignant plasma cells in approximately half of the MM patients, belonging to specific genetic subgroups, aberrantly express the homophilic adhesion molecule N-cadherin. N-cadherin-mediated cell-substrate or homotypic cell-cell adhesion does not contribute to MM cell growth in vitro. However, N-cadherin directly mediates the BM localization/retention of MM cells in vivo, and facilitates a close interaction between MM cells and N-cadherin positive osteoblasts. This N-cadherin-mediated interaction directly contributes to the inhibition of osteoblastogenesis. Taken together, our data show that N-cadherin plays an important role in the interaction of MM cells with the BM microenvironment, in particular the osteoblasts, and may play a crucial role in the pathogenesis of myeloma bone disease.

Introduction

Multiple Myeloma (MM) is a neoplasm, characterized by clonal expansion of malignant plasma cells. The transition of a normal plasma cell to a fully transformed, aggressive myeloma is considered to be a multistep process, which requires the acquisition of chromosomal translocations and mutations in multiple genes^{1,2}. Most of this evolution takes place in the bone marrow (BM), indicating that the interaction with the BM microenvironment plays a critical role in the pathogenesis of MM. As in normal plasma cell homing, a major player in the recruitment to and retention of MM plasma cells in the BM is the CXCL12/CXCR4 axis^{3,4}. The chemokine CXCL12 promotes transendothelial migration and induces $\alpha 4\beta 1$ -mediated adhesion to VCAM-1 and fibronectin⁵. Malignant plasma cells express several cell-surface molecules which mediate either homotypic cell adhesion, like N-CAM, or adhesion with the extracellular matrix or other cells in the BM microenvironment, like the integrins $\alpha 4\beta 1$ and $\alpha 5\beta 1$ and mucin1^{1,6}. These interactions control long-term survival and proliferation⁷, and may also render the MM cells resistant to the pro-apoptotic effects of conventional chemotherapies⁶, a process known as cell adhesion mediated drug resistance (CAM-DR). In addition, these interactions may also affect the BM microenvironment. Under physiologic conditions bone remodeling is a continuous process in which osteoclasts mediate resorption of “old” bone tissue, followed by new bone formation by the osteoblasts. These two processes are tightly regulated by signals involving the RANKL-RANK axis, the Wnt signaling pathway, and N-cadherin engagement⁸⁻¹⁰, of which the latter interaction serves an important role in osteoblast function and differentiation. One of the characteristic features of MM is osteolytic bone destruction, resulting from the activation of osteoclasts and inhibition of osteoblast function. Notably, the action of several factors produced by MM cells and involved in the deregulation of osteoblast differentiation, like DKK1¹¹, sFRP-2¹², and HGF¹³, was shown to be partially dependent on adhesion of myeloma cells to the osteoblasts via integrin $\alpha 4\beta 1$ ¹⁴. We have previously shown that malignant plasma cells of MM patients overexpress β -catenin, including the non-phosphorylated form, leading to active β -catenin/TCF-mediated transcription and MM cell proliferation¹⁵. Subsequent studies have confirmed the presence of Wnt pathway activation in MM and its importance for MM cell proliferation and survival¹⁶⁻¹⁸. Interestingly, our immunohistochemical studies revealed that β -catenin is localized in the nucleus as well as at the plasma membrane, at the site of cell-cell contact. Indeed, in addition to its role as a transcriptional regulator in the Wnt signaling pathway, β -catenin is also a key regulator of the cadherin-mediated adhesion¹⁹. Cadherins comprise a family of transmembrane adhesion molecules that mediate calcium-dependent cell-cell adhesion through homophilic interaction. In the “classical” cadherins, the conserved cytoplasmic domain forms a complex with the catenins p120catenin, β -catenin and α -catenin, which are possible regulators of cadherin function and link it to the cytoskeleton²⁰. In this study, we show that malignant plasma cells of a subset of MM patients express N-cadherin, which mediates homophilic adhesion. In addition, we demonstrate that N-cadherin is involved in the bone marrow localization of these malignant cells and that it contributes to the inhibition of osteoblast differentiation, thereby establishing a role for N-cadherin in myeloma bone disease.

Material and Methods

Antibodies

Monoclonal antibodies (mAb) were: anti-N-cadherin, clone 32 (IgG1); anti- β -catenin, clone 14 (IgG1) (all BD Biosciences, Erembodegem, Belgium); anti- β -actin, clone AC-15 (IgG1); anti-N-cadherin, clone GC-4 (IgG1) (both Sigma-Aldrich, St Louis, MO); anti-E-cadherin, clone HECD-1 (IgG1) (Takara Bio, Shiga, Japan); anti-CD138, clone B-B4 (IgG1) (IQ Products, Groningen, The Netherlands); IgG1 control antibody (DAKO, Carpinteria, CA). Polyclonal antibodies (pAb) used were: rabbit anti-human β -catenin, H-102 (Santa Cruz Biotechnology, Santa Cruz, CA); horseradish peroxidase (HRP)-conjugated rabbit anti-mouse; R-phycoerythrin (RPE)-conjugated streptavidin (both DAKO); biotinylated goat anti-mouse IgG1 (Southern Biotechnology, Birmingham, AL); Alexa488-conjugated goat anti-mouse and Alexa568-conjugated goat anti-rabbit (both Invitrogen Life technologies, Breda, The Netherlands).

Cell culture and osteoblast differentiation

MM cell lines, UM-1, UM-3, L363, OPM-1, NCI-H929, XG-1 and LME-1 were cultured as described previously¹⁵. C3H10T1/2 cells were grown in Dulbecco's Modified Eagle's Medium (DMEM; Invitrogen Life technologies) and KS483 cells were grown in Minimum Essential Medium (MEM) Alpha (Invitrogen Life technologies), both supplemented with 10% fetal calf serum (FCS), penicillin (50U/ml) and streptomycin (50 μ g/ml) (both from Invitrogen Life Technologies).

KS483 cells were seeded as 12000 cells/cm² and cultured until confluence. From confluence ascorbic acid (50 μ g/ml) was added to the medium, and medium was changed every three days. Co-cultures were initiated from the day of confluence, day 4, by addition of MM cells (25 x 10³ for alkaline phosphatase expression; 5 x 10⁵ for RNA samples) and maintained for a week, in the presence or absence of doxycycline (0.2 μ g/ml; Sigma-Aldrich). Subsequently, cultures were stained for alkaline phosphatase expression as described by van der Horst et al.²¹, or cells were lysed in Tri Reagent (Sigma-Aldrich).

A doxycycline-inducible cell line was generated as described previously²², using the T-REx™ System (H929 TR) (Invitrogen Life technologies) and a shRNA against CDH2, 5'-GAGCCTGAAGCCAACCTTA-3' (H929 shCDH2). N-cadherin knock down was obtained by incubating NCI-H929 shCDH2 cells for 5 days with 0.2 μ g/ml doxycycline.

Cell growth assessment

Cells were plated (5x10³) in a 96-wells plate coated with recombinant N-cadherin/Fc chimera (1 μ g/ml; R&D Systems, Abingdon, UK), or BSA as control. When assessing the growth of the doxycycline-inducible cell line, knock down was obtained by incubating NCI-H929 shCDH2 cells for 5 days with 0.2 μ g/ml doxycycline prior to the assay, and maintained by addition of 0.2 μ g/ml doxycycline to the culture medium.

Immunofluorescent microscopy

N-cadherin (clone 32) and β -catenin (pAb H-102) expression in MM cell lines was analyzed on PFA-fixed cytopins. Expression was detected, using Alexa488-conjugated goat anti-

mouse and Alexa568-conjugated goat anti-rabbit as secondary antibodies, and analyzed by confocal laser scan microscopy (CLSM).

Immunoprecipitation and western blot analysis

Immunoprecipitation and western blot analysis was performed as described previously²³. The immunoblots were stained with anti-N-cadherin (clone 32), anti-E-cadherin (HECD-1), or anti- β -catenin (clone 14). Equal loading was confirmed with anti- β -actin. Primary antibodies were detected by HRP-conjugated rabbit anti-mouse, followed by detection using LumiLightPLUS western blotting substrate (Roche, Basel, Switzerland).

Flow cytometry

N-cadherin expression was determined by incubation of cells with an anti-N-cadherin monoclonal antibody (clone GC-4, Sigma-Aldrich) followed by biotinylated goat anti-mouse IgG1 (Southern Biotechnology, Birmingham, AL) and subsequently RPE-conjugated streptavidin (DAKO). Analysis was carried out on a FACScalibur flow cytometer (BD Biosciences) with CellQuest™ software (BD Biosciences).

Sample preparation and microarray hybridization and analysis

Isolation of plasma cells (PCs) and profiling of RNA was performed as described²⁴. Gene expression was measured by U133 Plus2.0 Affymetrix oligonucleotide microarray probeset 203440_at of 559 newly diagnosed MM patients, summarized with MAS5, median normalized and plotted against genomic aberrations. In addition, publicly available U133 Plus2.0 Affymetrix oligonucleotide microarray data, provided by the Donna D. and Donald M. Lambert Laboratory of Myeloma Genetics, were used to analyze the expression of N-cadherin on the plasma cells of 345 MM patients from the total therapy 2 (TT2) patient set. MAS5 summarized data have been deposited in the NIH Gene Expression Omnibus (GEO; National Center for Biotechnology Information [NCBI], <http://www.ncbi.nlm.nih.gov/geo/under> accession number GSE2658).

Immunohistochemistry

Immunohistochemical staining was performed on formalin-fixed, plastic-embedded tissue sections. Endogenous peroxidase activity was blocked with 0.3 % H₂O₂ in methanol. For antigen retrieval sections were boiled for 10 minutes in a Tris/EDTA buffer (respectively 10 mM/1 mM) pH9, after which they were blocked with 10% normal goat serum. Followed by an incubation of either one hour at room temperature with CD138 or overnight at 4°C with N-cadherin (clone 32) or β -catenin (clone 14). Binding of the antibody was visualized using the PowerVision plus detection system (Immunovision Technologies, Duiven, The Netherlands) and 3,3-diaminobenzidine (Sigma). The sections were counterstained with hematoxylin (Merck, Darmstadt, Germany), washed and coverslipped.

Cell adhesion assays

Adhesion assays on recombinant N-cadherin/Fc chimera (1 μ g/ml; R&D Systems) were done as described²³. The monoclonal antibody GC-4 (10 μ g/ml) was used to block N-cadherin-mediated adhesion. Results are presented as percentage of maximum adhesion, as

measured by adhesion to poly-L-lysine coated surface, and the bars represent the means \pm SD of a triplicate experiment of at least three independent experiments.

C3H10T1/2 were seeded at a density of 7500 cells/200 μ l, in a 96-wells flat bottom tissue culture plates (Costar, Cambridge, MA). 24 Hours after plating an adhesion assay with MM cells (10^5 cells/100 μ l) was performed either in culture medium as a control, or in Hanks' balanced salts solution (HBSS) in the presence or absence of 2mM calcium chloride, and in the presence of an N-cadherin blocking antibody (10 μ g/ml), or an isotype antibody as a control. Images were captured using an EVOS original camera (AMG, Mill Creek, WA) and processed with Adobe Photoshop.

Migration assays

Migration assays were performed in triplicate as described previously²³, with transwells (Costar) coated with 1 μ g/ml recombinant N-cadherin/Fc chimera (R&D Systems), sVCAM-1 (R&D Systems), or BSA (fraction V; Sigma-Aldrich) coating as a control.

Transendothelial migration was performed by growing a confluent layer of HUVEC cells on a fibronectin coated transwell insert. Subsequently, H929 shCDH2 cells (5×10^5), either induced with or without doxycycline, were added and allowed to migrate for 5 hours towards 100 ng/ml SDF-1, in the presence or absence of blocking antibodies against N-cadherin (GC-4), or alpha4-integrin (HP2/1).

The amount of viable migrating cells was determined by fluorescence-activated cell sorting (FACS) and expressed as percentages of the input. The percentage of non-pretreated cells was normalized to 100%.

Homing assay

H929 shCDH2 cells were incubated for 5 days with (KD) or without (WT) 0.2 μ g/ml doxycycline. Cells were labeled with either 0.25 μ M Cell tracker Green (CMFDA; Invitrogen) or 2 μ M Cell tracker Orange (CMTMR; Invitrogen), mixed (1:1), and a total of 15×10^6 cells was injected intravenously in RAG2^{-/-} γ c^{-/-} mice. Each WT/KD combination was analyzed by adoptive transfer of 8 recipient mice, which included a dye-swap. After 24 hr, blood and bone marrow were collected and FACS analyzed to quantify dye-labeled cells. The percentage of homing cells was corrected for the input ratio.

Real-time reverse transcription-PCR

RNA isolation and cDNA synthesis were performed as described previously¹⁵. The quantitative reverse transcription-PCR (qRT-PCR) runs were performed on a Roche LightCycler 1.5 using FastStart DNA Master SYBR Green I kit (Roche, Basel, Switzerland). Results were analyzed using LinReg PCR analysis software (version 7.5;²⁵). Expression was normalized over β 2-microglobulin expression.

Mouse specific primers were designed recognizing alkaline phosphatase, AKP2, forward 5'-GGATAACGAGATGCCACC-3' and reverse 5'-CATCCAGTTCGTATTCCAC-3', and osteocalcin, BGLAP, forward 5'-CAATAAGGTAGTGAACAGACTCC-3', and reverse 5'-CTGGTCTGATAGCTCGTAC-3', and β 2M, forward 5'-CTGGTGCTTGCTCACTGACC-3', and reverse 5'-GGTGGAAGTGTACGTAGC-3'. All primers were manufactured by Sigma-Aldrich (Haverhill, UK).

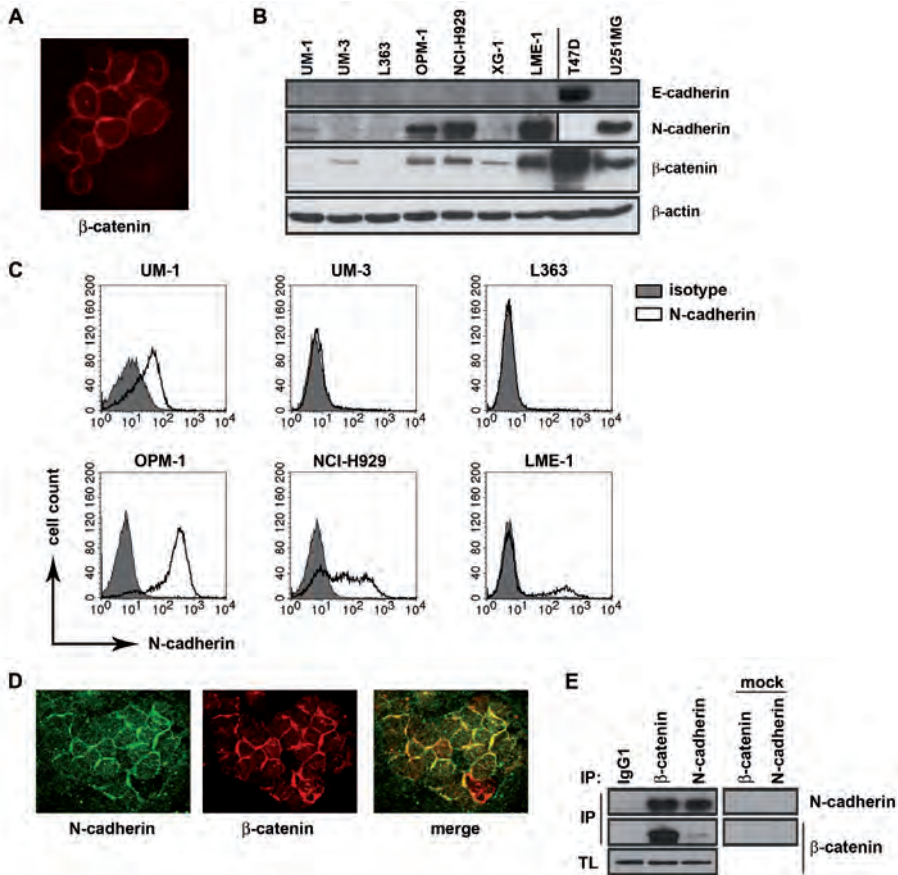


Figure 1. Multiple myeloma cells express N-cadherin.

(A) β -catenin is expressed in MM cells at the cell-cell junctions. The MM cell line OPM-1 is stained with a pAb H-102 against β -catenin and detected with Alexa568-conjugated goat anti-rabbit by confocal laser scan microscopy (CLSM). **(B)** Cadherin expression in MM cell lines. Cell lysates were immunoblotted using mAbs against E-cadherin (HECD-1), N-cadherin (clone 32) and β -catenin (clone 14). The breast carcinoma cell line T47D and the malignant glioma cell line U251 MG were used as positive controls for E-cadherin and N-cadherin, respectively. β -actin was used as loading control. **(C)** Fluorescence-activated cell sorting analysis (FACS) for N-cadherin protein expression in MM cell lines. Cells were stained with anti-N-cadherin mAb GC-4 (open histogram) or isotype control (filled histogram). **(D)** N-cadherin co-localizes with β -catenin at the cell-cell contacts. OPM-1 cells were double-stained with an antibody against N-cadherin (clone 32) and β -catenin (H-102), followed by secondary antibodies Alexa488-conjugated goat anti-mouse and Alexa568-conjugated goat anti-rabbit. Expression of N-cadherin (green; left panel) and β -catenin (red; middle panel) and co-localization (orange; right panel) was detected by CLSM. **(E)** Co-immunoprecipitation of N-cadherin with β -catenin. Cell lysates of the MM cell line OPM-1 were immunoprecipitated (IP) with mAb clone 32 (N-cadherin), clone 14 (β -catenin), or control IgG1 antibody, pre-coupled to Protein G-Sepharose beads. Immunoblots were stained with anti-N-cadherin (clone 32) and anti- β -catenin (clone 14). As a specificity control mock incubation, without lysates, were immunoblotted and stained. Total lysates (TL) were immunoblotted and stained with anti- β -catenin (clone 14), as an input control.

Results

MM cells express a functional β -catenin/N-cadherin complex at the plasma membrane.

Previously, we have reported that MM plasma cells overexpress β -catenin. Stimulation of Wnt signaling with either the glycogen synthase kinase-3 β (GSK3 β) inhibitor LiCl or Wnt3a led to a further accumulation and nuclear localization of β -catenin, resulting in enhanced TCF-mediated transcription and increased cell proliferation¹⁵. Interestingly, however, β -catenin was not only localized in the nucleus of the MM cells, but was also frequently observed at the plasma membrane, at the cell-cell contact sites between adjacent MM cells (Figure 1A). This observation suggested that β -catenin could also be involved in intercellular adhesion, presumably through interaction with a classical cadherin¹⁹. To explore this hypothesis, we screened a panel of MM cell lines for the expression of cadherins. Western blot analysis revealed that, while none of the myeloma cell lines tested expressed E-cadherin, 4 of 7 were N-cadherin positive (Figure 1B). This expression was confirmed by FACS analysis (Figure 1C). Furthermore, confocal laser scan microscopy revealed co-localization of N-cadherin and β -catenin at the cell-cell junctions between adjacent MM cells, suggesting a physical interaction between the two proteins (Figure 1D). Indeed, co-precipitation of N-cadherin and β -catenin confirmed the existence of an association between these molecules at the MM plasma membrane, with all N-cadherin attached to β -catenin (Figure 1E).

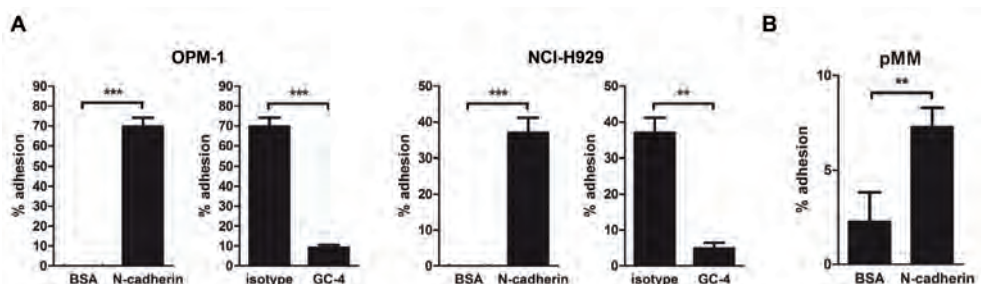


Figure 2. N-cadherin-mediated adhesion of multiple myeloma cells.

(A) Adhesion of MM cells to recombinant N-cadherin. OPM-1 (left panel) and NCI-H929 (right panel) cells adhere to a surface coated with recombinant N-cadherin (1 mg/ml), compared to BSA-coating as a negative control. This adhesion could be blocked by using an N-cadherin blocking antibody, GC-4 (10 μ g/ml). The results are expressed as a percentage of maximal adhesion. The bars represent the means \pm the standard deviation of a triplicate experiment, representative of at least three independent experiments. ** $P < 0.01$; *** $P < 0.001$ by student's t-test. **(B)** Adhesion of primary patient material to recombinant N-cadherin. Primary myeloma cells (pMM) were allowed to adhere to a surface coated with recombinant N-cadherin (1 mg/ml), compared to BSA-coating as a negative control. The results are expressed as a percentage of maximal adhesion. The bars represent the means \pm the standard deviation of a triplicate experiment. ** $P < 0.01$ by student's t-test.

Classical cadherins, including N-cadherin, mediate cell-cell adhesion via homophilic interaction. To assess the functional integrity of the N-cadherin/ β -catenin complexes on the MM cells we tested the ability of N-cadherin expressing MM cells to adhere to an N-cadherin-coated surface. As shown in Figure 2A, the N-cadherin positive MM cell lines OPM-1 and NCI-H929 specifically adhered to recombinant N-cadherin, which could be blocked completely by the N-cadherin blocking antibody (GC-4). Primary MM cells,

expressing N-cadherin, also showed specific adhesion to coated N-cadherin (Figure 2B), whereas primary MM cells without N-cadherin did not adhere (data not shown).

Expression of N-cadherin in primary MMs

To assess the prevalence of N-cadherin expression in primary MMs, we analyzed N-cadherin expression in purified plasma cells from a panel of 559 MM patients by Affymetrix oligonucleotide microarrays in relation to characteristic recurrent chromosomal translocations and expression of cyclin D1 and D2 (TC groups)²⁴. As depicted, CDH2, the gene encoding N-cadherin, is highly expressed (>2x) in 83% of the MM samples bearing translocation t(4;14)(p16;q32) involving MMSSET. Furthermore, the subgroups characterized by high expression of cyclin D1, either alone (D1) or together with high expression of cyclin D2 (D1+D2), consist of two distinct populations: one with high and one with low expression of CDH2. Expression of CDH2 was less prevalent in samples with the translocations involving 11q13, 6p21, or MAF, and in the subgroup characterized by low cyclin D1 but high cyclin D2 expression (D2) (Figure 3A left panel). Although the 4p16 translocation is known to correlate with poor prognosis, no independent prognostic value could be found for N-cadherin expression (data not shown). Importantly, analysis of the freely accessible microarray data of the Lambert Laboratory revealed that expression of N-cadherin is absent/low in normal bone marrow plasma cells (BMPC) of healthy donors, whereas expression is already elevated in MGUS (Figure 3A right panel). In agreement with our data, analysis of CDH2 expression in this data set, in which the major myeloma subtypes are defined by GEP-derived classification²⁶, revealed high expression of CDH2 in over 90% of the MMSSET expression subgroup (MS) characterized by the 4p16 MMSSET translocation, and low expression in the MAF expression subgroup (MF) characterized by MAF/MAFB translocations. Furthermore, the hyperdiploid subgroup (HY) reveals distinct populations with either high or low CDH2 expression, which is in line with the high concordance of the HY subgroup with our D1 subgroup²⁷. Consistent with the mRNA expression data, immunohistochemical study of bone marrow biopsies of MM patients (n=43) demonstrated N-cadherin protein expression in the malignant cells of approximately 50% of the patients (Figure 3B). Besides membrane expression, several of these tumors displayed a strong cytoplasmic N-cadherin staining. As in the MM cell lines (Figure 1D), N-cadherin and β -catenin in the primary MMs often localized at the cell-cell junctions between adjacent MM cells (Figure 3B), and between MM cells and the bone-lining cells (Figure 3C). Our observations identify N-cadherin as a myeloma associated protein displaying deregulated expression in a subset of MMs.

N-cadherin does not affect MM growth

Since N-cadherin expression has been described to both promote survival²⁰ and suppress cell proliferation in other cell types²⁸, we examined the role of both heterotypic as well as homotypic N-cadherin-mediated adhesion in MM growth. The direct effect of heterotypic adhesion was mimicked by seeding MM cell lines, with different levels of N-cadherin expression (Figure 1B), on recombinant N-cadherin and monitoring the growth for four days. Although the cells of the N-cadherin expressing cell lines essentially grew as single cells on the N-cadherin coating as compared to the formation of cell aggregates on the BSA coating (Figure 4A), no differences in growth rate were observed (Figure 4B). Similarly, no difference in cell proliferation was observed as determined by ³H-thymidine incorporation (data not shown). In addition, the survival of MM cells in a single cell growth assay was not altered by culturing on a recombinant N-cadherin coated surface either (data not shown).

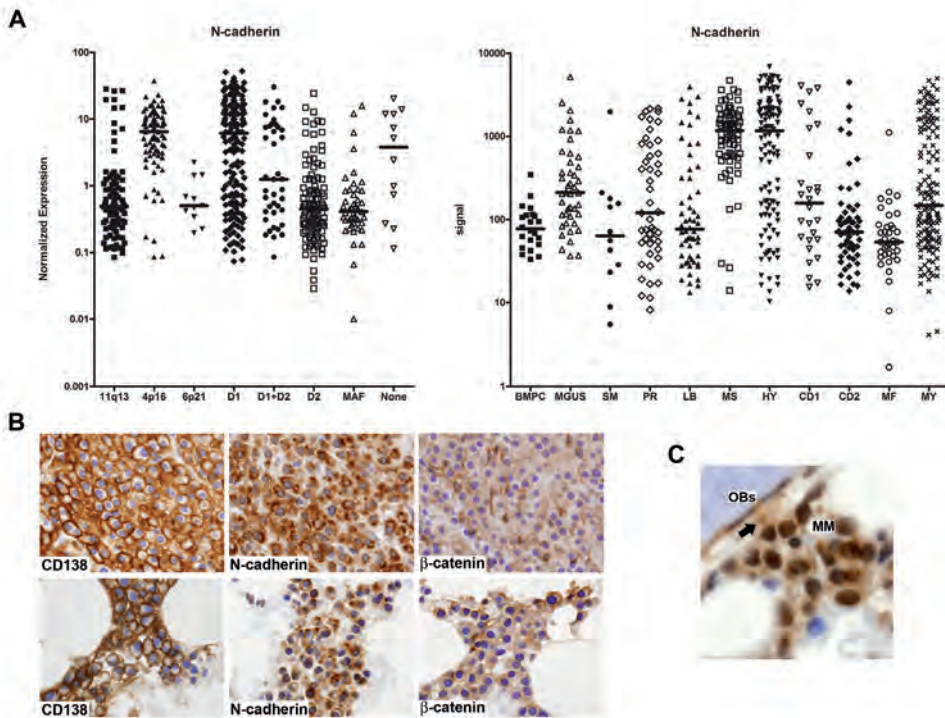


Figure 3. Expression of N-cadherin in primary MMs.

(A) Affymetrix expression profiles of N-cadherin in multiple myeloma. Gene expression of 559 newly diagnosed MM patients was measured by U133 Plus2.0 Affymetrix oligonucleotide microarray probeset 203440_at, summarized with MASS, median normalized and plotted against genomic aberrations (left panel); and public available genetic MM data of 345 MM patients from the total therapy 2 (TT2) patient set were plotted against disease progression and genetic profiles (right panel). N-cadherin was statistically higher expressed by plasma cells of patients in the MMSET expression (MS) and the hyperdiploid (HY) subgroups compared to normal bone marrow plasma cells (BMPC) of healthy donors ($P < 0.001$ by Kruskal-Wallis test). **(B)** Expression of N-cadherin in primary MM. Immunohistochemical staining of plastic-embedded sections of MM patients with antibodies against CD138 (B-B4; left panel), N-cadherin (clone 32; middle panels), and β -catenin (clone 14; right panel). Original magnifications $\times 64$. **(C)** N-cadherin expression on MM cells (MM) adjacent to N-cadherin positive bone lining osteoblasts (OBs). N-cadherin is often localized between MM cells and the bone-lining cells (arrow). Immunohistochemical staining of a plastic-embedded section of an MM patient with antibody against N-cadherin (clone 32). Original magnifications $\times 100$.

To examine the contribution of the homotypic adhesion to the growth of MM cells, we cultured MM cells in the presence of an N-cadherin blocking antibody. However, addition of antibodies to the culture did not result in altered proliferation (data not shown). To determine the direct effect of N-cadherin expression on MM growth, we generated NCI-H929 cells stably transfected with a doxycycline-inducible shRNA against CDH2 (H929 shCDH2). As shown in figure 4C, doxycycline treatment of the cells for five days results in a 70% reduction of N-cadherin expression. Assessment of the growth of the H929 shCDH2 cells in comparison to the negative control H929 TR cells, containing the TET repressor but not the CDH2 shRNA, showed that the doxycycline-induced knockdown of N-cadherin did not result in an aberrant growth pattern (Figure 4D). Performing similar experiments on a N-cadherin coating also did

not result in a difference in the growth rate of the cells (Figure 4E). Combined, these data show that neither N-cadherin expression as such, nor N-cadherin-mediated cell-substrate or homotypic cell-cell adhesion, directly affects MM cell growth in vitro.

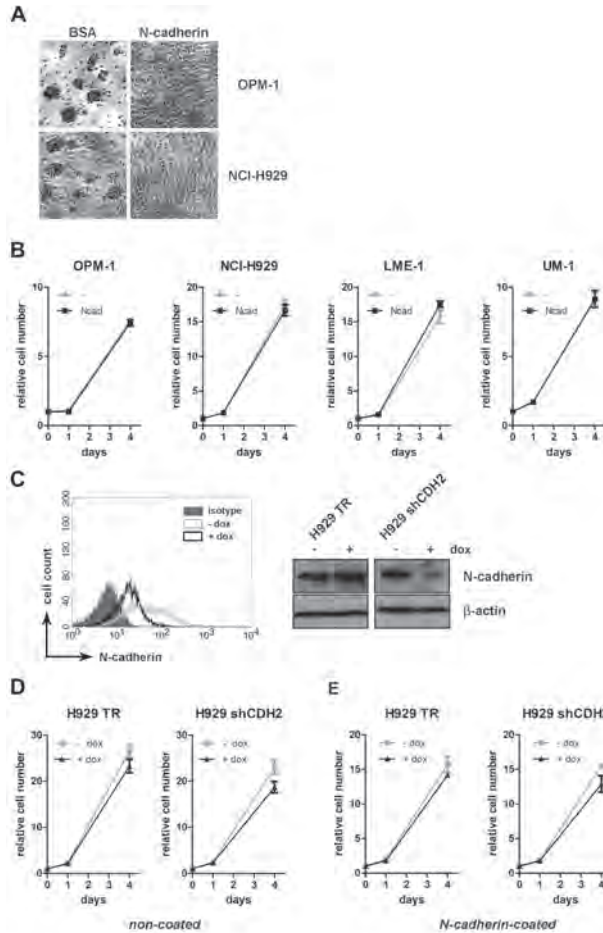


Figure 4. N-cadherin does not affect MM cell viability.

(A) Aggregation of MM cells blocked by N-cadherin coating. MM cell lines OPM-1 (top panel) and NCI-H929 (bottom panel) were plated on N-cadherin (1 mg/ml; right column) or on BSA as a control (left column). Representative pictures of the aggregation of the MM cell lines are shown. **(B)** MM cells (5×10^3) were plated on BSA (\circ) or N-cadherin (\blacksquare ; 1mg/ml) coated surfaces and cultured for 4 days. Cell viability was determined using FACS. The growth curves represent the means \pm SD of three measurements representative for at least 3 independent experiments. **(C)** Knock down of N-cadherin in the MM cell line NCI-H929, containing a doxycycline-inducible shRNA targeting N-cadherin (H929 shCDH2). Cells were incubated with (black line) or without doxycycline (gray line) for 5 days, and subsequently analyzed by FACS (left panel) using an N-cadherin mAb (clone GC-4) and an isotype control (filled gray histogram). By western blot analysis (right panel) knock down was confirmed (H929 shCDH2) and compared to the control cell line containing the TET repressor only (H929 TR), using a mAb N-cadherin (clone 32). β -actin was used as loading control. **D, E.** The growth rate of H929 shCDH2 (right panels) was compared with the H929 TR (left panels), in the presence (\blacktriangle) and absence (\circ) of doxycycline, with **(E)** or without **(D)** an N-cadherin coating (1 mg/ml), over a 4 day culture period. The growth curves represent the means \pm SD of three measurements representative for at least 3 independent experiments.

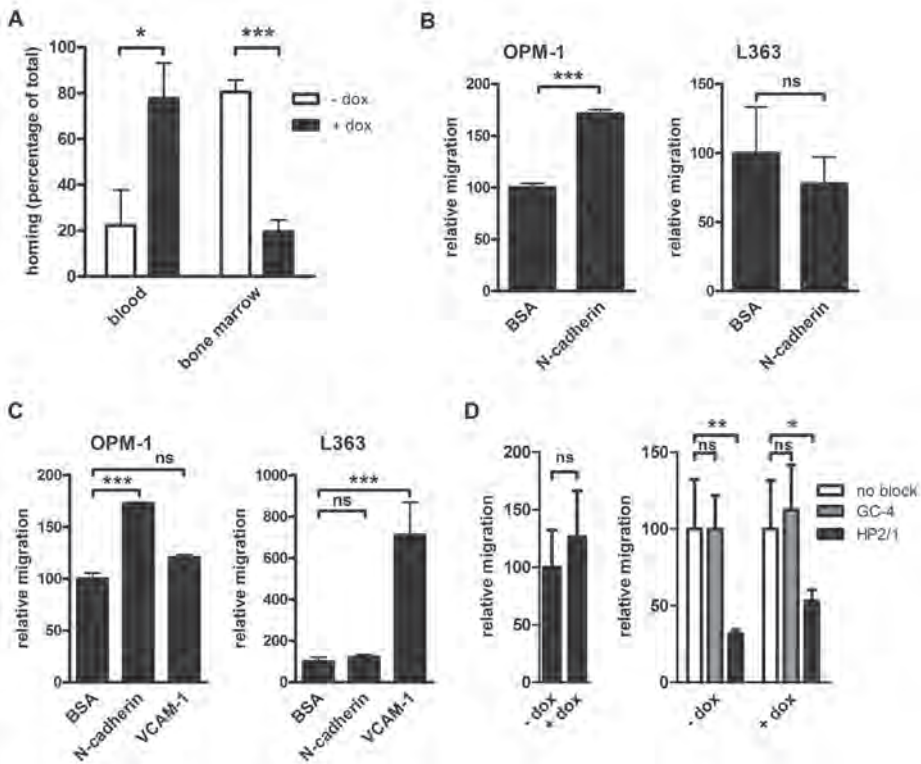


Figure 5. N-cadherin-mediated retention of MM cells in the bone marrow.

(A) H929 shCDH2 cells were incubated with or without doxycycline for 5 days, and subsequently labeled with either CMFDA or CMTMR. Cells were mixed (1:1), and injected intravenously in RAG2^{-/-}γc^{-/-} mice. Each CMFDA/CMTMR combination was analyzed by adoptive transfer of 8 recipient mice, which included a dye-swap. After 24 hr, blood and bone marrow were collected and FACS analyzed to quantify dye-labeled cells. The percentage of homing cells was corrected for the input ratio. The bars represent the means ± SD of 4 mice. * P<0.05; *** P<0.001 by student's t-test. **(B)** MM cells were allowed to migrate for 4 hours in the absence of SDF-1 in transwells coated with recombinant N-cadherin (1 mg/ml), compared to BSA-coating as a negative control. The results are expressed as relative migration with the migration on BSA-coating set to 100. The bars represent the means ± the standard deviation of three measurements, representative of at least three independent experiments. *** P<0.001; ns: not significant by student's t-test. **(C)** MM cells were allowed to migrate for 4 hours towards 100 ng/ml SDF-1 in transwells coated with recombinant N-cadherin (1 mg/ml), or sVCAM-1 (1 mg/ml) compared to BSA-coating as a negative control. The results are expressed as relative migration with the migration on BSA-coating set to 100. The bars represent the means ± the standard deviation of three measurements, representative of at least three independent experiments. *** P<0.001; ns: not significant by student's t-test. **(D)** H929 shCDH2 cells were allowed to migrate for 5 hours towards 100 ng/ml SDF-1 over an endothelial monolayer. H929 shCDH2 cells were cultured in the presence (+dox) or absence (-dox) of doxycycline for five days before migration (left panel). In addition to the doxycycline-treatment MM cells were coated with blocking antibodies against N-cadherin (GC-4) or alpha4-integrin (HP2/1) before migration (right panel). * P<0.05; ** P<0.01; ns: not significant by student's t-test. The results are expressed as relative migration with the migration of non-doxycycline treated without blocking set to 100. The bars represent the means ± the standard deviation of three measurements, representative of at least three independent experiments.

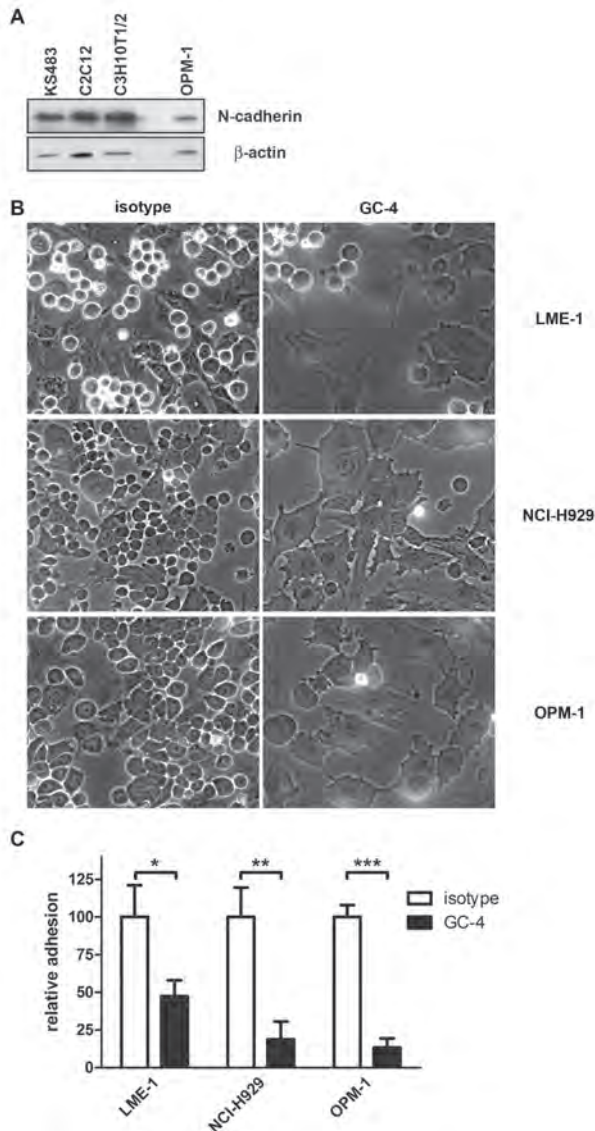


Figure 6. N-cadherin-mediated adhesion to osteoblasts.

(A) N-Cadherin expression in osteoblastic cell lines. Cell lysates were immunoblotted using a mAb against N-cadherin (clone 32), and β -actin was used as loading control. **(B)** N-cadherin-mediated adhesion of MM cells to osteoblasts. MM Cell lines were allowed to adhere to C3H10T1/2 cells in Hanks' balanced salt solution (HBSS) in the presence of calcium in combination with an N-cadherin blocking antibody (GC-4) or isotype control antibodies. Shown are representative pictures of the adhesion in HBSS supplemented with calcium and the isotype as a control (left column), and HBSS supplemented with calcium and the blocking antibody GC-4 (right column). **(C)** Quantification of the adhesion of the MM cells to C3H10T1/2 cells. The results are expressed as relative adhesion with the adhesion of the MM cells to C3H10T1/2 cells in HBSS supplemented with calcium and the isotype control normalized to 100. The bars represent the means \pm the standard deviation of four measurements, representative of at least three independent experiments. * $P < 0.05$; ** $P < 0.01$; *** $P < 0.001$ by student's t-test.

N-cadherin plays a role in the retention of MM cells in the bone marrow

Since N-cadherin has been implicated in migration and tumor metastasis^{20;29;30}, we investigated whether N-cadherin plays a role in MM cell homing. H929 shCDH2 cells were incubated with or without doxycycline for 5 days, and subsequently fluorescently labeled with either CMFDA or CMTMR. Cells were mixed (1:1), and injected intravenously in RAG2^{-/-}γc^{-/-} mice. Analysis of blood and bone marrow of these mice (n=4) revealed that reduced N-cadherin expression results in higher levels of circulating cells and a reduced homing to the bone marrow (Figure 5A), with a dye swap (n=4) resulting in similar results (data not shown). In support of these results, both basal motility (Figure 5B) and SDF-1-induced migration (Figure 5C) of the N-cadherin expressing OPM-1 cells is potentiated in transwell migration assays when the transwells are coated with recombinant N-cadherin, whereas migration of the N-cadherin negative L363 cells is not affected. Since endothelial cells express N-cadherin, we further explored a possible role for N-cadherin in MM cell homing by transendothelial migration assays using HUVEC cells. However, in contrast to the strong inhibition observed with an alpha4-integrin blocking antibody, neither blocking nor knock-down of N-cadherin affected transendothelial migration towards SDF-1 (Figure 5D). Taken together, our results establish the importance of N-cadherin in localization of MM cells in the bone marrow, most likely reflecting a role for N-cadherin in bone marrow retention rather than in active homing of MM cells.

N-cadherin-mediated adhesion of MM cells suppresses osteoblast differentiation

7

MM-related osteolytic bone disease is caused by an imbalance between osteoblast and osteoclast activity. MM cells have been shown to suppress osteoblast differentiation and activity via at least two different mechanisms, *i.e.* by secreting soluble factors¹¹⁻¹³ and by direct cell-cell contact with osteoblasts¹⁴. This, combined with the observations that N-cadherin positive MM cells reside in close proximity to the osteoblasts in the bone marrow of MM patients (Figure 3C) and that N-cadherin-mediated adhesion plays an important role in osteoblast maturation^{9;31;32}, prompted us to explore the possible contribution of N-cadherin-mediated adhesion to the contact-dependent suppression of osteoblast differentiation by MM cells. After confirming the high N-cadherin expression by pre-osteoblastic cells (Figure 6A), we determined whether MM cells could adhere to these cells in an N-cadherin dependent manner. To avoid integrin-mediated adhesion, experiments were performed in the presence of calcium as the only divalent cation. Indeed, N-cadherin-positive MM cells adhere to the osteoblasts (Figure 6B left panels), and, moreover, this adhesion could be blocked by pre-incubation of the MM cells with an antibody that blocks N-cadherin function (Figure 6B right panels and C). This heterotypic cell-cell interaction was further investigated with the use of the doxycycline-inducible H929 shCDH2 cells, which upon doxycycline-treatment display a ~ 70% reduction of N-cadherin expression (Figure 4C). In line with the blocking antibody results (Figure 6), these cells show a diminished adhesion to osteoblasts upon silencing of N-cadherin expression (Figure 7A lower panel and B), whereas no difference in adhesion was observed with the control H929 TR cells (Figure 7A upper panel and B).

To investigate the effect of N-cadherin-mediated MM adhesion on osteoblast differentiation, the doxycycline-inducible cells were co-cultured with KS483 pre-osteoblastic cells, which upon reaching confluence and the addition of ascorbic acid, differentiate into mature osteoblasts expressing alkaline phosphatase (ALP). Co-cultures of KS483 cells with either H929 shCDH2 cells or H929 TR cells resulted in a strong inhibition of ALP activity (Figure 7C). Interestingly, doxycycline-induced knock-down of N-cadherin markedly attenuated

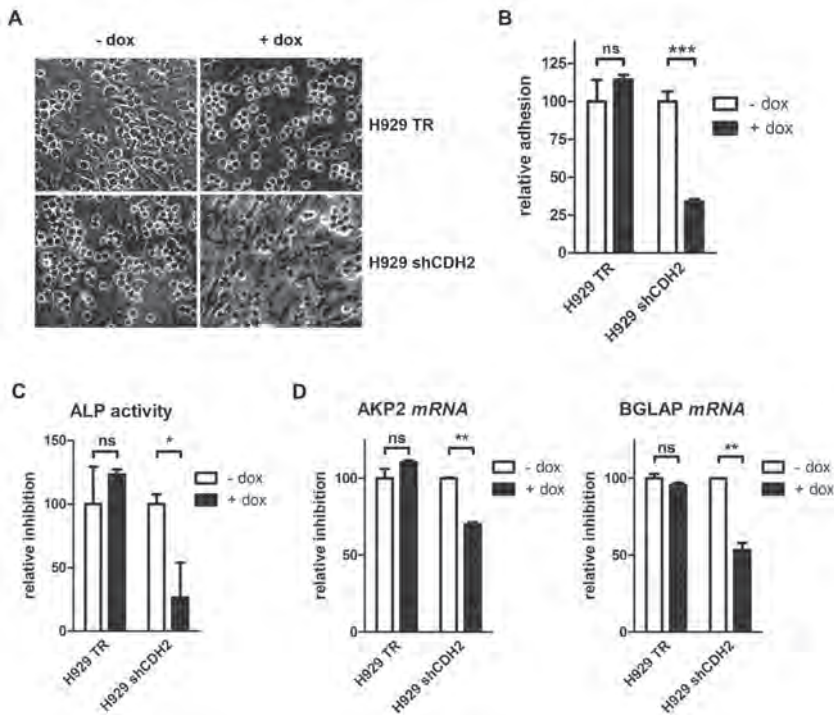


Figure 7. N-cadherin-mediated inhibition of osteoblast differentiation.

(A) N-cadherin knock-down abolishes N-cadherin-mediated adhesion of MM cells to osteoblasts. H929 TR (top panel) and H929 shCDH2 cells (bottom panel) were incubated with (right column) or without (left column) doxycycline for 5 days, and subsequently allowed to adhere to C3H10T1/2 cells in Hanks' balanced salt solution (HBSS) in the presence of calcium. Representative pictures of the adhesion are shown. (B) Quantification of the adhesion of the doxycycline-induced (black bars) H929 TR and H929 shCDH2 cells to C3H10T1/2 cells. The results are expressed as relative adhesion with the adhesion of the untreated cells (white bars) to C3H10T1/2 cells normalized to 100. The bars represent the means \pm the standard deviation of four measurements, representative of at least three independent experiments. *** $P < 0.001$; ns: not significant, by student's t-test. (C) N-cadherin mediates MM cell-controlled inhibition of osteoblast differentiation. KS483 cells were differentiated in the presence or absence of MM cells, either treated with (black bars) or without doxycycline (white bars), and subsequently stained for alkaline phosphatase (ALP) expression and quantified. The results are expressed as relative inhibition, with the co-incubation of KS483 and H929 TR in the absence of doxycycline normalized to 100. The bars represent the means \pm the standard deviation of three measurements, representative of at least three independent experiments. * $P < 0.05$; ns: not significant, by student's t-test. (D) N-cadherin represses alkaline phosphatase (AKP2) and osteocalcin (BGLAP) gene expression. KS483 cells were differentiated in the presence or absence of H929 shCDH2 cells with (black bars) or without doxycycline (white bars), and subsequently analyzed by qRT-PCR. The results are expressed as relative inhibition, with the co-incubation of KS483 in the absence of doxycycline set to 100. ** $P < 0.01$; ns: not significant, by student's t-test.

the ability of H929 shCDH2 cells to inhibit osteoblast differentiation, whereas doxycycline treatment of the control H929 TR cells had no effect (Figure 7C). The inhibitory effect of this N-cadherin-mediated interaction on osteoblast differentiation was further substantiated by measuring the mRNA levels of AKP2 and BGLAP (Figure 7D), encoding the osteoblast differentiation markers alkaline phosphatase and osteocalcin respectively. Like the expression of ALP, the ability of MM cells to inhibit the expression of AKP2 and BGLAP was significantly diminished upon N-cadherin knock-down. Taken together, these observations show that N-cadherin plays an important role in the interaction of MM cells with osteoblasts, and establish an important role for this N-cadherin-mediated interaction in the inhibition of osteoblastogenesis.

Discussion

Although MM cell growth is driven by genetic alterations like translocation and mutations, these cells still remain dependent upon the bone marrow (BM) microenvironment. The interactions of MM cells with the BM microenvironment, either directly via adhesion molecules or indirectly via the ensuing stimulation of autocrine/paracrine production of cytokines, activate a broad range of proliferative and anti-apoptotic signaling pathways^{6,7}. Here, we identified a new interactant of MM cells with the BM microenvironment, *i.e.* N-cadherin.

We observed high expression of N-cadherin on the malignant plasma cells in a subset of approximately 50% of primary MMs as well as MM cell lines, but not in normal BM plasma cells (Figures 1 and 3). To the best of our knowledge, with the exception of some T-cell leukemia cell-lines and two E2A-PBX1-positive B acute lymphoblastic leukemia cell-lines^{20,33,34}, expression of N-cadherin has not previously been reported in hematologic malignancies. N-cadherin is a transmembrane calcium-dependent homophilic cell-cell adhesion molecule, which is linked to the actin cytoskeleton through a conserved cytoplasmic domain that binds β -catenin. The functionality of the expressed N-cadherin was initially demonstrated by means of in vitro homophilic adhesion assays (Figure 2). As expected, N-cadherin co-localizes and physically interacts with β -catenin (Figures 1 and 3). Furthermore, high levels of N-cadherin seem to correlate with high levels of β -catenin (Figure 1B). This increase in β -catenin protein levels might be explained by the “protective” effect of N-cadherin binding to β -catenin, preventing degradation of the latter^{35,36}.

Our gene expression profiling analysis of a large group of MM patients revealed that CDH2, the gene encoding N-cadherin, is highly, but not exclusively, expressed in MM cells bearing a t(4;14)(p16;q32) translocation. Although this MM subtype is associated with poor prognosis^{37,38}, expression of CDH2 by itself does not predict prognosis. Notably, in a previous independent gene expression profiling study of 29 primary MM samples, CDH2 was among the genes upregulated in 5 patients carrying the t(4;14) MMSET translocation³⁹. Moreover, CDH2 was among the genes down-regulated upon silencing of the MMSET gene in the KMS-11 cell-line⁴⁰. Also, in our panel of MM cell-lines, the two cell-lines which carry the t(4;14) translocation, *i.e.* OPM-1 and NCI-H929, display prominent N-cadherin expression (Figure 1). Taken together, these data indicate that the aberrant expression of

N-cadherin in a subgroup of MM patients may, at least in part, be the indirect consequence of overexpression of the transcriptional repressor MMSET.

Increasing evidence indicates that the gain of N-cadherin expression in solid tumor cells is associated with an enhanced invasive potential and metastasis^{29,30}. Furthermore, Hazan et al. showed that exogenous expression of N-cadherin can induce migration of breast cancer cells⁴¹. In line with these reports, we here show that N-cadherin potentiates basal MM cell motility as well as SDF-1 induced migration (Figure 5B and C), and contributes to the homing to and/or retention in the bone marrow of MM cells (Figure 5A). In order to separate these two processes, we performed a transendothelial migration assay, showing that knock-down of N-cadherin and/or treatment with an N-cadherin blocking antibody, did not affect migration of MM cells across an endothelial barrier (Figure 5D), whereas a blocking antibody targeting $\alpha 4$ -integrin did suppress migration of the cells. In this context it is important to note that endothelial cells mainly display extrajunctional localization of N-cadherin^{42,43}, which might facilitate adhesion rather than migration in these static migration assays. Nevertheless, our results favor the hypothesis that N-cadherin is involved in the retention of MM cells in the bone marrow, which may be the consequence of homotypic and/or heterotypic cell-cell adhesion within the BM microenvironment.

Indeed, N-cadherin expression by MM cells participates in homophilic, heterotypic adhesion of MM cells with their environment, e.g., with osteoblasts (Figures 2 and 6). It has become apparent that the interplay between MM cells and bone is bidirectional. The BM microenvironment is not only radically perturbed by the presence of MM cells, but the microenvironment also changes the behavior of the tumor cells, for example by rendering the MM cells more resistant to the pro-apoptotic effects of conventional therapies. One of the important clinical sequela of these bidirectional interactions is enhanced osteoclastogenesis and osteoclast activity, resulting in osteolytic bone lesions. Under physiological conditions the remodeling of the bone is a homeostatic process in which osteoclasts mediate resorption of "old" bone tissue, followed by new bone formation by the osteoblasts. In MM, however, these two processes are uncoupled, due to increased osteoclast activation and a suppression of osteoblast function^{6,7}. Besides inhibition by soluble factors, like Wnt antagonists, IL-3 and IL-7, osteoblast function and maturation can also be suppressed through direct contact between MM cells and pre-osteoblastic cells mediated via $\alpha 4\beta 1$ -VCAM-1 and/or N-CAM-N-CAM interactions⁴⁴⁻⁴⁶. The latter findings in addition to the reported key role of cadherin-based interactions in osteoblast function and differentiation^{9,31,32}, prompted us to investigate whether N-cadherin-mediated adhesion of MM cells to osteoblasts (Figure 6, 7A and B) can contribute to inhibition of osteoblast differentiation. Indeed, doxycycline-induced knock-down of N-cadherin in myeloma cells impaired their capacity to inhibit osteoblast differentiation, as shown by reduced expression of differentiation markers, like alkaline phosphatase (Figures 7C and D) and osteocalcin (Figure 7D).

Apart from contributing to osteolytic bone disease, the N-cadherin-mediated interaction of MM with osteoblasts may also contribute to another sequela of MM, i.e. the development of pancytopenia. Since osteoblasts have a central role in the organization of the endosteal stem cell niche⁴⁷⁻⁴⁹, it is tempting to speculate that N-cadherin expression might enable MM cells to access this niche, leading to niche dysregulation and thereby contributing to the pancytopenia that is typically observed in MM patients.

In conclusion, our data indicate that N-cadherin-mediated interaction of MM cells with osteoblasts may be involved in bone marrow retention and results in reduced osteoblast

differentiation, which may hence play a crucial role in the pathogenesis of myeloma bone disease. Targeting N-cadherin, *e.g.* with a recently developed small cyclic peptide ADH-1⁵⁰, may prove to be a successful novel means of therapeutic intervention in a subgroup of MM patients.

Acknowledgements

The authors like to thank Dr. Clemens Löwik for providing us the C3H10T1/2 and KS483 cells. This work was supported by a grant from the Dutch Cancer Society to M.S. and S.T.P.

References

1. Hallek M, Bergsagel PL, Anderson KC. Multiple myeloma: increasing evidence for a multistep transformation process. *Blood*. 1998;91(1):3-21.
2. Kuehl WM, Bergsagel PL. Multiple myeloma: evolving genetic events and host interactions. *Nat.Rev.Cancer*. 2002;2(3):175-187.
3. Alsayed Y, Ngo H, Runnels J et al. Mechanisms of regulation of CXCR4/SDF-1 (CXCL12)-dependent migration and homing in multiple myeloma. *Blood*. 2007;109(7):2708-2717.
4. Pals ST, de Gorter DJ, Spaargaren M. Lymphoma dissemination: the other face of lymphocyte homing. *Blood*. 2007;110(9):3102-3111.
5. Sanz-Rodriguez F, Hidalgo A, Teixido J. Chemokine stromal cell-derived factor-1alpha modulates VLA-4 integrin-mediated multiple myeloma cell adhesion to CS-1/fibronectin and VCAM-1. *Blood*. 2001;97(2):346-351.
6. Hideshima T, Mitsiades C, Tonon G, Richardson PG, Anderson KC. Understanding multiple myeloma pathogenesis in the bone marrow to identify new therapeutic targets. *Nat.Rev.Cancer*. 2007;7(8):585-598.
7. Podar K, Chauhan D, Anderson KC. Bone marrow microenvironment and the identification of new targets for myeloma therapy. *Leukemia*. 2009;23(1):10-24.
8. Clohisy D. Cellular mechanisms of osteolysis. *J.Bone Joint Surg.Am*. 2003;85-A Suppl 1:S4-S6.
9. Mbalaviele G, Shin CS, Civitelli R. Cell-cell adhesion and signaling through cadherins: connecting bone cells in their microenvironment. *J.Bone Miner.Res*. 2006;21(12):1821-1827.
10. Chen Y, Alman BA. Wnt pathway, an essential role in bone regeneration. *J.Cell Biochem*. 2009;106(3):353-362.
11. Tian E, Zhan F, Walker R et al. The role of the Wnt-signaling antagonist DKK1 in the development of osteolytic lesions in multiple myeloma. *N.Engl.J.Med*. 2003;349(26):2483-2494.
12. Oshima T, Abe M, Asano J et al. Myeloma cells suppress bone formation by secreting a soluble Wnt inhibitor, sFRP-2. *Blood*. 2005;106(9):3160-3165.
13. Standal T, Abildgaard N, Fagerli UM et al. HGF inhibits BMP-induced osteoblastogenesis: possible implications for the bone disease of multiple myeloma. *Blood*. 2007;109(7):3024-3030.
14. Giuliani N, Colla S, Morandi F et al. Myeloma cells block RUNX2/CBFA1 activity in human bone marrow osteoblast progenitors and inhibit osteoblast formation and differentiation. *Blood*. 2005;106(7):2472-2483.
15. Derksen PWB, Tjin E, Meijer HP et al. Illegitimate WNT signaling promotes proliferation of multiple myeloma cells. *Proc.Natl.Acad.Sci.U.S.A*. 2004;101(16):6122-6127.
16. Sukhdeo K, Mani M, Zhang Y et al. Targeting the beta-catenin/TCF transcriptional complex in the treatment of multiple myeloma. *Proc.Natl.Acad.Sci.U.S.A*. 2007;104(18):7516-7521.

17. Dutta-Simmons J, Zhang Y, Gorgun G et al. Aurora kinase A is a target of Wnt/beta-catenin involved in multiple myeloma disease progression. *Blood*. 2009;114(13):2699-2708.
18. Mani M, Carrasco DE, Zhang Y et al. BCL9 promotes tumor progression by conferring enhanced proliferative, metastatic, and angiogenic properties to cancer cells. *Cancer Res*. 2009;69(19):7577-7586.
19. Harris TJ, Peifer M. Decisions, decisions: beta-catenin chooses between adhesion and transcription. *Trends Cell Biol*. 2005;15(5):234-237.
20. Derycke LD, Bracke ME. N-cadherin in the spotlight of cell-cell adhesion, differentiation, embryogenesis, invasion and signalling. *Int.J.Dev.Biol*. 2004;48(5-6):463-476.
21. van der Horst G, van Bezooijen RL, Deckers MM et al. Differentiation of murine preosteoblastic KS483 cells depends on autocrine bone morphogenetic protein signaling during all phases of osteoblast formation. *Bone*. 2002;31(6):661-669.
22. Reijmers RM, Groen RW, Rozemuller H et al. Targeting EXT1 reveals a crucial role for heparan sulfate in the growth of multiple myeloma. *Blood*. 2010;115(3):601-604.
23. de Gorter DJ, Beuling EA, Kersseboom R et al. Bruton's tyrosine kinase and phospholipase Cgamma2 mediate chemokine-controlled B cell migration and homing. *Immunity*. 2007;26(1):93-104.
24. Bergsagel PL, Kuehl WM, Zhan F et al. Cyclin D dysregulation: an early and unifying pathogenic event in multiple myeloma. *Blood*. 2005;106(1):296-303.
25. Ramakers C, Ruijter JM, Deprez RH, Moorman AF. Assumption-free analysis of quantitative real-time polymerase chain reaction (PCR) data. *Neurosci.Lett*. 2003;339(1):62-66.
26. Zhan F, Huang Y, Colla S et al. The molecular classification of multiple myeloma. *Blood*. 2006;108(6):2020-2028.
27. Fonseca R, Bergsagel PL, Drach J et al. International Myeloma Working Group molecular classification of multiple myeloma: spotlight review. *Leukemia*. 2009;23(12):2210-2221.
28. Kamei J, Toyofuku T, Hori M. Negative regulation of p21 by beta-catenin/TCF signaling: a novel mechanism by which cell adhesion molecules regulate cell proliferation. *Biochem.Biophys.Res.Commun*. 2003;312(2):380-387.
29. Wheelock MJ, Shintani Y, Maeda M, Fukumoto Y, Johnson KR. Cadherin switching. *J.Cell Sci*. 2008;121(Pt 6):727-735.
30. Blaschuk OW, Devemy E. Cadherins as novel targets for anti-cancer therapy. *Eur.J.Pharmacol*. 2009;625(1-3):195-198.
31. Cheng SL, Shin CS, Towler DA, Civitelli R. A dominant negative cadherin inhibits osteoblast differentiation. *J.Bone Miner.Res*. 2000;15(12):2362-2370.
32. Hay E, Laplantine E, Geoffroy V et al. N-cadherin interacts with axin and LRP5 to negatively regulate Wnt/beta-catenin signaling, osteoblast function, and bone formation. *Mol.Cell Biol*. 2009;29(4):953-964.
33. Tsutsui J, Moriyama M, Arima N et al. Expression of cadherin-catenin complexes in human leukemia cell lines. *J.Biochem*. 1996;120(5):1034-1039.
34. Nygren MK, en-Dahl G, Stubberud H et al. beta-catenin is involved in N-cadherin-dependent adhesion, but not in canonical Wnt signaling in E2A-PBX1-positive B acute lymphoblastic leukemia cells. *Exp.Hematol*. 2009;37(2):225-233.
35. Sadot E, Simcha I, Shtutman M, Ben-Ze'ev A, Geiger B. Inhibition of beta-catenin-mediated transactivation by cadherin derivatives. *Proc.Natl.Acad.Sci.U.S.A*. 1998;95(26):15339-15344.
36. Heuberger J, Birchmeier W. Interplay of cadherin-mediated cell adhesion and canonical wnt signaling. *Cold Spring Harb.Perspect.Biol*. 2010;2(2):a002915.
37. Keats JJ, Reiman T, Maxwell CA et al. In multiple myeloma, t(4;14)(p16;q32) is an adverse prognostic factor irrespective of FGFR3 expression. *Blood*. 2003;101(4):1520-1529.
38. Chng WJ, Kuehl WM, Bergsagel PL, Fonseca R. Translocation t(4;14) retains prognostic significance even in the setting of high-risk molecular signature. *Leukemia*. 2008;22(2):459-461.
39. Dring AM, Davies FE, Fenton JA et al. A global expression-based analysis of the consequences of the t(4;14) translocation in myeloma. *Clin.Cancer Res*. 2004;10(17):5692-5701.

40. Lauring J, Abukhdeir AM, Konishi H et al. The multiple myeloma associated MMSET gene contributes to cellular adhesion, clonogenic growth, and tumorigenicity. *Blood*. 2008;111(2):856-864.
41. Hazan RB, Phillips GR, Qiao RF, Norton L, Aaronson SA. Exogenous expression of N-cadherin in breast cancer cells induces cell migration, invasion, and metastasis. *J.Cell Biol.* 2000;148(4):779-790.
42. Salomon D, Ayalon O, Patel-King R, Hynes RO, Geiger B. Extrajunctional distribution of N-cadherin in cultured human endothelial cells. *J.Cell Sci.* 1992;102(Pt 1):7-17.
43. Navarro P, Ruco L, Dejana E. Differential localization of VE- and N-cadherins in human endothelial cells: VE-cadherin competes with N-cadherin for junctional localization. *J.Cell Biol.* 1998;140(6):1475-1484.
44. Barille S, Collette M, Bataille R, Amiot M. Myeloma cells upregulate interleukin-6 secretion in osteoblastic cells through cell-to-cell contact but downregulate osteocalcin. *Blood*. 1995;86(8):3151-3159.
45. Ely SA, Knowles DM. Expression of CD56/neural cell adhesion molecule correlates with the presence of lytic bone lesions in multiple myeloma and distinguishes myeloma from monoclonal gammopathy of undetermined significance and lymphomas with plasmacytoid differentiation. *Am.J.Pathol.* 2002;160(4):1293-1299.
46. Giuliani N, Rizzoli V, Roodman GD. Multiple myeloma bone disease: Pathophysiology of osteoblast inhibition. *Blood*. 2006;108(13):3992-3996.
47. Hosokawa K, Arai F, Yoshihara H et al. Function of oxidative stress in the regulation of hematopoietic stem cell-niche interaction. *Biochem.Biophys.Res.Commun.* 2007;363(3):578-583.
48. Kiel MJ, Acar M, Radice GL, Morrison SJ. Hematopoietic stem cells do not depend on N-cadherin to regulate their maintenance. *Cell Stem Cell.* 2009;4(2):170-179.
49. Li P, Zon LI. Resolving the controversy about N-cadherin and hematopoietic stem cells. *Cell Stem Cell.* 2010;6(3):199-202.
50. Williams E, Williams G, Gour BJ, Blaschuk OW, Doherty P. A novel family of cyclic peptide antagonists suggests that N-cadherin specificity is determined by amino acids that flank the HAV motif. *J.Biol.Chem.* 2000;275(6):4007-4012.

8

General discussion

General discussion

Malignant transformation of lymphocytes is caused by genetic aberrations that render the cells less sensitive to pro-apoptotic and/or more responsive to proliferative stimuli. However, interactions with the microenvironment, either directly via adhesion molecules or indirectly via stimulation by auto-/paracrine cytokines, may equally contribute to the proliferation and progression of these tumors. Therefore, the aim of the studies described in this thesis was to explore the role of the microenvironment, in particular the HGF/MET and Wnt signaling pathway, heparan sulfate proteoglycans (HSPGs), and N-cadherin, in the growth and survival of malignant lymphoma and multiple myeloma (MM).

HGF/MET signaling in malignant B cell lymphomas

Uncontrolled activation of the HGF/MET signaling pathway has been implicated in tumor growth, invasion and metastasis ¹. Previous work by others and our laboratory have established a role for HGF/MET signaling in B cell development and malignancies ²⁻¹⁰. However, a comprehensive analysis of MET expression in B-NHLs has not been performed. In chapter 2, we have investigated the expression of MET in a large panel of B cell malignancies. We have found that MET is frequently expressed in MM (48%) and diffuse large B cell lymphoma (DLBCL; 30%), but also, although at lower percentage, in chronic lymphatic leukemia/lymphoma (B-CLL), follicular lymphoma, and Burkitt's lymphoma (BL). These findings confirm and extend other studies, which also reported expression of MET in BL, MM and DLBCL ^{2,4,7}. Within the DLBCL microenvironment, HGF is most likely expressed by (activated) macrophages. This, combined with the lack of HGF expression by the DLBCL cell lines, as measured in conditioned medium, indicates a paracrine rather than an autocrine mechanism of MET activation in DLBCL. Activation of DLBCL cells, results in phosphorylation and activation of ERK, PKB, GSK3 and FOXO3a, which have been implicated in cell growth and survival. Furthermore, HGF induces PI3K-dependent, integrin-mediated adhesion of DLBCL cells. Similar to MM ⁸, and contrary to their normal counterparts the GC B cells⁹, DLBCL cells aberrantly produce HGFA themselves. This expression enables the DLBCL cells to activate HGF, and may facilitate active HGF/MET signaling. Hence, both MM and DLBCL cells have acquired self-supporting attributes, *i.e.* both HGF and HGFA expression, or HGFA expression alone, respectively, to more efficiently activate the HGF/MET pathway, emphasizing a key role for this signaling cascade in lymphomagenesis.

Besides auto- or paracrine activation, genetic aberrations, *e.g.* translocation, amplification, or mutation of the *MET* gene, can also cause inappropriate activation of MET ¹¹⁻¹⁵. Although amplification of *MET* has been reported in several types of human cancer ¹¹, it was not found in any of the MET-expressing lymphomas studied. This is in agreement with previous studies showing that amplification of the *MET* locus is a rare event in NHL ¹². However, we detected two germline missense mutations in *MET*: one mutation in the tyrosine kinase domain (R1166Q) in a DLBCL patient, and one in the juxtamembrane domain (R988C) in four patients with either DLBCL, CLL, FL or BL. No germline (or somatic) *MET* mutations had thus far been described for B cell malignancies. Interestingly, the R988C mutation has also been reported in small cell lung cancer and non- small cell lung cancer ¹⁶⁻¹⁸. Expression of the R988C MET-mutant in a small cell lung cancer line resulted in enhanced focus-formation

and soft-agar colony formation¹⁶. Furthermore, introduction of the R988C MET-mutant promoted proliferation, motility and overall tyrosine phosphorylation of the pre-B cell line BaF3^{16,19}. These data, combined with the recent demonstration that a mouse MET mutation homologous to R988C plays an important role in lung tumor susceptibility¹⁸, strongly suggest that the R988C mutation is a true gain-of-function mutation. Since it has been shown that mice carrying oncogenic MET mutations develop lymphomas²⁰, it is conceivable that the R988C MET mutation can convey B cell lymphoma susceptibility in humans.

Although overexpression of HGF/MET in patients with DLBCL has been associated with poor prognosis, our study is the first to show the functional consequences of active HGF/MET signaling in DLBCL cells and suggests that the pathway may contribute to the pathogenesis of DLBCL by controlling cell adhesion, growth and survival.

Aberrant Wnt pathway activation in the pathogenesis of lymphoproliferative disease

Wnt signaling plays an important role in early lymphocyte development, with TCF and LEF1 being essential for the maintenance of progenitor T- and B cell compartments in mice²¹⁻²³. In addition, it has been demonstrated that Wnts and β -catenin affect lymphocyte progenitor fate as well as hematopoietic stem cell self-renewal²⁴⁻³⁰, confirming the important role of Wnt signaling in lymphopoiesis. These observations, in combination with the key oncogenic role of Wnt signaling in several non-lymphoid tumors³¹, and our identification of illegitimate activation in MM³², prompted us to explore whether deregulation of the WNT pathway contributes to lymphoproliferative disease (chapter 3).

Immunohistochemical screening of a large panel of NHLs for nuclear accumulation of β -catenin, a hallmark of active canonical Wnt signaling, revealed that Wnt pathway activation is more common in T cell lymphomas (25%) than B cell lymphomas (3%). The three B cell tumors included one case of B-LBL/ALL carrying a t(1;19)(q23;p13) translocation, which results in a fusion of E2A and Pbx1. This fusion protein has been associated with enhanced Wnt16 expression^{33,34}. Interestingly, we also detected Wnt16 expression in MM³² and T-LBL/ALL (chapter 3), suggesting a role for this Wnt factor in lymphoid malignancies. Recent studies have suggested a role for uncontrolled WNT signaling in the pathogenesis of B-LBL/ALL^{35,36} and B-CLL³⁷, involving either epigenetic silencing of WNT inhibitors or deregulated expression of WNTs and/or other WNT pathway components. However, in line with our current findings, these studies did not reveal constitutive nuclear β -catenin expression in B-CLL and B-LBL/ALLs.

The aberrant activation of the WNT pathway in T cell lymphomas, was caused by *CTNNB1* mutations or, in lymphomas with mutations in neither *CTNNB1* nor *APC*, by the presence of an autocrine activation loop. Functional studies showed that this autocrine activating mechanism may promote the growth of T-LBL/ALL cells. In contrast to previously reported mutations in β -catenin in NK/T cell lymphomas^{38,39}, the current mutations all represented established gain-of-function mutations, identical to those previously reported in hepatocellular, prostate, and colorectal cancer⁴⁰. They involve phosphorylation sites important for ubiquitination and degradation of β -catenin. In agreement with our current findings in human T-LBL/ALL, it was recently shown that stabilization of β -catenin in mouse thymocytes is oncogenic, and results in the development of malignant T cell lymphomas⁴¹. Intriguingly, Kawaguchi-Ihara *et al.* recently showed that Wnt3A stimulation of T-LBL/ALL

cells did not induce growth in the whole cell population, but promoted the self-renewal of leukemic stem/progenitor cells in some T-LBL/ALL cell lines⁴². Since we did not detect Wnt3A expression in our T-LBL/ALL cell lines and patient, these data suggest that the maintenance of leukemic stem/progenitor cells in T cell lymphoma is regulated in a paracrine fashion. It is tempting to speculate that these putative cancer stem cells are regulated in a similar fashion as normal HSC, where paracrine Wnt signaling also regulates quiescence and self-renewal⁴³. In this context it is of interest that the expression of a set of Wnt pathway genes predicted relapse in 3 independent T-LBL/ALL patient sets⁴⁴. Taken together, these data show that Wnt signaling contributes to the pathogenesis of T cell lymphomas. Targeting WNT signaling components with recently developed small-molecule drugs may prove a successful novel means of therapeutic intervention in lymphoma patients displaying active WNT signaling. As already mentioned, we have previously demonstrated that the Wnt pathway is aberrantly activated in MM and can promote MM tumor growth³². Subsequent studies have confirmed the oncogenic potential of the Wnt pathway in MM by demonstrating that targeting the Wnt pathway by drugs or siRNAs leads to inhibition of MM growth^{32;45-49}. In addition, by knocking down the downstream effectors of Wnt, Dutta-Simmons *et al.* identified new Wnt/ β -catenin transcriptional targets involved in various aspects of cell-cycle progression⁴⁸. Interestingly, in three independent datasets of MM patients, we found a positive correlation between the expression of these Wnt target genes and the gene expression-based proliferation index (Kocemba *et al.* unpublished observation). This correlation provides support for our previous finding that aberrant activation of Wnt pathway is related to the growth of MM cells. Although the exact cause(s) of aberrant Wnt pathway activation in MM has not yet been established, the absence of detectable Wnt pathway mutations as well as the (over) expression of Wnt ligands in the BM microenvironment by both stromal cells and by the MM cells themselves suggests a key role for paracrine and/or autocrine stimulation. As a consequence, loss of secreted Wnt pathway antagonists, like DKK1, could have a major impact on the pathogenesis of MM. Indeed, we observed that whereas the DKK1 protein is strongly expressed in most primary MMs, the expression of this Wnt antagonist is down-regulated or even completely lost in a subgroup of advanced MMs. Interestingly, the loss of DKK1 protein expression in BM samples of MM patients was correlated with an increased nuclear expression of β -catenin, a hallmark of canonical Wnt signaling. Our observation, that DKK1 expression can be lost in advanced MM and that its restoration inhibits β -catenin/TCF transcriptional activity, suggests that silencing of DKK1 may contribute to activation of the canonical Wnt pathway during MM progression.

Studies by Shaughnessy and colleagues have previously reported that DKK1 expression by the malignant plasma cells may contribute to MM bone disease by inhibiting Wnt signaling in osteoblasts, thereby interfering with their differentiation⁵⁰⁻⁵². In addition to promoting bone disease, inhibition of osteoblast differentiation by DKK1 may also promote MM growth, since mature osteoblasts can suppress myeloma growth⁵³, whereas immature osteoblasts express high levels of IL-6, a central growth and survival factor for myeloma plasma cells⁵⁴. Furthermore, DKK1 enhances the expression of receptor activator of NF- κ B ligand (RANKL) and downregulates the expression of osteoprotegerin (OPG) in immature osteoblast⁵¹. The resulting increased RANKL/OPG ratio leads to osteoclast activation promoting osteolytic bone disease, and may also support the growth of myeloma cells through secretion of IL-6, osteopontin, and by adhesive interactions⁵⁵. Thus, DKK1 can both exercise paracrine effects on the BM microenvironment and affect the MM cells in an

autocrine fashion; the net effect could be either enhanced or reduced tumor growth.

In accordance with this hypothesis, Yaccoby *et al.* showed that treatment with an anti-DKK1 neutralizing antibody, stimulates osteoblast activity, reduces osteoclastogenesis, and promotes bone formation in myelomatous and nonmyelomatous bones. The inhibition of DKK1 activity was associated with reduced MM burden, although it should be noted that not in all mice bearing human myeloma cells this was observed⁵⁶. In addition, Fulciniti *et al.* demonstrated that the DKK1 neutralizing antibody BHQ880 increases bone formation and inhibits MM growth⁵⁷. Together, these studies suggest that MM bone disease and tumor growth are interdependent, at least at the medullary stage, and that increased bone formation in myelomatous bones, as a consequence of neutralization of DKK1 activity, can also control MM progression. However, in contrast with the overall response seen in the SCID/rab and SCID/hu mouse models, using a 5T2MM murine model of myeloma it has been demonstrated that the anti-DKK1 antibody BHQ880 also causes a reduction of osteolytic bone lesions, but without any significant effect on tumor burden⁵⁸.

Given the results of our study, demonstrating DKK1 mediated inhibition of canonical Wnt signaling in malignant plasma cells, we hypothesize that loss or inhibition of DKK1 activity could lead to hyperactivation of the Wnt pathway in malignant plasma cells, which could rather promote growth of the tumor, especially in the extramedullary location. Indeed, using yet another mouse model, *i.e.* 5TGM1, it was shown that stimulation of the Wnt signaling pathway by lithium chloride significantly increases subcutaneous tumor growth⁵⁹. Importantly, Dutta-Simmons *et al.* demonstrated that Wnt pathway controls not only proliferation of malignant plasma cells but also contributes to the metastatic potential of MM cells⁴⁸. In conclusion, although inhibition of DKK1 activity is clearly effective in prevention of MM osteolytic bone disease *in vivo*, the data presented in chapter 4 warrant clinical concerns regarding DKK1 targeting for therapeutic purpose in MM patients, since this could lead to hyperactivation of the Wnt pathway in malignant plasma cells and consequently increase metastatic potential and extramedullary tumor growth.

8 Heparan sulfate proteoglycans in the pathogenesis of multiple myeloma

In the last two decades, many studies have suggested a versatile role of the transmembrane heparan sulfate proteoglycan (HSPG) syndecan-1 in the interaction of MM plasma cells with the BM microenvironment^{32;60-62}. Furthermore, multiple growth factors, which have been implicated in the pathogenesis of MM can bind to the HS-chains of syndecan-1. This notion prompted us to specifically study the impact of targeting of EXT1, an enzyme indispensable for HS-chain synthesis, on MM growth, both *in vitro* and *in vivo*.

In the study presented in chapter 6, we have stably transfected MM cell lines with doxycycline-inducible shRNAs against either the syndecan-1 core protein or the HS co-polymerase EXT1 and analyzed the effects on growth. Doxycycline induced knockdown of either syndecan-1 or EXT1 led to a marked reduction of the *in vitro* growth rate of the myeloma cells, which was accompanied by a prominent increase in apoptosis. By employing our recently developed myeloma xenotransplant model in RAG2^{-/-}γC^{-/-} mice (chapter 5) we showed that induction of EXT1 knockdown *in vivo* dramatically suppresses the growth of bone marrow localized myeloma: Consistent with our previous observations using untransfected MM cells (chapter 5), mice that did not receive doxycycline displayed a rapid

exponential tumor growth, localized in various parts of the skeleton. Immunohistochemical analysis of the isolated bones confirmed the presence of highly proliferative tumor-foci. In striking contrast, treated doxycycline from the first day remained completely tumor free throughout the entire experiment. In addition, in mice with established tumors prior to doxycycline treatment, doxycycline administration from week 6 onwards led to either growth arrest or even a reduction in tumor size.

Consistent with our data, previous studies have shown that (partial) knock-down of the syndecan-1 core protein, results in a reduced growth of myeloma cell *in vivo*^{62;63}. Furthermore, Yang *et al.* showed that besides targeting syndecan-1, treatment with bacterial heparinase III, or an inhibitor of human heparanase blocked the growth of MM⁶². These latter findings confirm our results, and underscore the importance of HS side-chains, rather than the proteoglycan core protein per se, in the growth and survival of MM cells. Using the opposite approach, it was shown that overexpression of *HSulf-1* or *HSulf-2* attenuated tumor growth *in vivo*⁶⁴. These enzymes specifically remove 6-*O* sulfate groups from HS side-chains, thereby altering the signaling pathways of growth factors like bone morphogenic protein (BMP), Wnt, and FGF-2⁶⁵⁻⁶⁷. Furthermore, a recent study investigated the expression of genes encoding proteins involved in HS and chondroitin sulfate chain synthesis⁶⁸. This study showed that multiple genes that are implicated in the glycosaminoglycan chain synthesis or modifications, were significantly different expressed between normal and malignant plasma cells. Interestingly, it also showed that high expression of *EXT1* was correlated with bad prognosis. Taken together, these studies, including our own, demonstrate that the HS-chains decorating syndecan-1 are crucial for the growth and survival of MM cells within the bone marrow environment and indicate these HS-chains and their biosynthesis machinery as potential treatment targets in MM.

N-cadherin a novel player in multiple myeloma-BM interactions

In chapter 7, we describe a new interactant of MM cells with the BM microenvironment, *i.e.* N-cadherin. We observed high expression of N-cadherin on the malignant plasma cells in a subset of approximately 50% of primary MMs as well as MM cell lines, but not in normal BM plasma cells. Gene expression profiling analysis of a large group of MM patients revealed that *CDH2*, the gene encoding N-cadherin, is highly (>80%), but not exclusively, expressed in MM cells bearing a t(4;14)(p16;q32) translocation. Although this MM subtype is associated with poor prognosis^{69;70}, expression of *CDH2* by itself does not predict prognosis. In line with our current findings, previous studies found *CDH2* among the genes upregulated in 5 patients carrying the *MMSET* translocation⁷¹, and down-regulated upon silencing of the *MMSET* gene⁷². These data indicate a close association between the t(4;14) translocation and N-cadherin expression.

Furthermore, we show that N-cadherin potentiates MM cell motility, and contributes to the localization of MM cells in the BM. In line with these data, gain of N-cadherin expression in solid tumors is associated with an enhanced invasive potential and metastasis^{73;74}. In addition, Hazan *et al.* showed that the introduction of N-cadherin can induce migration of breast cancer cells⁷⁵. However, interference with N-cadherin-mediated adhesion did not affect migration of MM cells across an endothelial barrier. This observation, together with the mainly extrajunctional localization of N-cadherin on endothelial cells^{76;77}, suggests that N-cadherin is involved in the retention of MM cells in the BM. Indeed, N-cadherin participates

in homophilic, heterotypic adhesion of MM cells to their environment, *e.g.* to osteoblasts. One of the characteristic features of MM is osteolytic bone destruction, resulting from the activation of osteoclasts and inhibition of osteoblast function. Interestingly, N-cadherin is expressed by osteoblasts during all stages of bone formation and N-cadherin-mediated interactions have shown to be crucial for osteoblast differentiation and function^{78;79}. In addition, loss of N-cadherin-mediated cell-cell adhesion results in osteoblast apoptosis^{78;80}. These findings prompted us to investigate whether N-cadherin-mediated adhesion of MM cells to osteoblasts affects osteoblast differentiation. Indeed, we observed that knock-down of N-cadherin in myeloma cells impaired their capacity to inhibit osteoblast differentiation. However, it should be noted that the inhibition was only partial, suggesting the contribution of other (soluble) factors. Consistent with this notion, recent studies have identified several factors produced by MM cells that are involved in the deregulation of osteoblast differentiation, like DKK1⁵⁰, sFRP-2⁸¹, HGF⁸², and IL-7^{83;84}. Furthermore, it was shown that these inhibitory effects were also partially dependent on adhesion of myeloma cells to the osteoblasts via integrin $\alpha4\beta1$ ⁸⁴. Apart from contributing to osteolytic bone disease, the N-cadherin-mediated interaction of MM with osteoblasts may also contribute to another sequela of MM, *i.e.* the development of pancytopenia. Since osteoblasts have a central role in the organization of the endosteal stem cell niche⁸⁵⁻⁸⁷, it is tempting to speculate that N-cadherin expression might enable MM cells to access this niche, leading to niche dysregulation and thereby contributing to the pancytopenia that is typically observed in MM patients. Taken together, our data indicate that N-cadherin, besides its role in bone homeostasis, may hence play a central role in the pathogenesis of myeloma bone disease.

Multiple myeloma mouse models

Despite the introduction of several novel agents such as bortezomib, thalidomide and lenalidomide, MM still remains incurable, indicating the necessity for novel therapies. Unfortunately, clinical testing of (combinations of) several potentially promising drugs is cumbersome and requires large controlled studies. Together, this emphasizes the need for representative and convenient animal models that permit preclinical testing of novel (combination) therapies against MM.

To develop a model that offers an optimal platform for preclinical evaluation of cellular immunotherapies, we tested the feasibility of using the immunodeficient RAG2^{-/-} γ C^{-/-} mice. These mice completely lack B, T and NK cells⁸⁸ and are far more suitable than NOD/SCID mice for reproducible engraftment of human T and B cells^{89;90}. In chapter 5, we show that intravenous transfer of human myeloma cell lines, marked with a fusion construct of green fluorescent protein (GFP) and luciferase, results in predominantly BM localized tumors in five out of seven MM cell lines tested. Despite the use of cell lines, these tumors present with a dissemination and growth pattern highly similar to that of human MM patients. Previously, other investigators developed MM models by injecting MM cell lines into SCID-mice⁹¹⁻⁹³. However, these models display subcutaneous and/or intraperitoneal tumor growth^{91;92}, lacking the interaction with the BM microenvironment, or use human fetal bone implants⁹³, which raises a lot of ethical concerns. Another recently developed model exploited the advantages of fluorescence-based optical imaging, by using NOD/SCID-mice and GFP-tagged cells, which allows frequent and serial non-invasive monitoring⁹⁴. While highly useful and convenient, an important drawback of this recent model is the extramedullary growth of

tumors, which is not a typical feature of MM. Furthermore, outgrowth of human T cells in the NOD/SCID-mice is far less reproducible than that in RAG2^{-/-}γC^{-/-} mice⁸⁹, making the latter model also more suitable for allogeneic stem cell transplantation. Thus, in our opinion, the RAG2^{-/-}γC^{-/-} model offers several advantages over the (NOD/SCID)-models and may, therefore, be better suited for preclinical testing. Nevertheless, it should be noted that our model, which uses cell lines rather than primary tumor cells, may be less suitable for studying a number of the biological aspects of myeloma such as stroma-myeloma interactions or natural growth kinetics.

An important reason for employing MM cell lines instead of primary MM cells was that cell lines allowed us to exploit the advantages of bioluminescent imaging (BLI) as a sensitive and non-invasive technology for tumor monitoring. In our model BLI proved superior to free Ig light chain-based monitoring. BLI was not only suitable for quantitative detection of the tumor load in the whole body, but it was also highly useful for visualization and quantitative analysis of individual foci of myeloma growth throughout the BM. Bioluminescence is a very sensitive method for the detection of low levels of marker gene expression⁹⁵, allowing the detection of even small tumors, an aspect which becomes relevant when monitoring small tumors after therapy. To evaluate the preclinical applicability of our model, we treated established full-blown tumors with radiotherapy as well as with allogeneic cellular immunotherapy. Radiotherapy resulted in a slow decay in tumor load, initially diminishing the tumor load to below the detection limits of the BLI. While for small individual lesions radiotherapy seemed to be sufficient for tumor eradication, this was clearly not the case for the larger tumor foci. However, these radiotherapy experiments illustrated the feasibility of using BLI as a sensitive technology for tumor monitoring. Finally, the allogeneic cellular immunotherapy experiments demonstrated that the MM model developed in RAG2^{-/-}γC^{-/-} mice is very useful for preclinical testing of cellular immune therapies, as the mice easily permit the engraftment and outgrowth of human T cells. The potent graft versus myeloma (GvM) effect obtained by infusion of allogeneic, thus MHC-mismatched, human T cells suggests that it may be possible to eradicate fullblown MM by potent allo-immune cellular therapies. In conclusion, we present here a model of human MM growth in an immunodeficient mouse, strongly resembling human MM. This model can be used to monitor the outgrowth of MM cells non-invasively and quantitatively. It offers the possibility for preclinical evaluation of several therapeutic strategies and may, therefore, facilitate the design of optimal protocols for the treatment of MM.

Concluding remarks

The studies described in this thesis, show that HGF, Wnt, HSPGs, and N-cadherin play an important role in the environmental regulation of multiple myeloma and malignant lymphoma. Although the different signaling cascades and surface molecules were analyzed separately and in different disease settings, it is tempting to speculate how these pathways might interact (Figure 1). In MM the expression of these different components is established. Here auto- and /or paracrine HGF or Wnts can bind the transmembrane HSPG syndecan-1. This HSPG has been shown to be involved in the presentation of many growth factors/cytokines, including HGF⁹⁶ and Wnts⁹⁷, resulting in efficient downstream signaling. Moreover, activation of both the HGF/MET and Wnt pathway have been implicated in the proliferation, survival as well as the migration of MM cells^{2;6;8;32;45;48;96;98}. Furthermore, matrix

metalloproteinase-9 (MMP9) was recently found to be a direct target of the Wnt signaling pathway⁹⁹, while in a different study it was shown that HGF stimulation of MM cells resulted in enhanced MMP9 secretion¹⁰⁰ (Figure 1a). MMP9 is one of the two MMPs that can cleave/degrade collagen type IV, a major component of the basement membrane, and therefore considered to play a crucial role in lymphocyte trafficking¹⁰¹. In addition, MMP9 has been shown to be involved in the cleavage of N-cadherin¹⁰², and thereby can contribute to the enhanced invasion of cells^{75;103;104}. Interestingly, we have identified N-cadherin as an important player in the pathogenesis of MM, *e.g.* inducing enhanced motility and interaction with osteoblasts (this thesis). Another place where these signaling molecules meet is the endosteal niche. Here, both HGF/MET⁸² and Wnt signaling, *i.e.* inhibition by DKK1⁵⁰, as well as adhesion by N-cadherin (this thesis), have shown to contribute to the inhibition of osteoblast differentiation (Figure 1b). Besides, as has already been discussed for N-cadherin, the interaction of MM cells with osteoblasts may also contribute to another sequela of MM, *i.e.* the development of pancytopenia. Because osteoblasts have a central role in the organization of the endosteal stem cell niche⁸⁵⁻⁸⁷, N-cadherin expression might enable MM cells to access this niche. This, together with the inhibitory effect of HGF, DKK1, and N-cadherin on osteoblast differentiation, could lead to niche dysregulation and thereby contribute to the pancytopenia. Furthermore, these signaling molecules have all been associated with hematopoietic stem cell (HSC) function^{43;105;106} (Figure 1b). Where N-cadherin keeps the HSCs localized in the endosteal stem cell niche¹⁰⁶, Wnt pathway activation in the niche is required to limit HSC proliferation and preserve the reconstituting function of endogenous hematopoietic stem cells⁴³. In contrast, DKK1 expression induces cell cycling in HSCs, and a progressive decline in regenerative function⁴³. Thus, the HGF/MET and Wnt signaling cascades, and N-cadherin have shown to play an important role in the pathogenesis of MM, by facilitating the growth and survival of the MM cells and may contribute to characteristic features of this disease, *e.g.* osteolytic lesions and pancytopenia.

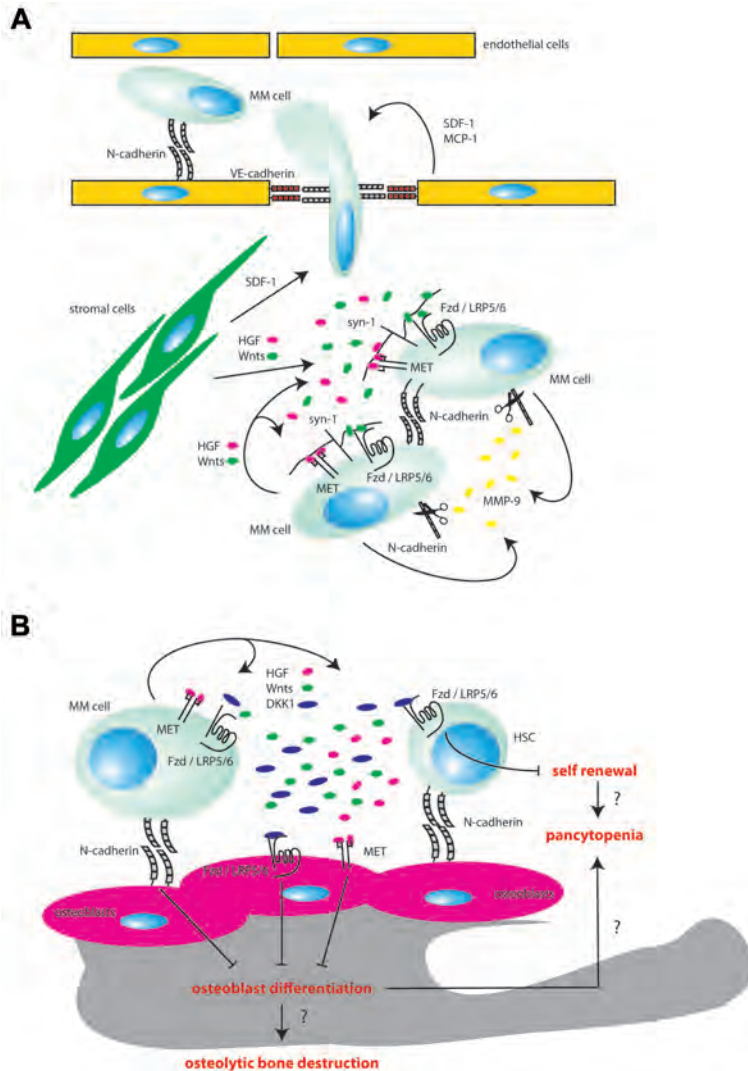


Figure 1. The role of HGF, Wnts, heparan sulfate proteoglycans, and N-cadherin in the pathogenesis of multiple myeloma.

(A) Auto- and/or paracrine activation of the Wnt and HGF/Met signaling cascade can be potentiated by the transmembrane HSPG, syndecan-1. Downstream signaling of these cascades could result in enhanced secretion of MMP-9, which is able to cleave N-cadherin. Together, these pathways might contribute to enhanced motility/migration of MM cells. **(B)** Potential interactions in the endosteal stem cell niche. The Wnt and HGF/Met signaling pathways, as well as N-cadherin, have been implicated in the development of osteolytic bone disease, via the inhibition of osteoblast differentiation. Besides, these molecules have been shown to play a role in the self renewal of hematopoietic stem cells, which suggest that these pathways could contribute to another characteristic of MM, *i.e.* pancytopenia. For details see text. Fzd, Frizzled; HSC, hematopoietic stem cell; MMP9, matrix metalloproteinase 9; syn-1, syndecan-1.

References

1. van der Voort R, Taher TE, Derksen PW et al. The hepatocyte growth factor/Met pathway in development, tumorigenesis, and B-cell differentiation. *Adv.Cancer Res.* 2000;79:39-90.
2. Borset M, Hjorth-Hansen H, Seidel C, Sundan A, Waage A. Hepatocyte growth factor and its receptor c-met in multiple myeloma. *Blood* 1996;88:3998-4004.
3. van der Voort, Taher TE, Keehnen RM et al. Paracrine regulation of germinal center B cell adhesion through the c-met-hepatocyte growth factor/scatter factor pathway. *J.Exp.Med.* 1997;185:2121-2131.
4. Weimar IS, de JD, Muller EJ et al. Hepatocyte growth factor/scatter factor promotes adhesion of lymphoma cells to extracellular matrix molecules via alpha 4 beta 1 and alpha 5 beta 1 integrins. *Blood* 1997;89:990-1000.
5. Seidel C, Borset M, Turesson I et al. Elevated serum concentrations of hepatocyte growth factor in patients with multiple myeloma. The Nordic Myeloma Study Group. *Blood* 1998;91:806-812.
6. Derksen PWB, de Gorter DJJ, Meijer HP et al. The hepatocyte growth factor/Met pathway controls proliferation and apoptosis in multiple myeloma. *Leukemia* 2003;17:764-774.
7. Hsiao LT, Lin JT, Yu IT et al. High serum hepatocyte growth factor level in patients with non-Hodgkin's lymphoma. *Eur.J.Haematol.* 2003;70:282-289.
8. Tjin EP, Derksen PW, Kataoka H, Spaargaren M, Pals ST. Multiple myeloma cells catalyze hepatocyte growth factor (HGF) activation by secreting the serine protease HGF-activator. *Blood* 2004;104:2172-2175.
9. Tjin EP, Bende RJ, Derksen PW et al. Follicular dendritic cells catalyze hepatocyte growth factor (HGF) activation in the germinal center microenvironment by secreting the serine protease HGF activator. *J.Immunol.* 2005;175:2807-2813.
10. Mahtouk K, Tjin EP, Spaargaren M, Pals ST. The HGF/MET pathway as target for the treatment of multiple myeloma and B-cell lymphomas. *Biochim.Biophys.Acta* 2010
11. Comoglio PM, Giordano S, Trusolino L. Drug development of MET inhibitors: targeting oncogene addiction and expedience. *Nat.Rev.Drug Discov.* 2008;7:504-516.
12. Trusolino L, Comoglio PM. Scatter-factor and semaphorin receptors: cell signalling for invasive growth. *Nat. Rev.Cancer* 2002;2:289-300.
13. Schmidt L, Duh FM, Chen F et al. Germline and somatic mutations in the tyrosine kinase domain of the MET proto-oncogene in papillary renal carcinomas. *Nat.Genet.* 1997;16:68-73.
14. Olivero M, Valente G, Bardelli A et al. Novel mutation in the ATP-binding site of the MET oncogene tyrosine kinase in a HPRCC family. *Int.J.Cancer* 1999;82:640-643.
15. Schmidt L, Junker K, Nakaigawa N et al. Novel mutations of the MET proto-oncogene in papillary renal carcinomas. *Oncogene* 1999;18:2343-2350.
16. Ma PC, Kijima T, Maulik G et al. c-MET mutational analysis in small cell lung cancer: novel juxtamembrane domain mutations regulating cytoskeletal functions. *Cancer Res.* 2003;63:6272-6281.
17. Ma PC, Jagadeeswaran R, Jagadeesh S et al. Functional expression and mutations of c-Met and its therapeutic inhibition with SU11274 and small interfering RNA in non-small cell lung cancer. *Cancer Res.* 2005;65:1479-1488.
18. Zaffaroni D, Spinola M, Galvan A et al. Met proto-oncogene juxtamembrane rare variations in mouse and humans: differential effects of Arg and Cys alleles on mouse lung tumorigenesis. *Oncogene* 2005;24:1084-1090.
19. Jagadeeswaran R, Jagadeeswaran S, Bindokas VP, Salgia R. Activation of HGF/c-Met pathway contributes to the reactive oxygen species generation and motility of small cell lung cancer cells. *Am.J.Physiol Lung Cell Mol. Physiol* 2007;292:L1488-L1494.
20. Graveel C, Su Y, Koeman J et al. Activating Met mutations produce unique tumor profiles in mice with selective duplication of the mutant allele. *Proc.Natl.Acad.Sci.U.S.A* 2004;101:17198-17203.

21. Verbeek S, Izon D, Hofhuis F et al. An HMG-box-containing T-cell factor required for thymocyte differentiation. *Nature* 1995;374:70-74.
22. Schilham MW, Wilson A, Moerer P et al. Critical involvement of Tcf-1 in expansion of thymocytes. *J.Immunol.* 1998;161:3984-3991.
23. Okamura RM, Sigvardsson M, Galceran J et al. Redundant regulation of T cell differentiation and TCRalpha gene expression by the transcription factors LEF-1 and TCF-1. *Immunity.* 1998;8:11-20.
24. Gounari F, Aifantis I, Khazaie K et al. Somatic activation of beta-catenin bypasses pre-TCR signaling and TCR selection in thymocyte development. *Nat.Immunol.* 2001;2:863-869.
25. Ioannidis V, Beermann F, Clevers H, Held W. The beta-catenin--TCF-1 pathway ensures CD4(+)CD8(+) thymocyte survival. *Nat.Immunol.* 2001;2:691-697.
26. Reya T, O'Riordan M, Okamura R et al. Wnt signaling regulates B lymphocyte proliferation through a LEF-1 dependent mechanism. *Immunity.* 2000;13:15-24.
27. Reya T, Duncan AW, Ailles L et al. A role for Wnt signalling in self-renewal of haematopoietic stem cells. *Nature* 2003;423:409-414.
28. Kirstetter P, Anderson K, Porse BT, Jacobsen SE, Nerlov C. Activation of the canonical Wnt pathway leads to loss of hematopoietic stem cell repopulation and multilineage differentiation block. *Nat.Immunol.* 2006;7:1048-1056.
29. Scheller M, Huelsken J, Rosenbauer F et al. Hematopoietic stem cell and multilineage defects generated by constitutive beta-catenin activation. *Nat.Immunol.* 2006;7:1037-1047.
30. Baba Y, Yokota T, Spits H et al. Constitutively active beta-catenin promotes expansion of multipotent hematopoietic progenitors in culture. *J.Immunol.* 2006;177:2294-2303.
31. Clevers H. Wnt/beta-catenin signaling in development and disease. *Cell* 2006;127:469-480.
32. Derksen PWB, Tjin E, Meijer HP et al. Illegitimate WNT signaling promotes proliferation of multiple myeloma cells. *Proc.Natl.Acad.Sci.U.S.A* 2004;101:6122-6127.
33. McWhirter JR, Neuteboom ST, Wancewicz EV et al. Oncogenic homeodomain transcription factor E2A-Pbx1 activates a novel WNT gene in pre-B acute lymphoblastoid leukemia. *Proc.Natl.Acad.Sci.U.S.A* 1999;96:11464-11469.
34. Mazieres J, You L, He B et al. Inhibition of Wnt16 in human acute lymphoblastoid leukemia cells containing the t(1;19) translocation induces apoptosis. *Oncogene* 2005;24:5396-5400.
35. Nygren MK, Dosen G, Hystad ME et al. Wnt3A activates canonical Wnt signalling in acute lymphoblastic leukaemia (ALL) cells and inhibits the proliferation of B-ALL cell lines. *Br.J.Haematol.* 2007;136:400-413.
36. Khan NI, Bradstock KF, Bendall LJ. Activation of Wnt/beta-catenin pathway mediates growth and survival in B-cell progenitor acute lymphoblastic leukaemia. *Br.J.Haematol.* 2007;138:338-348.
37. Lu D, Zhao Y, Tawatao R et al. Activation of the Wnt signaling pathway in chronic lymphocytic leukemia. *Proc. Natl.Acad.Sci.U.S.A* 2004;101:3118-3123.
38. Hoshida Y, Hongyo T, Jia X et al. Analysis of p53, K-ras, c-kit, and beta-catenin gene mutations in sinonasal NK/T cell lymphoma in northeast district of China. *Cancer Sci.* 2003;94:297-301.
39. Takahara M, Kishibe K, Bando N, Nonaka S, Harabuchi Y. P53, N- and K-Ras, and beta-catenin gene mutations and prognostic factors in nasal NK/T-cell lymphoma from Hokkaido, Japan. *Hum.Pathol.* 2004;35:86-95.
40. Polakis P. Wnt signaling and cancer. *Genes Dev.* 2000;14:1837-1851.
41. Guo Z, Dose M, Kovalovsky D et al. Beta-catenin stabilization stalls the transition from double-positive to single-positive stage and predisposes thymocytes to malignant transformation. *Blood* 2007;109:5463-5472.
42. Kawaguchi-Ihara N, Murohashi I, Nara N, Tohda S. Promotion of the self-renewal capacity of human acute leukemia cells by Wnt3A. *Anticancer Res.* 2008;28:2701-2704.
43. Fleming HE, Janzen V, Lo CC et al. Wnt signaling in the niche enforces hematopoietic stem cell quiescence and is necessary to preserve self-renewal in vivo. *Cell Stem Cell* 2008;2:274-283.
44. Cleaver AL, Beesley AH, Firth MJ et al. Gene-based outcome prediction in multiple cohorts of pediatric T-cell acute lymphoblastic leukemia: a Children's Oncology Group study. *Mol.Cancer* 2010;9:105.

45. Qiang YW, Walsh K, Yao L et al. Wnts induce migration and invasion of myeloma plasma cells. *Blood* 2005;106:1786-1793.
46. Sukhdeo K, Mani M, Zhang Y et al. Targeting the beta-catenin/TCF transcriptional complex in the treatment of multiple myeloma. *Proc.Natl.Acad.Sci.U.S.A* 2007;104:7516-7521.
47. Ashihara E, Kawata E, Nakagawa Y et al. beta-catenin small interfering RNA successfully suppressed progression of multiple myeloma in a mouse model. *Clin.Cancer Res.* 2009;15:2731-2738.
48. Dutta-Simmons J, Zhang Y, Gorgun G et al. Aurora kinase A is a target of Wnt/beta-catenin involved in multiple myeloma disease progression. *Blood* 2009;114:2699-2708.
49. Schmidt M, Sievers E, Endo T et al. Targeting Wnt pathway in lymphoma and myeloma cells. *Br.J.Haematol.* 2009;144:796-798.
50. Tian E, Zhan F, Walker R et al. The role of the Wnt-signaling antagonist DKK1 in the development of osteolytic lesions in multiple myeloma. *N.Engl.J.Med.* 2003;349:2483-2494.
51. Qiang YW, Chen Y, Stephens O et al. Myeloma-derived Dickkopf-1 disrupts Wnt-regulated osteoprotegerin and RANKL production by osteoblasts: a potential mechanism underlying osteolytic bone lesions in multiple myeloma. *Blood* 2008;112:196-207.
52. Qiang YW, Barlogie B, Rudikoff S, Shaughnessy JD, Jr. Dkk1-induced inhibition of Wnt signaling in osteoblast differentiation is an underlying mechanism of bone loss in multiple myeloma. *Bone* 2008;42:669-680.
53. Yaccoby S, Wezeman MJ, Zangari M et al. Inhibitory effects of osteoblasts and increased bone formation on myeloma in novel culture systems and a myelomatous mouse model. *Haematologica* 2006;91:192-199.
54. Klein B, Zhang XG, Jourdan M et al. Paracrine rather than autocrine regulation of myeloma-cell growth and differentiation by interleukin-6. *Blood* 1989;73:517-526.
55. Abe M, Hiura K, Wilde J et al. Osteoclasts enhance myeloma cell growth and survival via cell-cell contact: a vicious cycle between bone destruction and myeloma expansion. *Blood* 2004;104:2484-2491.
56. Yaccoby S, Ling W, Zhan F et al. Antibody-based inhibition of DKK1 suppresses tumor-induced bone resorption and multiple myeloma growth in vivo. *Blood* 2007;109:2106-2111.
57. Fulciniti M, Tassone P, Hideshima T et al. Anti-DKK1 mAb (BHQ880) as a potential therapeutic agent for multiple myeloma. *Blood* 2009;114:371-379.
58. Heath DJ, Chantry AD, Buckle CH et al. Inhibiting Dickkopf-1 (Dkk1) removes suppression of bone formation and prevents the development of osteolytic bone disease in multiple myeloma. *J.Bone Miner.Res.* 2009;24:425-436.
59. Edwards CM, Edwards JR, Lwin ST et al. Increasing Wnt signaling in the bone marrow microenvironment inhibits the development of myeloma bone disease and reduces tumor burden in bone in vivo. *Blood* 2008;111:2833-2842.
60. Borset M, Hjertner O, Yaccoby S, Epstein J, Sanderson RD. Syndecan-1 is targeted to the uropods of polarized myeloma cells where it promotes adhesion and sequesters heparin-binding proteins. *Blood* 2000;96:2528-2536.
61. Mahtouk K, Cremer FW, Reme T et al. Heparan sulphate proteoglycans are essential for the myeloma cell growth activity of EGF-family ligands in multiple myeloma. *Oncogene* 2006;25:7180-7191.
62. Yang Y, MacLeod V, Dai Y et al. The syndecan-1 heparan sulfate proteoglycan is a viable target for myeloma therapy. *Blood* 2007;110:2041-2048.
63. Khotskaya YB, Dai Y, Ritchie JP et al. Syndecan-1 is required for robust growth, vascularization, and metastasis of myeloma tumors in vivo. *J.Biol.Chem.* 2009;284:26085-26095.
64. Dai Y, Yang Y, MacLeod V et al. HSulf-1 and HSulf-2 are potent inhibitors of myeloma tumor growth in vivo. *J.Biol.Chem.* 2005;280:40066-40073.
65. Ai X, Do AT, Lozynska O et al. QSulf1 remodels the 6-O sulfation states of cell surface heparan sulfate proteoglycans to promote Wnt signaling. *J.Cell Biol.* 2003;162:341-351.
66. Viviano BL, Paine-Saunders S, Gasiunas N, Gallagher J, Saunders S. Domain-specific modification of heparan sulfate by QSulf1 modulates the binding of the bone morphogenetic protein antagonist Noggin. *J.Biol.Chem.* 2004;279:5604-5611.

67. Wang S, Ai X, Freeman SD et al. QSulf1, a heparan sulfate 6-O-endosulfatase, inhibits fibroblast growth factor signaling in mesoderm induction and angiogenesis. *Proc.Natl.Acad.Sci.U.S.A* 2004;101:4833-4838.
68. Bret C, Hose D, Reme T et al. Expression of genes encoding for proteins involved in heparan sulphate and chondroitin sulphate chain synthesis and modification in normal and malignant plasma cells. *Br.J.Haematol.* 2009;145:350-368.
69. Keats JJ, Reiman T, Maxwell CA et al. In multiple myeloma, t(4;14)(p16;q32) is an adverse prognostic factor irrespective of FGFR3 expression. *Blood* 2003;101:1520-1529.
70. Chng WJ, Kuehl WM, Bergsagel PL, Fonseca R. Translocation t(4;14) retains prognostic significance even in the setting of high-risk molecular signature. *Leukemia* 2008;22:459-461.
71. Dring AM, Davies FE, Fenton JA et al. A global expression-based analysis of the consequences of the t(4;14) translocation in myeloma. *Clin.Cancer Res.* 2004;10:5692-5701.
72. Lauring J, Abukhdeir AM, Konishi H et al. The multiple myeloma associated MMSET gene contributes to cellular adhesion, clonogenic growth, and tumorigenicity. *Blood* 2008;111:856-864.
73. Wheelock MJ, Shintani Y, Maeda M, Fukumoto Y, Johnson KR. Cadherin switching. *J.Cell Sci.* 2008;121:727-735.
74. Blaschuk OW, Devemy E. Cadherins as novel targets for anti-cancer therapy. *Eur.J.Pharmacol.* 2009;625:195-198.
75. Hazan RB, Phillips GR, Qiao RF, Norton L, Aaronson SA. Exogenous expression of N-cadherin in breast cancer cells induces cell migration, invasion, and metastasis. *J.Cell Biol.* 2000;148:779-790.
76. Salomon D, Ayalon O, Patel-King R, Hynes RO, Geiger B. Extrajunctional distribution of N-cadherin in cultured human endothelial cells. *J.Cell Sci.* 1992;102 (Pt 1):7-17.
77. Navarro P, Ruco L, Dejana E. Differential localization of VE- and N-cadherins in human endothelial cells: VE-cadherin competes with N-cadherin for junctional localization. *J.Cell Biol.* 1998;140:1475-1484.
78. Marie PJ. Role of N-cadherin in bone formation. *J.Cell Physiol* 2002;190:297-305.
79. Stains JP, Civitelli R. Cell-cell interactions in regulating osteogenesis and osteoblast function. *Birth Defects Res.C.Embryo.Today* 2005;75:72-80.
80. Hunter I, McGregor D, Robins SP. Caspase-dependent cleavage of cadherins and catenins during osteoblast apoptosis. *J.Bone Miner.Res.* 2001;16:466-477.
81. Oshima T, Abe M, Asano J et al. Myeloma cells suppress bone formation by secreting a soluble Wnt inhibitor, sFRP-2. *Blood* 2005;106:3160-3165.
82. Standal T, Abildgaard N, Fagerli UM et al. HGF inhibits BMP-induced osteoblastogenesis: possible implications for the bone disease of multiple myeloma. *Blood* 2007;109:3024-3030.
83. Weitzmann MN, Roggia C, Toraldo G, Weitzmann L, Pacifici R. Increased production of IL-7 uncouples bone formation from bone resorption during estrogen deficiency. *J.Clin.Invest* 2002;110:1643-1650.
84. Giuliani N, Colla S, Morandi F et al. Myeloma cells block RUNX2/CBFA1 activity in human bone marrow osteoblast progenitors and inhibit osteoblast formation and differentiation. *Blood* 2005;106:2472-2483.
85. Hosokawa K, Arai F, Yoshihara H et al. Function of oxidative stress in the regulation of hematopoietic stem cell-niche interaction. *Biochem.Biophys.Res.Commun.* 2007;363:578-583.
86. Kiel MJ, Acar M, Radice GL, Morrison SJ. Hematopoietic stem cells do not depend on N-cadherin to regulate their maintenance. *Cell Stem Cell* 2009;4:170-179.
87. Li P, Zon LI. Resolving the controversy about N-cadherin and hematopoietic stem cells. *Cell Stem Cell* 2010;6:199-202.
88. Weijer K, Uittenbogaart CH, Voordouw A et al. Intrathymic and extrathymic development of human plasmacytoid dendritic cell precursors in vivo. *Blood* 2002;99:2752-2759.
89. van Rijn RS, Simonetti ER, Hagenbeek A et al. A new xenograft model for graft-versus-host disease by intravenous transfer of human peripheral blood mononuclear cells in RAG2-/- gammac-/- double-mutant mice. *Blood* 2003;102:2522-2531.
90. Mutis T, van Rijn RS, Simonetti ER et al. Human regulatory T cells control xenogeneic graft-versus-host disease induced by autologous T cells in RAG2-/-gammac-/- immunodeficient mice. *Clin.Cancer Res.* 2006;12:5520-5525.

91. Bellamy WT, Odeleye A, Finley P et al. An in vivo model of human multidrug-resistant multiple myeloma in SCID mice. *Am.J.Pathol.* 1993;142:691-697.
92. Reme T, Gueydon E, Jacquet C, Klein B, Brochier J. Growth and immortalization of human myeloma cells in immunodeficient severe combined immunodeficiency mice: a preclinical model. *Br.J.Haematol.* 2001;114:406-413.
93. Tassone P, Neri P, Carrasco DR et al. A clinically relevant SCID-hu in vivo model of human multiple myeloma. *Blood* 2005;106:713-716.
94. Mitsiades CS, Mitsiades NS, Bronson RT et al. Fluorescence imaging of multiple myeloma cells in a clinically relevant SCID/NOD in vivo model: biologic and clinical implications. *Cancer Res.* 2003;63:6689-6696.
95. Caceres G, Zhu XY, Jiao JA et al. Imaging of luciferase and GFP-transfected human tumours in nude mice. *Luminescence.* 2003;18:218-223.
96. Derksen PWB, Keehnen RMJ, Evers LM et al. Cell surface proteoglycan syndecan-1 mediates hepatocyte growth factor binding and promotes Met signaling in multiple myeloma. *Blood* 2002;99:1405-1410.
97. Alexander CM, Reichsman F, Hinkes MT et al. Syndecan-1 is required for Wnt-1-induced mammary tumorigenesis in mice. *Nat.Genet.* 2000;25:329-332.
98. Hov H, Tian E, Holien T et al. c-Met signaling promotes IL-6-induced myeloma cell proliferation. *Eur.J.Haematol.* 2009;82:277-287.
99. Wu B, Crampton SP, Hughes CC. Wnt signaling induces matrix metalloproteinase expression and regulates T cell transmigration. *Immunity.* 2007;26:227-239.
100. Vande Broek I, Asosingh K, Allegaert V et al. Bone marrow endothelial cells increase the invasiveness of human multiple myeloma cells through upregulation of MMP-9: evidence for a role of hepatocyte growth factor. *Leukemia* 2004;18:976-982.
101. Kessenbrock K, Plaks V, Werb Z. Matrix metalloproteinases: regulators of the tumor microenvironment. *Cell* 2010;141:52-67.
102. Dwivedi A, Slater SC, George SJ. MMP-9 and -12 cause N-cadherin shedding and thereby beta-catenin signalling and vascular smooth muscle cell proliferation. *Cardiovasc.Res.* 2009;81:178-186.
103. Suyama K, Shapiro I, Guttman M, Hazan RB. A signaling pathway leading to metastasis is controlled by N-cadherin and the FGF receptor. *Cancer Cell* 2002;2:301-314.
104. Hulit J, Suyama K, Chung S et al. N-cadherin signaling potentiates mammary tumor metastasis via enhanced extracellular signal-regulated kinase activation. *Cancer Res.* 2007;67:3106-3116.
105. Weimar IS, Miranda N, Muller EJ et al. Hepatocyte growth factor/scatter factor (HGF/SF) is produced by human bone marrow stromal cells and promotes proliferation, adhesion and survival of human hematopoietic progenitor cells (CD34+). *Exp.Hematol.* 1998;26:885-894.
106. Zhang J, Niu C, Ye L et al. Identification of the haematopoietic stem cell niche and control of the niche size. *Nature* 2003;425:836-841.

9

Summary

Nederlandse samenvatting

Dankwoord

Curriculum Vitae

Publications by the author

Summary

B and T cell development and differentiation are regulated multistep processes, which highly depend on the interactions with the microenvironment. This microenvironment, composed of APCs, supporting cells as FDCs (in B cell development) and thymic epithelial cells (in T cell development), and co-stimulatory molecules (on T-helper cells), provides proliferation and survival factors, but more importantly selects the lymphocytes based on antigen recognition. This highly proliferative process of selection also comes with a risk and is the probable source of many types of lymphoproliferative disease, due to unfortunate introduction of mutation in oncogenes and tumor suppressor genes, and chromosomal translocations. Despite the presence of these genetic aberrations, which renders lymphoma cell more resistant for apoptotic stimuli, these cells still need microenvironmental stimuli for proliferation and progression. In this thesis we have explored the role of two potent oncogenic pathways, *i.e.* the HGF/MET and Wnt signaling pathways, substantiated the role of HSPGs and identified a new player, *i.e.* N-cadherin, in the pathogenesis of malignant lymphoma and myeloma.

In chapter 2, we examined the expression of MET in a large panel of B cell malignancies. We have found that MET is expressed in some cases of follicular lymphoma, Burkitt's lymphoma, and chronic lymphocytic leukemia, and more frequently expressed in multiple myeloma (MM; 48%) and diffuse large B cell lymphoma (DLBCL; 30%). No indication of amplification of the MET gene was found, whereas occasional missense mutations in the juxtamembrane and tyrosine kinase domain were detected. Furthermore, we have demonstrated that HGF is produced within the DLBCL microenvironment, probably by cells of the monocyte/macrophage lineage, suggesting that DLBCL cells are stimulated in a paracrine fashion. In addition, we show that DLBCL cells themselves produce HGFA, which efficiently autocatalyzes HGF activation, thereby generating a constant source of active HGF in the microenvironment. HGF stimulation of DLBCL phosphorylated multiple downstream targets, including MAPKs ERK1 and -2, and PKB and its substrates GSK3 and FOXO3a, which are linked to proliferative- and survival functions. Finally, HGF induced PI3K-dependent adhesion of DLBCL cells to VCAM-1 and fibronectin.

In Chapter 3, we have explored the role of the Wnt signaling pathway in non Hodgkin lymphoma (NHL) by screening a substantial set of NHL, including all major WHO categories, for nuclear expression of β -catenin, a hallmark of "active" Wnt signaling. This screening showed that nuclear β -catenin was predominantly expressed in T cell lymphomas, *i.e.* precursor-T lymphoblastic lymphoma (T-LBL/ALL; 33%) and mature T cell lymphomas (40%), and could be detected in some case of B-NHL, namely B-LBL/ALL and DLBCL. In non-malignant B and T cells, within a lymph node and the thymus respectively, nuclear β -catenin expression was absent. In the majority of the mature T cell lymphomas with aberrant Wnt pathway activation this was caused by *CTNNB1* mutations (3/4), whereas in T-LBL/ALL mutations in *CTNNB1* were not so frequent (1/9). All these mutations were gain-of-function mutations, resulting in the hyperactivation of the Wnt pathway. Although activation of the Wnt pathway was more frequently observed in single positive T cells, it was not restricted to a single state of maturation. Next we showed that the Wnt pathway is constitutively activated in T-LBL/ALL cell lines and that conditioned medium obtained from these cells can activate TCF-mediated transcription, suggesting the presence of an autocrine loop, constitutively

activating the pathway. Functional studies indicate that Wnt pathway activation results in enhanced non-phosphorylated (active) β -catenin, which translocates to the nucleus and may promote lymphoma growth.

In MM, the malignant plasma cells can secrete the Wnt signaling inhibitor Dickkopf-1 (DKK1), which contributes to osteolytic bone disease by inhibiting osteoblast differentiation. Paradoxically, however, the Wnt/ β -catenin pathway is frequently aberrantly activated in MM cells, most likely by para- and/or autocrine produced Wnts, resulting in enhanced proliferation. Thus, DKK1 could also act as a tumor suppressor by inhibition of Wnt signaling in the MM cells. In chapter 4 we reconcile these apparently conflicting findings by showing that DKK1 expression is lost in most MM cell lines and a subset of patients with advanced MM. This loss is correlated with activation of the Wnt pathway, as demonstrated by increased nuclear accumulation of β -catenin. Furthermore, analysis of 345 MM patients by microarray for Wnt components, *i.e.* Wnts, Fzds, and LRP6, revealed frequent co-expression of Fzs, LRP6, as well as various Wnts, suggesting the ability to respond to Wnts produced within the BM microenvironment or to evoke autocrine activation of the Wnt pathway. In addition, we show that expression of Wnt/ β -catenin target genes correlates with an increased gene expression-based proliferation index, indicating that Wnt pathway activation contributes to increased proliferation of MM cells. Analysis of the DKK1 promoter revealed CpG island methylation in several MM cell lines as well as in MM cells from patients with advanced MM. Moreover, demethylation of the DKK1 promoter restores DKK1 expression, which results in inhibition of β -catenin/TCF-mediated gene transcription in MM lines.

Chapter 5 describes the development of a new mouse model for MM that offers an optimal platform for preclinical evaluation of therapies. To this end we transduced seven different human MM cell lines with a retroviral vector encoding a green fluorescent protein (GFP)-luciferase fusion protein and injected them in RAG2^{-/-} γ c^{-/-} mice. Bioluminescence imaging was used to semi-quantitatively monitor the *in vivo* engraftment, outgrowth and distribution of the MM cell lines. Five out of seven tested MM cell lines progressed as myeloma-like tumors predominantly in the bone marrow (BM); the two other lines showed additional growth in soft tissues, *i.e.* liver and intestinal tract. In our model bioluminescent imaging appeared superior to free light chain-based monitoring and also allowed semi-quantitative monitoring of individual foci of MM. Tumors treated with radiotherapy showed temporary regression. However, infusion of allogeneic peripheral blood mononuclear cells resulted in the development of xenogeneic graft-versus-host-disease and a powerful cell dose-dependent graft-versus-myeloma effect, resulting in complete eradication of established tumors, depending on the *in vitro* immunogenicity of the inoculated MM cells.

In chapter 6, we show that inducible RNAi-mediated knockdown of syndecan-1 in human MM cells leads to reduced syndecan-1 and total cell surface heparan sulfate expression, resulting in diminished growth rates and a strong increase of apoptosis. Next, we show that knockdown of exostin-1 (EXT1), a co-polymerase critical for HS-chain biosynthesis, had similar *in vitro* functional effects. By employing the innovative myeloma xenotransplant model, described in chapter 5, we demonstrate that induction of EXT1 knockdown *in vivo* dramatically suppresses the growth of BM-localized myeloma. These *in vivo* effects were seen both in mice treated following inoculation, as well as in mice treated with established tumors, and absent in mice infused with control MM cell lines.

Within the BM microenvironment, N-cadherin plays an important role in bone homeostasis and has been implicated in the interaction between hematopoietic stem cells and osteoblasts.

In chapter 7, we show that a subset of human MM cell lines express N-cadherin at the cell-cell junctions, which associates with β -catenin, and mediates homophilic adhesion. Furthermore, the malignant plasma cells in approximately half of the MM patients, belonging to specific genetic subgroups including the 4p16 translocation, aberrantly express the homophilic adhesion molecule N-cadherin. Functional evaluation of N-cadherin-mediated cell-substrate or homotypic cell-cell adhesion, showed that these interactions do not contribute to MM cell growth *in vitro*. However, N-cadherin seems to potentiate MM motility *in vitro*, and directly mediates the BM localization/retention of MM cells *in vivo*. This facilitates a close interaction between MM cells and N-cadherin positive osteoblasts. In addition, we show that N-cadherin-mediated interaction with osteoblasts directly contributes to the inhibition of osteoblastogenesis.

Nederlandse samenvatting

Het lichaam staat onder constante bedreiging van infectie van micro-organisme (bijvoorbeeld bacteriën, virussen en parasieten). Het afweersysteem biedt ons de bescherming tegen deze ziekteverwekkers. Binnen het afweersysteem spelen B en T cellen een centrale rol. De B cellen zijn verantwoordelijk voor de productie van antistoffen, terwijl de T cellen geïnfecteerde cellen onschadelijk maken. Alvorens een B cel antistoffen kan produceren, moet de B cel zich ontwikkelen tot een antistof-producerende plasma cel. Deze ontwikkeling start in het beenmerg, waarna de B cellen het beenmerg verlaten en door het lichaam circuleren via bloed- en lymfobaan naar secundaire lymfoïde organen zoals de milt. Wanneer B cellen daar in contact komen met een antigeen (= een deeltje dat een afweerreactie veroorzaakt), raken de B cellen geactiveerd, gaan delen en ontwikkelen zich tot plasma cellen en geheugen B cellen, welke snel kunnen reageren op een herhaalde infectie met hetzelfde micro-organisme. T cellen ontwikkelen zich in de thymus, waar voorloper cellen zich via een aantal selectie-processen ontwikkelen tot rijpe T cellen. Deze rijpe T cellen verlaten de thymus via de bloedbaan en circuleren evenals de B cellen naar de secundaire lymfoïde organen, waar ze “wachten” tot een antigeen wordt gepresenteerd. Na presentatie van het antigeen, vermeerderen deze cellen zich en vallen de geïnfecteerde cellen aan. Tijdens het leven en het doorlopen van de verschillende ontwikkelingsstadia bestaat er een redelijke kans dat B en T cellen fouten in het erfelijke materiaal (bijvoorbeeld mutaties) oplopen, die onder normale omstandigheden worden hersteld. Niet gerepareerde fouten in genen die betrokken zijn bij de groei, overleving, adhesie, en migratie van cellen, kunnen leiden tot ontregelde expressie en/of functie. Voor het ontstaan van kanker echter, zijn meerdere fouten in de genen nodig. Ondanks het optreden van fouten in het genetische materiaal, is de micro-omgeving van de tumor erg bepalend voor de groei. In dit proefschrift hebben we gekeken naar de rol van de micro-omgeving, in het bijzonder twee groeifactoren met bijbehorende signaleringsroutes, de hepatocyte groeifactor (HGF) en Wnt, heparansulfaat proteoglycanen, en N-cadherin, in de ontwikkeling van non Hodgkin lymfomen en multipel myeloom (MM, ook: de ziekte van Kahler).

In hoofdstuk 2 hebben we gekeken naar de expressie van MET, de receptor voor HGF, in een groot aantal B cel non Hodgkin lymfomen (NHL). Verhoogde MET expressie werd gedetecteerd in een klein aantal folliculair lymfomen, Burkitt's lymfomen, en chronische lymfatische leukemie, en in een hoog percentage van de MM en diffuus grootcellige B cel lymfomen (DLBCL). Amplificaties van het MET gen werden niet gevonden. Wel hebben wij twee verschillende missense mutaties in MET gevonden (in de juxtamembraan- en tyrosine kinase domein) in meerdere lymfomen. HGF expressie is in veel van de MET-positieve primaire DLBCL tumoren gedetecteerd. De HGF wordt waarschijnlijk geproduceerd door de aanwezige monocytten en/of macrofagen en suggereert dat DLBCL cellen via een paracrine activatie mechanisme worden gestimuleerd. Stimulatie van DLBCL cellen met HGF resulteert in de fosforylatie van een reeks signaleringsmoleculen, waaronder de MAPKs, PKB en zijn substraten GSK3 en Foxo3a. Activatie van deze eiwitten kan leiden tot biologische effecten als celdgroei en –overleving. Verder laten wij zien dat HGF activatie van DLBCL cellen kan leiden tot adhesie, wat afhankelijk is van het signaleringsmolecuul PI3K. HGF kan alleen in een actieve vorm MET activeren en biologische effecten induceren. Activatie van HGF is de bepalende stap in de HGF/MET signaleringsroute. Wij laten hier zien dat DLBCL cellen HGFA

produceren, wat efficiënt HGF activatie katalyseert. Hierdoor is er een continue aanmaak van actief HGF in de tumor micro-omgeving, wat de groei en progressie van DLBCL kan bevorderen.

Onder normale omstandigheden is de Wnt signalering betrokken bij de overleving en expansie van lymfocyten voorloper cellen. Actieve Wnt signalering wordt gekenmerkt door ophoping en nucleaire lokalisatie van β -catenin. In hoofdstuk 3 hebben we gekeken naar de rol van Wnt signalering in B en T cel maligniteiten, door een groot aantal lymfomen te evalueren voor nucleaire lokalisatie van β -catenin. Wij laten zien dat nucleaire lokalisatie van β -catenin voornamelijk voorkomt in T cel lymfomen. In een deel van deze tumoren wordt deze ophoping en nucleaire lokalisatie veroorzaakt door mutaties in β -catenin. Deze mutaties voorkomen dat β -catenin wordt afgebroken en veroorzaken een voortdurende (constitutieve) activatie van de Wnt signaleringsroute. Verder laten wij zien dat de resterende T cel lymfomen zelf Wnts produceren, hetgeen suggereert dat ze zichzelf kunnen activeren (=autocriene activatie). Activatie van de Wnt signaleringsroute in deze tumoren leidt inderdaad tot ophoping en nucleaire translocatie van β -catenin, wat de groei van de T cel lymfomen zou kunnen bevorderen.

MM is de op één na meest voorkomende bloedkanker en wordt veroorzaakt door woekering van kwaadaardige plasma cellen (myeloom cellen) in het beenmerg (BM). Deze ziekte gaat vaak gepaard met botafbraak, nierafwijking, anemie (=bloedarmoede) en verstoorde afweer. Myeloom cellen scheiden een remmer van de Wnt signalering, genaamd Dickkopf-1 (DKK1) uit, wat een bijdrage levert aan de botafbraak in deze patiënten. Hier staat tegenover dat de Wnt signaleringsroute in MM vaak ontspoord is, waarschijnlijk door para- en/of autocrien geproduceerde Wnts, resulterend in verbeterde proliferatie. Dit zou er op kunnen duiden dat DKK1 functioneert als een tumor suppressor door Wnt signalering in MM te remmen.

In hoofdstuk 4 hebben we geprobeerd deze ogenschijnlijk tegenstrijdige bevindingen met elkaar te verzoenen, door aan te tonen dat de DKK1 expressie verloren gaat in de meeste MM cellijnen en een subset van patiënten met gevorderde MM. Dit verlies is gecorreleerd met de activatie van de Wnt signaleringsroute, zoals blijkt uit de toegenomen nucleaire lokalisatie van β -catenin. Analyse van 345 MM patiënten door middel van microarray voor de Wnt componenten, zoals Wnts, Frizzled receptors en LRP6, laat zien dat deze componenten vaak gezamenlijk tot expressie komen. Dit suggereert dat myeloom cellen in staat zijn om te reageren op Wnts geproduceerd in de micro-omgeving en/of de aanwezigheid van autocriene activatie van de Wnt signaleringsroute. Daarnaast laten microarray analyses van MM patiënten een correlatie zien tussen actieve Wnt signalering en proliferatie, wat aangeeft dat Wnt signalering bijdraagt aan verhoogde proliferatie van MM cellen. Een van de redenen waardoor DKK1 expressie in de progressie van de ziekte verloren zou kunnen gaan is door methylering van de DKK1 promotor. Analyse van de DKK1 promotor laat inderdaad zien dat methylering van de DKK1 promotor voorkomt in verschillende MM cellijnen alsook in myeloom cellen van patiënten met gevorderde MM. Demethylering van de DKK1 promotor herstelt DKK1 expressie, wat resulteert in remming van Wnt signaleringsroute in MM cellijnen.

Om een ziektebeeld goed te kunnen bestuderen zijn representatieve diermodellen een vereiste. Hoofdstuk 5 beschrijft de ontwikkeling van een nieuw muismodel voor MM dat een optimaal platform voor preklinische evaluatie van therapieën biedt. Daartoe hebben we zeven verschillende MM cellijnen gemarkeerd met een fusie-eiwit, bestaande uit green fluorescent protein (GFP) en luciferase, die vervolgens in immuundeficiënte muizen

(RAG2^{-/yc^{-/-}}) werden geïnjecteerd. Luciferase is een enzym dat in de aanwezigheid van zuurstof en ATP, luciferine kan omzetten in oxoluciferine en licht (fotonen). Dit licht kan met behulp van bioluminescentie imaging (BLI) worden gedetecteerd en gekwantificeerd. Wij laten hier zien dat, door de muizen in te spuiten met luciferine, wij in staat zijn om m.b.v. BLI op een semikwantitatieve manier toezicht te houden op de *in vivo* implantatie, uitgroei en de distributie van de MM cellijnen. Vijf van de zeven geteste MM cellijnen groeide als myeloom-achtige tumoren voornamelijk in het BM, de twee andere lijnen groeide ook in zachte weefsels, dat wil zeggen in de lever en het darmstelsel. In ons model bleek BLI superieur ten opzichte van het monitoren van de immunoglobuline lichte keten in de urine, een gebruikelijke methode voor de diagnose van MM. Behandeling van tumoren met radiotherapie laat een tijdelijke afname van het tumorvolume zien. Echter, een infusie van allogene perifere bloed mononucleaire cellen resulteerde in de ontwikkeling van xenogene graft-versus-host ziekte en een celdosis-afhankelijke graft-versus-myeloom effect. Met als gevolg het volledig verdwijnen van de tumoren.

Syndecan-1 expressie is een van de kenmerken waarmee een (maligne) plasma cel zich onderscheidt van andere B cellen. Dit transmembraan eiwit, met zijn heparansulfaat (HS) zijketens, speelt een belangrijke rol in de presentatie van groeifactoren en hierdoor ook in de pathogenese van MM. In hoofdstuk 6 laten we zien dat induceerbare RNAi-gemedieerde knockdown van syndecan-1 in myeloom cellen leidt tot een vermindering van syndecan-1 en de totale HS expressie, wat resulteert in verminderde groei en een sterke toename van apoptose. Vervolgens laten we zien dat knock-down van exostin-1 (EXT1), een enzym dat van cruciaal belang is voor HS-keten biosynthese, *in vitro* vergelijkbare effecten heeft. Door toepassing van het myeloom muizenmodel, beschreven in hoofdstuk 5, laten we zien dat knockdown van EXT1 *in vivo* de groei van BM-gelokaliseerde tumoren drastisch onderdrukt. Deze *in vivo* effecten werden waargenomen in muizen behandeld direct na inspuiten van de myeloom cellen, evenals in muizen pas behandeld na vorming van tumoren. In muizen ingespoten met controle myeloom cellijnen waren deze effecten afwezig.

Binnen de BM micro-omgeving speelt het adhesiemolecuul N-cadherin een belangrijke rol in de bothomeostase en is het betrokken bij de interactie tussen hematopoietische stamcellen en osteoblasten. In hoofdstuk 7 laten we zien dat een subset van de MM cellijnen N-cadherin tot expressie brengt en dat er een fysieke interactie bestaat tussen N-cadherin en β -catenin. Verder laten we zien dat N-cadherin adhesie van myeloom cellen aan andere N-cadherin moleculen (bijvoorbeeld op andere cellen) veroorzaakt. In ongeveer de helft van de MM patiënten brengen de myeloom cellen N-cadherin tot expressie. Expressie van N-cadherin lijkt vooral voor te komen bij patienten met een 4p16 translocatie. Uit functionele evaluatie van de N-cadherin-gemedieerde cel-substraat of homotypische cel-cel adhesie, blijkt dat deze interacties niet bijdragen aan MM celgroei *in vitro*. Echter, N-cadherin lijkt het migrerend vermogen van de myeloom cellen te versterken *in vitro*, en speelt een belangrijke rol bij de BM-lokalisatie van MM *in vivo*. Hierdoor zou er een directe interactie met de N-cadherin-positieve osteoblasten in het BM kunnen ontstaan. Hierop voortbordurend, laten wij zien dat deze N-cadherin-gemedieerde interactie met osteoblasten rechtstreeks bijdraagt aan de remming van osteoblastogenese (=botontwikkeling).

Dankwoord

Ook dit proefschrift eindigt met een dankwoord. Een dank aan een ieder die mij experimenteel en/of mentaal hebben bijgestaan tijdens deze zware, maar ook vooral mooie periode.

Laat ik beginnen met het bedanken van de degene die mij oorspronkelijk heeft geïnspireerd om de wetenschap te gaan beoefenen, Paola Casarosa. Jouw enthousiasme en bevoegenheid werkten erg aanstekelijk en hebben bijgedragen aan de keuze om na mijn studie het onderzoek in te gaan.

Vervolgens wil ik graag mijn promotor Steven en mijn co-promotor Marcel bedanken voor hun vertrouwen en de mogelijkheid die jullie mij hebben geboden om te promoveren. Steven, onze bezoeken aan de Wnt-meetings waren gezellig en leerzaam. Maar vooral onze gesprekken, jouw kritische houding en jouw ideeën over de wetenschap zijn altijd erg interessant. Marcel, jouw ervaring en inzicht hebben de manuscripten gemaakt tot wat ze nu zijn. Verder is de balans die jij tussen thuis en werk weet te behouden bewonderenswaardig. Ook de biertjes en de discussies tot in de late uurtjes op de congressen waren een aangename afwisseling. Ik heb veel van jullie beiden geleerd.

Kamergenoten: Febe, Jurrit en in het bijzonder Rogier, wat een mooie tijd heb ik met jullie beleefd. Onze uitstapjes naar de “Ep” zijn onvergetelijk. Febe onze “vrouwelijke” touch van de kamer. Jouw kijk op data is verfrissend en verhelderend. Maar ook de gesprekken met jou over eten en wijn, waren zeer welkom. Jurrit onze “whizzkid” met kantoorhumor, jouw kennis van computers en software heeft mij toch meer malen uit de brand geholpen, met name je hulp toen mijn laptop met al mijn promotiedata crashte zal mij altijd bijblijven. En dan natuurlijk Rogier, mijn paranimf en “tweelingbroer”, ook al begrijpen wij allebei de verwisselingen nog steeds niet. Jouw rust en relaxte houding zijn een voorbeeld voor mij. Ik heb met veel plezier met jou samengewerkt. Onze nachtelijke experimenten in het UMCU en de lol die we hadden tijdens deze langdurige metingen zijn prachtige herinneringen aan een mooie periode. Ik hoop dat we de vriendschap die ontstaan is, zullen voortzetten.

De “oude garde”: Ronald, Elles, David, Esther T. en Laura, ik heb veel van jullie geleerd, maar bovenal was het natuurlijk enorm gezellig, bedankt daarvoor! Richard B., ook jij behoort eigenlijk tot de oude garde, maar toch ook weer niet. De steunpilaar van onze kamer, een wandelende encyclopedie. Je was een fijne collega, ik mis de gezamenlijke treinreis naar Zaandam en onze conversaties nog steeds. Jij kon alles weer in perspectief zetten.

Het bestaan van een “oude garde” houdt automatisch in dat er een jonge nieuwe garde bestaat, Robbert, Martine, Martin en Harmen, ook al heb ik kort met jullie gewerkt, bedankt voor de morele en experimentele steun. Ik wens jullie ook veel succes met het afronden van jullie projecten. Kinga, ook jij behoort tot deze groep, maar jij zult bij mij altijd een speciale plek hebben. Je begon als mijn student, maar al snel was duidelijk dat jij meer in je mars hebt. Toen Steven vervolgens vroeg of ik dacht dat jij in staat was om een promotietraject succesvol af te ronden, kon ik daar ook alleen maar instemmend op reageren. Er schuilt een geweldige wetenschapper in jou, veel succes met de laatste loodjes.

En dan de analytische ondersteuning die ik heb mogen genieten, allereerst Esther S., Monique en Helen, zonder jullie voorwerk was de β -catenin paper er nooit geweest. Helen, die mij in de eerste periode aan het handje moest nemen, die mij heeft leren FACS'en, ach, wat heb je me niet geleerd. Esther en Monique, altijd in voor een geintje, maar serieus als het moet. Heel veel dank voor al het DNA-werk dat jullie voor mij hebben gedaan. Marije,

de ambitieuze en goedlachse analiste, toen jij binnen kwam was mij al snel duidelijk dat wij het project niet samen zouden afronden. Jij had geen aanwijzingen nodig, maar leidde vanaf het begin al meteen je eigen projecten. Het was prettig om met jou te werken. Ik was dan ook niet verbaasd om te horen dat je bij je huidige werkgever een promotiepositie hebt gekregen. Anneke, de laatste analiste waar ik mee heb gewerkt, jouw inzet is onmisbaar geweest bij het afronden van de projecten. Ook al sta jij om politieke redenen op een andere plaats op het N-cadherin manuscript, voor mij sta je op plaats twee. Ik vond het erg fijn dat ik in de laatste fase van mijn project een luisterend oor bij jou kon vinden. Meiden, bedankt voor al jullie inzet!

Maar dit was nog niet de gehele groep Pals: Leonie, Annemieke, Sander en Esther B. zonder jullie inbreng was de sfeer in onze groep nooit zo goed geweest. Tamas, onze SBS6-Hongaar (en nu zelfs directeur), de bunker zonder jou is toch minder leuk, bedankt voor het helpen met de muizen. En Carel, ik heb jou medewerkers (Richard, Laura, Febe, en Robbert), in dit dankwoord gerekend tot onze grote gezamenlijke groep, maar dat is denk ik illustrerend voor de inspirerende werkomgeving die jij en Steven creëren. Verder koester ik mooie herinneringen aan het AMC hockeytoernooi dat jij voor onze afdeling organiseerde.

Van de mensen buiten onze groep gaat een speciale dank uit naar: Pran, Wilfried, Wim, Peter, Nike, Jos en Chris. Pran, ik ken jou al vanaf mijn jonge jaren op het hockeyveld, toen ik nog niet wist wat onderzoek inhield. Ik hecht grote waarde aan onze gesprekken over wetenschap en het leven, en ben er van overtuigd dat we dit gaan voortzetten. Ik wens jou en Lucie heel veel geluk in Engeland en hoop dat jullie daar de wel verdiende rust kunnen vinden. Wilfried bedankt voor alle grafische ondersteuning en in het bijzonder voor de lay-out van mijn proefschrift. Wim bedankt voor de cover lay-out. Heren, het is een mooi exemplaar geworden. Peter en Nike, zonder jullie leiding en hulp zou het lab stuurloos geweest zijn. Ik vind het bewonderenswaardig hoe jullie deze taak uitvoeren. Ook wil ik Jos en Chris niet vergeten in dit dankwoord, de mannen die mij wegwijs hebben gemaakt in de wondere wereld van de immunohistochemie. Ik gebruik nog dagelijks de van jullie geleerde technieken. Verder wil ik de mensen van de diagnostiek bedanken voor al het snijwerk, zonder jullie hulp en inzet was het onmogelijk om zoveel botbiopten te onderzoeken. Natuurlijk bestaat een researchlab niet uit één groep, maar uit meerdere, en onmisbaar in elke organisatie is het secretariaat. Ik wil hier dan ook de andere mensen die de afdeling pathologie tot een geheel maken, bedanken voor jullie inbreng bij mijn presentaties en de goede sfeer tijdens de labuitjes.

Mijn huidige groep in Utrecht: Frans, Linda, Petra, Henk R. en Henk-Jan bedankt voor de fijne werkplek die jullie creëren. Henk R. bedankt voor de technieken die ik al tijdens mijn promotietijd van je heb geleerd. Frans en Linda, jullie wil ik graag bedanken voor het goede team dat wij nu vormen. Maar ik had deze mensen nooit ontmoet, als ik jou niet had ontmoet, Anton, mijn huidige "mentor". Het is aangenaam om samen met jou te werken. Jouw stijl past helemaal bij mij en ik leer erg veel van je. Dank voor je steun en het vertrouwen dat je me gegeven hebt! Ook de mensen van de groep van Tuna en Henk L., en het Coffe-lab wil ik graag bedanken voor de prettige werkomgeving.

Naast het werk bestaat er ook nog zoiets als een privéleven, waarin ik de dagelijkse stress van het werk kon vergeten. Mark, Tessa, Femke, Boris, Eelco en Anneke wil ik graag bedanken voor de welkome afleiding in het weekend, en de heerlijke diners (en natuurlijk de nodige drank) die we hebben genuttigd. Zonder deze afleiding was het nooit gelukt.

Jelmer, mijn tweede paranimf, ik vind het erg plezierig en ben er trots op dat jij naast mij zal

staan tijdens dit belangrijke moment in mijn leven. Ik kan altijd op jou bouwen en zal nooit vergeten hoe jij er voor mij was toen mijn moeder overleed. Ik hoop nog lang van onze vriendschap te mogen genieten.

Papa, wat hebben we een tijd achter de rug. Ik wil jou en mama, helaas kan zij dit alles niet meer meemaken, bedanken voor alles wat jullie mij in mijn leven hebben meegegeven. Jullie steun, vertrouwen en liefde hebben dit alles mogelijk gemaakt. Ik weet zeker dat mama erg trots zou zijn geweest. Esther, mijn lieve zusje, op jou kan ik altijd terugvallen voor een dikke knuffel. Theo en Petra, 'surrogaat'-opa en -oma van Tijmen, bedankt voor alle interesse, het luisterende oor en de wijze raad, maar bovendien ook voor alle gezelligheid. HJ en Digna, ik kan me geen betere schoonouders wensen. HJ jouw rust en wijsheid, vormen een fijn klankbord. Digna, jij creëert altijd een veilige en gezellige thuisbasis voor de meiden, en dus automatisch voor de aanhang. Ook Tijmen mag hier veel van genieten, dank hiervoor. Charlotte en Evelien, ik vind het leuk dat ik af en toe zo'n groot gezin heb ;). Het is altijd erg gezellig met jullie. Ook de rest van mijn familie en mijn schoonfamilie wil ik bedanken voor hun interesse en support.

Hier aangekomen wil ik graag alle mensen bedanken die een bijdrage hebben geleverd en die ik nog niet met naam heb genoemd!

En dan tot slot de mensen waar ik het meeste van hou: Tijmen en Anne Marie. Tijmen, ook al ben je nog niet zo lang in mijn leven, ik kan me geen dag meer zonder jou indenken. Jouw glimlach doet elke dag goed beginnen en eindigen. Lieve Anne, mijn rots in de branding, waar zou ik zijn zonder jou! Jouw planning en overzicht hebben mij er doorheen geleid en ons overeind gehouden. Ik zou deze klus nooit geklaard hebben zonder jouw steun, je eeuwige geduld, en de onvoorwaardelijke liefde die jij mij de afgelopen jaren geschonken hebt. Het is heerlijk om te weten en te voelen dat er altijd iemand is waar je blind op kunt vertrouwen. Het zit er dan eindelijk op, ik hou van je!

Richard

Curriculum Vitae

Richard Groen werd geboren op 21 oktober 1978 in Heemskerk. En groeide vervolgens op in Uitgeest, alwaar hij de lagere school doorliep. In 1997 runde hij het atheneum af aan het Bonhoeffercollege te Castricum, waarna hij Farmacochemie is gaan studeren aan de Vrije Universiteit van Amsterdam. Gedurende deze studie werden er twee wetenschappelijke stages doorlopen. De eerste stage werd uitgevoerd aan de afdeling Toxicologie onder leiding dr. Martijn Rooseboom en dr. Jan Commandeur. Dit onderzoek was gericht op het bestuderen van de mogelijke bescherming van selenocysteine Se-conjugaten tegen de door paracetamol geïnduceerde toxiciteit. De tweede stage aan de afdeling Farmacochemie werd uitgevoerd onder leiding van dr. Paola Casarosa en prof. dr. Martine Smit, binnen deze stage werd onderzoek gedaan naar het effect van mutaties in de cytomegalovirus-gecodeerde chemokine receptor homoloog US28 op signaaltransductie. De opleiding Farmacochemie werd afgerond met het behalen van het doctoraalexamen in juni 2003.

Aansluitend werd gestart met het promotieonderzoek aan de afdeling Pathologie van het Academisch Medisch Centrum te Amsterdam, onder leiding van prof. dr. Steven Pals en dr. Marcel Spaargaren. Hier heeft hij tot mei 2008 onderzoek gedaan naar de rol van de micro-omgeving in de ontwikkeling van non-Hodgkin lymfomen en multipel myeloom (ook: de ziekte van Kahler), waarvan de resultaten zijn beschreven in dit proefschrift.

Sinds juni 2008 is Richard werkzaam aan de afdeling Immunologie van het Universitair Medisch Centrum Utrecht, waar hij in de groep van dr. Anton Martens in samenwerking met de groep van prof. dr. Henk Lokhorst (Hematologie) en de groep van prof. dr. Paul Coffey (Moleculaire Immunologie) een nieuw muizenmodel heeft ontwikkeld. Dit model maakt het mogelijk om onderzoek te doen naar de humane hematopoietische niche en de interactie met tumorcellen.

Publications by the author

Tjin EP, **Groen RW**, Vogelzang I, Derksen PW, Klok MD, Meijer HP, van Eeden S, Pals ST, Spaargaren M. Functional analysis of HGF/MET signaling and aberrant HGF-activator expression in diffuse large B-cell lymphoma. *Blood*. 2006;107(2):760-8.

Rozemuller H, van der Spek E, Bogers-Boer LH, Zwart MC, Verweij V, Emmelot M, **Groen RW**, Spaapen R, Bloem AC, Lokhorst HM, Mutis T, Martens AC. A bioluminescence imaging based in vivo model for preclinical testing of novel cellular immunotherapy strategies to improve the graft-versus-myeloma effect. *Haematologica*. 2008;93(7):1049-57.

Groen RW, Oud ME, Schilder-Tol EJ, Overdijk MB, ten Berge D, Nusse R, Spaargaren M, Pals ST. Illegitimate WNT pathway activation by beta-catenin mutation or autocrine stimulation in T-cell malignancies. *Cancer Res*. 2008;68(17):6969-77.

Groen RW*, Reijmers RM*, Rozemuller H, Kuil A, de Haan-Kramer A, Csikós T, Martens AC, Spaargaren M, Pals ST. Targeting EXT1 reveals a crucial role for heparan sulfate in the growth of multiple myeloma. *Blood*. 2010;115(3):601-4.

Spaapen RM, **Groen RW**, van den Oudenalder K, Guichelaar T, van Elk M, Aarts T, Bloem AC, Storm G, Martens AC, Lokhorst HM and Mutis T. Eradication of medullary multiple myeloma by CD4+ cytotoxic human T lymphocytes directed at a single minor histocompatibility antigen. Accepted for publication 2010 Oct. 1.

Groen RW*, Kocemba KA*, de Rooij MFM, Reijmers RM, de Haan-Kramer A, Overdijk MB, Rozemuller H, Martens ACM, Bergsagel PL, Kersten MJ, Pals ST, Spaargaren M. N-cadherin-mediated adhesion of Multiple Myeloma cells inhibits osteoblast differentiation. Submitted for publication.

Reijmers RM, **Groen RW**, Kuil A, Weijer K, Kimberley FC, Medema JP, van Kuppevelt TH, Li JP, Spaargaren M, Pals ST. Disruption of Glce reveals a role for heparan sulfate proteoglycans in B cell maturation and APRIL-mediated plasma cell survival. Submitted for publication.

* These authors share first authorship

